INSIGHTS IN CANCER ENDOCRINOLOGY: 2021

EDITED BY: Claire Perks and Antonino Belfiore
PUBLISHED IN: Frontiers in Endocrinology

frontiers Research Topics

ISSN 1664-8714
ISBN 978-2-83250-032-3
DOI 10.3389/978-2-83250-032-3

About Frontiers

Frontiers is more than just an open-access publisher of scholarly articles: it is a pioneering approach to the world of academia, radically improving the way scholarly research is managed. The grand vision of Frontiers is a world where all people have an equal opportunity to seek, share and generate knowledge. Frontiers provides immediate and permanent online open access to all its publications, but this alone is not enough to realize our grand goals.

Frontiers Journal Series

The Frontiers Journal Series is a multi-tier and interdisciplinary set of open-access, online journals, promising a paradigm shift from the current review, selection and dissemination processes in academic publishing. All Frontiers journals are driven by researchers for researchers; therefore, they constitute a service to the scholarly community. At the same time, the Frontiers Journal Series operates on a revolutionary invention, the tiered publishing system, initially addressing specific communities of scholars, and gradually climbing up to broader public understanding, thus serving the interests of the lay society, too.

Dedication to Quality

Each Frontiers article is a landmark of the highest quality, thanks to genuinely collaborative interactions between authors and review editors, who include some of the world's best academicians. Research must be certified by peers before entering a stream of knowledge that may eventually reach the public - and shape society; therefore, Frontiers only applies the most rigorous and unbiased reviews.
Frontiers revolutionizes research publishing by freely delivering the most outstanding research, evaluated with no bias from both the academic and social point of view. By applying the most advanced information technologies, Frontiers is catapulting scholarly publishing into a new generation.

What are Frontiers Research Topics?

Frontiers Research Topics are very popular trademarks of the Frontiers Journals Series: they are collections of at least ten articles, all centered on a particular subject. With their unique mix of varied contributions from Original Research to Review Articles, Frontiers Research Topics unify the most influential researchers, the latest key findings and historical advances in a hot research area! Find out more on how to host your own Frontiers Research Topic or contribute to one as an author by contacting the Frontiers Editorial Office: frontiersin.org/about/contact

INSIGHTS IN CANCER ENDOCRINOLOGY: 2021

Topic Editors:
Claire Perks, University of Bristol, United Kingdom
Antonino Belfiore, University of Catania, Italy

Citation: Perks, C., Belfiore, A., eds. (2022). Insights in Cancer Endocrinology: 2021. Lausanne: Frontiers Media SA. doi: 10.3389/978-2-83250-032-3

Table of Contents

frontiers | Frontiers in Endocrinology

TYPE Editorial
PUBLISHED 29 July 2022
DOI 10.3389/fendo.2022.987764

OPEN ACCESS

EDITED AND REVIEWED BY
Jeff M P Holly,
University of Bristol, United Kingdom

*CORRESPONDENCE
Claire M. Perks
Claire.M.Perks@bristol.ac.uk

SPECIALTY SECTION
This article was submitted to Cancer Endocrinology, a section of the journal Frontiers in Endocrinology

RECEIVED 06 July 2022
ACCEPTED 13 July 2022
PUBLISHED 29 July 2022

CITATION
Perks CM and Belfiore A (2022) Editorial: insights in cancer endocrinology 2021. *Front. Endocrinol.* 13:987764. doi: 10.3389/fendo.2022.987764

Editorial: insights in cancer endocrinology 2021

Claire M. Perks[1]* and Antonino Belfiore[2]

[1]Bristol Medical School, Department of Translational Health Sciences, University of Bristol, Bristol, United Kingdom, [2]Endocrinology Unit, Department of Clinical and Experimental Medicine, University of Catania, Garibaldi-Nesima Hospital, Catania, Italy

KEYWORDS

cancer, cell signalling, prostate, breast, neuroendocrine tumors

Editorial on the Research Topic
Insights in Cancer Endocrinology: 2021

This Research Topic entitled "Insights in Cancer Endocrinology: 2021" provides a collection of work highlighting important issues in the field, for example, furthering our understanding of important cell signalling pathways and optimization of treatment options in different cancers. Panigoro et al. report on a multicentre, case-control study conducted in six public referral hospitals in Indonesia and assessed the use of triglyceride glucose index (TyG) as a reliable and cost-effective surrogate marker of insulin resistance. The authors found it to be associated with the risk of breast cancer in a non-linear fashion. Mutations in the breast and ovarian cancer susceptibility gene (BRCA1) are also associated with an increased risk of developing cancers, including those of the breast and ovary. Werner's review emphasizes the emerging non-genomic roles of BRCA1, for example being an important regulator of endocrine and metabolic axes, including the insulin/IGF1 signalling pathway. BRCA1 mutations are also correlated with metabolic disorders, such as metabolic syndrome and diabetes. A mini-review written by Bulatowitcz et al. discusses the role of another important regulator of cell behavior in cancer progression, the insulin-like growth factor 1 receptor (IGF-1R). The IGF-1R has mostly been described as pro-tumorigenic, but the authors highlight that both pro- and anti-tumorigenic roles have been described mainly in mouse models of breast cancer and they provide hypotheses to support these conflicting data [IN PRESS].

Prostate cancer (PCa) remains the second most common cancer in men globally and Wang et al. describe the 'burden' of PCa in China from 1990- 2019. Whilst the incidence in China is still relatively low compared with other countries, it appears to be on the increase and the rates and disease burden amongst the provinces in China are very different. The authors conclude that based on this, implementing more targeted and effective strategies should be considered [IN PRESS]. In terms of new therapeutic options for men with advanced PCa, Licitra et al. have written a review highlighting the limited approaches available. They report that a better understanding in recent years of for example, the role of the tumor micro-environment, has led to the emergence of novel therapeutic approaches.

There are many adverse side effects of cancer therapies and a vitally important one is highlighted by Eugeni et al. who reviewed current available approaches to protect or restore fertility in young prepubertal male patients, before they undergo potentially damaging treatments, such as radiotherapy [IN PRESS]. In addition, immune checkpoint inhibitors are currently now used to treat cancer patients and Barnabei et al. have reported that a rare side-effect of these drugs is central diabetes insipidus (CDI) and to provide better management of the adverse effects and the specific drugs that trigger it, they describe a new, improved grading system for CDI.

Von Hippel-Lindau (VHL) disease is a hereditary condition associated with tumors occurring in multiple organs, including the brain, spine, eyes, kidneys, pancreas, adrenal glands, inner ears, reproductive tract, liver, and lung, and is caused by mutations in a tumor suppressor gene called *VHL*. Mathó et al. characterise two novel variants of this gene, to help understand how they may affect the function and fate of VHL protein and impact on disease progression.

Neuroendocrine tumors (NETs) are rare cancers and can develop in different locations, as neuroendocrine cells are found in most organs of the body. Puliani et al. have written a mini review to provide a new vision for the potential increased use, safety and prognostic and predictive factors of two radiopharmaceuticals, ^{177}Lu-DOTATATE and ^{90}Y-DOTATOC in peptide receptor radionuclide therapy (PPRT) for NETs. Contarino et al. focused on medullary thyroid carcinoma and in their case series and review of the literature they asked the question: "Is encapsulated medullary carcinoma associated with a better prognosis?". Cui et al. retrospectively analysed clinical data from patients with local-regional recurrence of pheochromocytoma/paraganglioma and reported on their characteristics, risk factors and outcome. Giuffrida et al. analyzed the methylation profile from eleven growth hormone-secreting (GH-omas) and ten non-functioning (NF-omas) pituitary adenomas and report that the epigenetic landscape of these tumors is complicated. Whilst hypermethylation is considerably more prevalent in NFPA compared with GH-omas, its contribution to the disease is still to be determined. Furthermore, Mangili et al. performed *in vitro* studies to examine if cabergoline in combination with mTOR inhibitors may be a potential treatment specifically for patients with β-arrestin2 expressing pituitary neuroendocrine tumors or other subtypes also resistant to conventional therapy [IN PRESS].

It has been our pleasure to host this exciting Research Topic and we thank all the authors for their excellent contributions.

Author contributions

CP wrote and AB & CP read, commented and edited the article. All authors contributed to the article and approved the submitted version.

Conflict of interest

The authors declare that the research was conducted in the absence of any commercial or financial relationships that could be construed as a potential conflict of interest.

Publisher's note

frontiers in Endocrinology

ORIGINAL RESEARCH
published: 11 October 2021
doi: 10.3389/fendo.2021.745236

The Association Between Triglyceride-Glucose Index as a Marker of Insulin Resistance and the Risk of Breast Cancer

Sonar Soni Panigoro[1], Noorwati Sutandyo[2], Fiastuti Witjaksono[3], Nurjati Chairani Siregar[4], Ramadhan Ramli[5], Ririn Hariani[6], Eko Adhi Pangarsa[7], Yan Wisnu Prajoko[8], Niken Puruhita[9], William Hamdani[10], Dimas Bayu[11], Mardiana Madjid[12], Dedy Yulidar[13], Jane Estherina Fransiska[14], Retno Widyawati[15], Effif Syofra Tripriadi[16], Wiwit Ade F. W.[17], Dewi Krisna Yunda[18] and Raymond Pranata[19]*

[1] Department of Surgical Oncology, Dr. Cipto Mangunkusumo Hospital, Faculty of Medicine, Universitas Indonesia, Jakarta, Indonesia, [2] Department of Hematology and Medical Oncology, Dharmais Hospital National Cancer Center, Jakarta, Indonesia, [3] Department of Nutrition, Dr. Cipto Mangunkusumo Hospital, Faculty of Medicine, Universitas Indonesia, Jakarta, Indonesia, [4] Department of Pathological Anatomy, Dr. Cipto Mangunkusumo Hospital, Faculty of Medicine, Universitas Indonesia, Jakarta, Indonesia, [5] Department of Surgical Oncology, Dharmais Hospital National Cancer Center, Jakarta, Indonesia, [6] Department of Nutrition, Dharmais Hospital National Cancer Center, Jakarta, Indonesia, [7] Department of Hematology and Medical Oncology, Dr. Kariadi General Hospital, Faculty of Medicine, Diponegoro University, Semarang, Indonesia, [8] Department of Surgical Oncology, Dr. Kariadi General Hospital, Faculty of Medicine, Diponegoro University, Semarang, Indonesia, [9] Department of Nutrition, Dr. Kariadi General Hospital, Faculty of Medicine, Diponegoro University, Semarang, Indonesia, [10] Department of Surgical Oncology, Wahidin Sudirohusodo General Hospital, Faculty of Medicine, Hasanuddin University, Makassar, Indonesia, [11] Division of Hematology-Medical Oncology, Department of Internal Medicine, Hasanuddin University General Hospital, Faculty of Medicine, Hasanuddin University, Makassar, Indonesia, [12] Department of Nutrition, Faculty of Medicine, Wahidin Sudirohusodo General Hospital, Hasanuddin University, Makassar, Indonesia, [13] Department of Surgical Oncology, Prof. Dr. WZ Johannes General Hospital, Kupang, Indonesia, [14] Division of Hematology and Medical Oncology, Department of Internal Medicine, Prof. Dr. WZ Johannes General Hospital, Kupang, Indonesia, [15] Department of Pathological Anatomy, Prof. Dr. WZ Johannes General Hospital, Kupang, Indonesia, [16] Department of Surgical Oncology, Arifin Achmad General Hospital, Faculty of Medicine, Riau University, Pekanbaru, Indonesia, [17] Department of Pathological Anatomy, Arifin Achmad General Hospital, Faculty of Medicine, Riau University, Pekanbaru, Indonesia, [18] Department of Nutrition, Arifin Achmad General Hospital, Faculty of Medicine, Riau University, Pekanbaru, Indonesia, [19] Department of Nutrition, Nutrition Cancer Reaserch Team, Dharmais Hospital National Cancer Center, Jakarta, Indonesia*

OPEN ACCESS

Edited by:
Antonino Belfiore, University of Catania, Italy

Reviewed by:
Rosario Le Moli, University of Catania, Italy
Annalisa De Silvestri, Fondazione IRCCS Policlinico San Matteo, Italy

***Correspondence:**
Sonar Soni Panigoro
sonarpanigoro@gmail.com

Specialty section:
This article was submitted to Cancer Endocrinology, a section of the journal Frontiers in Endocrinology

Received: *21 July 2021*
Accepted: *14 September 2021*
Published: *11 October 2021*

Citation:
Panigoro SS, Sutandyo N, Witjaksono F, Siregar NC, Ramli R, Hariani R, Pangarsa EA, Prajoko YW, Puruhita N, Hamdani W, Bayu D, Madjid M, Yulidar D, Fransiska JE, Widyawati R, Tripriadi ES, F. W. WA, Yunda DK and Pranata R (2021) The Association Between Triglyceride-Glucose Index as a Marker of Insulin Resistance and the Risk of Breast Cancer. Front. Endocrinol. 12:745236. doi: 10.3389/fendo.2021.745236

Background: This study aims to evaluate the association and dose-response between triglyceride-glucose (TyG) index and breast cancer.

Method: This is a multicenter case-control study conducted in six public referral hospitals in Indonesia. Cases are individuals aged 19 years or above who were diagnosed with breast cancer within 1 year of diagnosis, based on histopathology and immunohistochemistry. Controls were recruited from corresponding hospitals. TyG index was determined by the formula: ln (fasting TG [mg/dl] × fasting glucose [mg/dl]).

Results: There were 212 participants in the breast cancer group and 212 participants in the control group. TyG index was higher in patients with breast cancer (median 8.65 [7.38, 10.9] vs. 8.30 [7.09, 10.84], $p < 0.001$). When compared with TyG quartile of Q1, Q4 was associated with an OR of 2.42 (1.77, 3.31), $p < 0.001$, Q3 was associated with an OR of 1.53 (1.21, 1.93), $p < 0.001$, Q2 was associated with an OR of 1.39 (1.12, 1.73), $p = 0.002$

for the risk of breast cancer. The dose-response relationship was nonlinear ($p < 0.001$). On univariate analysis, smoking (OR 2.15 [1.44, 3.22], $p < 0.001$), use of contraception (1.73 [1.15, 2.60], $p = 0.008$), alcohol consumption (OR 2.04 [0.96, 4.35], $p = 0.064$), and TyG Index >8.87 (OR 3.08 [1.93, 4.93], $p < 0.001$) were associated with risk of breast cancer. Independently associated with increased risk of breast cancer included smoking (OR 1.93 [1.23, 3.01], $p = 0.004$), use of contraception (OR 1.59 [1.02, 2.48], $p = 0.039$), and TyG Index >8.87 (OR 2.93 [1.72, 4.98], $p < 0.001$)

Conclusion: TyG index was associated with breast cancer in a nonlinear dose-response fashion.

Keywords: breast cancer, insulin resistance, triglyceride, glucose, insulin

INTRODUCTION

Breast cancer is the most common cancer worldwide (1, 2). There were an estimated 2.3 million new cases of female breast cancer out of 19.3 million new cases of cancer (i.e., breast cancer represents 11.7% of all new cancer cases) worldwide in 2020 (2). Breast cancer accounts for one in six cancer deaths and has become the leading cause of cancer death in the majority of countries. This trend also occurs in Indonesia where the incidence rate of breast cancer is 44.0 and mortality rate is 15.3 out of 100,000 (2, 3). Breast cancer is associated with several risk factors which numerous studies have investigated (4–7). Risk factors are commonly differentiated into two categories namely nonmodifiable and modifiable risk factors. The nonmodifiable risk factors consist of age, age of menarche, genetic factors, family history, and history of breast cancer, while the modifiable category includes weight status, fat intake, parity, breastfeeding status, alcohol consumption, smoking habit, and the use of contraception (4–6, 8).

Recent studies suggest that insulin resistance was associated with breast cancer and may affect its prognosis (9, 10). Euglycemic-hyperinsulinemic clamp (clamp-IR) is the gold standard for IR diagnosis (11); however, its use is impractical (12). Triglyceride-glucose (TyG) index is a reliable surrogate marker of insulin resistance (13), which is calculated by formula comprising fasting glyceride and glucose, which is usually assessed in apparently healthy individuals (14). Thus, risk stratification for breast cancer using TyG index is practical, feasible, and cost-effective. Although ideally evaluated using a prospective cohort study, this case-control study may provide early evidence regarding the association between insulin resistance and breast cancer. This study aims to evaluate the association between TyG index and breast cancer and assess the dose-response between TyG index and breast cancer.

PATIENTS AND METHODS

Study Population

This was a multicenter case-control study conducted in six public referral hospitals in Indonesia, namely, Ciptomangunkusumo Hospital in Jakarta, Dharmais Cancer Center in Jakarta, Arifin Achmad General Hospital in Pekanbaru, Dr. Kariadi Hospital in Semarang, Wahidin Sudirohusodo Hospital in Makassar, and Prof. Dr. WZ. Johannes Hospital in Kupang. Recruitment of study participants was performed consecutively between April to August 2019. A total of 432 women consisting of 216 cases and 216 controls were recruited. The sample size was derived from proportion estimate of two population with the formula $(Z1-\alpha/2\sqrt{2PQ} + Z1-\beta\sqrt{P1Q\ 1+P2Q2})^2/(P1-P2)^2$.

The inclusion criteria for the case group are as follows (1): individuals aged 19 years or above who were diagnosed with breast cancer based on histopathology and immunohistochemistry between April to August 2019. The maximum year postdiagnosis was 1 year (2), patients with breast cancer that has not received therapy, (3) can read, understand, and provide consent, and (4) complete medical record and paraffin block. Those with incomplete questionnaire data were excluded. Controls were recruited from corresponding hospitals. Inclusion criteria for the control group were as follows: (1) women aged 19 years or above (matched 5 years), (2) in healthy conditions based on anamnesis and physical examination results, (3) no evidence of cancer or history of cancer, and (4) no evidence of chronic disease. Most individuals recruited as controls were hospital employees. The study was approved by Ethical Committee of Health Research in the Faculty of Medicine, Universitas Indonesia, Rumah Sakit Cipto Mangunkusumo, Jakarta, Indonesia (450/UN2.F1/ETIK/2018).

Measurements

Data were collected through medical records and a self-administered structured questionnaire. The questionnaire included information on age at menarche, smoking history, reproductive risk factors (i.e., breastfeeding and use of contraception), family history of malignancy, alcohol consumption, and nutrition intake.

TyG index was determined by the formula: ln (fasting TG [mg/dl] × fasting glucose [mg/dl]) (14).

Weight and height were measured to the nearest 0.1 kg and 0.5 cm according to standardized procedures. The study participants wore light clothes and no shoes during the measurement. Body mass index (BMI) was calculated as weight in kilograms divided by the square of height in meters. BMI was classified according to WHO into underweight (<18.5 kg/m^2),

normal weight (18.5–24.9 kg/m^2), and overweight and obese (>24.9 kg/m^2).

Menarche was defined as the age when the first menstruation occurred. The use of contraception, breastfeeding history, smoking status, and alcohol consumption were defined from the questionnaire. Participants were classified as using contraception/breastfeeding/having smoking history/consuming alcohol if they answered "yes" to the question "have you ever used contraception/breastfed/smoked cigarettes/drunk alcohol during your entire life?". Those who answered yes were then asked for the duration of using contraception/breastfeeding/having smoking history/consuming alcohol. Type of contraception was also asked to those who ever used contraception.

Statistical Analysis

Categorical data are presented as proportions. The distribution of continuous data was inspected using QQ plots, histograms, Kolmogorov-Smirnoff, and Shapiro-Wilk test. Normally distributed data are presented as means and standard deviations (SD), while nonparametric data are presented as median, minimum, and maximum values (median (min-max)). Comparison of categorical variables was tested using Chi-square test. Continuous variables were compared using independent *t*-test or Mann-Whitney *U* test, where appropriate.

The TyG was divided into four quartiles, and the odds ratios (ORs) for each quartile were calculated using the first quartile as the reference. Restricted cubic spline model was constructed using four knots at 7.9, 8.3, 8.7, and 9.4; nonlinearity of the dose-response curve was also assessed. The ORs for TyG index and breast cancer were calculated using logistic regression. A cutoff point for TyG index was set at the beginning of the fourth quartile for multivariate analysis. Multivariate logistic regression was used to test the association between breast cancer and each independent variable. The results are presented as ORs with 95% confidence intervals (CIs). Statistical significance was defined as $p < 0.05$. Data were managed and analyzed using SPSS 25.0 (IBM, Armonk, US) and STATA® version 16 (StataCorp, College Station, TX, USA).

RESULTS

Baseline Characteristics

There were 212 participants in the breast cancer group and 212 participants in the control group. The baseline characteristics of the participants in this study can be seen in **Table 1**. The distribution of BMI categories was more or less the same, except in the underweight group, in which there was a significantly higher breast cancer patient in the underweight group.

Triglyceride-Glucose Index and Breast Cancer

TyG index was higher in patients with breast cancer (median 8.65 [7.38, 10.9] vs. 8.30 [7.09, 10.84], $p < 0.001$). The patients were divided into four quartiles based on the TyG index, namely, Q1 (7.09–8.12), Q2 (8.13–8.47), Q3 (8.48–8.86), and Q4 (8.87–10.90); comprising of 101, 108, 108, and 107 patients, respectively. When compared with TyG quartile of Q1, Q4 was associated with an OR of 2.42 (1.77, 3.31), $p < 0.001$, Q3 was associated with an OR of 1.53 (1.21, 1.93), $p < 0.001$, Q2 was associated with an OR of 1.39 (1.12, 1.73), $p = 0.002$ for the risk of breast cancer (**Table 2**). There was a non-linear relationship between TyG index and breast cancer ($p < 0.001$) (**Figure 1**).

Univariate Analysis

On univariate analysis, variables that contribute to increased risk of breast cancer were smoking (OR 2.15 [1.44, 3.22], $p < 0.001$),

TABLE 1 | Baseline characteristics of study participants.

	Breast cancer (+) *n* = 212	Breast cancer (–) *n* = 212	*p*-Value
Age (year)	48 (22–78)	46 (22–75)	0.001
Smoking	100 (49.3)	65 (31.1)	0.001
Age at menarche (year)	13 (9–19)	13 (8–18)	<0.001
Breastfeeding ≥12 months	81 (42)	87 (43.7)	0.726
Use of contraception	96 (48.7)	67 (35.4)	0.008
Family history of malignancy	35 (16.6)	45 (21.5)	0.197
Alcohol consumption	21 (10.1)	11 (5.2)	0.060
Body mass index (kg/m^2)			
Underweight	15 (7.2)	2 (1)	0.001
Normal	60 (28.8)	47 (22.5)	0.137
Overweight	39 (18.8)	46 (22)	0.409
Obese	94 (45.2)	114 (54.5)	0.056
TyG index	8.65 (7.38–10.9)	8.30 (7.09–10.84)	<0.001
Q1 (7.09–8.12)	28 (13.2)	73 (34.4)	<0.001
Q2 (8.13–8.47)	52 (24.5)	56 (26.4)	0.656
Q3 (8.48–8.86)	57 (26.9)	51 (24.1)	0.504
Q4 (8.87–10.90)	75 (35.4)	32 (15.1)	<0.001
Total cholesterol	201.5 (71–343)	206 (113–561)	0.190
LDL	135 (39–268)	136 (67–268)	<0.001

TyG index, triglyceride-glucose index.

use of contraception (1.73 [1.15, 2.60], p = 0.008), alcohol consumption (OR 2.04 [0.96, 4.35], p = 0.064), and TyG Index >8.87 (OR 3.08 [1.93, 4.93], p < 0.001) (**Table 3**).

Multivariate Analysis

On multivariate analysis, variables that were independently associated with increased risk of breast cancer included smoking (OR 1.93 [1.23, 3.01], p = 0.004), use of contraception (OR 1.59 [1.02, 2.48], p = 0.039), and TyG Index >8.87 (OR 2.93 [1.72, 4.98], p < 0.001) (**Table 3**).

DISCUSSION

This study indicates that TyG index was associated with breast cancer in a nonlinear dose-response fashion. TyG index >8.87 was independently associated with a threefold risk of breast cancer. Although there was no statistically significant difference in terms of overweight and obesity between the two groups, TyG index, which is a marker of insulin resistance, was higher in patients with breast cancer.

Hyperinsulinemia has been shown to be a risk factor for breast cancer as shown by previous studies using fasting insulin or c-peptide measurement (15–18). A Post Genome-Wide Gene–Environment Interaction Study identify insulin resistance single-nucleotide polymorphisms (SNPs) in combination with lifestyle as a synergistic factors for the risk of breast cancer (9). A study involving 22,837 postmenopausal women found that insulin resistance measured using homeostatic model assessment for insulin resistance in postmenopausal women were associated with higher incidence of breast cancer and mortality (10). Interestingly, a study by Kabat et al. indicates that although elevated serum insulin was associated with breast cancer, glucose alone was not (18). A study by Zhu et al. on 2,536 patients with breast cancer and 2528 patients with benign breast disease showed that insulin and insulin resistance was associated with breast cancer risk in Chinese women (19).

Gunter et al. showed that insulin resistance, and not adiposity per se, is a risk factor for postmenopausal breast cancer (20). Several reports indicate that overweight with normal insulin sensitivity does not have increased risk for cardiovascular disease (21–23), which might also be the case for breast cancer. In our study, alike to that of the study of Gunter et al. (20), TyG index was independently associated with breast cancer despite similar baseline BMI characteristics. Since the dose-response relationship between TyG index and risk of breast cancer was nonlinear, a TyG index >8.87 which marks the beginning of the fourth quartile was used as the cutoff point.

This present study showed that contraception use was positively associated with the risk of breast cancer, although statistical significance was lost in the multivariate analyzed. This finding was well-reported in previous studies (24–26). In the present study, we did not distinguish the type of hormonal contraception. Several studies indicated no significant differences regarding the type of oral contraception being used by individuals with breast cancer (24, 25), while another study in the USA shows that progestin-only pill consumption was not correlated with the risk of breast cancer (27). Moreover, some studies found that the duration of hormonal contraception use was correlated with increased risk of breast cancer (24, 25).

Although there is tendency towards increased risk of breast cancer related to alcohol consumption in the present study, it did not reach statistical significance. Previous studies have shown that alcohol was associated with breast cancer (28–32). A meta-analysis reported that there is a significant association between light drinking and breast cancer (32). Another study identified that increased alcohol intake in postmenopausal women was linked to a higher risk of breast cancer (31). It has been widely accepted that the biological mechanism underlying the correlation between alcohol and breast cancer is through the effects of alcohol on circulating estrogen levels and thus mostly associated with positive estrogen receptor breast cancer (28, 33). This study did not stratify the amount of alcohol consumption, the association might be dose related.

We did not found association of breast cancer with age at menarche and breastfeeding. Yet, the association between age at menarche and breast cancer has been established in previous studies. Several studies showed that early age at menarche was associated with increased risk of breast cancer (6, 34–36). A meta-analysis of 117 studies reported that every year younger at

TABLE 2 | Quartiles of triglyceride-glucose index and the risk of breast cancer.

TyG index quartiles	Odds ratio	*p*-Value
Q1 (7.09–8.12) [*n* = 101]	Reference value	Reference value
Q2 (8.13–8.47) [*n* = 108]	1.39 (1.12, 1.73)	p = 0.002
Q3 (8.48–8.86) [*n* = 108]	1.53 (1.21, 1.93)	p < 0.001
Q4 (8.87–10.90) [*n* = 107]	2.42 (1.77, 3.31)	p < 0.001

TyG index, triglyceride-glucose index.

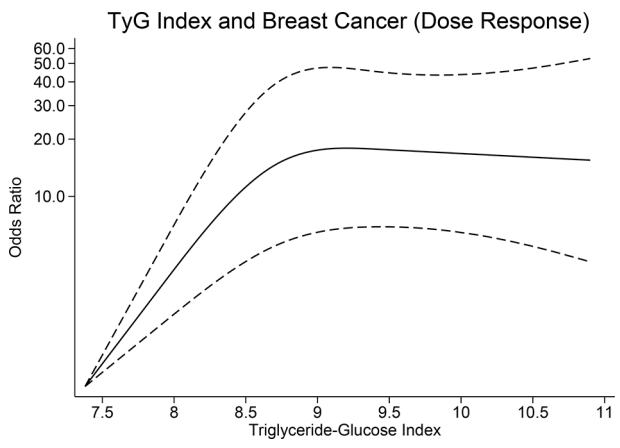

FIGURE 1 | Dose-response relationship between triglyceride-glucose index and breast cancer.

TABLE 3 | Univariate and multivariate analysis of risk factors for breast cancer.

	Univariate analysis	Multivariate analysis
Age >60 years old	1.64 [0.85, 3.16], $p = 0.142$	1.46 [0.71, 3.04], $p = 0.305$
Early menarche (<12 years old)	1.19 [0.62, 2.27], $p = 0.599$	1.32 [0.64, 2.74], $p = 0.450$
Family history of malignancy	0.73 [0.44, 1.18], $p = 0.197$	0.66 [0.38, 1.15], $p = 0.143$
Smoking	2.15 [1.44, 3.22], $p < 0.001$	1.93 [1.23, 3.01], $p = 0.004$
Use of contraception	1.73 [1.15, 2.60], $p = 0.008$	1.59 [1.02, 2.48], $p = 0.039$
Alcohol consumption	2.04 [0.96, 4.35], $p = 0.064$	2.24 [0.97, 5.18], $p = 0.059$
TyG index >8.87	3.08 [1.93, 4.93], $p < 0.001$	2.93 [1.72, 4.98], $p < 0.001$
Total cholesterol > 200 mg/dl	0.86 [0.59, 1.26], $p = 0.436$	0.87 [0.53, 1.41], $p = 0.565$
LDL >100 mg/dl	0.68 [0.39, 1.18], $p = 0.164$	0.75 [0.38, 1.47], $p = 0.400$

TyG index, triglyceride-glucose index; LDL, low-density lipoprotein.

menarche led to increasing the risk of breast cancer by the odds of 1.050 (95% CI 1.044–1.057, $p < 0.0001$) (35). In the present study, the crude analysis indicated a significant association between age at menarche and breast cancer, while such association was not shown in the adjusted model. Lack of power may be a reason for this null association.

The association between breastfeeding and breast cancer has been contradictive. The present study found a null association of breastfeeding with breast cancer. This finding is in line with several studies (6, 37). In contrast, other studies reported that breastfeeding has a protective effect on breast cancer (8, 38, 39). The risk of breast cancer who breastfed exclusively was 28% lower compared with those who had never breastfed (38). One of the biological explanations for this association is that prolonged breastfeeding leads to decreased exposure to the cyclic reproductive hormones (39).

A few studies have shown association between smoking and breast cancer (40, 41). This study support the link between smoking and breast cancer. A study in the UK found that women who smoked have a higher risk of breast cancer, particularly those who smoked >5 cigarettes per day, 10+pack-years of use (40). This finding indicated that relationship between smoking and breast cancer is stronger in a dose-response pattern, rather than as a binary association.

Limitations

One of the limitations was due to self-reported measurements used in the study, recall bias and social desirability bias might have occurred. Furthermore, selection bias might have occurred due to hospital-based study design. In addition, as different histological subtypes of breast cancer might have different risk factors, a larger longitudinal study is needed to assess factors associated with histological subtypes of breast cancer. Finally, levels of triglycerides and glucose are variable and are related to the time since the last meal.

CONCLUSION

TyG index was associated with increased risk for breast cancer in a non-linear fashion. Further prospective studies are required to confirm this finding.

DATA AVAILABILITY STATEMENT

The raw data supporting the conclusions of this article will be made available by the authors, without undue reservation.

ETHICS STATEMENT

The studies involving human participants were reviewed and approved by Ethical Committee of Health Research in the Faculty of Medicine, Universitas Indonesia, Rumah Sakit Cipto Mangunkusumo, Jakarta, Indonesia (450/UN2.F1/ETIK/2018). The patients/participants provided their written informed consent to participate in this study.

AUTHOR CONTRIBUTIONS

SP: conceptualization, design, data curation, investigation, and writing (original draft). NS: data curation, investigation, and writing (original draft). FW: data curation, investigation, and writing (original draft). NS: data curation, investigation, and writing (original draft). RR: data curation, investigation, and writing (review and editing). RH: data curation, investigation, and writing (review and editing). EP: data curation, investigation, and writing (review and editing). YP: data curation, investigation, and writing (review and editing). NP: Data curation, investigation, and writing (review and editing). WH: data curation, investigation, and writing (review and editing). DB: data curation, investigation, and writing (review and editing). MM: data curation, investigation, and writing (review and editing). DY: data curation, investigation, and writing (review and editing). JF: data curation, investigation, writing (review and editing). RW: data curation, investigation, and writing (review and editing). ET: data curation, investigation, and writing (review and editing). WF: data curation, investigation, and writing (review and editing). DY: data curation, investigation, and writing (review and editing). RP: conceptualization, investigation, formal analysis, and writing (original draft). All authors contributed to the article and approved the submitted version.

REFERENCES

1. IARC. *World Cancer Report 2020*. World Health Organization (2020).
2. Sung H, Ferlay J, Siegel RL, Laversanne M, Soerjomataram I, Jemal A, et al. Global Cancer Statistics 2020: GLOBOCAN Estimates of Incidence and Mortality Worldwide for 36 Cancers in 185 Countries. *CA Cancer J Clin* (2021) 0:1–41. doi: 10.3322/caac.21492
3. International Agency for Research on Cancer (IARC). Indonesia - Global Cancer Observatory. In: *Globocan*, vol. 858. (2020). The International Agency for Research on Cancer. p. 1–2.
4. Sun YS, Zhao Z, Yang ZN, Xu F, Lu HJ, Zhu ZY, et al. Risk Factors and Preventions of Breast Cancer. *Int J Biol Sci* (2017) 13:1387–97. doi: 10.7150/ijbs.21635
5. Kamińska M, Ciszewski T, Łopacka-Szatan K, Miotła P, Starosławska E. Breast Cancer Risk Factors. *Prz Menopauzalny* (2015) 14:196–202. doi: 10.5114/pm.2015.54346
6. Ozsoy A, Barca N, Akdal Dolek B, Aktas H, Elverici E, Araz L, et al. The Relationship Between Breast Cancer and Risk Factors: A Single-Center Study. *Eur J Breast Heal* (2017) 13:145–9. doi: 10.5152/tjbh.2017.3180
7. Ataollahi MR, Sharifi J, Paknahad MR, Paknahad A. Breast Cancer and Associated Factors: A Review. *J Med Life* (2015) 8:6–11.
8. Fortner RT, Sisti J, Chai B, Collins LC, Rosner B, Hankinson SE, et al. Parity, Breastfeeding, and Breast Cancer Risk by Hormone Receptor Status and Molecular Phenotype: Results From the Nurses' Health Studies. *Breast Cancer Res* (2019) 21:1–9. doi: 10.1186/s13058-019-1119-y
9. Jung SY, Papp JC, Sobel EM, Yu H, Zhang ZF. Breast Cancer Risk and Insulin Resistance: Post Genome-Wide Gene-Environment Interaction Study Using a Random Survival Forest. *Cancer Res* (2019) 79:2784–94. doi: 10.1158/0008-5472.CAN-18-3688
10. Pan K, Chlebowski RT, Mortimer JE, Gunther MJ, Rohan T, Vitolins MZ, et al. Insulin Resistance and Breast Cancer Incidence and Mortality in Postmenopausal Women in the Women's Health Initiative. *Cancer* (2020) 126:3638–47. doi: 10.1002/cncr.33002
11. Tam CS, Xie W, Johnson WD, Cefalu WT, Redman LM, Ravussin E. Defining Insulin Resistance From Hyperinsulinemic-Euglycemic Clamps. *Diabetes Care* (2012) 35:1605–10. doi: 10.2337/dc11-2339
12. Pranata R, Huang I, Irvan, Lim MA, Vania R. The Association Between Triglyceride-Glucose Index and the Incidence of Type 2 Diabetes Mellitus—a Systematic Review and Dose–Response Meta-Analysis of Cohort Studies. *Endocrine* (2021). doi: 10.1007/s12020-021-02780-4
13. Sánchez-García A, Rodríguez-Gutiérrez R, Mancillas-Adame L, González-Nava V, Díaz González-Colmenero A, Solis RC, et al. Diagnostic Accuracy of the Triglyceride and Glucose Index for Insulin Resistance: A Systematic Review. *Int J Endocrinol* (2020) 2020:1–7. doi: 10.1155/2020/4678526
14. Park K, Ahn CW, Lee SB, Kang S, Nam JS, Lee BK, et al. Elevated TYG Index Predicts Progression of Coronary Artery Calcification. *Diabetes Care* (2019) 42:1569–73. doi: 10.2337/dc18-1920
15. Toniolo P, Bruning PF, Akhmedkhanov A, Bonfrer JMG, Koenig KL, Lukanova A, et al. Serum Insulin-Like Growth Factor-I and Breast Cancer. *Int J Cancer* (2000) 88:828–32. doi: 10.1002/1097-0215(20001201)88:5<828::AID-IJC22>3.0.CO;2-8
16. Verheus M, Peeters PHM, Rinaldi S, Dossus L, Biessy C, Olsen A, et al. Serum C-Peptide Levels and Breast Cancer Risk: Results From the European Prospective Investigation Into Cancer and Nutrition (EPIC). *Int J Cancer* (2006) 119:659–67. doi: 10.1002/ijc.21861
17. Keinan-Boker L, Bueno De Mesquita HB, Kaaks R, Van Gils CH, Van Noord PAH, Rinaldi S, et al. Circulating Levels of Insulin-Like Growth Factor I, Its Binding Proteins -1, -2, -3, C-Peptide and Risk of Postmenopausal Breast Cancer. *Int J Cancer* (2003) 106:90–5. doi: 10.1002/ijc.11193
18. Kabat GC, Kim M, Caan BJ, Chlebowski RT, Gunter MJ, Ho GYF, et al. Repeated Measures of Serum Glucose and Insulin in Relation to Postmenopausal Breast Cancer. *Int J Cancer* (2009) 125:2704–10. doi: 10.1002/ijc.24609
19. Zhu Y, Wang T, Wu J, Huang O, Zhu L, He J, et al. Biomarkers of Insulin and the Insulin-Like Growth Factor Axis in Relation to Breast Cancer Risk in Chinese Women. *Onco Targets Ther* (2020) 13:8027–36. doi: 10.2147/OTT.S258357
20. Gunter MJ, Xie X, Xue X, Kabat GC, Rohan TE, Wassertheil-Smoller S, et al. Breast Cancer Risk in Metabolically Healthy But Overweight Postmenopausal Women. *Cancer Res* (2015) 75:270–4. doi: 10.1158/0008-5472.CAN-14-2317
21. Durward CM, Hartman TJ, Nickols-Richardson SM. All-Cause Mortality Risk of Metabolically Healthy Obese Individuals in NHANES III. *J Obes* (2012) 2012:1–12. doi: 10.1155/2012/460321
22. Wildman RP, Muntner P, Reynolds K, McGinn AP, Rajpathak S, Wylie-Rosett J, et al. The Obese Without Cardiometabolic Risk Factor Clustering and the Normal Weight With Cardiometabolic Risk Factor Clustering: Prevalence and Correlates of 2 Phenotypes Among the US Population (NHANES 1999-2004). *Arch Intern Med* (2008) 168:1617–24. doi: 10.1001/archinte.168.15.1617
23. Stefan N, Kantartzis K, Machann J, Schick F, Thamer C, Rittig K, et al. Identification and Characterization of Metabolically Benign Obesity in Humans. *Arch Intern Med* (2008) 168:1609–16. doi: 10.1001/archinte.168.15.1609
24. Mørch LS, Skovlund CW, Hannaford PC, Iversen L, Fielding S, Lidegaard Ø. Contemporary Hormonal Contraception and the Risk of Breast Cancer. *N Engl J Med* (2017) 377:2228–39. doi: 10.1056/nejmoa1700732
25. Bardaweel SK, Akour AA, Al-Muhaissen S, Alsalamat HA, Ammar K. Oral Contraceptive and Breast Cancer: Do Benefits Outweigh the Risks? A Case - Control Study From Jordan. *BMC Womens Health* (2019) 19:1–7. doi: 10.1186/s12905-019-0770-x
26. Busund M, Bugge NS, Braaten T, Waaseth M, Rylander C, Lund E. Progestin-Only and Combined Oral Contraceptives and Receptor-Defined Premenopausal Breast Cancer Risk: The Norwegian Women and Cancer Study. *Int J Cancer* (2018) 142:2293–302. doi: 10.1002/ijc.31266
27. Samson M, Porter N, Orekoya O, Hebert JR, Adams SA, Bennett CL, et al. Progestin and Breast Cancer Risk: A Systematic Review. *Breast Cancer Res Treat* (2016) 155:3–12. doi: 10.1007/s10549-015-3663-1.Progestin
28. Chen WY, Rosner B, Hankinson SE, Colditz GA, Willett WC. Moderate Alcohol Consumption During Adult Life, Drinking Patterns, and Breast Cancer Risk. *JAMA* (2011) 306:1884–90. doi: 10.1001/jama.2011.1590.Moderate
29. de Menezes RF, Bergmann A, Thuler LCS. Alcohol Consumption and Risk of Cancer: A Systematic Literature Review. *Asian Pacific J Cancer Prev* (2013) 14:4965–72. doi: 10.7314/APJCP.2013.14.9.4965
30. Shield KD, Soerjomataram I, Rehm J. Alcohol Use and Breast Cancer: A Critical Review. *Alcohol Clin Exp Res* (2016) 40:1166–81. doi: 10.1111/acer.13071
31. Dam MK, Hvidtfeldt UA, Tjønneland A, Overvad K, Grønbæk M, Tolstrup JS. Five Year Change in Alcohol Intake and Risk of Breast Cancer and Coronary Heart Disease Among Postmenopausal Women: Prospective Cohort Study. *BMJ* (2016) 353:1–10. doi: 10.1136/bmj.i2314
32. Seitz HK, Pelucchi C, Bagnardi V, La Vecchia C. Epidemiology and Pathophysiology of Alcohol and Breast Cancer: Update 2012. *Alcohol Alcohol* (2012) 47:204–12. doi: 10.1093/alcalc/ags011
33. Zhu J, Jiang X, Niu Z. Alcohol Consumption and Risk of Breast and Ovarian Cancer: A Mendelian Randomization Study. *Cancer Genet* (2020) 245:35–41. doi: 10.1016/j.cancergen.2020.06.001
34. Khalis M, Charbotel B, Chajès V, Rinaldi S, Moskal A, Biessy C, et al. Menstrual and Reproductive Factors and Risk of Breast Cancer: A Case-Control Study in the Fez Region, Morocco. *PloS One* (2018) 13:1–12. doi: 10.1371/journal.pone.0191333
35. Hamajima N, Hirose K, Tajima K, Rohan T, Friedenreich CM, Calle EE, et al. Menarche, Menopause, and Breast Cancer Risk: Individual Participant Meta-Analysis, Including 118 964 Women With Breast Cancer From 117 Epidemiological Studies. *Lancet Oncol* (2012) 13:1141–51. doi: 10.1016/S1470-2045(12)70425-4
36. Suh JS, Yoo KY, Kwon OJ, Yun IJ, Han SH, Noh DY, et al. Menstrual and Reproductive Factors Related to the Risk of Breast Cancer in Korea. *J Korean Med Sci* (1996) 11:501–8. doi: 10.3346/jkms.1996.11.6.501
37. Tan MM, Ho WK, Yoon SY, Mariapun S, Hasan SN, Shin-Chi Lee D, et al. A Case-Control Study of Breast Cancer Risk Factors in 7,663 Women in Malaysia. *PloS One* (2018) 13:1–12. doi: 10.1371/journal.pone.0203469
38. Unar-Munguía M, Torres-Mejía G, Colchero MA, González De Cosío T. Breastfeeding Mode and Risk of Breast Cancer: A Dose-Response Meta-Analysis. *J Hum Lact* (2017) 33:422–34. doi: 10.1177/0890334416683676
39. Zhou Y, Chen J, Li Q, Huang W, Lan H, Jiang H. Association Between Breastfeeding and Breast Cancer Risk: Evidence From a Meta-Analysis. *Breastfeed Med* (2015) 10:175–82. doi: 10.1089/bfm.2014.0141

40. Jones ME, Schoemaker MJ, Wright LB, Ashworth A, Swerdlow AJ. Smoking and Risk of Breast Cancer in the Generations Study Cohort. *Breast Cancer Res* (2017) 19:1–14. doi: 10.1186/s13058-017-0908-4
41. Catsburg C, Miller AB, Rohan TE. Active Cigarette Smoking and Risk of Breast Cancer. *Int J Cancer* (2015) 136:2204–9. doi: 10.1002/ijc.29266

Conflict of Interest: The authors declare that the research was conducted in the absence of any commercial or financial relationships that could be construed as a potential conflict of interest.

Publisher's Note: All claims expressed in this article are solely those of the authors and do not necessarily represent those of their affiliated organizations, or those of the publisher, the editors and the reviewers. Any product that may be evaluated in this article, or claim that may be made by its manufacturer, is not guaranteed or endorsed by the publisher.

frontiers in Endocrinology

ORIGINAL RESEARCH
published: 19 October 2021
doi: 10.3389/fendo.2021.762548

Local-Regional Recurrence of Pheochromocytoma/Paraganglioma: Characteristics, Risk Factors and Outcomes

*Yunying Cui[1], Xiaosen Ma[1], Yinjie Gao[1], Xiaoyan Chang[2], Shi Chen[1], Lin Lu[1] and Anli Tong[1]**

[1] Key Laboratory of Endocrinology, Department of Endocrinology, National Health Commission of the People's Republic of China, Peking Union Medical College Hospital, Peking Union Medical College, Chinese Academy of Medical Sciences, Beijing, China, [2] Department of Pathology, Peking Union Medical College Hospital, Peking Union Medical College, Chinese Academy of Medical Sciences, Beijing, China

OPEN ACCESS

Edited by:
Claire Perks, University of Bristol, United Kingdom

Reviewed by:
Carl Christofer Juhlin, Karolinska Institutet (KI), Sweden
Letizia Canu, University of Florence, Italy

***Correspondence:**
Anli Tong
tonganli@hotmail.com

Specialty section:
This article was submitted to Cancer Endocrinology, a section of the journal Frontiers in Endocrinology

Received: *22 August 2021*
Accepted: *28 September 2021*
Published: *19 October 2021*

Citation:
Cui Y, Ma X, Gao Y, Chang X, Chen S, Lu L and Tong A (2021) Local-Regional Recurrence of Pheochromocytoma/Paraganglioma: Characteristics, Risk Factors and Outcomes. Front. Endocrinol. 12:762548. doi: 10.3389/fendo.2021.762548

Objective: To study the characteristics, risk factors, and outcomes of local-regional recurrence of pheochromocytoma and paraganglioma (PPGL).

Methods: Clinical data of 96 PPGL patients with local-regional recurrence and 112 patients without recurrence were retrospectively analyzed.

Results: Recurrent patients exhibited a median recurrence time of 6.0 (4.0, 9.0) years after resection of the primary tumor. *SDHB* mutation [HR 4.1 (1.7, 9.5), p=0.001), primary tumor size ≥5cm [HR 2.3 (1.1, 4.7), p=0.028], and average Ki-67 count ≥3% in the primary tumor [HR 2.6 (1.4, 4.9), p=0.003] were independent predictors for recurrence of PPGL. Primary tumor sizes ≥5cm [HR 5.1 (1.7, 15.3), p=0.003] and average Ki-67 counts ≥3% of the primary tumor [HR 2.4 (1.1, 5.2), p=0.035] were independent predictors for recurrence of pheochromocytoma, while *SDHB* mutation [HR 4.6 (1.5, 13.9), p=0.007] was a predictor for paraganglioma recurrence. Among recurrent patients, 47% (45/96) had multiple nodules in recurrent sites, and 58% (56/96) had metastases, with 20% (19/96) being implantation metastases. The risk of metastases (42% vs. 25%, p=0.030) and death (15% vs. 8%, p=0.003) was significantly increased in untreated patients after recurrence compared with treated patients.

Conclusion: Long-term follow-up is necessary for all PPGL patients. Risk factors for recurrence of pheochromocytoma and paraganglioma differ, with primary tumor size and average Ki-67 count representing independent predictors for pheochromocytoma patients and *SDHB* mutations predicting paraganglioma recurrence. Although the treatment of recurrence can be difficult, patients should be treated once recurrence is detected as it decreases the risk of metastases and death.

Keywords: recurrence, characteristics, risk factors, outcomes, pheochromocytoma/paraganglioma

INTRODUCTION

Pheochromocytoma (PHEO) and paraganglioma (PGL), together referred to herein as PPGL, are rare neuroendocrine tumors arising from chromaffin cells of the adrenal medulla and extra-adrenal autonomic paraganglia, respectively. The incidence of PPGL is approximately 0.6 cases per 100,000 personyears (1). Once PPGL is diagnosed, surgery is the mainstay of treatment. Long-term follow-up is recommended for patients who have undergone surgery as even tumor-free patients are at risk of recurrence and metastases. Recurrence after resection is reported to occur in 3-16% of patients (2–7) and can be difficult to treat, especially if diagnosis is delayed. So far, few studies focused on the characteristics of local-regional PPGL recurrence, all which were small scale studies (2, 3, 7). The aim of this study was to study the characteristics, risk factors, and outcomes of local-regional recurrence of PPGL. The data presented in this article represents the largest study of PPGL recurrence to date.

METHODS

Patients

We retrospectively studied clinical data of 96 patients diagnosed with local-regional recurrent PPGL in Peking Union Medical College Hospital, China. Local-regional recurrence referred to a reappearance of disease at the original site with or without metastases after complete surgical resection of the original tumor which had been confirmed by negative biochemical and imaging tests. Radiological features of local recurrence were often irregular in shape and closely adhered to surrounding tissues, and may be multiple nodules fused together. The recurrence-free survival was defined as the time elapsed from initial surgery until recurrence. Patients with metastases at onset, failure of complete resection of the primary tumor or new lesions which were not located at the original site of disease were excluded. We also retrospectively analyzed clinical data of 112 patients without recurrence with a median follow-up time of 8.0 (7.0, 9.8) years to study risk factors for recurrence. Patients without local-regional recurrence referred to those patients without recurrence or metastasis after complete resection of the primary tumor during the entire follow-up. Metastases were defined in accordance with the 2017 WHO classification of endocrine tumors. Metastases-free survival was defined as the time elapsed from initial surgery until metastasis. Clinical data, including gender, age at diagnosis, recurrence and metastases, symptoms, blood pressure (BP), primary tumor location, the maximum diameter of primary tumor, tumor secretion function (24-hour urinary catecholamine excretion), primary tumor pathology, genetic characteristics, treatment, and prognosis of recurrence were collected. The study was approved by the Institutional Review Board of Peking Union Medical College Hospital(S-K431). Written informed consent was obtained from all included patients.

Statistical Analysis

All statistical analyses were conducted using Statistical Product and Service Solutions, version 21.0. Categorical data are presented as frequencies and percentages. Normally distributed data are expressed as mean ± standard deviation ($\bar{x} \pm s$). Non-normally distributed data are presented as median and quartile range (25%, 75%). The association between two independent samples with a normal distribution was determined using independent sample T tests, while the association between two independent samples with a non-normal distribution was assessed using Wilcoxon rank sum tests. Associations between two dichotomous parameters were evaluated utilizing the Chi-square test. Kaplan-Meier testing was employed to describe progression-free recurrence. Factors validated in univariate analysis were further tested in multivariate analysis using Cox proportional hazard models. Results are reported as hazard ratios (HR) with 95% confidence intervals. All tests were conducted two-sided, with P values< 0.05 being considered statistically significant.

RESULTS

Patient Characteristics

The 96 PPGL patients with local-regional recurrence included in this study, consisting of 67 PHEO patients and 29 PGL patients, exhibited an average diagnosis age of 32.2 ± 14.9 years, average recurrence age of 39.0 ± 15.4 years, and a median recurrence time of 6.0 (4.0, 9.0) years after resection of the primary tumor (**Figure 1**). Twenty-one percent of patients (20/96) exhibited recurrence between 10 to 20 years after the initial surgery, and one patient exhibited recurrence 23 years after the initial surgery. Among recurrent patients, 47% (45/96) had multiple nodules in recurrent site, and 58% (56/96) had metastases, of which 71% (40/56) were synchronous metastases (recurrence accompanied with metastases) and 34% (19/56) were implantation metastases. At the current follow-up, seven recurrent patients had died. The 112 non-recurrent patients included 75 PHEO patients, 33 PGL patients and 4 patients with both PHEO and PGL. Non-recurrent patients had an average diagnosis age of 40.5 ± 12.9 years and a median follow-up of 8.0 (7.0, 9.8) years. Germline mutations were screened in 182 patients by using next-generation sequencing (including genes *VHL, RET, NF1, SDHA, SDHB, SDHC, SDHD, SDHAF2, MAX, TMEM127, FH and KIF1B*) (8), and Sanger sequencing. 33% (60/182) patients carried pathogenetic mutations in genes including *SDHB, VHL, RET, MAX, SDHD* and *SDHA*.

The Characteristics and Risk Factors of Recurrent PPGL

Compared with non-recurrent patients, recurrent patients exhibited at a younger diagnosis age (32.2 ± 14.9 in recurrent *vs*. 40.5 ± 12.9 in non-recurrent patients, p=0.000). Moreover, among the recurrent patients was a higher proportion of patients with primary tumor sizes ≥ 5cm (78% *vs*. 51% in non-recurrent patients, p=0.000), and a higher proportion of patients with gene mutations (42% *vs*. 26%, p=0.020), in particular in the *SDHB* gene (19% *vs*. 6% p=0.005). The proportion of patients with a primary tumor resection by laparotomy was higher than in the non-recurrent group (54% *vs*. 27% p=0.001) and the pathological

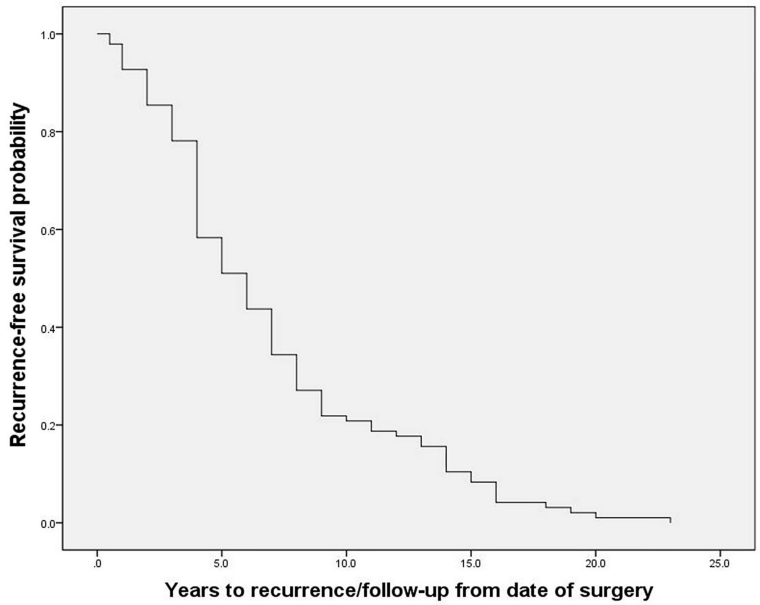

FIGURE 1 | The recurrence-free survival of recurrent patients with pheochromocytoma and paraganglioma.

features of the primary tumors of recurrent patients were more aggressive, manifesting more frequently as capsular invasion (20% *vs*. 5%, p=0.002), with vascular tumor emboli occurring more frequently (14% *vs*. 4%, p=0.018). Moreover, both the average Ki-67 count [4.5% (2%, 8%) *vs*. 1% (<1%, 2%), P=0.001] or the proportion of patients with an average Ki-67 count ≥ 3% (43% *vs*. 17%, p=0.001) were higher in recurrent than in non-recurrent patients. In contrast, there were no statistically significant differences in tumor functionality, levels of serum neuron specific enolase, primary tumor sites, proportion of patients presenting with typical symptoms, or *RET/VHL/SDHD/SDHA/MAX* mutation frequencies between the two groups (**Table 1**).

SDHB mutation [HR 2.1 (1.2, 3.4), p=0.014], primary tumor size ≥5cm [HR 2.0 (1.2, 3.4), p=0.007], capsular invasion of the primary tumor [HR 2.0 (1.1, 3.7), p=0.016], and an average Ki-67 count ≥3% [HR 2.6 (1.5, 4.4), p=0.001] in the primary pathology were risk factors for recurrence in PPGL patients in univariable COX regression analysis (**Table 2**). *SDHB* mutation [HR 4.1 (1.7, 9.5), p=0.001), a primary tumor size ≥5cm [HR 2.3 (1.1, 4.7), p=0.028], and average Ki-67 count ≥3% [HR 2.6 (1.4, 4.9), p=0.003] represented independent predictors for recurrence in multivariate analysis (**Table 2** and **Figure 2**).

The Characteristics and Risk Factors of Recurrent PHEO

The study included 146 PHEO patients, including 67 recurrent patients and 79 non-recurrent patients. Compared with non-recurrent PHEO patients, recurrent patients of PHEO presented at a younger diagnosis age (32.8 ± 15.3 in recurrent *vs*. 39.4 ± 13.3 in non-recurrent patients, p=0.007) and exhibited a larger primary tumor size (6.3 ± 2.3 *vs*. 5.5 ± 2.5 p=0.048). Among patients with recurrence there was a larger proportion of patients with a primary tumor size ≥5cm (75% *vs*. 46%). Both the average Ki-67 count [2% (1%, 5%) *vs*. 1% (1%, 2%), P=0.005] or the proportion of patients with an average Ki-67 count ≥3% (38% *vs*. 13%, p=0.002) were higher in recurrent patients (**Table 3**). Primary tumor sizes ≥5cm [HR 5.1 (1.7,15.3), p=0.003] and an average Ki-67 count ≥3% of primary tumor [HR 2.4 (1.1, 5.2), p=0.035] were independent predictors for recurrence of PHEO in multivariate COX regression analysis (**Figure 3**).

The Characteristics and Risk Factors of Recurrent PGL

The study consisted of 66 PGL patients, including 29 recurrent patients (27 retroperitoneal PGL, 1 bladder PGL, and 1 cardiac PGL) and 37 non-recurrent patients (33 retroperitoneal PGL, 3 bladder PGL, and 1 cardiac PGL). Compared with the non-recurrent PGL patients, recurrent patients of PGL presented at a younger diagnosis age (30.7 ± 13.8 in recurrent patients *vs*. 43.7 ± 11.9 years in non-recurrent patients, p=0.000) and a higher proportion of patients with a *SDHB* mutation (40% *vs*. 9%, p=0.004). The primary tumors pathological characteristics of recurrent patients were more aggressive, manifesting more frequently as capsular invasion (29% *vs*. 6% in non-recurrent patients, p=0.023), vascular tumor emboli happened more frequently (17% *vs*. 0%, p=0.008), and both the average Ki-67 count [3% (1%, 4%) *vs*. 1% (1%, 3%), p=0.021] or the proportion of patients with an average Ki-67 count ≥ 3% was higher in recurrent patients (53% *vs*. 23%, p=0.049) (**Table 4**). *SDHB* mutations [HR 4.6 (1.5, 13.9), p=0.007] were independent predictors for PGL recurrence in multivariate analysis (**Figure 4**).

TABLE 1 | Differences in clinical characteristics between pheochromocytoma/paraganglioma patients with and without recurrence.

Patients	Total patients	Recurrence group	No recurrence group	P value
Male	42% (87/208)	39% (37/96)	45% (50/112)	0.400
Age at diagnosis,y	36 ± 15	32.2 ± 14.9	40.5 ± 12.9	**0.000**
Follow-up time,y	7.0 (4.0,9.3)	6.0 (4.0,9.0)	8.0 (7.0,9.8)	
BPmax, mmHg				
Systolic BP	189 ± 39	196 ± 36	179 ± 51	0.203
Diastolic BP	115 ± 26	120 ± 25	108 ± 32	0.104
Typical symptoms[a]	80% (167/208)	77% (74/96)	72% (81/106)	0.911
Functionality				
NE, ug/24h.	166 (58,386)	220 (73,555)	127 (42,323)	0.099
E, ug/24h.	3.7 (2.7,7.6)	3.8 (2.5,7.4)	3.6 (2.7,10.4)	0.592
DA, ug/24h.	221 (156,319)	252 (166,327)	212 (149,304)	0.244
NSE, ng/mL	14.1 (11.0, 17.2)	14.7 (12.0,18.1)	12.7 (10.6,16.7)	0.801
Primary tumor size	5.8 ± 2.4	6.2 ± 2.3	5.6 ± 2.5	0.078
Tumor size≥5cm	64% (124/195)	78% (69/88)	51% (55/107)	**0.000**
Tumor site				
Left adrenal gland	28% (59/208)	30% (29/96)	27% (30/112)	0.585
Right adrenal gland	28% (60/208)	29% (27/96)	29% (33/112)	0.832
Bilateral adrenal glands	11% (23/208)	10% (10/96)	12% (13/112)	0.785
Paragangliomas	32% (66/208)	30% (29/96)	33% (37/112)	0.662
Multiple primary tumors	15% (31/208)	16% (15/96)	14% (16/112)	0.787
Laparotomy	36% (70/196)	54% (42/87)	27% (28/109)	**0.001**
Gene mutation	33% (60/182)	42% (33/78)	26% (27/104)	**0.020**
SDHB	12% (21/182)	19% (15/78)	6% (6/104)	**0.005**
VHL	6% (11/182)	9% (7/78)	4% (4/104)	0.210
RET	10% (19/182)	8% (6/78)	13% (13/104)	0.336
SDHD	3% (5/182)	3% (2/78)	3% (3/104)	0.896
SDHA	1% (2/182)	1% (1/78)	1% (1/104)	0.837
MAX	1% (2/182)	3% (2/78)	0% (0/104)	0.101
Capsular invasion	11% (21/186)	20% (15/76)	5% (6/110)	**0.002**
Vascular tumor embolus	9% (16/186)	14% (11/76)	4% (5/110)	**0.018**
Ki-67 count	1% (<1%, 3%))	4.5% (2%, 8%)	1% (<1%,2%)	**0.001**
Ki-67 count ≥3%	26% (40/154)	43% (23/54)	17% (17/100)	**0.001**

BP, blood pressure; a, the classic triad of headache, palpitation, and profuse sweating; NE, 24-hour urinary norepinephrine excretion (normal range: 17-41 μg/24 h); E, 24-hour urinary epinephrine excretion (normal range: 1.74-6.42 μg/24 h; DA, 24-hour urinary dopamine excretion (normal range: 121-331 μg/24 h); NSE, neuron specific enolase (normal range: 0-16.3 ng/mL). Bold values indicate significant P values.

The Characteristics of Metastatic Patients

Among recurrent patients, 58% (56/96) had metastases. Most of these patients exhibited multi-system metastases, including 34% (19/56) implantation metastases, 34% (19/56) lung metastases, 30% (17/56) bone metastases, 27% (15/56) lymph node metastases, and 21% (12/56) liver metastases. *SDHB* mutations [HR 3.6 (1.3, 10.2), p=0.017] were an independent predictor for metastases by multivariate analysis (**Figure 5**). The study included 19 patients with implantation metastases. These patients exhibited an average diagnosis age of 37.1 ± 15.3 years, an average recurrence age of 42.8 ± 15.5 years, and a median recurrence time of 5 (4, 7) years. The average primary tumor diameter was 6.1 ± 1.8 cm, and 89% (17/19) were PHEO, of which 37% (7/19) were left adrenal PHEO, 42% (8/19) were right adrenal PHEO, 10% (2/19) were bilateral adrenal PHEO. Ten percent of patient with implantation metastases (2/19) had distant metastases, with one patient exhibiting a liver metastasis and the other exhibiting bone and lymph node metastasis. No independent predictors for implantation metastases were found in multivariate analysis.

Treatment of Recurrence

Thirty-two percent of recurrent patients (31/96) underwent surgery, of which 81% (25/31) patients underwent surgery only. However, 48% (12/25) exhibited recurrence after reoperation with a median time of recurrence of 3 (1.8, 4.2) years (**Figure 6**). Recurrent lesions in 19% (6/25) of these recurrent patients had not been completely

TABLE 2 | Hazard ratios for the risk of recurrence of pheochromocytoma/paraganglioma.

Factors	Univariable			Multivariate		
	HR	95%CI	*P*	HR	95%CI	*P*
SDHB mutation	2.1	1.2, 3.4	**0.014**	4.1	1.7, 9.5	**0.001**
Tumor size≥5cm	2.0	1.2, 3.4	**0.007**	2.3	1.1, 4.7	**0.028**
Capsular invasion	2.0	1.1, 3.7	**0.016**	1.4	0.6, 3.3	0.424
Ki-67 count ≥3%	2.6	1.5, 4.4	**0.001**	2.6	1.4, 4.9	**0.003**

Bold values indicate significant P values.

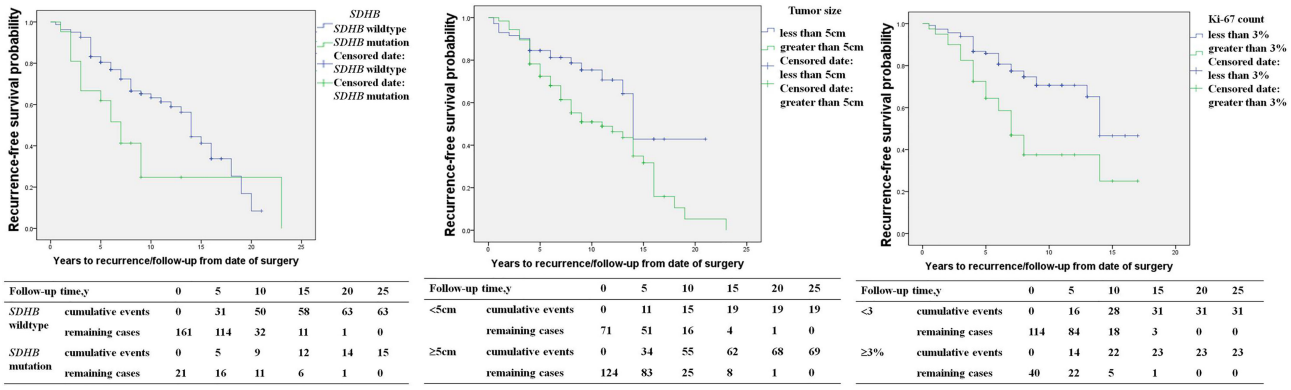

Follow-up time,y		0	5	10	15	20	25
SDHB wildtype	cumulative events	0	31	50	58	63	63
	remaining cases	161	114	32	11	1	0
SDHB mutation	cumulative events	0	5	9	12	14	15
	remaining cases	21	16	11	6	1	0

Follow-up time,y		0	5	10	15	20	25
<5cm	cumulative events	0	11	15	19	19	19
	remaining cases	71	51	16	4	1	0
≥5cm	cumulative events	0	34	55	62	68	69
	remaining cases	124	83	25	8	1	0

Follow-up time,y		0	5	10	15	20	25
<3	cumulative events	0	16	28	31	31	31
	remaining cases	114	84	18	3	0	0
≥3%	cumulative events	0	14	22	23	23	23
	remaining cases	40	22	5	1	0	0

FIGURE 2 | The recurrence-free survival in pheochromocytoma/paraganglioma patients (SDHB mutation patients *versus SDHB* wildtype patients; primary tumor size <5 *versus* primary tumor size ≥5cm; average Ki-67 count <3% *versus* Ki-67 count ≥3%).

resected, and patients therefore received MIBG, radiotherapy, and chemotherapy, amongst other therapeutic options. Forty-three percent of recurrent patients (41/96) could not undergo surgery. Of these patients, 78% (32/41) patients received MIBG treatment, 12% (5/41) patients underwent chemotherapy/targeted therapy, and 10% (4/41) patients underwent radiotherapy. Fourteen percent of recurrent patients (13/96) were recommended for surgery, but refused and did not receive any other treatment. Of these patients, five developed metastases during the observation period, one patient could not undergo surgery during the observation peried as the lesion progressed and invaded surrounding organs, and 2 patients died of metastases. Compared with the treated patients, the risk of metastases and death was significantly increased in the untreated patients (42% *vs.* 25%, p=0.030, and 15% *vs.* 8%, p=0.003, respectively). The treatment records of the remaining 11% (11/96) recurrent patients were unclear due to lost to follow-up after the diagnosis of recurrence.

DISCUSSION

Recurrence of PPGL after resection occurred in 13.3% patients who were followed up for more than five years after tumor resection in our center (unpublished data). A recent systematic review showed that the overall rate of recurrent PPGL was 0.98 events/100 person-years, which suggested the risk of recurrence after complete resection was previously underestimated (9). In a meta-analysis of 13 studies, the mean time to recurrence was approximately 4 years (0.5-12) (6). In our study, recurrent patients exhibited a median recurrence time of 6.0 (4.0, 9.0) years after resection of the primary tumor, which is longer than previous reports (2, 6). Our data suggest that the follow-up of all patients after tumor resection should be at least 10-20 years, as recurrences may occur after a prolonged time after initial treatment.

In our study, we found *SDHB* mutation, primary tumor sizes ≥5cm, and average Ki-67 counts ≥3% in the primary

TABLE 3 | Differences in clinical characteristics between pheochromocytoma patients with and without recurrence.

Patients	Total patients	Recurrence group	No recurrence group	P value
Male	43% (63/146)	39% (26/67)	47% (37/79)	0.329
Age at diagnosis, y	36 ± 15.0	32.8 ± 15.3	39.4 ± 13.3	**0.007**
Follow-up time, y	7.0 (5.0,9.0)	6.0 (4.0,9.0)	8.0 (7.0,9.0)	**0.000**
Primary tumor size	5.8 ± 2.4	6.3 ± 2.3	5.5 ± 2.5	**0.048**
Tumor size≥5cm	64% (86/135)	75% (50/67)	46% (36/79)	**0.000**
Gene mutation	33% (42/126)	39% (21/53)	29% (21/73)	0.067
SDHB	6% (8/126)	9% (5/53)	4% (3/73)	0.226
VHL	8% (10/126)	13% (7/53)	4% (3/73)	0.062
RET	13% (19/126)	11% (6/53)	18% (13/73)	0.315
MAX	2% (2/126)	4% (2/53)	0% (0/73)	0.090
Tumor site				
Left adrenal gland	41% (59/146)	45% (29/67)	38% (30/79)	0.515
Right adrenal gland	40% (60/146)	40% (27/67)	41% (32/79)	0.857
Bilateral adrenal glands	16% (23/146)	15% (10/67)	16% (13/79)	0.800
Multiple primary tumors	18% (27/146)	16% (11/67)	20% (16/79)	0.552
Laparotomy	25% (34/136)	40% (24/60)	13% (10/76)	**0.000**
Capsular invasion	9% (12/130)	15% (8/52)	5% (4/78)	0.064
Vascular tumor embolus	8% (11/130)	12% (6/52)	6% (5/78)	0.303
Ki-67 count	1% (1%,2%))	2% (1%, 5%)	1% (1%,2%)	**0.005**
Ki-67 count ≥3%	22% (24/108)	38% (15/39)	13% (9/69)	**0.002**

Bold values indicate significant P values.

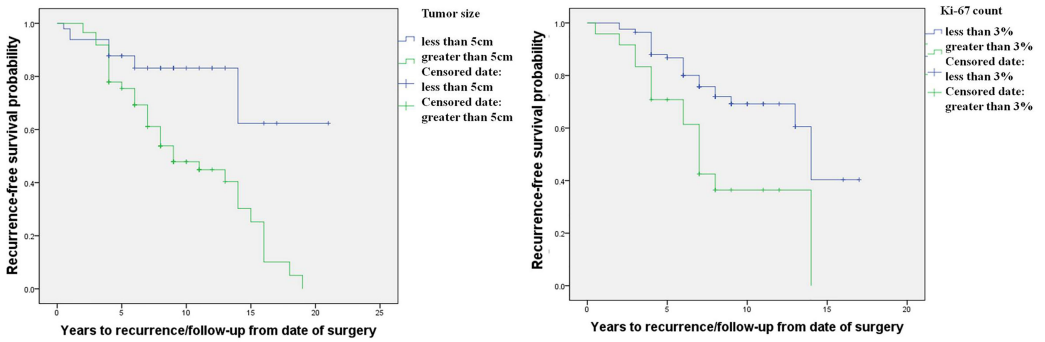

Follow-up time,y		0	5	10	15	20	25
<5cm	cumulative events	0	6	8	9	9	9
	remaining cases	49	38	10	3	1	0
≥5cm	cumulative events	0	21	40	45	50	50
	remaining cases	86	61	16	5	0	0

Follow-up time,y		0	5	10	15	20	25
<3	cumulative events	0	11	22	24	24	24
	remaining cases	83	65	12	2	1	0
≥3%	cumulative events	0	7	14	15	15	15
	remaining cases	24	15	3	0	0	0

FIGURE 3 | The recurrence-free survival (primary tumor size <5 *versus* primary tumor size ≥5cm, average Ki-67 count <3% *versus* Ki-67 count ≥3%) in pheochromocytoma patients.

tumor were independent predictors of recurrence. The results in our study were similar to previous reports (3, 7, 10–13). Moreover, we separately studied the predictors of PHEO and PGL, and found that the risk factors for recurrence of PHEO and PGL were different. The risk of recurrence was 5.1- and 2.4-fold higher in PHEO patients with primary tumor sizes≥ 5cm and average Ki-67 counts ≥3%, respectively. *SDHB* mutations were predictors for recurrence in PGL patients and not for PHEO, with the risk of recurrence being 4.6 fold higher in PGL patients with *SDHB* mutation than those without. Recent studies have shown that higher Pheochromocytoma of the Adrenal Gland Scaled Score (PASS) and Grading system for Adrenal Pheochromocytoma and Paraganglioma(GAPP) score were significantly associated with recurrence, and it was, respectively, 1.2- and 3.4-fold higher in patients with higher PASS and GAPP scores (13, 14).

In our study, 19 patients unfortunately exhibited implantation metastases which are considered to be related to tumor cells scattered in peritoneal cavity during surgical resection (15). The initial surgery of most patients was not performed in our hospital. Laparoscopic surgery may be more challenging if the tumor is large since these tumors more likely to be broken and tumor cells scattered when manipulated. The guideline recommends open resection for large (>6 cm) PHEO and PGL to ensure complete tumor resection, preventing tumor rupture and avoiding local recurrence (16). However, several studies have suggested that larger PPGL may be amenable to laparoscopy with safety levels similar to those for smaller tumors (4, 17). Here, we did not find that laparoscopic surgery can increase the risk of recurrence. The key to preventing implantation metastases is an endocrine surgeon with expertise in laparoscopic techniques and operating on PPGL. Furthermore, in cases of tumor rupture during surgical resection, careful follow-up is mandatory.

Recurrence is difficult to treat especially if diagnosis is delayed. Unfortunately, surgery was not an option in 43% of recurrent patients included in this study. Several reasons can lead to difficulty of recurrence treatment, for instance, 47% recurrent patients had multiple nodules in recurrent site in our study,

TABLE 4 | Clinical characteristics of paraganglioma with and without recurrence.

Patients	Total patients	Recurrence group	No recurrence group	P value
Male	39% (26/66)	38% (11/29)	19% (15/37)	0.830
Age at diagnosis, y	37 ± 14	30.7 ± 13.8	43.7 ± 11.9	**0.000**
Follow-up time, y	7.0 (4.0,9.3)	5 (2.5,10.0)	7.0 (5.5,9.5)	
Primary tumor size	5.8 ± 2.3	5.8 ± 2.4	5.6 ± 2.3	0.654
Tumor size≥5cm	61% (39/64)	66% (19/29)	57% (20/35)	0.494
Gene mutation	30% (18/60)	44% (11/25)	23% (8/35)	0.082
SDHB	22% (13/60)	40% (10/25)	9% (3/35)	**0.004**
Multiple primary tumors	12% (8/66)	14% (4/29)	11% (4/37)	0.713
Laparotomy	55% (35/64)	67% (18/27)	46% (17/37)	0.100
Capsular invasion	15% (9/60)	29% (7/24)	6% (2/36)	**0.023**
Vascular tumor embolus	8% (5/60)	17% (5/29)	0% (0/36)	**0.008**
Ki-67 count	2% (1%, 3%)	3% (1%, 4%)	1% (1%, 3%)	**0.021**
Ki-67 count ≥3%	32% (16/50)	53% (8/15)	23% (8/35)	**0.049**

Bold values indicate significant P values.

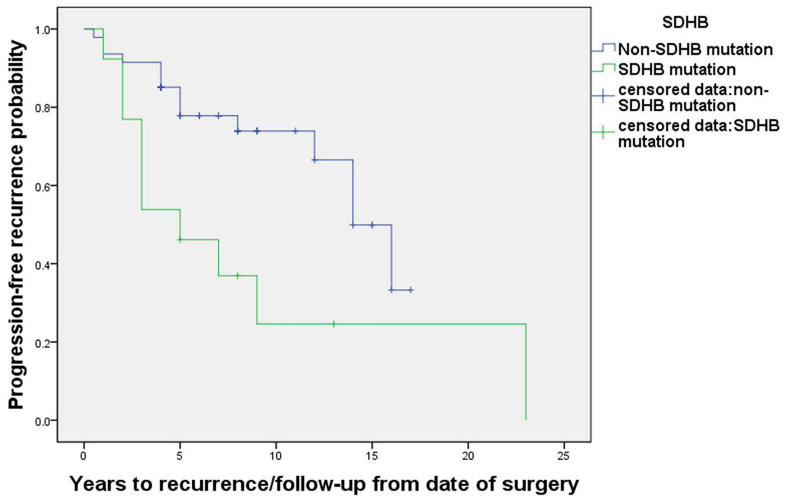

Follow-up time,y		0	5	10	15	20	25
SDHB wildtype	cumulative events	0	10	11	14	15	15
	remaining cases	47	42	11	4	0	0
SDHB mutation	cumulative events	0	7	9	9	10	10
	remaining cases	13	5	2	1	0	0

FIGURE 4 | The recurrence-free survival (*SDHB* mutation patients *versus SDHB* wildtype patients) in paraganglioma patients.

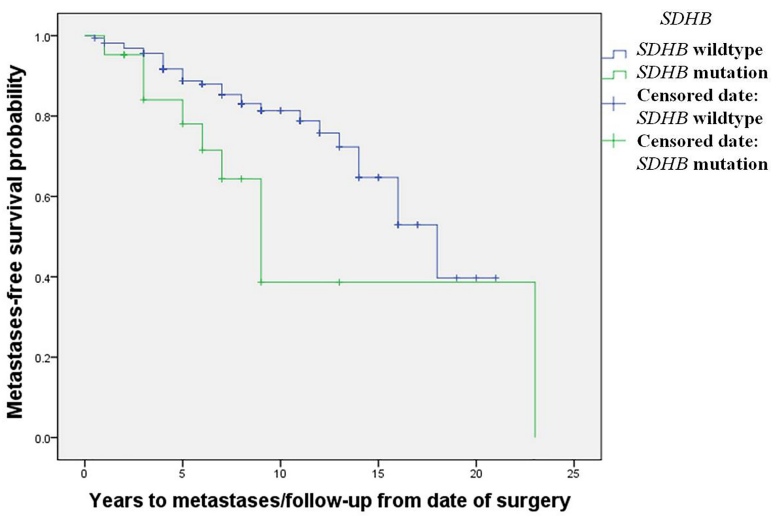

Follow-up time,y		0	5	10	15	20	25
SDHB wildtype	cumulative events	0	17	24	29	32	32
	remaining cases	161	114	32	11	1	0
SDHB mutation	cumulative events	0	2	5	6	8	9
	remaining cases	21	16	11	6	1	0

FIGURE 5 | Progression-free metastases (*SDHB* mutation patients *versus SDHB* wildtype patients) in PPGL patients.

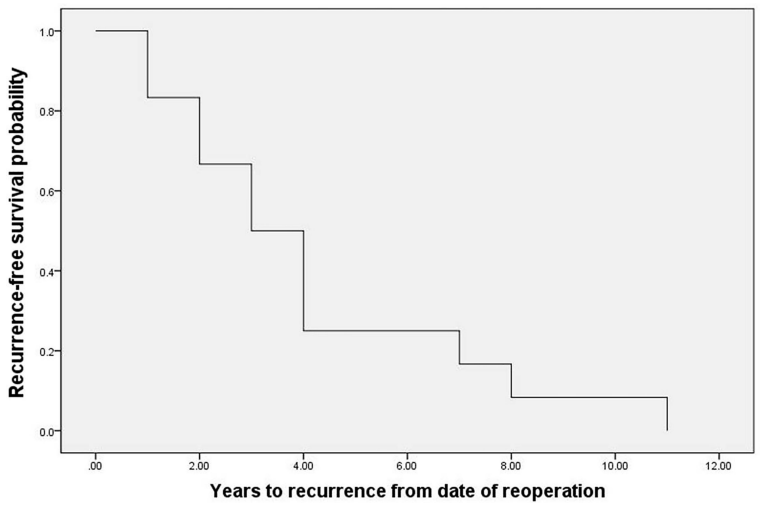

FIGURE 6 | The recurrence-free survival probability after reoperations.

recurrent patients were often accompanied by metastases, 58% had metastases in our study (7). Although treatment of recurrences is challenging, patients should be treated as soon as possible after detection of recurrence as we found that treatment significantly decreased the risk of metastases and death compared to untreated patients.

There were some limitations in our study. Firstly, local-regional recurrence referred to a reappearance of disease at the original site after complete surgical resection which had been confirmed by negative biochemical and imaging tests. However we cannot completely exclude the situation that a separate, metachronous PPGL arising in the same location. Another weakness of our study was the lack of PASS/GAPP scores which may be beneficial to predicting tumor recurrences.

CONCLUSION

Long-term follow-up in all PPGL patients is necessary. PHEO patients with primary tumor sizes ≥5cm, average Ki-67 counts ≥3%, and PGL patients with *SDHB* mutation exhibited an elevated risk of recurrence. Recurrence is difficult to treat as it is often accompanied by multiple nodes in recurrent sites, distant metastases, and implantation metastases, however it is recommended as it can reduce the risk of further metastases and death.

DATA AVAILABILITY STATEMENT

The original contributions presented in the study are included in the article/supplementary material. Further inquiries can be directed to the corresponding author.

ETHICS STATEMENT

The study was approved by the Institutional Review Board of Peking Union Medical College Hospital(S-K431). Written informed consent was obtained from the patients included.

AUTHOR CONTRIBUTIONS

YC performed the study and drafted the manuscript. AT contributed to the concept and design for the study. YG, XM, SC, and LL contributed to the manuscript preparation. XC prepared histopathological results. All authors contributed to the article and approved the submitted version.

FUNDING

This work was supported by CAMS Innovation Fund for Medical Sciences (CIFMS) of China (Grant No. 2021-I2M-C&T-B-002, and 2017-I2M-1-001), and National Natural Science Foundation of China (Grant No. 81770427, and 82070822).

ACKNOWLEDGMENTS

The authors gratefully acknowledge the invaluable support of the members of the Department of Endocrinology and Urology, Peking Union Medical College Hospital, and, especially, Professor Zhengpei Zeng and Hanzhong Li.

REFERENCES

1. Berends A, Buitenwerf E, de Krijger RR, Veeger N, van der Horst-Schrivers A, Links TP, et al. Incidence of Pheochromocytoma and Sympathetic Paraganglioma in the Netherlands: A Nationwide Study and Systematic Review. *Eur J Intern Med* (2018) 51:68–73. doi: 10.1016/j.ejim.2018.01.015
2. Johnston PC, Mullan KR, Atkinson AB, Eatock FC, Wallace H, Gray M, et al. Recurrence of Phaeochromocytoma and Abdominal Paraganglioma After Initial Surgical Intervention. *Ulster Med J* (2015) 84(2):102–6.
3. Slycke SV, Caiazzo R, Pigny P, Cardot-Bauters C, Arnalsteen L, D'Herbomez M, et al. Local-Regional Recurrence of Sporadic or Syndromic Abdominal Extra-Adrenal Paraganglioma: Incidence, Characteristics, and Outcome. *Surgery* (2009) 146(6):986–92. doi: 10.1016/j.surg.2009.10.055
4. Shen WT, Grogan R, Vriens M, Clark OH, Duh Q. One Hundred Two Patients With Pheochromocytoma Treated at a Single Institution Since the Introduction of Laparoscopic Adrenalectomy. *Arch Surg (Chicago 1960)* (2010) 145(9):893. doi: 10.1001/archsurg.2010.159
5. Amar L, Fassnacht M, Gimenez-Roqueplo A, Januszewicz A, Prejbisz A, Timmers H, et al. Long-Term Postoperative Follow-Up in Patients With Apparently Benign Pheochromocytoma and Paraganglioma. *Horm Metab Res* (2012) 44(5):385. doi: 10.1055/s-0031-1301339
6. Holscher I, van den Berg TJ, Dreijerink KMA, Engelsman AF, Nieveen Van Dijkum EJM, et al. Recurrence Rate of Sporadic Pheochromocytomas After Curative Adrenalectomy: A Systematic Review and Meta-Analysis. *J Clin Endocrinol Metab* (2021) 106(2):588–97. doi: 10.1210/clinem/dgaa794
7. Amar L, Servais A, Gimenez-Roqueplo A, Zinzindohoue F, Chatellier G, Plouin P. Year of Diagnosis, Features at Presentation, and Risk of Recurrence in Patients With Pheochromocytoma or Secreting Paraganglioma. *J Clin Endocrinol Metab* (2005) 90(4):2110–6. doi: 10.1210/jc.2004-1398
8. Ma X, Li M, Tong A, Wang F, Cui YY, Li YX, et al. Genetic and Clinical Profiles of Pheochromocytoma and Paraganglioma: A Single Center Study. *Front Endocrinol (Lausanne)* (2020) 11:574662. doi: 10.3389/fendo.2020.574662
9. Amar L, Lussey-Lepoutre C, Lenders JWM, Djadi-Prat J, Plouin P, Steichen O. Management of Endocrine Disease: Recurrence or New Tumors After Complete Resection of Pheochromocytomas and Paragangliomas: A Systematic Review and Meta-Analysis. *Eur J Endocrinol* (2016) 175(4):R135–45. doi: 10.1530/EJE-16-0189
10. Moog S, Castinetti F, DoCao C, Amar L, Hadoux J, Lussey-Lepoutre C, et al. Recurrence-Free Survival Analysis in Locally Advanced Pheochromocytoma: First Appraisal. *J Clin Endocrinol Metab* (2021) 106(9):2726–37. doi: 10.1210/clinem/dgab202
11. Press D, Akyuz M, Dural C, Aliyev S, Monteiro R, Mino J, et al. Predictors of Recurrence in Pheochromocytoma. *Surgery* (2014) 156(6):1523–8. doi: 10.1016/j.surg.2014.08.044
12. Gimenez-Roqueplo A, Favier J, Rustin P, Rieubland C, Crespin M, Corvol P, et al. Mutations in the SDHB Gene are Associated With Extra-Adrenal and/or Malignant Phaeochromocytomas. *Cancer Res (Chicago Ill)* (2003) 63(17):5615–21.
13. Parasiliti-Caprino M, Lucatello B, Lopez C, Burrello J, Maletta F, Mistrangelo M, et al. Predictors of Recurrence of Pheochromocytoma and Paraganglioma: A Multicenter Study in Piedmont, Italy. *Hypertens Res* (2020) 43(6):500–10. doi: 10.1038/s41440-019-0339-y
14. Wachtel H, Hutchens T, Baraban E, Schwartz LE, Montone K, Baloch Z, et al. Predicting Metastatic Potential in Pheochromocytoma and Paraganglioma: A Comparison of PASS and GAPP Scoring Systems. *J Clin Endocrinol Metab* (2020) 105(12):4661–70. doi: 10.1210/clinem/dgaa608
15. Rafat C, Zinzindohoue F, Hernigou A, Hignette C, Favier J, Tenenbaum F, et al. Peritoneal Implantation of Pheochromocytoma Following Tumor Capsule Rupture During Surgery. *J Clin Endocrinol Metab* (2014) 99(12):E2681–5. doi: 10.1210/jc.2014-1975
16. Lenders JW, Duh QY, Eisenhofer G, Gimenez-Roqueplo AP, Grebe SK, Murad MH, et al. Pheochromocytoma and Paraganglioma: An Endocrine Society Clinical Practice Guideline. *J Clin Endocrinol Metab* (2014) 99(6):1915–42. doi: 10.1210/jc.2014-1498
17. Walz MK, Alesina PF, Wenger FA, Koch JA, Neumann HP, Petersenn S, et al. Laparoscopic and Retroperitoneoscopic Treatment of Pheochromocytomas and Retroperitoneal Paragangliomas: Results of 161 Tumors in 126 Patients. *World J Surg* (2006) 30(5):899–908. doi: 10.1007/s00268-005-0373-6

Conflict of Interest: The authors declare that the research was conducted in the absence of any commercial or financial relationships that could be construed as a potential conflict of interest.

frontiers in Endocrinology

REVIEW
published: 11 February 2022
doi: 10.3389/fendo.2022.840787

New Insights and Emerging Therapeutic Approaches in Prostate Cancer

Fabrizio Licitra, Pia Giovannelli, Marzia Di Donato, Alessandra Monaco, Giovanni Galasso, Antimo Migliaccio and Gabriella Castoria**

Department of Precision Medicine, University of Campania 'L. Vanvitelli', Naples, Italy

Prostate cancer is the second most frequently diagnosed cancer in men and several therapeutic approaches are currently available for patient's care. Although the androgen receptor status represents a good predictor of response to androgen deprivation therapy, prostate cancer frequently becomes resistant to this approach and spreads. The molecular mechanisms that contribute to progression and drug-resistance of this cancer remain still debated. However, few therapeutic options are available for patient's management, at this stage. Recent years have seen a great expansion of the studies concerning the role of stromal-epithelial interactions and tumor microenvironment in prostate cancer progression. The findings so far collected have provided new insights into diagnostic and clinical management of prostate cancer patients. Further, new fascinating aspects concerning the intersection of the androgen receptor with survival factors as well as calcium channels have been reported in cultured prostate cancer cells and mouse models. The results of these researches have opened the way for a better understanding of the basic mechanisms involved in prostate cancer invasion and drug-resistance. They have also significantly expanded the list of new biomarkers and druggable targets in prostate cancer. The primary aim of this manuscript is to provide an update of these issues, together with their translational aspects. Exploiting the power of novel promising therapeutics would increase the success rate in the diagnostic path and clinical management of patients with advanced disease.

Keywords: nerve growth factor signalling, calcium influx, cancer-associated fibroblasts, prostate cancer, new drugs

OPEN ACCESS

Edited by:
Claire Perks,
University of Bristol, United Kingdom

Reviewed by:
Marcello Maggiolini,
University of Calabria, Italy
Silvère Baron,
U1103 Génétique Reproduction et Développement (GReD)(INSERM), France

****Correspondence:***
Gabriella Castoria
gabriella.castoria@unicampania.it
Antimo Migliaccio
antimo.migliaccio@unicampania.it

Specialty section:
This article was submitted to Cancer Endocrinology, a section of the journal Frontiers in Endocrinology

Received: *21 December 2021*
Accepted: *20 January 2022*
Published: *11 February 2022*

Citation:
Licitra F, Giovannelli P, Di Donato M, Monaco A, Galasso G, Migliaccio A and Castoria G (2022) New Insights and Emerging Therapeutic Approaches in Prostate Cancer. Front. Endocrinol. 13:840787. doi: 10.3389/fendo.2022.840787

Abbreviations: α-SMA, α-smooth muscle actin; ADT, androgen deprivation therapy; AR, androgen receptor; B2R, bradykinin 2 receptor; BDNF, brain-derived neurotrophic factor; BPH, benign prostatic hyperplasia; CAF, cancer associated fibroblast; CHRM4, cholinergic receptor muscarinic 4; CRPC, castration resistant prostate cancer; CTD, C-terminal domain; EMT, epithelial-to-mesenchymal transition; FAP, fibroblast activating protein; FlnA, filamin A; HER3, Receptor tyrosine-protein kinase erbB-3; HIF-1α, hypoxia-induced factor 1 α; IFN-γ, interferon-γ; IHC, immunohistochemistry; M-CSF, macrophage colony stimulating factor; MAPK, mitogen-activated protein kinase; MHR, melastatin homology region; MMP, matrix metalloproteinase; NEPC, neuroendocrine prostate cancer; NGF, nerve growth factor; NGFR, nerve growth factor receptor; NGS, next generation sequencing; NRG1, neuregulin-1; NT, neurotrophin; PC, prostate cancer; PGC1α, peroxisome proliferator-activated receptor gamma coactivator 1-α; PI3-K, phosphatidylinositol 3-kinase; PIN, prostatic intraepithelial neoplasia; PLCγ, phospholipase C γ; PSA, prostate specific antigen; RTK, receptor tyrosine-kinase; SIRT1, sirtuin 1; TGF-β, transforming growth factor-β; TMD, transmembrane domain; TME, tumor microenvironment; TrkA/B/C, tropomyosin receptor kinase A/B/C; TRPM8, transient receptor potential melastatin-8; VEGF-A, vascular endothelial growth factor-A.

INTRODUCTION

Prostate cancer (PC) still remains the second most commonly diagnosed neoplasia in men (1). Depending on the availability of specific screenings, including the prostate-specific antigen (PSA) assay, the lifestyle and environmental factors, PC incidence varies among men of different ethnicities (2). Despite the recent advances in early diagnosis and detection, the disease's onset is often asymptomatic, accounting for numerous late diagnoses. Additionally, the prognosis can be favorable at early stage's disease, given the progresses of advanced radiotherapy technology (3, 4 and refs therein). However, PC still represents the second leading cause of cancer-related death in men, albeit its mortality rate is relatively low (almost 20-30%), as compared with other solid cancers (5). New therapeutic options are needed for patients with advanced disease.

PC pathogenesis and progression depend on androgen/androgen-receptor (AR) circuit. As such, the mainstream pharmacological approach relies on the androgen deprivation therapy (ADT), which shows a satisfactory response in a significant number of cases. However, many PC relapse and progress towards a more aggressive phenotype, often characterized by ADT insensitivity and androgen-independence. Such phenotype, also called castrate-resistant prostate cancer (CRPC), may be metastatic or not (6, 7). Additionally, a subset of PC might further differentiate into neuroendocrine phenotype, also called neuroendocrine PCs (NEPCs). These cancers lose AR signaling, become more aggressive and exhibit androgen-independence in a quite scantly known molecular landscape (8). Among the various factors elsewhere excellently discussed (9–11), PC progression is often characterized by abnormal AR-mediated signaling activation or AR variants (12), which might help the tumor to achieve ADT unresponsiveness. However, emerging findings have identified unexpected drivers of PC progression. Some of them are implied in the survival response elicited by the receptor tyrosine-kinase (RTK) signaling, such as the nerve growth factor (NGF) and its high-affinity receptor, tropomyosin-related kinase receptor A (TrkA; 13). Recent papers, including ours, have investigated this issue in PC (14–18). Other findings have identified the transient receptor potential melastatin-8 (TRPM-8) as a playmaker in PC (19–21 and refs therein), likely because of its role in connecting the androgen endocrine system with intracellular calcium levels (22). At last, the role of cancer-associated fibroblasts (CAFs) in PC progression is undeniable (23). The finding that CAFs harbor significant amounts of AR has opened new ways for a better understanding of the role of tumor microenvironment in PC progression and more tailored approaches of this cancer (23–29).

In search for a link between these three apparently unlinked items, it might be argued that NGF and other neurotrophins secreted from PC cells or CAFs sustain tumor survival and aggressiveness through a paracrine loop, as it occurs in breast cancer (30–33). However, NGF and calcium signaling might intersect each other in PC, as it occurs in neurons (34) or Schwann cells (35). In this manuscript, we will discuss these emerging findings and their connections. The potential application of these data in diagnostic and therapeutic guidance of PC will be outlined.

NERVE GROWTH FACTOR AND ITS RECEPTORS IN PROSTATE CANCER

The action of neurotrophins is mediated by the binding to membrane receptors, mainly the neurotrophin receptor p75NTR (also called NGF receptor; NGFR) and the neurotrophin tyrosine kinase receptor (Trk) family, which consists of three members, TrkA, B and C, with a variable affinity for the four identified neurotrophins (NGF; brain-derived neurotrophic factor, BDNF; neurotrophin 3 and 4, NT3 and NT4; **Figure 1**). Their dependent signaling mediates, indeed, the activation of several downstream effectors, such as MAPK, PI3-K, PLCγ as well as the small GTP binding proteins that strongly impact differentiation and survival, cytoskeletal remodeling, receptor cross-talk and ion channels in various cell types, other than neurons (13). Beyond their role in neuronal cells, neurotrophic factors are emerging as potential drivers of cancer progression, and therapies specifically affecting the neurotrophin-mediated signaling might hold value for innovative treatments of human cancers (36, 37).

PCs release NGF and express the neurotrophin receptors, which undergo significant changes during PC progression, as primary PC express both TrkA and NGFR, while losing NGFR during the disease progression. This behavior has been linked with PC onset and androgen-resistance development (38). At last, NGFR is almost completely absent in metastatic PC, making the TrkA receptor the lead driver of NGF signaling in aggressive PC (16). Previous findings have reported that NGF triggers mitogenesis and promotes PSA release through TrkA activation in LNCaP cells, and this effect is additive to that exerted by androgens (39). As such, it was thereafter found that the tyrosine kinase inhibitor, CEP-701 blocks the TrkA-mediated events, thereby reducing invasiveness of PC cultured cells (40). Derangements of NGF and its dependent signaling can be often detected in PC (41), where the neurotrophin might be released by PC cells and/or the surrounding stromal cells. As such, a paracrine loop between the two counterparts occurs (42). We recently reported that a reciprocal cross-talk between AR and TrkA fosters the mitogenesis or motility of LNCaP cells in response to NGF or androgens (15). The obvious impact of these findings is that combinatorial treatment with antiandrogens and TrkA inhibitors might be explored in PC patients. Consistent with the hypothesis that TrkA is involved in PC motility and spreading, it has been shown that non-proteolytic ubiquitination of TrkA by the ubiquitin-ligase TRAF4 increases the kinase activity of the receptor and mediates PC spreading. The finding that TRAF4 is overexpressed in advanced PC specimens strongly supports the involvement of this mechanism in PC aggressiveness (14). The role of NGF in PC malignancy has been further highlighted by the finding that NGF-elicited activation of TrkA increases mitogenesis, epithelial-mesenchyme transition (EMT) and

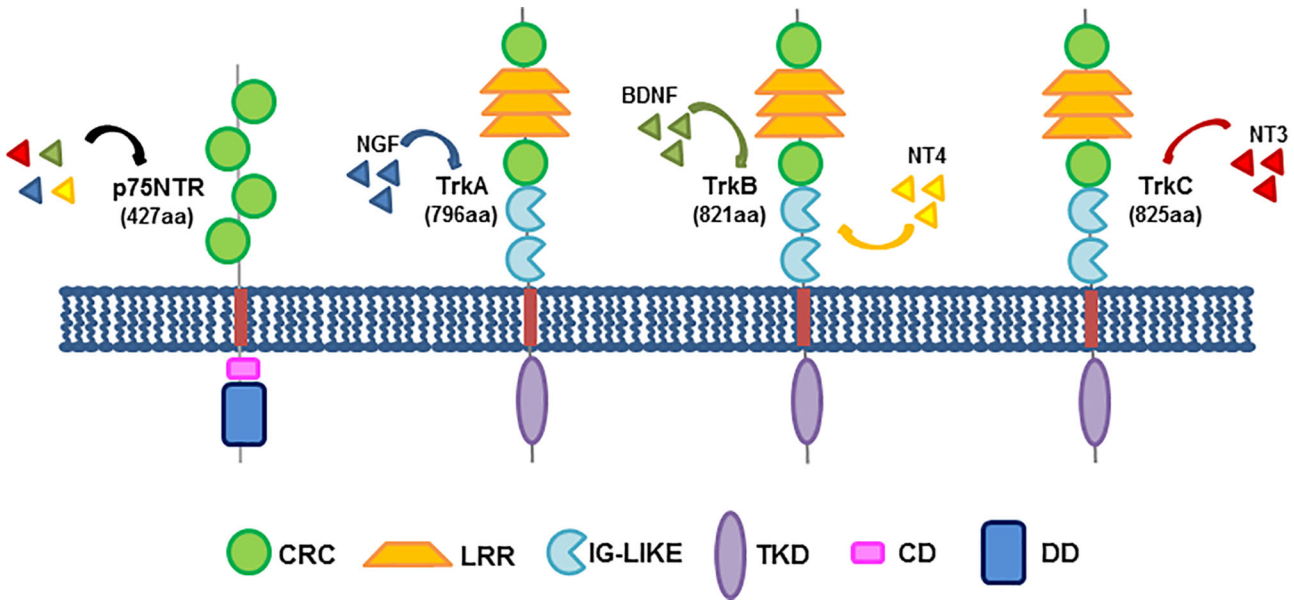

FIGURE 1 | Neurotrophin receptors and their structure. The three members of the Trk family share a common structure, encompassing a cysteine-rich cluster (CRC), three leucine-rich repeats (LRR), a second cysteine cluster and two immunoglobulin-like domains (IG-Like), responsible for ligand binding, in their extracellular domains. A transmembrane domain (TMD) anchors the receptor to the plasma membrane. The intracellular region consists of the tyrosine kinase domain (TKD). On the left, the low-affinity neurotrophin receptor, p75NTR (called NGFR) is also depicted. It consists of four cysteine-rich clusters in the extracellular domain, a transmembrane region and an intracellular region exhibiting a chopper domain (CD) and a death domain (DD). Shown beside each Trk member is reported the corresponding high-affinity binding neurotrophin. p75NTR might bind all neurotrophins at low affinity. The indicated domains are colored as follows: CRC, green; LRR, yellow; IG-Like, light blue; TMD, red; TKD, purple; CD, pink; DD, dark blue.

invasion of various CRPC-derived cells through activation of the downstream Ras- and PI3-K-dependent signaling cascades. Chemical inhibitors of TrkA or siRNA approaches have definitely indicated a role for this receptor in NGF-elicited responses of CRPC-derived cells or spheroids (16). In addition to suggesting the clinical benefit from TrkA inhibitor usage in PC patients (37), the findings so far presented point to the role of NGF axis in PC survival. This circuit might substitute the androgens in controlling PC cell survival and lead to disease's progression towards the CRPC stage. As before stated, similar findings have been reported in various 'hormone-dependent' cancers, including breast cancers. Thus NGF might intersect the steroid endocrine system in various solid cancers.

Beyond the well described mechanism(s) responsible for PC progression and drug-resistance, neuroendocrine differentiation of PC is recently emerging as a process by which a subset of CRPC escapes the ADT. These tumors acquire some signatures (low or absent AR signaling, Rb and p53 loss, amplification of Myc-N and epigenetic changes) which lead to a highly aggressive phenotype and patient's death within 2 years (8 and therein refs). To date, no therapies are available for NEPC patients. Therefore, the identification of NEPC drivers represents a major challenge. Some years ago, it was shown that PC cells overexpress Myc-N after a prolonged ADT. The oncogene activation correlated with a low or absent AR expression. It was proposed that this feature leads to development of undifferentiated, invasive PC cells that exhibit characteristics similar to those of human NEPC (43). Subsequent reports have confirmed that a small fraction of PCs differentiate into NEPCs upon protracted ADT. These cancers lose the AR-dependent signaling and progress towards an aggressive phenotype, whose molecular drivers are still under investigation (44). Simultaneously, it was shown that ZBTB46 transcription factor might act as one of these key players. It induces NGF expression upon a prolonged ADT treatment in PC patients. Mechanistically, NGF interacts with the peripheral nerve cholinergic receptor muscarinic 4 (CHRM4) to trigger PC cell differentiation by AKT and Myc-N activation. These events might finally lead to the development of neuroendocrine phenotype and ADT-resistance (18). In addition to identifying ZBTB46 as a signature for NEPC, these findings significantly contribute to the understanding of unwanted effects caused by prolonged ADT in PC patients.

Although the role of NGF and its dependent signaling in PC pathogenesis and progression is well established, genetic aberrations of NGF receptors have not been so far reported in PC (45). Thus, derangements of NGF-signaling caused by deregulation of the NGF-RTK or excessive production of NGF might be involved in PC progression. An increased expression and/or release of NGF was firstly detected in human PC specimens and PC-derived cell lines (46) and subsequently confirmed by several labs. Neurotrophic factors can be currently assayed in urine samples from PC patients (47), thus indicating a reliable, non-invasive approach for detection of novel PC biomarkers in body fluids. Extension of these

findings to a large cohort of PC patients might expand the current strategies for patient's stratification. By contrast, RTK derangements cannot be easily detected. Nevertheless, from the findings previously discussed, it appears that some biomarkers, such as TRAF4 or ZBTB46, emerge as predictors of TrkA activation. Their overexpression correlates with aberrant TrkA activation and metastatic events or would predict, as in the case of ZBTB46, the increase in NGF levels with the subsequent signaling derangement in PC patients. These findings, together with the well-established role of neurotrophins for autonomic innervation of PC into the tumor microenvironment, indicate that NGF and their receptors are clinically actionable in PC (48 and therein refs). On the basis of preclinical findings (40, 49), the RTK inhibitor, lestaurtinib (CEP-701) entered clinical trials (NCT00081601) in PC patients, with promising data from phase I studies. However, the drug failed to show a significant PSA response in patients with localized hormone-refractory PC (50). Subsequently, another small-molecule RTK inhibitor, cabozantinib was approved for the treatment of metastatic PC. Noteworthy, these and other currently used inhibitors, such as NCT02219711, block a broad range of RTK and frequently induce side-effects, mainly the drug-resistance. Thus, only in-depth investigation in 3D models from PC specimens or patient's derived xenografts might allow a more tailored therapy. In this regard, the design and synthesis of small bioavailable peptides specifically perturbing the key signaling functions of NGF receptors can be envisaged. Similar approaches have been successfully applied in our lab to disrupt the upstream interactions of sex steroid receptors with signaling effectors in quite different experimental settings (15, 29, 51–55).

Lastly, it cannot be neglected the role of NGF in PC-related pain, which is the most common symptom of PC bone metastasis (56). Anti-NGF blocking antibodies were firstly used to reduce PC-related bone pain in mouse models. Interestingly, this pharmacologic approach showed limited adverse effects, as compared with nonselective non-steroidal drugs or opioids (57). After many years of investigations, we are now aware that neurotrophins control the autonomic innervation of tumor microenvironment and, hence, PC progression. As such, neurotrophic factor assays would predict the progression and metastatic events in PC patients. Their pharmacologic manipulation can be used to prevent PC progression, reduce the PC-related bone pain and improve the quality of life in patients (48).

THE ROLE OF TRANSIENT RECEPTOR POTENTIAL MELASTATIN-8 (TRPM8) IN PROSTATE CANCER

The calcium channels mediate activation of several intracellular pathways by modulating the influx of cations (58 and therein refs). Some of them have emerged in recent years as important players in PC pathogenesis. As such, they represent 'druggable' targets in PC therapy (59, 60).

The transient receptor potential melastatin-8 (TRPM8) is a Ca^{2+}-permeable cold-sensing channel, which has received increasing attention for its role in a *plethora* of human solid cancers, including PC (20, 61–63). TRPM8 belongs to a family of eight members, classified from TRPM1 to TRPM8. They share a common structure, including a N-terminal region of almost 700 amino-acids, which endows four Melastatin Homology Regions (MHRs). MHRs are required for channel assembly and ion trafficking. The channels also exhibit a trans-membrane domain (TMD) with six helices, together with an additional intracellular helix (TRP helix). The C-terminal coiled-coil domain links the C-terminal domain (CTD) to the TRP helix (64). **Figure 2** illustrates the TRPM8 molecular organization. Among the various members, TRPM8 is involved in ion's homeostasis and it is sensitive to redox-state and temperature changes. Additionally, the channel can be activated by thermal stimuli (cold), depolarization of cell membranes or chemical compounds, such as the menthol and icilin (65).

TRPM8 expression was initially discovered in sensory neurons (66, 67). Subsequent studies of genome wide expression profiling showed that it is abundantly expressed in prostate tissue and PC samples (68, 69). TRPM8 expression is regulated by androgens, while ADT and the androgen-independence status both reduce its expression in PC tissues (69). Again, negligible levels of TRPM8 can be detected in PC3 and DU145 cells (22, 68, 70). These data highlight the importance of the TRPM8 channel in PC progression and hint at the usage of TRPM8 as a prognostic marker of PC progression.

Low levels of TRPM8 were detected at plasma membrane or endoplasmic reticulum of the androgen-dependent LNCaP cells. In these cells, the channel activation leads to mitogenesis by regulating Ca^{2+} and Na^{+} homeostasis (70). Subsequent studies in the same cells have shown that the *trpm8* gene is responsive to androgens, as its hormone regulation can be mediated by an androgen response element (ARE). Beyond this transcriptional regulation, a ligand-regulated degradation of TRPM8 has been detected in LNCaP cells (71). These findings underline the importance of hormone regulation in TRPM8 expression, at both transcriptional or post-translational level. Such regulation might impact the proliferation, survival and motility of PC cells. However, TRPM8 can also be regulated by PSA. In PC3 cells engineered to overexpress TRPM8, PSA acts as a channel agonist, prompting the Ca^{2+} intake. As such, bradykinin 2 receptor (B2R) activation occurs, with the consequent activation of protein kinase C pathway and inhibition of cell migration (72). Thus, once released, PSA activates TRPM8 by an autocrine loop, thereby impairing the invasive potential of PC cells. These findings point to the protective role for TRPM8 in PC. Recent findings have consistently shown that WS-12, a selective TRPM8 agonist, sensitizes the locally advanced PC to a sublethal dose of X-rays. These findings indicate that pharmacologic manipulation of TRPM8 by agonists would avoid the side effects correlated to high-dose ionizing radiation approach in PC patients (63).

We have recently reported that androgen stimulation of various PC-derived cells rapidly induces the complexation of

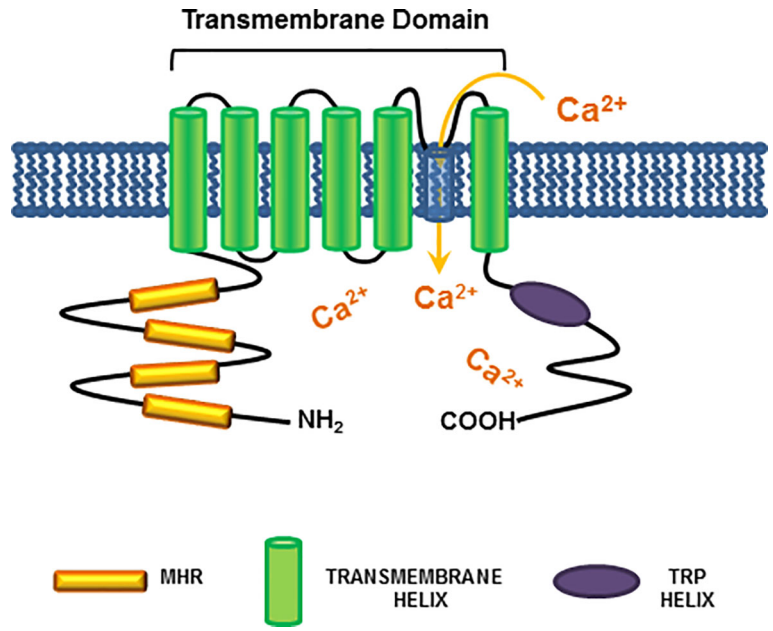

FIGURE 2 | TRPM8 structure. A schematic representation of the TRPM8 channel shows all the common structures between TRPM members. The cytosolic N-terminal region is connected to four Melastatin Homology Regions (MHRs), which are required for channel assembly and ion trafficking. The MHRs are connected to six helices within the plasma membrane, which constitute the trans-membrane domain (TMD). At last, the intracellular TRP helix is connected *via* a coiled-coil domain to the C-terminal domain (CTD). The indicated domains are colored as follows: MHR, orange; TMD helices: green; TRP helix: purple. As indicated in Figure, TRPM8 channel activation leads to an increase in cytosolic calcium levels.

AR with TRPM8 at extra-nuclear level. Previous findings have consistently shown that androgens trigger the AR/TRPM8 interaction within the lipid rafts microdomains of PC3 cells engineered to express AR (73). Whatever the intracellular localization of the complex, our data indicate that the androgen-induced AR/TRPM8 complex assembly controls the aggressive behaviour of PC cells through the increase in cytosolic [Ca^{2+}] levels. Newly synthesized TRPM8 antagonists revert these effects, impair the mitogenesis and invasion of PC cells and reduce the growth of PC cell-derived spheroids. Remarkably, the designed antagonists impair the proliferation and invasion of CRPC cells still expressing AR or the AR-V7 variant (22). As this mutant confers the anti-androgen resistance to PC patients (74), our recent study indicates that TRPM8 channel is clinically actionable in CRPC patients. In summary, we posit that TRPM8 acts as a molecular link between the androgen- and calcium-dependent signaling in PC. Therefore, the discovery of new selective TRPM8 antagonists hold promising results in PC therapy, since the lead compounds we used combine the selective modulation of AR-mediated rapid actions with the release of intracellular calcium. This combinatorial approach may be more effective than the currently used ADT. The arguments put forward here, together with the recent identification of TRPM8 mRNA as a bloodstream signature for PC aggressiveness (75), strongly encourage further studies in this direction.

The finding that TRPM8 regulates key features of PC cells call for additional comments. Other members of the same family can be regulated by sex steroids. TRPM4 and TRPM6, for instance, have been linked to non-transcriptional estrogen action in various cell types (76, 77). Pregnenolone sulfate, the precursor of steroid hormones, transiently activates TRPM3, thereby increasing the calcium influx and the insulin secretion from pancreatic islets (78). As such, the TRPM family members connect the steroid endocrine system with calcium and insulin pathways. Notably, NGF induces through TrkA signaling activation the up-regulation of TRPM8 in neuronal cells. This process requires the reversible activation of the Src tyrosine kinase as well as PI3-K (79), the two mainstream effectors activated by rapid actions mediated by AR in target cells. Thus, it might be argued that an intricate network made up of TrkA/TRPM8/AR components sustains the activation of pathways triggered by NGF or androgens or calcium in PC. If that were to happen, drug escape would easily occur. As such, ADT or TrkA inhibitors or even TRPM8 antagonists might fail in monotherapy.

THE ROLE OF CANCER ASSOCIATED FIBROBLASTS IN PROSTATE CANCER PATHOGENESIS AND PROGRESSION

CAFs represent the most important component of the tumor microenvironment (TME), which surrounds the neoplastic tissue. Together with the extracellular matrix (ECM), blood vessels and immune cells, CAFs have emerged as key regulators of cancer cell proliferation and metastasis. They

respond to the tumor-released growth factors or cytokines and secrete cytokines, chemokines and growth factors of their own. Again, by depositing or degrading ECM proteins, CAFs also influence the TME architecture, thus creating a favorable or a disadvantageous environment for the onset and progression of several tumors. The study of CAFs origin and analysis of their actions have emerged during the last years as a main road for a better understanding of cancer pathogenesis and progression, as well as the design of novel strategies for diagnostic and therapeutic guidance in patients (*reviewed in* 80, 81).

In normal tissues, fibroblasts contribute to the production of ECM and are major players in restoring the tissue integrity upon injury or chronic damage. Under such conditions, they acquire an activated phenotype, characterized by the expression of a subset of mesenchymal markers, including α-smooth muscle actin (α-SMA), fibroblast activating protein (FAP) and vimentin (82, 83). At this stage, they become myofibroblasts, contribute to the tissue recovery by releasing cytokines, chemokines and growth factors, such as the TGF-β and the vascular endothelial growth factor A (VEGF-A), and also recruit immune cells. CAFs derived from neoplastic tissues lack the markers for epithelial/endothelial lineages, show a decrease in CD36 expression and exhibit few genetic mutations, in the presence of an elongated cell morphology. They can be detected before the onset of a proper neoplasia, as a consequence of a tissue injury or damage. However, CAFs may also arise from a population of fibroblasts surrounding primitive lesions, with the initial aim to suppress the tumor growth. Additional events might switch this function, addressing them towards a tumor-supporting activity. Other studies have also indicated a possible, though less likely, origin of CAFs from mesenchymal stem cells, pericytes or adipocytes in different tumor types. Finally, CAF activation typically depends on soluble molecules, including interleukins and growth factors, which activate several intracellular signaling pathways, such as the TGF-β, Notch and NF-κB ones. Direct contact between cancer cells and fibroblasts could be also responsible for their activation, even if only in some cancer types. Simultaneously, other TME components could induce fibroblasts activation, regardless of cancer cells presence (81, 84).

Pioneering studies have pointed to the fundamental role of CAFs in supporting the onset of PC (85). Currently available data indicate that prostate CAFs establish a reciprocal, paracrine interaction with PC cells, resulting in EMT of the latter. Interleukin-6 (IL-6) produced by PC3 cells activates fibroblasts derived from patients with benign prostatic hyperplasia (BPH). Interestingly, different markers of fibroblast activation can be detected in these conditions, as compared with those expressed upon TGF-β-mediated activation (86). At the same time, CAFs activated by IL-6 promote EMT of PC3 cells and increase invasiveness in a similar fashion to that achieved by TGF-β-activated fibroblasts. Interestingly, only transformed prostate cells trigger CAFs activation, and such skill strictly depends on cell aggressiveness. Unlike PC3 or DU145, androgen-sensitive LNCaP cells seem, indeed, unable to activate CAFs. The mechanism by which PC cells acquire invasive phenotype, together with the EMT, depends on secretion of matrix metalloproteinases 2 and 9 (MMP2, MMP9) by CAFs. This response can be only detected on IL-6 stimulation and is reversed by MMPs inhibitors, thus indicating a role for MMPs in the observed findings. Additionally, CAFs are required for PC onset and metastatic spreading in mouse xenograft models, since their absence impairs the PC3 cell ability to generate subcutaneous tumors. Again, CAF-induced EMT of PC cells contributes to the formation of PC stem cells, thus enhancing cancer stemness (87). CAFs also play an energy-supporting role in PC, since prolonged exposure of PC3 and DU145 cells to CAF-conditioned media increases PC cell mitochondrial activity through sirtuin 1/peroxisome proliferator-activated receptor gamma coactivator 1-α (SIRT1/PGC-1α) axis. SIRT1 or PGC-1α silencing impairs the CAF-induced EMT in PC3 cells. Moreover, metabolic deregulation of PC cells by CAFs ultimately increases PC cells invasive potential by stabilization of hypoxia-induced factor 1α (HIF-1α), a reported feature of enhanced PC cell malignancy. Additionally, CAFs are also able to transfer horizontally and unidirectionally their dispensable, functional mitochondria to PC cells, thus contributing to their increased metabolic capacity, both directly or through activation of the SIRT1/PGC-1α pathway. By this mechanism, CAFs establish a symbiotic interaction with PC cells, which sustains their proliferative and metastatic behavior through metabolic regulation, production of high-energy metabolites and mitochondria supply (88). Recent findings have also indicated a role for CAFs in the development of castration-resistance. Accordingly, PC resistance to the 2nd generation antiandrogen, enzalutamide, would depend on CAFs, as shown in a PC mouse model progressing from castration-sensitive to castration-resistant state. The process seems mediated by the activation of the specific NRG1 receptor, HER3, by CAFs-secreted neuregulin-1 (NRG-1). Altogether, the proposed findings identify the NRG1/HER3 axis as a main candidate in the antiandrogen resistance. In support of this concept, high levels of NRG1, together with an enhanced NRG1 mRNA expression, can be detected in CAFs from ADT-treated PC patients (17). These results suggest that targeting of the NRG1/HER3 axis may be beneficial in CRPC patients. **Figure 3** schematically depicts the interplay between CAFs and PC cells.

However, the findings so far presented raise an important question. It concerns the expression of AR in CAFs. Previous findings from prostate CAFs have shown that the receptor is expressed at lower levels, as compared with LNCaP cells. Its somatic knockdown reduced the proliferative and migratory potential of PC3 cells, suggesting a role for stromal AR in sustaining the growth and invasion of PC cells (24). By contrast, subsequent studies reported that inhibition of AR in murine CAFs increases the expression of stemness markers in co-cultured PC cells. This effect was attributed to the release of interferon-γ (IFN-γ) and macrophage colony stimulating factor (M-CSF) by AR-depleted murine CAFs (25). Consistent with a protective role for stromal AR, it has been reported that expression of the receptor reduces the release of CCL2 and CXCL8 by CAFs, thereby inhibiting PC cell motility (89). These findings further corroborate the idea that PC

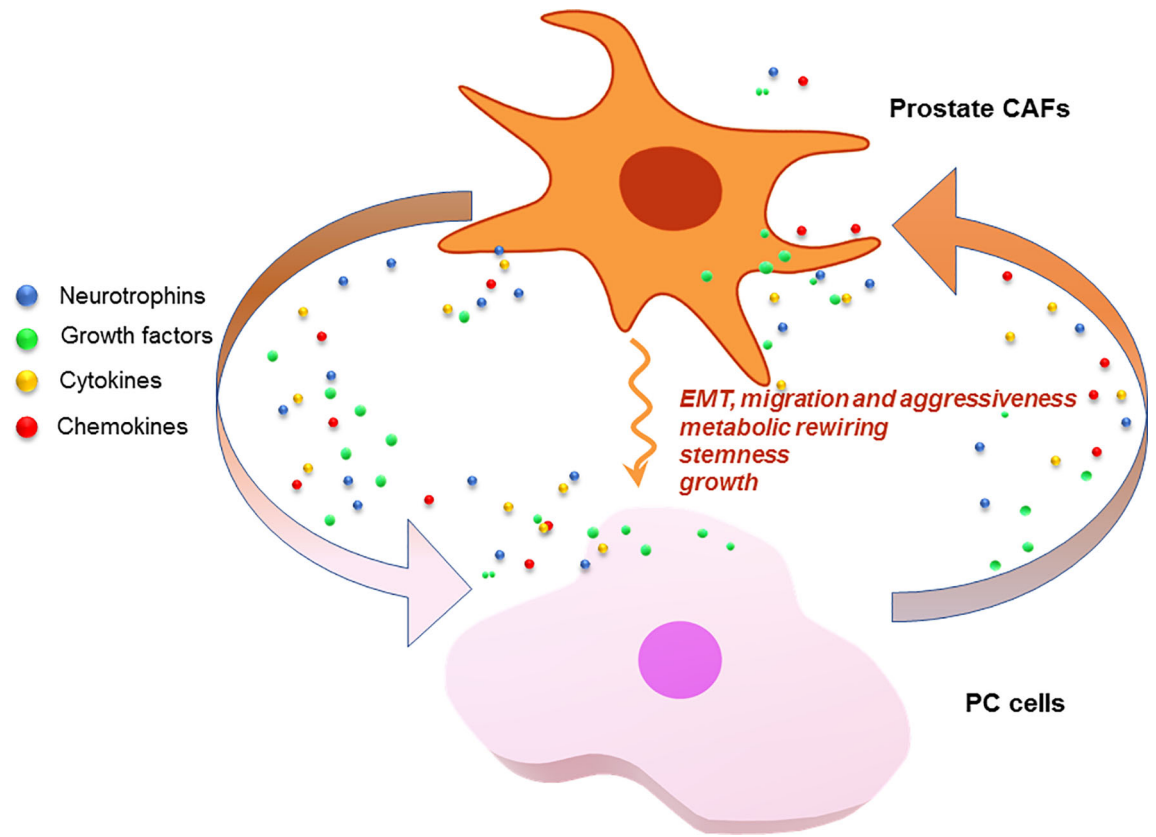

FIGURE 3 | CAFs and PC cells as signal exchangers. CAFs or PC cells release neurotrophins, growth factors, cytokines and chemokines. These signals are exchanged by the cells to foster a *plethora* of responses that lead to PC progression and drug-resistance.

progression might be paradoxically fostered by ADT or AR blocking therapies. Additional findings have supported an inverse correlation between stromal AR and disease's malignancy. Immunohistochemistry (IHC) analysis has shown, indeed, that expression of AR is more abundant in non-malignant stroma, as compared with PC-related stroma, further suggesting a protective and antioncogenic role for stromal AR (90–92). In contrast with these findings, our recent study in short-term primary culture of CAFs derived from PC specimens has revealed low, but appreciable AR levels in almost all the CAFs analyzed, even in about 30% of CAFs from PC patients at high Gleason's score (29). The conflicting findings so far reported might be explained by different considerations. Firstly, the IHC approach for detection of sex steroid receptors often exhibits pitfalls because of the type of cell permeabilization or the primary antibody used (93). Again, AR might be lost in stromal cells as a consequence of CAF selection and/or cell culture manipulation. Additionally, the receptor might undergo degradation as a consequence of ubiquitin-proteasome pathway activation (94) or epigenetic changes (95). Whatever the case, many studies support an oncogenic role for stromal AR, which might induce prostatic intraepithelial neoplasia (PIN; 96) or even metastatic events (97). We have consistently reported that stromal AR directs CAFs towards PC epithelial cells. This process requires AR complexation with filamin A (FlnA) and is strongly stimulated by androgens in 2 and 3D cell culture models. As such, a significant increase in PC-derived organoid's size can be detected (29). A similar process might occur *in vivo* when the local androgen levels increase, as it frequently occurs in PC (98). Nevertheless, the role of other factors, including NGF, cannot be neglected. In such a way, stromal AR might change the TME composition and allow metastatic events. In support of a role for stromal AR in cancer aggressiveness, it has been shown that AR targeting in CAFs reduces skin cancer aggressiveness traits (26) or even inhibit the development of chemo-resistant skin cancers (27). Thus, AR-directed therapies in CAFs might help the therapeutic approach of different cancer types. We designed and successfully used a small modified peptide that perturbs the androgen-induced AR/FlnA complex assembly (53). By this way, the peptide inhibits the androgen-induced invasion of CAFs in 2D models and reduces the overall tumor size in androgen-treated 3D co-culture (29). Our translational findings identify the AR/FlnA complex as a new 'druggable' biomarker in prostate CAFs. The strategy we propose might be profitably used for a more efficient PC treatment.

CONCLUDING REMARKS

PC still represents the second leading cause of cancer death in men in Western society. In most cases (~70%), PC has a slow and symptom-free growth, whereas it is more aggressive in the remaining patients. Current therapies for advanced PC remain unsatisfactory and new inhibitors of androgen synthesis and AR activation have been designed to improve patient survival. Despite these therapies, PC often progress towards a metastatic and/or CRPC phenotype. Preclinical and clinical studies currently aim at identifying the molecular basis for PC spreading and drug-resistance. Nevertheless, few biomarkers predictive of metastatic phenotype have as yet been identified and few efficient therapeutic options are available for advanced PC. Recent years, have seen important advances in large scale –omics approaches to identify novel biomarkers of PC malignancy and ameliorate patients' stratification as well as clinical management of the disease. The combination of next generation sequencing (NGS) approaches with proteomic profiling has revealed important differences between malignant and benign specimens, together with the identification of clinically actionable biomarkers. Additionally, tools for transcriptional expression classification have allowed the PCs characterization based on their pathological features, thereby addressing the patients towards a proper care (99). Several epigenetic modifications have been also identified and linked to altered gene expression, resulting in increased PC risk. Transcriptome-wide association studies confirmed the correlation with the expression of several predicted genes (100). Similar tools have been also applied to prostate CAFs to show that increased expression of ECM remodelling proteins is linked to cancer-supporting properties (101) or that specific epigenetic alterations are correlated to PC malignancy (102). These approaches might further provide important information on PC molecular landscape.

In this review, we aimed to address novel aspects of PC biology, which impinge on the interconnections between AR and other key intracellular signalling regulated by NGF or calcium channels. Communications between these partners seem relevant, since their breakdown might underly PC pathogenesis and progression. Current PC therapies prevalently target proliferative functions of AR and may only be effective within a short time frame. Primary PC show, instead, a marked heterogeneity and tumor cells may rapidly change as a consequence of pressures exerted by CAFs. Thus, further analysis of tumor microenvironment, identification of its molecular signatures, including the AR expression and its main partners, together with in depth study of signals delivered by PC- or CAF-derived exosomes (103), would provide additional information for patient's stratification, avoiding expensive therapies with considerable side effects. In this context, the synthesis of new biologically active molecules, such as the new calcium-channel antagonists or the small bioavailable peptides, specifically perturbing the extranuclear AR functions in TME or PC cells, should improve the pharmacologic response in patients and ameliorate their quality of life.

AUTHOR CONTRIBUTIONS

FL and GC conceptualized the paper and performed the initial and final editing. FL, MD, and AnM conceptualized and arranged the Figure's images. All the authors contributed to paper writing and revision. All authors contributed to the article and approved the submitted version.

FUNDING

This work was supported by Italian Ministry of University and Scientific Research (P.R.I.N. 2017EKMFTN_002 to GC); VALERE Program (Vanvitelli per la Ricerca Program; GoMAGIC to A.M., AdipCARE to GC and DESIRE to PG). Marzia Di Donato is supported by iCURE Project (B21C17000030007- Regione Campania).

REFERENCES

1. Sung H, Ferlay J, Siegel RL, Laversanne M, Soerjomataram I, Jemal A, et al. Global Cancer Statistics 2020: GLOBOCAN Estimates of Incidence and Mortality Worldwide for 36 Cancers in 185 Countries. *CA: Cancer J Clin* (2021) 71(3):209–49. doi: 10.3322/caac.21660
2. Pernar CH, Ebot EM, Wilson KM, Mucci LA. The Epidemiology of Prostate Cancer. *Cold Spring Harbor Perspect Med* (2018) 8(12):a030361. doi: 10.1101/cshperspect.a030361
3. Cuccurullo V, Di Stasio GD, Evangelista L, Castoria G, Mansi L. Biochemical and Pathophysiological Premises to Positron Emission Tomography With Choline Radiotracers. *J Cell Physiol* (2017) 232(2):270–5. doi: 10.1002/jcp.25478
4. Miralbell R. Stereotactic Beam Radiotherapy for Prostate Cancer: Is Less, More? *Lancet Oncol* (2019) 20(11):1471–2. doi: 10.1016/S1470-2045(19)30652-7
5. Siegel RL, Miller KD, Fuchs H, Jemal A. Cancer Statistic, 2021. *CA: A Cancer J Clin* (2021) 71:7– 33. doi: 10.3322/caac.21654
6. Attard G, Parker C, Eeles RA, Schröder F, Tomlins SA, Tannock I, et al. Prostate Cancer. *Lancet (London England)* (2016) 387(10013):70–82. doi: 10.1016/S0140-6736(14)61947-4
7. Nuhn P, De Bono JS, Fizazi K, Freedland SJ, Grilli M , Kantoff, et al. Update on Systemic Prostate Cancer Therapies: Management of Metastatic Castration-Resistant Prostate Cancer in the Era of Precision Oncology. *Eur Urol* (2019) 75(1):88–99. doi: 10.1016/j.eururo.2018.03.028
8. Davies AH, Beltran H, Zoubeidi A. Cellular Plasticity and the Neuroendocrine Phenotype in Prostate Cancer. *Nat Rev Urol* (2018) 15 (5):271–86. doi: 10.1038/nrurol.2018.22
9. Shen MM, Abate-Shen C. Molecular Genetics of Prostate Cancer: New Prospects for Old Challenges. *Genes Dev* (2010) 24(18):1967–2000. doi: 10.1101/gad.1965810
10. Logothetis CJ, Gallick GE, Maity SN, Kim J, Aparicio A, Efstathiou E, et al. Molecular Classification of Prostate Cancer Progression: Foundation for Marker-Driven Treatment of Prostate Cancer. *Cancer Discov* (2013) 3 (8):849–61. doi: 10.1158/2159-8290.CD-12-0460
11. Howard N, Clementino M, Kim D, Wang L, Verma A, Shi X, et al. New Developments in Mechanisms of Prostate Cancer Progression. *Semin Cancer Biol* (2019) 57:111–6. doi: 10.1016/j.semcancer.2018.09.003
12. Luo J, Attard G, Balk SP, Bevan C, Burnstein K, Cato L, et al. Role of Androgen Receptor Variants in Prostate Cancer: Report From the 2017

Mission Androgen Receptor Variants Meeting. *Eur Urol* (2018) 73(5):715–23. doi: 10.1016/j.eururo.2017.11.038
13. Huang EJ, Reichardt LF. Trk Receptors: Roles in Neuronal Signal Transduction. *Annu Rev Biochem* (2003) 72:609–42. doi: 10.1146/annurev.biochem.72.121801.161629
14. Singh R, Karri D, Shen H, Shao J, Dasgupta S, Huang S, et al. TRAF4-Mediated Ubiquitination of NGF Receptor Trka Regulates Prostate Cancer Metastasis. *J Clin Invest* (2018) 128(7):3129–43. doi: 10.1172/JCI96060
15. Di Donato M, Cernera G, Auricchio F, Migliaccio A, Castoria G. Cross-Talk Between Androgen Receptor and Nerve Growth Factor Receptor in Prostate Cancer Cells: Implications for a New Therapeutic Approach. *Cell Death Discovery* (2018) 4:5. doi: 10.1038/s41420-017-0024-3
16. Di Donato M, Cernera G, Migliaccio A, Castoria G. Nerve Growth Factor Induces Proliferation and Aggressiveness in Prostate Cancer Cells. *Cancers* (2019) 11(6):784. doi: 10.3390/cancers11060784
17. Zhang Z, Karthaus WR, Lee YS, Gao VR, Wu C, Russo JW, et al. Tumor Microenvironment-Derived NRG1 Promotes Antiandrogen Resistance in Prostate Cancer. *Cancer Cell* (2020) 38(2):279–296.e9. doi: 10.1016/j.ccell.2020.06.005
18. Chen WY, Wen YC, Lin SR, Yeh HL, Jiang KC, Chen WH, et al. Nerve Growth Factor Interacts With CHRM4 and Promotes Neuroendocrine Differentiation of Prostate Cancer and Castration Resistance. *Commun Biol* (2021) 4(1):22. doi: 10.1038/s42003-020-01549-1
19. Zhang L, Barritt GJ. TRPM8 in Prostate Cancer Cells: A Potential Diagnostic and Prognostic Marker With a Secretory Function? *Endoc Relat Cancer* (2006) 13(1):27–38. doi: 10.1677/erc.1.01093
20. Grolez GP, Gkika D. TRPM8 Puts the Chill on Prostate Cancer. *Pharmaceuticals (Basel Switzerland)* (2016) 9(3):44. doi: 10.3390/ph9030044
21. Alaimo A, De Felice D, Genovesi S, Lorenzoni M, Lunardi A. Tune the Channel: TRPM8 Targeting in Prostate Cancer. *Oncoscience* (2021) 8:97–100. doi: 10.18632/oncoscience.543
22. Di Donato M, Ostacolo C, Giovannelli P, Di Sarno V, Monterrey I, Campiglia P, et al. Therapeutic Potential of TRPM8 Antagonists in Prostate Cancer. *Sci Rep* (2021) 11(1):23232. doi: 10.1038/s41598-021-02675-4
23. Cioni B, Zwart W, Bergman AM. Androgen Receptor Moonlighting in the Prostate Cancer Microenvironment. *Endoc Relat Cancer* (2018) 25(6):R331–49. doi: 10.1530/ERC-18-0042
24. Yu S, Xia S, Yang D, Wang K, Yeh S, Gao Z, et al. Androgen Receptor in Human Prostate Cancer-Associated Fibroblasts Promotes Prostate Cancer Epithelial Cell Growth and Invasion. *Med Oncol (Northwood London England)* (2013) 30(3):674. doi: 10.1007/s12032-013-0674-9
25. Liao CP, Chen LY, Luethy A, Kim Y, Kani K, MacLeod AR, et al. Androgen Receptor in Cancer-Associated Fibroblasts Influences Stemness in Cancer Cells. *Endoc Relat Cancer* (2017) 24(4):157–70. doi: 10.1530/ERC-16-0138
26. Clocchiatti A, Ghosh S, Procopio MG, Mazzeo L, Bordignon P, Ostano P, et al. Androgen Receptor Functions as Transcriptional Repressor of Cancer-Associated Fibroblast Activation. *J Clin Invest* (2018) 128(12):5531–48. doi: 10.1172/JCI99159
27. Chan J, Sng MK, Teo ZQ, Chong HC, Twang JS, Tan NS. Targeting Nuclear Receptors in Cancer-Associated Fibroblasts as Concurrent Therapy to Inhibit Development of Chemoresistant Tumors. *Oncogene* (2018) 37 (2):160–73. doi: 10.1038/onc.2017.319
28. Mishra R, Haldar S, Suchanti S, Bhowmick NA. Epigenetic Changes in Fibroblasts Drive Cancer Metabolism and Differentiation. *Endoc Relat Cancer* (2019) 26(12):R673–88. doi: 10.1530/ERC-19-0347
29. Di Donato M, Zamagni A, Galasso G, Di Zazzo E, Giovannelli P, Barone MV, et al. The Androgen Receptor/Filamin a Complex as a Target in Prostate Cancer Microenvironment. *Cell Death Dis* (2021) 12(1):127. doi: 10.1038/s41419-021-03402-7
30. Dollé L, El Yazidi-Belkoura I, Adriaenssens E, Nurcombe V, Hondermarck H. Nerve Growth Factor Overexpression and Autocrine Loop in Breast Cancer Cells. *Oncogene* (2003) 22(36):5592–601. doi: 10.1038/sj.onc.1206805
31. Pundavela J, Roselli S, Faulkner S, Attia J, Scott RJ, Thorne RF, et al. Nerve Fibers Infiltrate the Tumor Microenvironment and are Associated With Nerve Growth Factor Production and Lymph Node Invasion in Breast Cancer. *Mol Oncol* (2015) 9(8):1626–35. doi: 10.1016/j.molonc.2015.05.001
32. Chakravarthy R, Mnich K, Gorman AM. Nerve Growth Factor (NGF)-Mediated Regulation of P75(NTR) Expression Contributes to Chemotherapeutic Resistance in Triple Negative Breast Cancer Cells. *Biochem Biophys Res Commun* (2016) 478(4):1541–7. doi: 10.1016/j.bbrc.2016.08.149
33. Di Donato M, Galasso G, Giovannelli P, Sinisi AA, Migliaccio A, Castoria G. Targeting the Nerve Growth Factor Signaling Impairs the Proliferative and Migratory Phenotype of Triple-Negative Breast Cancer Cells. *Front Cell Dev Biol* (2021) 9:676568. doi: 10.3389/fcell.2021.676568
34. Cheng B, Mattson MP. NGF and Bfgf Protect Rat Hippocampal and Human Cortical Neurons Against Hypoglycemic Damage by Stabilizing Calcium Homeostasis. *Neuron* (1991) 7(6):1031–41. doi: 10.1016/0896-6273(91)90347-3
35. Huang J, Ye Z, Hu X, Lu L, Luo Z. Electrical Stimulation Induces Calcium-Dependent Release of NGF From Cultured Schwann Cells. *Glia* (2010) 58 (5):622–31. doi: 10.1002/glia.20951
36. Jobling P, Pundavela J, Oliveira SM, Roselli S, Walker MM, Hondermarck H. Nerve-Cancer Cell Cross-Talk: A Novel Promoter of Tumor Progression. *Cancer Res* (2015) 75(9):1777–81. doi: 10.1158/0008-5472.CAN-14-3180
37. Meldolesi J. Neurotrophin Trk Receptors: New Targets for Cancer Therapy. *Rev Physiol Biochem Pharmacol* (2018) 174:67–79. doi: 10.1007/112_2017_6
38. Geldof AA, Van Haarst EP, Newling DW. Neurotrophic Factors in Prostate and Prostatic Cancer. *Prostate Cancer Prostatic Dis* (1998) 1(5):236–41. doi: 10.1038/sj.pcan.4500247
39. Sortino MA, Condorelli F, Vancheri C, Chiarenza A, Bernardini R, Consoli U, et al. Mitogenic Effect of Nerve Growth Factor (NGF) in Lncap Prostate Adenocarcinoma Cells: Role of the High- and Low-Affinity NGF Receptors. *Mol Endocrinol (Baltimore Md)* (2000) 14(1):124–36. doi: 10.1210/mend.14.1.0402
40. Festuccia C, Muzi P, Gravina GL, Millimaggi D, Speca S, Dolo V, et al. Tyrosine Kinase Inhibitor CEP-701 Blocks the NTRK1/NGF Receptor and Limits the Invasive Capability of Prostate Cancer Cells *In Vitro*. *Int J Oncol* (2007) 30(1):193–200. doi: 10.3892/ijo.30.1.193
41. Arrighi N, Bodei S, Zani D, Simeone C, Cunico SC, Missale C, et al. Nerve Growth Factor Signaling in Prostate Health and Disease. *Growth Factors (Chur Switzerland)* (2010) 28(3):191–201. doi: 10.3109/08977190903578678
42. Bradshaw RA, Pundavela J, Biarc J, Chalkley RJ, Burlingame AL, Hondermarck H. NGF and Prongf: Regulation of Neuronal and Neoplastic Responses Through Receptor Signaling. *Adv Biol Regul* (2015) 58:16–27. doi: 10.1016/j.jbior.2014.11.003
43. Dardenne E, Beltran H, Benelli M, Gayvert K, Berger A, Puca L, et al. N-Myc Induces an EZH2-Mediated Transcriptional Program Driving Neuroendocrine Prostate Cancer. *Cancer Cell* (2016) 30(4):563–77. doi: 10.1016/j.ccell.2016.09.005
44. Wang Y, Wang Y, Ci X, Choi S, Crea F, Lin D, et al. Molecular Events in Neuroendocrine Prostate Cancer Development. *Nat Rev Urol* (2021) 18 (10):581–96. doi: 10.1038/s41585-021-00490-0
45. Rosen EY, Goldman DA, Hechtman JF, Benayed R, Schram AM, Cocco E, et al. TRK Fusions are Enriched in Cancers With Uncommon Histologies and the Absence of Canonical Driver Mutations. *Clin Cancer Res an Off J Am Assoc Cancer Res* (2020) 26(7):1624–32. doi: 10.1158/1078-0432.CCR-19-3165
46. Dalal R, Djakiew D. Molecular Characterization of Neurotrophin Expression and the Corresponding Tropomyosin Receptor Kinases (Trks) in Epithelial and Stromal Cells of the Human Prostate. *Mol Cell Endocrinol* (1997) 134 (1):15–22. doi: 10.1016/s0303-7207(97)00165-2
47. March B, Lockhart KR, Faulkner S, Smolny M, Rush R, Hondermarck H. ELISA-Based Quantification of Neurotrophic Growth Factors in Urine From Prostate Cancer Patients. *FASEB bioAdvances* (2021) 3(11):888–96. doi: 10.1096/fba.2021-00085
48. March B, Faulkner S, Jobling P, Steigler A, Blatt A, Denham J, et al. Tumour Innervation and Neurosignalling in Prostate Cancer. *Nat Rev Urol* (2020) 17 (2):119–30. doi: 10.1038/s41585-019-0274-3
49. Weeraratna AT, Dalrymple SL, Lamb JC, Denmeade SR, Miknyoczki S, Dionne CA, et al. Pan-Trk Inhibition Decreases Metastasis and Enhances Host Survival in Experimental Models as a Result of its Selective Induction of Apoptosis of Prostate Cancer Cells. *Clin Cancer Res an Off J Am Assoc Cancer Res* (2001) 7(8):2237–45.

50. Collins C, Carducci MA, Eisenberger MA, Isaacs JT, Partin AW, Pili R, et al. Preclinical and Clinical Studies With the Multi-Kinase Inhibitor CEP-701 as Treatment for Prostate Cancer Demonstrate the Inadequacy of PSA Response as a Primary Endpoint. *Cancer Biol Ther* (2007) 6(9):1360–7. doi: 10.4161/cbt.6.9.4541
51. Migliaccio A, Castoria G, Auricchio F. Src-Dependent Signalling Pathway Regulation by Sex-Steroid Hormones: Therapeutic Implications. *Int J Biochem Cell Biol* (2007) 39(7-8):1343–8. doi: 10.1016/j.biocel.2006.12.009
52. Varricchio L, Migliaccio A, Castoria G, Yamaguchi H, de Falco A, Di Domenico M, et al. Inhibition of Estradiol Receptor/Src Association and Cell Growth by an Estradiol Receptor Alpha Tyrosine-Phosphorylated Peptide. *Mol Cancer Res MCR* (2007) 5(11):1213–21. doi: 10.1158/1541-7786.MCR-07-0150
53. Castoria G, Giovannelli P, Di Donato M, Ciociola A, Hayashi R, Bernal F, et al. Role of non-Genomic Androgen Signalling in Suppressing Proliferation of Fibroblasts and Fibrosarcoma Cells. *Cell Death Dis* (2014) 5(12):e1548. doi: 10.1038/cddis.2014.497
54. Di Donato M, Bilancio A, D'Amato L, Claudiani P, Oliviero MA, Barone MV, et al. Cross-Talk Between Androgen Receptor/Filamin a and Trka Regulates Neurite Outgrowth in PC12 Cells. *Mol Biol Cell* (2015) 26 (15):2858–72. doi: 10.1091/mbc.E14-09-1352
55. Di Donato M, Giovannelli P, Barone MV, Auricchio F, Castoria G, Migliaccio A. A Small Peptide Targeting the Ligand-Induced Androgen Receptor/Filamin a Interaction Inhibits the Invasive Phenotype of Prostate Cancer Cells. *Cells* (2021) 11(1):14. doi: 10.3390/cells11010014
56. Coleman RE. Skeletal Complications of Malignancy. *Cancer* (1997) 80(8 Suppl):1588–94. doi: 10.1002/(sici)1097-0142(19971015)80:8+<1588::aid-cncr9>3.3.co;2-z
57. Halvorson KG, Kubota K, Sevcik MA, Lindsay TH, Sotillo JE, Ghilardi JR, et al. A Blocking Antibody to Nerve Growth Factor Attenuates Skeletal Pain Induced by Prostate Tumor Cells Growing in Bone. *Cancer Res* (2005) 65 (20):9426–35. doi: 10.1158/0008-5472.CAN-05-0826
58. Gautier M, Trebak M, Fleig A, Vandier C, Ouadid-Ahidouch H. Ca^{2+} Channels in Cancer. *Cell Calcium* (2019) 84:102083. doi: 10.1016/j.ceca.2019.102083
59. Yu S, Xu Z, Zou C, Wu D, Wang Y, Yao X, et al. Ion Channel TRPM8 Promotes Hypoxic Growth of Prostate Cancer Cells *via* an O2 -Independent and RACK1-Mediated Mechanism of HIF-1α Stabilization. *J Pathol* (2014) 234(4):514–25. doi: 10.1002/path.4413
60. Maly IV, Hofmann WA. Calcium and Nuclear Signaling in Prostate Cancer. *Int J Mol Sci* (2018) 19(4):1237. doi: 10.3390/ijms19041237
61. Wondergem R, Ecay TW, Mahieu F, Owsianik G, Nilius B. HGF/SF and Menthol Increase Human Glioblastoma Cell Calcium and Migration. *Biochem Biophys Res Commun* (2008) 372(1):210–5. doi: 10.1016/j.bbrc.2008.05.032
62. Liu Z, Wu H, Wei Z, Wang X, Shen P, Wang S, et al. TRPM8: A Potential Target for Cancer Treatment. *J Cancer Res Clin Oncol* (2016) 142(9):1871–81. doi: 10.1007/s00432-015-2112-1
63. Alaimo A, Lorenzoni M, Ambrosino P, Bertossi A, Bisio A, Macchia A, et al. Calcium Cytotoxicity Sensitizes Prostate Cancer Cells to Standard-of-Care Treatments for Locally Advanced Tumors. *Cell Death Dis* (2020) 11 (12):1039. doi: 10.1038/s41419-020-03256-5
64. Huang Y, Fliegert R, Guse AH, Lü W, Du J. A Structural Overview of the Ion Channels of the TRPM Family. *Cell Calcium* (2020) 85:102111. doi: 10.1016/j.ceca.2019.102111
65. Yin Y, Wu M, Zubcevic L, Borschel WF, Lander GC, Lee SY. Structure of the Cold- and Menthol-Sensing Ion Channel TRPM8. *Sci (New York NY)* (2018) 359(6372):237–41. doi: 10.1126/science.aan4325
66. McKemy DD, Neuhausser WM, Julius D. Identification of a Cold Receptor Reveals a General Role for TRP Channels in Thermosensation. *Nature* (2002) 416(6876):52–8. doi: 10.1038/nature719
67. Peier AM, Moqrich A, Hergarden AC, Reeve AJ, Andersson DA, Story GM, et al. A TRP Channel That Senses Cold Stimuli and Menthol. *Cell* (2002) 108 (5):705–15. doi: 10.1016/s0092-8674(02)00652-9
68. Tsavaler L, Shapero MH, Morkowski S, Laus R. Trp-P8, a Novel Prostate-Specific Gene, is Up-Regulated in Prostate Cancer and Other Malignancies and Shares High Homology With Transient Receptor Potential Calcium Channel Proteins. *Cancer Res* (2001) 61(9):3760–9.
69. Henshall SM, Afar DE, Hiller J, Horvath LG, Quinn DI, Rasiah KK, et al. Survival Analysis of Genome-Wide Gene Expression Profiles of Prostate Cancers Identifies New Prognostic Targets of Disease Relapse. *Cancer Res* (2003) 63(14):4196–203.
70. Zhang L, Barritt GJ. Evidence That TRPM8 is an Androgen-Dependent Ca2+ Channel Required for the Survival of Prostate Cancer Cells. *Cancer Res* (2004) 64(22):8365–73. doi: 10.1158/0008-5472.CAN-04-2146
71. Asuthkar S, Velpula KK, Elustondo PA, Demirkhanyan L, Zakharian E. TRPM8 Channel as a Novel Molecular Target in Androgen-Regulated Prostate Cancer Cells. *Oncotarget* (2015) 6(19):17221–36. doi: 10.18632/oncotarget.3948
72. Gkika D, Flourakis M, Lemonnier L, Prevarskaya N. PSA Reduces Prostate Cancer Cell Motility by Stimulating TRPM8 Activity and Plasma Membrane Expression. *Oncogene* (2010) 29(32):4611–6. doi: 10.1038/onc.2010.210
73. Grolez GP, Gordiendko DV, Clarisse M, Hammadi M, Desruelles E, Fromont G, et al. TRPM8-Androgen Receptor Association Within Lipid Rafts Promotes Prostate Cancer Cell Migration. *Cell Death Dis* (2019) 10 (9):652. doi: 10.1038/s41419-019-1891-8
74. Antonarakis ES, Lu C, Wang H, Luber B, Nakazawa M, Roeser JC, et al. AR-V7 and Resistance to Enzalutamide and Abiraterone in Prostate Cancer. *New Engl J Med* (2014) 371(11):1028–38. doi: 10.1056/NEJMoa1315815
75. Souza MF, Kuasne H, Barros-Filho MC, Cilião HL, Marchi FA, Fuganti PE, et al. Circulating Mrna Signature as a Marker for High-Risk Prostate Cancer. *Carcinogenesis* (2020) 41(2):139–45. doi: 10.1093/carcin/bgz129
76. Cao G, van der Wijst J, van der Kemp A, van Zeeland F, Bindels RJ, Hoenderop JG. Regulation of the Epithelial Mg2+ Channel TRPM6 by Estrogen and the Associated Repressor Protein of Estrogen Receptor Activity (REA). *J Biol Chem* (2009) 284(22):14788–95. doi: 10.1074/jbc.M808752200
77. Wong KK, Hussain FA. TRPM4 Is Overexpressed in Breast Cancer Associated With Estrogen Response and Epithelial-Mesenchymal Transition Gene Sets. *PloS One* (2020) 15(6):e0233884. doi: 10.1371/journal.pone.0233884
78. Wagner TF, Loch S, Lambert S, Straub I, Mannebach S, Mathar I, et al. Transient Receptor Potential M3 Channels are Ionotropic Steroid Receptors in Pancreatic Beta Cells. *Nat Cell Biol* (2008) 10(12):1421–30. doi: 10.1038/ncb1801
79. Kayama Y, Shibata M, Takizawa T, Ibata K, Nakahara J, Shimizu T, et al. Signaling Pathways Relevant to Nerve Growth Factor-Induced Upregulation of Transient Receptor Potential M8 Expression. *Neuroscience* (2017) 367:178–88. doi: 10.1016/j.neuroscience.2017.10.037
80. Kalluri R. The Biology and Function of Fibroblasts in Cancer. *Nat Rev Cancer* (2016) 16(9):582–98. doi: 10.1038/nrc.2016.73
81. Sahai E, Astsaturov I, Cukierman E, DeNardo DG, Egeblad M, Evans RM, et al. A Framework for Advancing Our Understanding of Cancer-Associated Fibroblasts. *Nat Rev Cancer* (2020) 20(3):174–86. doi: 10.1038/s41568-019-0238-1
82. Tomasek JJ, Gabbiani G, Hinz B, Chaponnier C, Brown RA. Myofibroblasts and Mechano-Regulation of Connective Tissue Remodelling. *Nat Rev Mol Cell Biol* (2002) 3(5):349–63. doi: 10.1038/nrm809
83. Roberts EW, Deonarine A, Jones JO, Denton AE, Feig C, Lyons SK, et al. Depletion of Stromal Cells Expressing Fibroblast Activation Protein-α From Skeletal Muscle and Bone Marrow Results in Cachexia and Anemia. *J Exp Med* (2013) 210(6):1137–51. doi: 10.1084/jem.20122344
84. Gascard P, Tlsty TD. Carcinoma-Associated Fibroblasts: Orchestrating the Composition of Malignancy. *Genes Dev* (2016) 30(9):1002–19. doi: 10.1101/gad.279737.116
85. Olumi AF, Grossfeld GD, Hayward SW, Carroll PR, Tlsty TD, Cunha GR. Carcinoma-Associated Fibroblasts Direct Tumor Progression of Initiated Human Prostatic Epithelium. *Cancer Res* (1999) 59(19):5002–11. doi: 10.1186/bcr138
86. Kalluri R, Zeisberg M. Fibroblasts in Cancer. *Nat Rev Cancer* (2006) 6 (5):392–401. doi: 10.1038/nrc1877
87. Giannoni E, Bianchini F, Masieri L, Serni S, Torre E, Calorini L, et al. Reciprocal Activation of Prostate Cancer Cells and Cancer-Associated Fibroblasts Stimulates Epithelial-Mesenchymal Transition and Cancer Stemness. *Cancer Res* (2010) 70(17):6945–56. doi: 10.1158/0008-5472.CAN-10-0785

88. Ippolito L, Morandi A, Taddei ML, Parri M, Comito G, Iscaro A, et al. Cancer-Associated Fibroblasts Promote Prostate Cancer Malignancy *via* Metabolic Rewiring and Mitochondrial Transfer. *Oncogene* (2019) 38 (27):5339–55. doi: 10.1038/s41388-019-0805-7
89. Cioni B, Nevedomskaya E, Melis M, van Burgsteden J, Stelloo S, Hodel E, et al. Loss of Androgen Receptor Signaling in Prostate Cancer-Associated Fibroblasts (Cafs) Promotes CCL2- and CXCL8-Mediated Cancer Cell Migration. *Mol Oncol* (2018) 12(8):1308–23. doi: 10.1002/1878-0261.12327
90. Henshall SM, Quinn DI, Lee CS, Head DR, Golovsky D, Brenner PC, et al. Altered Expression of Androgen Receptor in the Malignant Epithelium and Adjacent Stroma is Associated With Early Relapse in Prostate Cancer. *Cancer Res* (2001) 61(2):423–7.
91. Ricciardelli C, Choong CS, Buchanan G, Vivekanandan S, Neufing P, Stahl J, et al. Androgen Receptor Levels in Prostate Cancer Epithelial and Peritumoral Stromal Cells Identify non-Organ Confined Disease. *Prostate* (2005) 63(1):19–28. doi: 10.1002/pros.20154
92. Wikström P, Marusic J, Stattin P, Bergh A. Low Stroma Androgen Receptor Level in Normal and Tumor Prostate Tissue is Related to Poor Outcome in Prostate Cancer Patients. *Prostate* (2009) 69(8):799–809. doi: 10.1002/pros.20927
93. Di Zazzo E, Galasso G, Giovannelli P, Di Donato M, Bilancio A, Perillo B, et al. Estrogen Receptors in Epithelial-Mesenchymal Transition of Prostate Cancer. *Cancers* (2019) 11(10):1418. doi: 10.3390/cancers11101418
94. Lin HK, Wang L, Hu YC, Altuwaijri S, Chang C. Phosphorylation-Dependent Ubiquitylation and Degradation of Androgen Receptor by Akt Require Mdm2 E3 Ligase. *EMBO J* (2002) 21(15):4037–48. doi: 10.1093/emboj/cdf406
95. Keil KP, Abler LL, Laporta J, Altmann HM, Yang B, Jarrard DF, et al. Androgen Receptor DNA Methylation Regulates the Timing and Androgen Sensitivity of Mouse Prostate Ductal Development. *Dev Biol* (2014) 396 (2):237–45. doi: 10.1016/j.ydbio.2014.10.006
96. Lai KP, Yamashita S, Huang CK, Yeh S, Chang C. Loss of Stromal Androgen Receptor Leads to Suppressed Prostate Tumourigenesis via Modulation of Pro-Inflammatory Cytokines/Chemokines. *EMBO Mol Med* (2012) 4 (8):791–807. doi: 10.1002/emmm.201101140
97. Ricke EA, Williams K, Lee YF, Couto S, Wang Y, Hayward SW, et al. Androgen Hormone Action in Prostatic Carcinogenesis: Stromal Androgen Receptors Mediate Prostate Cancer Progression, Malignant Transformation and Metastasis. *Carcinogenesis* (2012) 33(7):1391–8. doi: 10.1093/carcin/bgs153
98. Montgomery RB, Mostaghel EA, Vessella R, Hess DL, Kalhorn TF, Higano CS, et al. Maintenance of Intratumoral Androgens in Metastatic Prostate Cancer: A Mechanism for Castration-Resistant Tumor Growth. *Cancer Res* (2008) 68(11):4447–54. doi: 10.1158/0008-5472.CAN-08-0249
99. Nevedomskaya E, Baumgart SJ, Haendler B. Recent Advances in Prostate Cancer Treatment and Drug Discovery. *Intern J Mol Sci* (2018) 19(5):1359. doi: 10.3390/ijms19051359
100. Wu L, Yang Y, Guo X, Shu XO, Cai Q, Shu X, et al. An Integrative Multi-Omics Analysis to Identify Candidate DNA Methylation Biomarkers Related to Prostate Cancer Risk. *Nat Commun* (2020) 11(1):3905. doi: 10.1038/s41467-020-17673-9
101. Nguyen EV, Pereira BA, Lawrence MG, Ma X, Rebello RJ, Chan H, et al. Proteomic Profiling of Human Prostate Cancer-Associated Fibroblasts (CAF) Reveals LOXL2-dependent Regulation of the Tumor Microenvironment. *Mole Cell Proteo: MCP* (2019) 18(7):1410–27. doi: 10.1074/mcp.RA119.001496
102. Lawrence MG, Pidsley R, Niranjan B, Papargiris M, Pereira BA, Richards M, et al. Alterations in the Methylome of the Stromal Tumour Microenvironment Signal the Presence and Severity of Prostate Cancer. *Clin Epigen* (2020) 12 (1):48. doi: 10.1186/s13148-020-00836-2
103. Giovannelli P, Di Donato M, Galasso G, Monaco A, Licitra F, Perillo B, et al. Communication Between Cells: Exosomes as a Delivery System in Prostate Cancer. *Cell Commun Signal: CCS* (2021) 19(1):110. doi: 10.1186/s12964-021-00792-1

Conflict of Interest: The authors declare that the research was conducted in the absence of any commercial or financial relationships that could be construed as a potential conflict of interest.

Publisher's Note: All claims expressed in this article are solely those of the authors and do not necessarily represent those of their affiliated organizations, or those of the publisher, the editors and the reviewers. Any product that may be evaluated in this article, or claim that may be made by its manufacturer, is not guaranteed or endorsed by the publisher.

frontiers in Endocrinology

ORIGINAL RESEARCH
published: 21 March 2022
doi: 10.3389/fendo.2022.854365

VHL-P138R and VHL-L163R Novel Variants: Mechanisms of VHL Pathogenicity Involving HIF-Dependent and HIF-Independent Actions

Cecilia Mathó[1†], María Celia Fernández[1], Jenner Bonanata[2], Xian-De Liu[3], Ayelen Martin[1], Ana Vieites[1], Gabriela Sansó[1], Marta Barontini[1], Eric Jonasch[3], E. Laura Coitiño[2] and Patricia Alejandra Pennisi[1]*

[1] Centro de Investigaciones Endocrinológicas Dr. César Bergadá (CEDIE), Consejo Nacional de Investigaciones Científicas y Técnicas- Fundación de Endocrinología Infantil (CONICET-FEI) División de Endocrinología, Hospital de Niños Dr. Ricardo Gutiérrez, Buenos Aires, Argentina, [2] Laboratorio de Química Teórica y Computacional (LQTC), Instituto de Química Biológica, Facultad de Ciencias and Centro de Investigaciones Biomédicas (CEINBIO), Universidad de la República, Montevideo, Uruguay, [3] University of Texas MD Anderson Cancer Center, Houston, TX, United States

OPEN ACCESS

Edited by:
Claire Perks,
University of Bristol, United Kingdom

Reviewed by:
Paraskevi Xekouki,
University of Crete, Greece
Anne Barlier,
Aix Marseille Université, France

***Correspondence:**
Patricia Pennisi
ppennisi@cedie.org.ar

†Present address:
Cecilia Mathó,
Departamento de Genética, Facultad de Medicina, Universidad de la República, Montevideo, Uruguay

Specialty section:
This article was submitted to Cancer Endocrinology, a section of the journal Frontiers in Endocrinology

Received: 13 January 2022
Accepted: 15 February 2022
Published: 21 March 2022

Citation:
Mathó C, Fernández MC, Bonanata J, Liu X-D, Martin A, Vieites A, Sansó G, Barontini M, Jonasch E, Coitiño EL and Pennisi PA (2022) VHL-P138R and VHL-L163R Novel Variants: Mechanisms of VHL Pathogenicity Involving HIF-Dependent and HIF-Independent Actions. Front. Endocrinol. 13:854365. doi: 10.3389/fendo.2022.854365

The von Hippel–Lindau (VHL) disease is an autosomal dominant cancer syndrome caused by mutations in the *VHL* tumor suppressor gene. VHL protein (pVHL) forms a complex (VBC) with Elongins B-C, Cullin2, and Rbx1. Although other functions have been discovered, the most described function of pVHL is to recognize and target hypoxia-inducible factor (HIF) for degradation. This work comprises the functional characterization of two novel variants of the VHL gene (P138R and L163R) that have been described in our center in patients with VHL disease by *in vitro*, *in vivo*, and *in silico* approaches. *In vitro*, we found that these variants have a significantly shorter half-life compared to wild-type VHL but still form a functional VBC complex. Altered fibronectin deposition was evidenced for both variants using immunofluorescence. *In vivo* studies revealed that both variants failed to suppress tumor growth. By means of molecular dynamics simulations, we inspected *in silico* the nature of the changes introduced by each variant in the VBC complex. We have demonstrated the pathogenicity of P138R and L163R novel variants, involving HIF-dependent and HIF-independent mechanisms. These results provide the basis for future studies regarding the impact of structural alterations on posttranslational modifications that drive pVHL's fate and functions.

Keywords: VHL, von Hippel–Lindau, novel variants, P138R, L163R, functional characterization, molecular dynamics, simulations

1 INTRODUCTION

The von Hippel–Lindau (VHL) disease is a hereditary autosomal dominant syndrome (1, 2) that predisposes to the formation of cysts and benign and malignant tumors in different organs (3). Clinically, VHL disease can be divided into two subtypes based on the absence (type 1) or presence (type 2) of pheochromocytoma (4).

VHL disease's incidence ranges from 1/36,000 to 1/45,000 live births (3, 5) and is caused by mutations in the *VHL* tumor suppressor gene, which is located in the short arm of chromosome 3 (3p25-26) (3). Its coding sequence spans three exons and encodes a 213-amino acid protein (pVHL) widely expressed in human tissues (4, 6).

The correct folding of pVHL is coupled to the formation of the VBC complex with Elongin B and Elongin C (7, 8). The VBC complex together with Cullin 2 is part of the substrate-binding subunit of an E3 ubiquitin ligase that negatively regulates the expression of the hypoxia-inducible factors (HIFs) (9, 10). At normal oxygen level, HIF-α is hydroxylated at proline residues, in this form is recognized by pVHL, leading to rapid ubiquitination and degradation by the proteasome (11, 12). In hypoxic conditions, the prolyl-hydroxylases are inactive and HIF-α is stabilized, dimerizes with HIF-β (constitutively expressed), and translocates to the nucleus (12, 13). The dimer functions as a transcription factor, negatively regulating the expression of diverse hypoxia-inducible genes involved in metabolism, angiogenesis, and apoptosis (12, 14). In the past years, research has demonstrated that the SUMOylation of pVHL by the protein RSUME prevents the formation of the VBC complex, thus HIF-α is not degraded even under normal oxygen conditions (15, 16). On the other hand, pVHL has HIF-independent actions, such as microtubule stabilization (17), primary cilium formation (18), and extracellular matrix fibronectin assembly (19, 20), which are also important for tumor development.

To this day, more than 500 *VHL* mutations have been reported according to the Human Gene Mutation Database (HGMD® Professional 2020.3, accessed on November 5, 2020). Interestingly, most of the families presenting with pheochromocytoma (type 2 VHL disease) harbor missense mutations, while families with type 1 VHL disease usually present with gene deletions or nonsense mutations (21–24). In the present work, we performed functional characterization of two genetic variants (P138R and L163R) that have been described at our center in patients with VHL disease (25). P138R variant was identified in 5 patients of a family with Type 2B VHL. L163R variant was identified in 2 patients of a family with pheochromocytoma only (Type 2C VHL). The P138R variant implies the change of a proline for an arginine in the β domain of pVHL, involved in the interaction with HIF-α, while the L163R (25) variant is located in the α domain, involved in the union with Elongins B and C. Through *in vitro*, *in vivo*, and *in silico* studies, we demonstrated the pathogenicity of P138R and L136R variants affecting not only pVHL capacity to form HIF's recognition complex and its functioning in pseudo hypoxic conditions but also some of HIF's independent actions.

2 MATERIALS AND METHODS

2.1 Site-Directed Mutagenesis

The vector *VHL*-wild-type (WT)-Venus-Retro (26) and the Quikchange II XL Site-Directed Mutagenesis Kit were used following manufacturer's protocols to perform the specific mutations P138R (CCA➔CGA) and L163R (CTC➔CGC). Mutations were verified by DNA sequencing in ABI PRISM 310 Genetic Analyzer (Applied Biosystems, Foster City, CA, USA).

2.2 Stable Cell Line Development

HEK293T cells were used as a helper cell line in order to obtain retrovirus with the desired vectors as previously described by Ding et al. (27). Briefly, HEK293T cells were transfected with 3 different vectors: 1) pcGp, 2) pVSVG, and 3) either one of the following: GFP-Retro/*VHL*-WT-Venus-Retro/*VHL*-P138R-Venus-Retro/*VHL*-L163R-Venus-Retro using Lipofectamine 3000 (Invitrogen, Carlsbad, CA, USA). Upon assembly, supernatant was used to infect RCC 786-0 cells (ATCC® CRL-1932™, American Type Culture Collection, Manassas, VA, USA), and after 20h, selection was performed with 1 mg/ml of G418 antibiotic (Sigma Aldrich, St. Louis, MO, USA). Four different cell lines were obtained expressing green fluorescent protein (GFP), *VHL*-WT-Venus, VHL-P138R-Venus, and VHL-L163R-Venus. All cell lines were cultured in high-glucose Dulbecco's modified Eagle's medium (DMEM) supplemented with 10% fetal bovine serum (FBS) and maintained at 37°C in a humidified 5% CO_2 environment.

2.3 Western Blotting

Proteins were obtained as previously described (28) and resolved on a 12.5% sodium dodecyl-sulfate polyacrylamide gel electrophoresis (SDS-PAGE). After transferring to polyvinylidene fluoride (PVDF) membranes, blots were blocked and probed with different primary antibodies: VHL (BD Biosciences, # 556347, diluted 1/5,000), GFP (Santa Cruz, sc-8334, diluted 1/1,000), HIF-2α (Novus Biologicals, NB100-122, diluted 1/1,000), β-actin (Cell Signaling, #4970, diluted 1/1,000), Elongin B (Santa Cruz, sc-133090, diluted 1/500), and Elongin C (Santa Cruz, sc-1559, diluted 1/500). The following secondary antibodies were used accordingly: anti-rabbit (Cell Signaling, #7074, diluted 1/5,000), anti-goat (Santa Cruz, sc 2020, diluted 1/2,000), and anti-mouse (Cell Signaling, #7076, diluted 1/2,000).

2.4 Cell Treatments

Cell lines were seeded on 6-well plates and incubated with 50 μg/ml cycloheximide to interfere with protein synthesis, or 5 μg/ml MG132 to inhibit the proteasome, or 100 μM $CoCl_2$ (29) to simulate hypoxia. After treatment, proteins or RNA was extracted.

2.5 Immunoprecipitation

The amount of protein coming from GFP, WT VHL-Venus, P138R VHL-Venus, and L163R VHL-Venus cell lines was determined by Bradford assay, and 1 mg of protein was immunoprecipitated using GFP-Trap®_A kit (Chromotek GmbH, Germany). The immunocomplexes were detected by Western blot using the antibodies described above. Protein from WT VHL-Venus cell line was used as positive control and that from the cell line expressing GFP as a negative one.

2.6 Real-Time PCR

Total RNA from the different cell lines was extracted with Direct-Zol RNA Kit (Zymo Research, Irvine, CA, USA) following manufacturer's protocol. To perform RT-qPCR, 1 μg of RNA

from each sample was used together with random hexamers and Super Script II (Invitrogen, Carlsbad, CA, USA). Resulting cDNA was diluted by 1:10, and 3 µl from each dilution was subject to qPCR in triplicate using Kapa Syber Fast qPCR master mix (Kapa Biosystems, Boston, MA, USA) in Step One Plus Real-Time PCR System (Life Technologies, Carlsbad, CA, USA). mRNA values were calculated using relative quantitation method and are presented as fold change compared to control conditions. Specific primers were designed to assess fibronectin, vascular endothelial growth factor A (VEGF-A), and glucose transporter 1 (GLUT1) normalized to TATA box-binding protein (TBP) or *VHL* and α subunit α of HIF-2 (HIF-2α) normalized to glyceraldehyde 3-phosphate dehydrogenase (GAPDH).

2.7 Fibronectin Deposition by Immunofluorescence

Using anti-fibronectin antibody combined with a secondary antibody conjugated with Cy5, matrix deposition by all cell lines was analyzed according to the protocol of Debnath et al. (30). Briefly, cells were plated on coverslips, fixed, and permeabilized after 6 days of culture. Nuclei were dyed with Hoechst (5 µg/ml), and pictures were taken on a Carl-Zeiss AxioScope A1 microscope.

2.8 Xenografts

Immunodeficient mice [N:NIH (S)-Fox 1^{nu}] were housed in standard conditions of 12-h light/12-h dark cycle with water and food *ad libitum*, in accordance with National Institutes of Health guide for the care and use of laboratory animals (31).

A solution of 1×10^7 viable cells was injected subcutaneously on 6–8-week-old male mice and monitored weekly for tumor development. At 16 weeks post cell injection or when tumor reached 2-cm diameter, mice were sacrificed, and tumor histology was evaluated by hematoxylin and eosin (H&E) staining.

All animals were treated and cared for in accordance with standard international animal care protocols. All procedures were approved by the Animal Care and Use Committee of the Hospital de Niños Dr. Ricardo Gutiérrez.

2.9 Database Search and Online Predictions

We searched for these variants in the Genome Aggregation Database (gnomAD) (32), dbSNP (33), and ClinVar (34) databases to look at allele frequency, and if they had been reported by other groups. We also used online tools that predict the effect of protein variants: SIFT (35), Polyphen (36), Mutation Taster (37), and Human Splicing Finder (38). To classify these variants according to the American College of Medical Genetics Guidelines (39), we used VarSome (40).

2.10 *In Silico* Studies: Molecular Dynamics Simulations

The crystal structure of a human VBC: HIF-1α complex PDB 4AJY (X-Ray diffraction, 1.73 Å resolution) was used as starting structure (41). Missing residues of EloC (amino acids 106–118) were added using the SWISS-MODEL workspace (42, 43). The following six macromolecular systems were considered: WT and P138R and L163R variants of pVHL inserted in VBC: HIF-1α complexes, both under normoxia or hypoxia (the latter simulated replacing Hyp564 by Pro564 in HIF-1α). Lacking experimental structures of the two variants considered, *in silico* mutations were introduced by replacing the residue of interest at the native structure using the SWISS-PDB Viewer software (42). Protonation states of titratable residues were determined with PROPKA 3.0 (44), then all missing hydrogen atoms were added with the ProToss utility of the Proteins Plus server. All the systems were solvated with a truncated-octahedral box of TIP3P water 12 Å around the solute and neutralized with K^+ ions using the *leap* module of AmberTools17 (45). Each of the systems was minimized (2,000 steps applying a 500 kcal mol^{-1} $Å^{-2}$ harmonic potential over solute atoms, followed by 20,000 steps without restraints), then heated to 310 K [500 ps molecular dynamics (MD) simulation in NVT ensemble] and equilibrated at 1 atm (1 ns MD simulation at 310 K in NPT ensemble), prior to run 400 ns of productive MD simulations (NPT, 310 K and 1 atm). Minimizations and MD simulations were carried out with the *pmemd.cuda* module of AMBER16 (45). Protein residues were treated using the AMBER *ff14SB* force field. An integration step of 2 fs was used, constraining bonds involving hydrogen with SHAKE algorithm (46). Temperature and pressure were controlled applying the Langevin thermostat (47) and the Monte Carlo barostat (48), respectively. An 8.0-Å cutoff was used for direct non-bonded interactions, and the Particle Mesh Ewald (PME) method (49) was applied to long-range electrostatic interactions. Trajectory processing and analysis were performed with *cpptraj* module of AmberTools 17. Trajectory convergence was monitored following Cα-RMSDs, and flexibility was examined by means of per-residue Cα-RMSF. Snapshots of the trajectory were clustered into 5 clusters—each one with a representative structure—using a hierarchical agglomerative algorithm. Binding free energies of HIF-1α to the VBC complex were calculated using the MM-PB (GB)SA methods (50). For those calculations, the first 50 ns of the trajectories were discarded, then 100 snapshots separated by 3.5 ns were used. Representative structures of clusters with appreciable population (>10%) were used to calculate the electrostatic potential of VBC using the APBS software (51) implemented in the APBS/PDB2PQR web server (52).

2.11 Statistical Analysis

For real-time PCR analysis, one-way ANOVA was used with a Tukey test post evaluation. The chi-square test was used to analyze the differences in tumor incidence, and crosstabs were created. Statistical significance was defined as a p-value <0.05, and all data were graphed as mean ± standard deviation unless indicated otherwise.

3 RESULTS

3.1 P138R and L163R pVHL Variants Exhibit Lower Protein Levels Than Wild-Type pVHL

We analyzed the effect of P138R and L163R novel variants on VHL protein stability using Venus-tagged proteins. Human 786–0 RCC cell line (*VHL*-deficient) was infected with retroviral vectors to stably express VHL-P138R-Venus, VHL-L163R-Venus, and *VHL*-WT-Venus. Protein levels for both variants were significantly lower

than those for VHL-WT-Venus (**Figure 1A**). Assessed by RT-qPCR, mRNA levels showed that VHL-P138R-Venus and VHL-L163R-Venus variants were similar and even higher than VHL-WT-Venus mRNA levels (**Figure 1B**), suggesting that transcription levels are not responsible for the differences in protein levels evidenced by Western blot.

Cell lines were treated with cycloheximide to inhibit protein translation and enable the determination of half-lives for both VHL variants and WT pVHL. After 6 h, results showed that *VHL*-P138R-Venus and VHL-L163R-Venus have a significantly shorter half-life (≈1.2 h and 1 h, respectively) compared to that of VHL-WT-Venus (≈3.4 h) (**Figure 1C**).

Inhibiting the proteasome with MG132 (proteasome inhibitor) significantly increased both variants' protein levels, achieving quantities comparable to WT pVHL levels after MG132 treatment for the case of P138R and slightly lower for L163R (**Figure 1D**).

3.2 VBC Complex Formation Is Apparently Diminished but Still Functional for P138R and L163R

To date, pVHL's most described function is its interaction and consequent downregulation of HIF-α protein subunits (53). To this end, pVHL needs to form the VBC complex (pVHL-Elongin B-Elongin C). Immunoprecipitation of GFP Trap showed a specific band of 25 kD for GFP alone and 50 kD on cells expressing GFP-pVHL-Venus Tag (**Figure 2A**). Consistent with previous results (**Figure 1A**), pVHL levels are different for

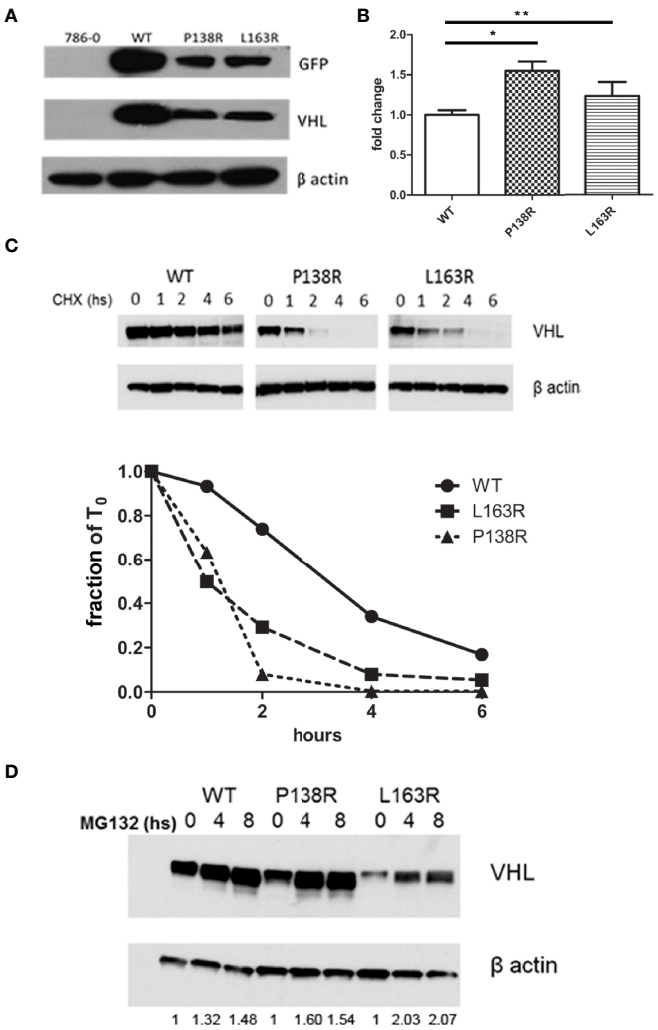

FIGURE 1 | Reduction in protein levels and half-life for P138R and L163R pVHL variants. **(A)** Representative Western blot showing the levels of GFP and VHL protein obtained in each cell line and β-actin as loading control. **(B)** Expression of VHL measured by qrPCR and graphed as fold change for P138R and L163R pVHL variants compared to pVHL WT. *p < 0.0001, **p = 0.0424, one-way ANOVA and Tukey's posttest. **(C)** Proteins levels obtained by Western blot after treatment with 50 μg/ml cycloheximide to inhibit protein translation. Quantification was done in order to plot the proportion of protein levels on the different time points evaluated. The dotted line indicates the 50%. **(D)** Inhibition of proteasome by 5 μg/ml MG 132 for cell lines expressing WT, and P138R and L163R pVHL variants. Results are shown by a representative Western blot for VHL and β-actin. Relative quantification of the bands is shown under each line.

the WT and P138R and L163R variants, resulting in less coimmunoprecipitation of Elongin B and C for the variants compared to WT *VHL* cell line (**Figure 2A**). We calculated the ratio between the bands obtained: Elongin C/pVHL and Elongin B/pVHL for WT pVHL, P138R and L163R pVHL-expressing cell lines. Ratios were normalized to WT pVHL's set as 1, and we observed that P138R immunoprecipitates less Elongin B and Elongin C (approximately 0.6) and L163R manages to immunoprecipitate a similar proportion of Elongin C but a lower quantity of Elongin B (0.25).

Since VBC complex was evidenced for both variants, we sought to evaluate its functionality. Firstly, the capacity of pVHL variants to downregulate HIF-2α was assessed. HIF-2α is overexpressed in the parental cell line used (786-0) (54), and its levels decrease significantly in the derived cell line expressing *VHL*-WT-Venus (**Figure 2B**, lanes 1 and 2). Protein levels for both P138R and L163R cell lines (**Figure 2B**, lanes 3 and 4) were intermediate for HIF-2α assessed by Western blot, although mRNA levels did not change in the different cell lines (**Figure 2B**). To evidence the consequence of these intermediate levels of HIF-2α protein, we quantified mRNA levels of two of its downstream targets: *VEGF-A* and *GLUT1* using qRT-PCR in normoxic and pseudohypoxic conditions (**Figure 2C**). Despite different HIF-2α protein levels, mRNA levels in normoxia for *VEGF-A* and *GLUT1* were similar among cell lines expressing WT and P138R and L163R pVHL (**Figure 2C**, upper panel). Under pseudohypoxic conditions, we

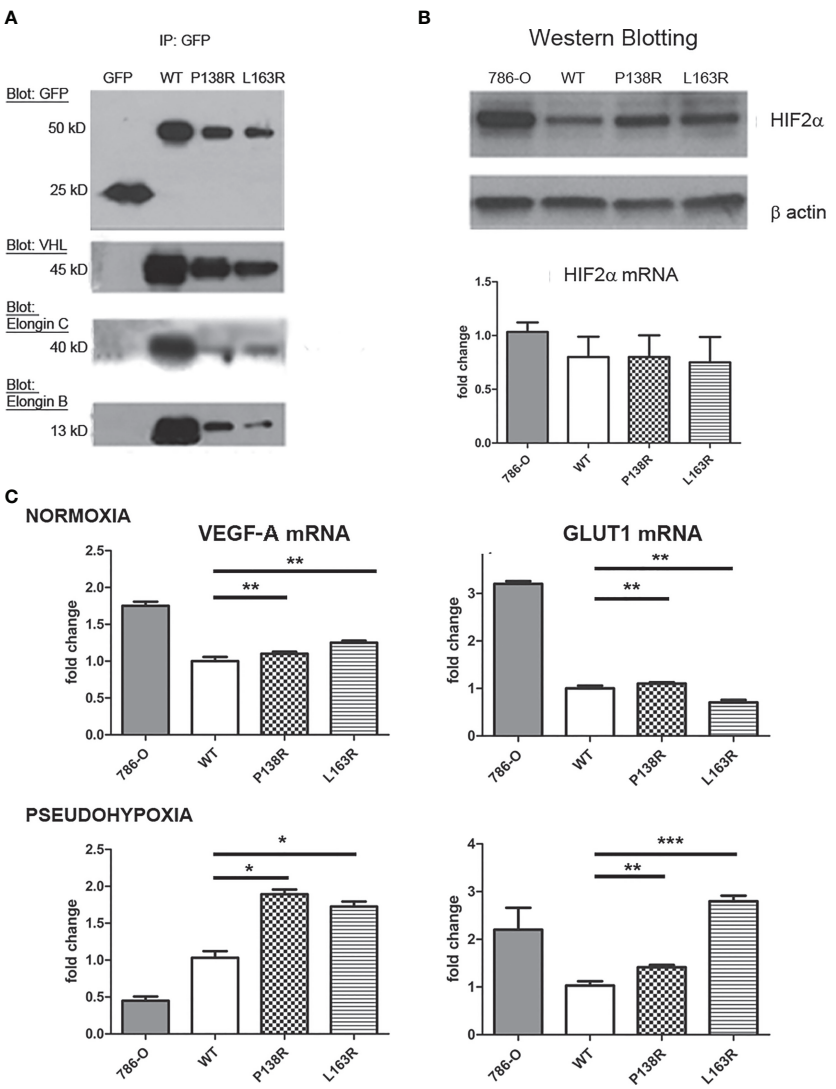

FIGURE 2 | P138R and L163R pVHL variants form less VBC complexes without losing functionality. **(A)** Representative Western blot showing immunoprecipitation of GFP-trap for each cell line expressing GFP, VHL-WT, P138R, or L163R. Membranes were blotted with anti-GFP, anti-VHL, anti-Elongin C, and anti-Elongin B. **(B)** Representative Western blot showing the levels of HIF-2α protein and mRNA measured by RT-qPCR and graphed as fold change for 786-O, WT, P138R, and L163R cell lines. **(C)** *VEG-F* and *GLUT1* mRNA expression was calculated by RT-qPCR under normoxia or 24 h of pseudohypoxia generated with 100 μM $CoCl_2$. Results are presented as fold change relative to pVHL WT expression. ns, not significant; *p < 0.0001, **p = 0.0401, ***p = 0.0002, one-way ANOVA and Tukey's posttest.

found significantly higher levels of *VEGF-A* and *GLUT1* mRNAs on the variant cell lines compared to the one expressing WT pVHL (**Figure 2C**, lower panel).

3.3 Altered Fibronectin Deposition in P138R pVHL and L163R pVHL With Different RNA Levels

pVHL is known to regulate fibronectin mRNA levels, although the underlying molecular mechanism has not been yet described. We assessed fibronectin mRNA levels in the 786-0 and 786-0-derived cell lines expressing *VHL*-WT-Venus, VHL-P138R-Venus, and *VHL*-L163R-Venus by RT-qPCR. Cells expressing WT-VHL have higher fibronectin mRNA levels than the parental 786-0, which is pVHL null (**Figure 3A**). Regarding the variants, P138R expression shows similar fibronectin mRNA levels to that of WT-*VHL*-expressing cell line. On the other hand, L163R expression resulted in diminished fibronectin mRNA levels and significantly different to the WT-*VHL* but comparable to the levels obtained for 786-0 cell line (**Figure 3A**).

Fibronectin expression *per se* does not ensure its proper extracellular matrix organization. Using immunofluorescence,

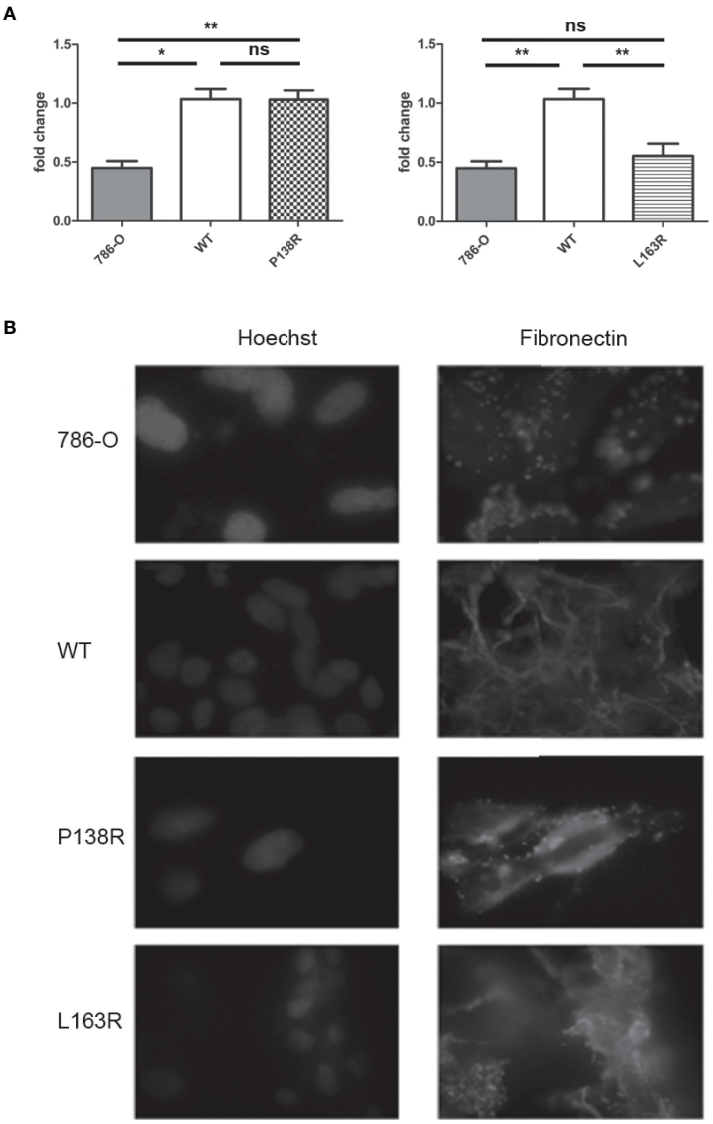

FIGURE 3 | Differences in mRNA fibronectin expression for P138R and L163R pVHL variants with similar disrupted deposition patterns. **(A)** Fibronectin mRNA expression of 786-O, WT, P138R, and L163R cell lines. Results are presented as fold change compared to WT cells. Values are expressed as ± SD of three independent experiments performed in triplicate. ns, not significant; *p = 0.0011, **p = 0.0030, one-way ANOVA and Tukey's posttest. **(B)** Cell lines were cultured on coverslips to assess fibronectin deposition with anti-fibronectin Cy5 conjugated (in red) by immunofluorescence. Nuclei were dyed with 5 μg/ml Hoechst as shown in blue. Images were taken at ×40 on a Carl-Zeiss AxioScope A1 microscope.

we evidenced fibronectin deposition in the 786-0 cell line as a dotted pattern, while in *VHL*-WT-Venus resulted in fibrillar network of fibronectin deposition (**Figure 3B**). Both variants, P138R and L163R, failed to generate this fibrillar organization, demonstrating a pattern similar to that observed in the parental 786-0 cell line where pVHL is absent (**Figure 3B**).

3.4 Cells Expressing P138R and L163R pVHL Do Not Suppress Tumor Growth as Wild-Type pVHL Does

To test the tumor suppressor role of the novel variants, we injected the cell lines expressing WT-*VHL* and P138R and L163R pVHL into male nude mice. Also, 786-0 cell line was injected as an internal control for the experiments. In our hands, visible tumors were developed, on average, 9 weeks after injection for all the tested cell lines (**Figure 4A**).

As expected, the ratio between the number of tumors developed and the number of sites injected was significantly higher in 786-0 compared to the cells expressing the WT-*VHL* protein. Moreover, P138R and L163R pVHL-expressing cells developed more tumors when compared to WT-*VHL* cell line (**Figure 4B**). Contingency tables were obtained, showing a significant difference between P138R, L163R, or 786-0 cells with WT pVHL, where tumors developed in 55% (11/20 for both variants) or 40% (4/10 for 786-0 cells) of the sites injected compared to a 10% for WT pVHL (3/30) (**Figure 4B**). Also, the variants showed a similar ratio of developed tumors to that of the parental cell line.

H&E staining confirmed that developed tumors had histological characteristics that are compatible with clear cell renal carcinoma (**Figure 4C**). These solid tumors were composed of atypical polyhedral cells that have a large, acidophilic, or

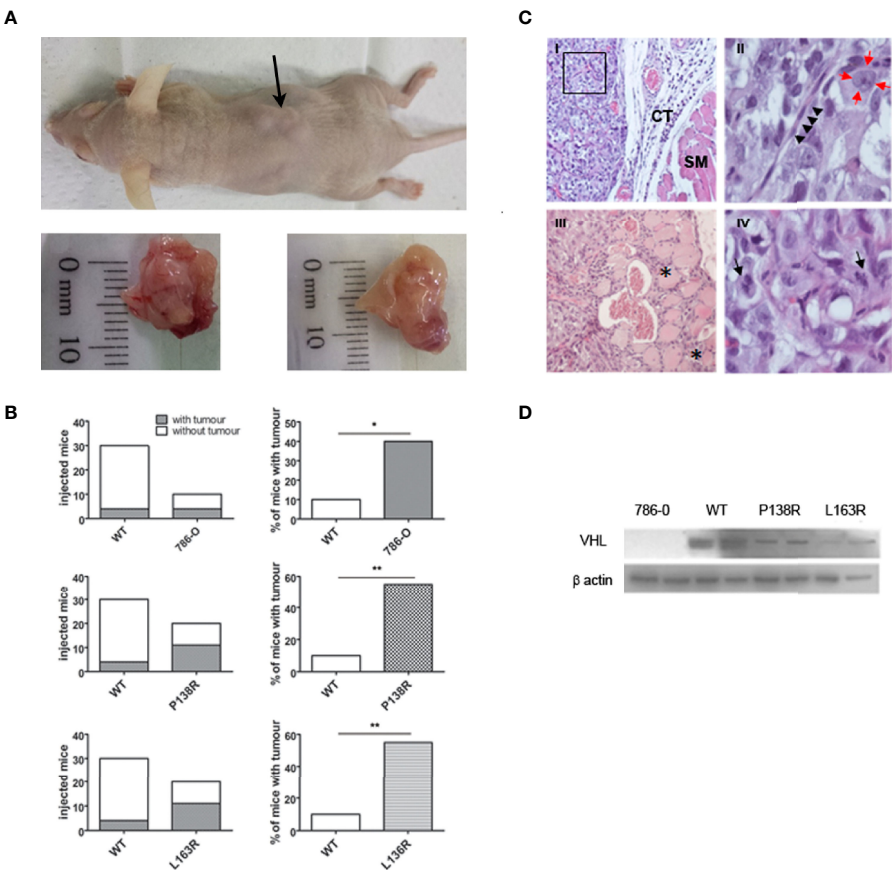

FIGURE 4 | *In vivo* studies showed tumor development for P138R and L163R pVHL variants. **(A)** Representative picture of nude mice and the tumors developed. The arrow points toward a tumor (upper panel). The bottom panel shows the macroscopical aspect of the tumors. **(B)** Left plots represent the incidence obtained for each cell line when injected on immunodeficient mice, and percentages are plotted on the right panels. ns, not significant; *p = 0.0306, **p = 0.0005, two-tailed chi-square test. **(C)** Histological features of the experimentally obtained tumors and stained with H&E. Panel I, Tumor cells distributed as lobes of polyhedral cells separated by fine fibers of connective tissue (CT) and striated muscle (SM) ×20 (Panel I). Panel II, a magnification of a sector of panel I shows a connective septum with central endothelial nuclei corresponding to the capillary vessel (marked with black arrowheads), surrounded by tumor cells with nuclei (red arrows) with prominent central nucleolus; ×100. Panel III presented tumor infiltrating the neighboring striated muscle, and the asterisks (*) indicate traces of tumor progression between the muscle bundles. Panel IV shows mitotic figures indicated with black arrows; ×100. **(D)** Representative Western blot showing the expression of VHL protein in the tumors developed by 786-O, WT, P138R, and L163R cell lines. β-Actin was blotted as loading control.

optically empty cytoplasm with large nuclei where its membrane was observed thickened and a prominent central nucleolus. Cells are grouped into clusters separated by thin collagen tracts through which small blood vessels pass (**Figures 4C**, I, II). Tumors had infiltrating growth toward neighboring tissues (**Figures 4C**, III) and showed histological signs of proliferative activity, evidenced by the numerous mitotic figures found (**Figures 4C**, IV).

pVHL protein expression was verified on tumors developed by 786-0 cells, WT pVHL, P138R, and L163R cell lines by Western blot. As shown in **Figure 4D**, pVHL was not detectable on 786-0 cells and had higher levels on WT pVHL-expressing cells compared to both variants (P138R and L163R).

3.5 Database Search and Online Predictions

The results of our database and online prediction tools are summarized in **Table 1**.

Our variants were not found in the Genome Aggregation Database (gnomAD) that includes thousands of genomes and exomes; this information allows us to infer that they have a very low allelic frequency. Most of the effect prediction tools used suggest that both variants are deleterious. L163R was previously reported by our group and reported in ClinVar by a genetic testing laboratory that classifies it as a variant of unknown significance (VUS). Using VarSome to follow the ACMG guidelines for classification of new variants, they are classified as likely pathogenic (P138R) and pathogenic (L163R).

3.6 *In Silico* Studies of VBC: HIF-1α Complexes by Molecular Dynamics Simulations

MD simulations enabled us to inspect at a molecular level the effects of introducing P138R and L163R pVHL variants in the VBC: HIF complex structure (**Figure 5A**) and stability, flexibility of the protein components, and other features relevant toward molecular recognition of pVHL by HIF (here represented by a 559-577 peptide fragment from HIF-1α containing either hydroxyproline Hyp564 or P564 in a carboxyl-terminal oxygen-dependent CODD motif, as representative of normoxia and hypoxia, respectively) in the VBC complex and by other possible interactors (**Figure 5A**).

All of the six MD 400-ns simulations promptly converged, showing formation of structurally stable complexes in all the cases. Introducing variants P138R and L163R in pVHL (**Figure 5B**) appears not to considerably disrupt HIF-1α binding to VBC under normoxic conditions: as shown in **Table 2**, the three complexes display similar binding strength values. Although VBC: HIF-1α complexes still form as evidenced *in vitro* (**Figure 2A**), binding strength is significantly reduced in all the cases under hypoxia, particularly for variant P138R (**Table 2**).

Global structural fluctuations in protein backbones appear to be smaller under hypoxia (when HIF-1α Hyp564 is replaced by P564) with respect to normoxia (See **Figure S1** in the **Supplementary Material**). Differences in dynamic behavior among WT and P138R and L163R variants of pVHL are more pronounced under conditions representative of normoxia and accompanied by side-chain shifts in residues relevant for the pathophysiological functions of pVHL.

3.6.1 Structure and Dynamics of VBC: HIF Involving Wild Type and P138R/L163R Variants

No major changes are detected in the tertiary and secondary structure of the pVHL: HIF complexes after introduction of variants P138R and L163R. Introducing variants affects specific interactions at the level of amino acid side chains directly in their local environment, and for L163R, it is propagated far away into the pVHL: HIF-1α interface. P138R introduces changes in a loop composed of residues 136–151.

3.6.2 Flexibility of the Components of the Multiproteic Complex–Root-Mean-Square Fluctuation (RMSF)

pVHL backbone flexibility and VCB interunit adaptation in the VBC complex are essential features toward successfully recruiting Cullin 2 (Cul2) E3 ubiquitin ligase and HIF-1α (55). Under high oxygen conditions, P138R variant significantly increases pVHL backbone flexibility in the region around P138 substitution comprising residues 136–151 (**Figure S1**, left bottom). More precisely, while lining the floor of the β-domain in native pVHL, this flexibilized region constitutes a hydrophobic patch from where P138 establishes direct hydrogen-bonding interactions with H115 (one of the residues clamping Hyp564 from HIF-1α at the B-interface of pVHL) and

TABLE 1 | Databases and online predictions for our pVHL variants.

Variant	ACMG Classification using VarSome	Databases			Mutation Effect Predictions			
		gnomAD (v3.1.2&2.1.1)	dbSNP	ClinVar	SIFT	Polyphen	Mutation Taster	Human Splicing Finder
P138R	Likely pathogenic	NA	NA	NA	Affect protein function	Probably damaging	Deleterious	New donor splice site
L163R	Pathogenic	NA	rs28940297	VUS	Affect protein function	Probably damaging	Deleterious	No significant impact on splicing signals

NA, not available; VUS, Variant of Unknown Significance.

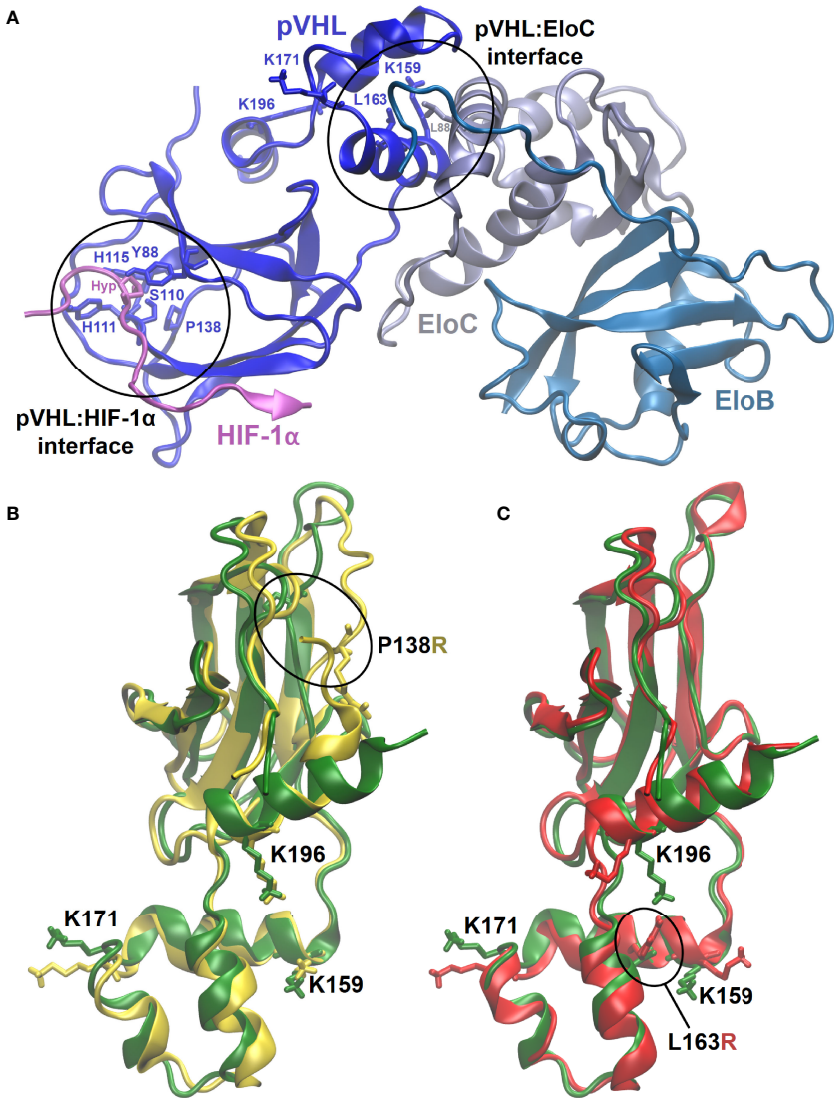

FIGURE 5 | 3D representative structures from MD simulations. **(A)** VBC complex with pVHL : HIF-1α and pVHL : EloC interfaces where variants are located circled and evidencing relevant residues. **(B, C)** Overlapped representative structures for the most populated clusters from 400-ns MD simulation under normoxia. Circled residues correspond to pVHL variants amino acids P138R and L163R in **(B, C)**, respectively. Color code: green, wild type pVHL; yellow, P138R pVHL variant; red, L163R pVHL variant.

TABLE 2 | MMPB(GB)SA-binding free-energies ($\Delta_b G$) for VBC: HIF-1α complexes.

System	$\Delta_b G$ (MMPBSA, kcal mol^{-1})		$\Delta(\Delta_b G)$
	Normoxia	Hypoxia	
Wild type	−34 ± 12	−23 ± 12	**11**
P138R	−33 ± 08	−12 ± 10	**21**
L163R	−33 ± 09	−24 ± 10	**9**

MMPBSA, Molecular Mechanics Poisson-Boltzmann Surface Area MMPBSA.

Y112. In the P138R variant, the more extended and charged Arg138 lies at the bottom of the β-domain but displaced outward from the hydrophobic *core* and oriented toward helix H4. On the opposite direction, both variants slightly reduce the flexibility of the protein in the region 86–96, also in the β-domain of pVHL, as a part of the HIF-1α binding surface [primary binding site S1, quite shallow, rigid (13, 56)] including some of the well-conserved residues lining the Hyp564 binding cavity. No

significant alterations are introduced by the L163R variant located in the α-domain of pVHL at the hydrophobic surface patch defining the interface with EloC where L163 establishes hydrophobic interactions with pVHL residues K159, L188, and a leucine from EloC. No significant alterations in flexibility are observed under conditions representative of hypoxia (**Figure S1**, panel C) other than a small reduction in the native protein around 86–96. Introducing variants in pVHL does not affect in a significant way HIF-1α flexibility (**Figure S1**, left bottom), which remains bound to VBC in all the cases with similar strengths under normoxia (**Table 2**). In the case of P138R, a small increase in flexibility is noticed under hypoxia in the region after Pro564, partially comprising the primary (S1) and secondary (S2) HIF-binding sites to pVHL. Introduction of variants in pVHL also reduces EloB flexibility in the region comprising residues 77–90. Whereas L163R does not alter EloC flexibility with respect to VBC formed with native pVHL, P138R induces a reduction mainly in the region defined by residues 83–93.

3.7 Changes Toward Molecular Interactions After Introducing Variants in pVHL

3.7.1 Electrostatic Reorganization Influencing Molecular Recognition Properties

As shown in **Figure 6**, front-view representations, HIF-1α binding site in the native VBC complex has two regions of clearly defined positive and negative electrostatic potential that may be guiding HIF-1α recognition and proper positioning. Introduction of both variants in pVHL induces charge

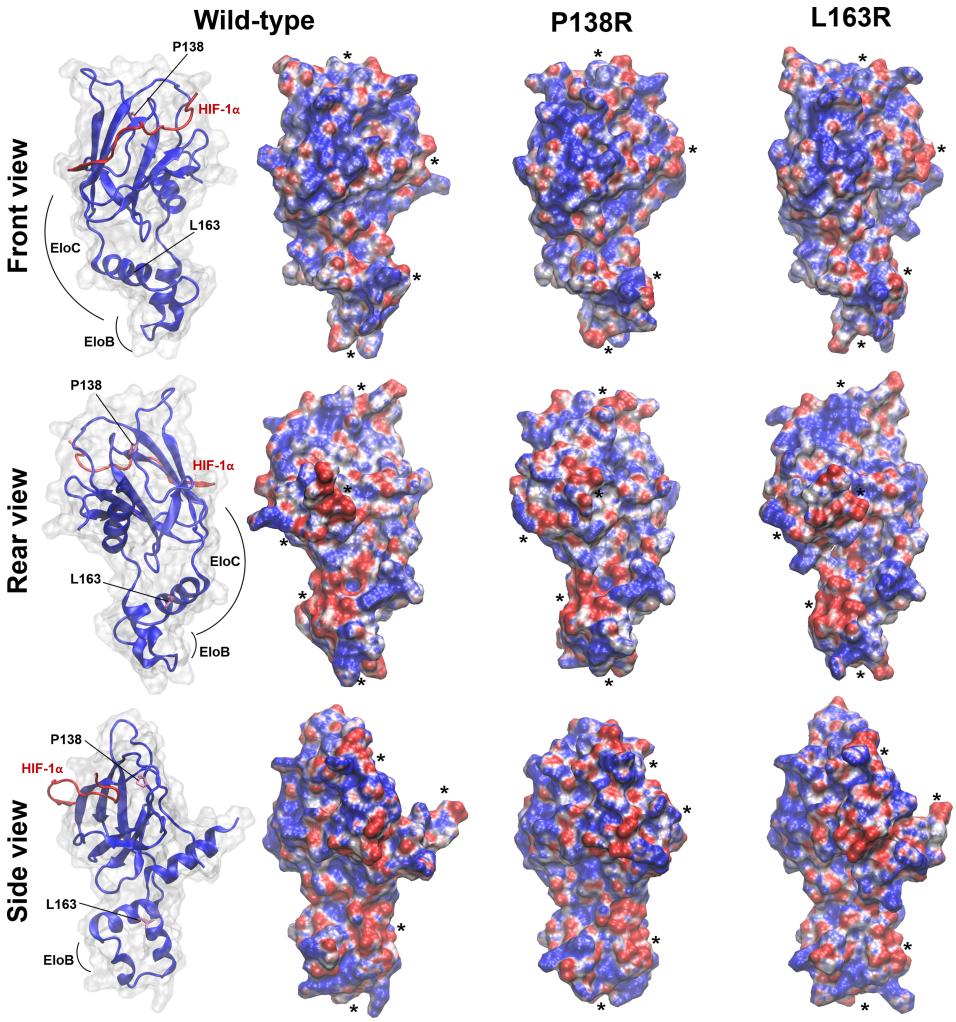

FIGURE 6 | *In silico* studies showed both reorganization in shape and/or surface electrostatic potential in pVHL variants. Molecular electrostatic potential (MEP) is mapped on the Connolly surface as calculated for WT and P138R or L163R pVHL variants. Representative structures were extracted from the most populated cluster from each MD simulation. Units of potential range from -7 to 7 kT/e (red, negative values; blue, positive values). Relevant modifications in shape and/or surface MEP between WT and mutants are evidenced by placing black asterisks nearby. The interaction domains of pVHL with HIF and EloC/EloB are shown in the left for each of the three views displayed.

redistribution reflected in the molecular electrostatic potential (MEP) and changes in the surface molecular shape, with an influence in molecular recognition.

3.7.2 Exposition to Solvent (SASA) of Relevant pVHL Lys Residues: K159, K171, and K196

We calculated the solvent-accessible surface area (SASA) for lysine residues 159, 171, and 196 (see **Figures 5B, C** for their location and orientation in each variant), which are targets for posttranslational modifications. **Figure S2** and **Table S1** in the **Supplementary Material** show the results for each of these. K159 is the most buried of the three Lys identified as relevant in the interaction with NEDD8. L163R variant further reduces solvent exposure of K159 in several frames of simulation, and this residue is reoriented. K171 is the most exposed of the three Lys inspected, and none of the variants affected its exposition. K196 is less exposed to solvent for the case of the L163R variant.

4 DISCUSSION

In this study, we aimed to describe two novel variants of the VHL protein: P138R and L163R, which have been found in families with VHL disease and have not been functionally characterized before.

Firstly, by Western blot, we observed lower protein levels of the variants when compared to WT pVHL and showed that they have significantly lower half-lives compared to WT pVHL. Other groups have reported similar results for other pVHL variants such as S65W (57), N78S (57), Y98H (57, 58), W117A (26), P138L (59), V155A (60), L158P (57), L158Q (60), Q164R (60), R167Q (57, 61), R167W (58), L188Q (57), and L188V (60). There are striking differences among other authors' results regarding the absolute value of WT pVHL and variant half-lives, even if we only consider those that use the same cycloheximide concentration (50 μg/ml). To compare our results with previous studies, we calculated the ratio between WT pVHL and our variants' half-lives, resulting in 2.8 (P138R) and 3.4 (L163R) approximately. Lanikova et al. (59) have described P138L variant, obtaining different absolute values for the half-lives, but a similar ratio to the one reported here for P138R. If we compare mutations near L163R, Park et al. (58) have shown that Q164R's half-life was reduced ≈3-fold compared to WT, while V155A and L158Q ≈5.5–6-fold. Ding et al. (61) showed a ≈3-fold reduction of R167Q's half-life. When regarding absolute half-life values, Bangiyeva et al. (57) showed that after 2 h of cycloheximide treatment, levels of L158P and R167Q diminished drastically, becoming very low or undetectable by Western blot, resembling our results.

On the other hand, when cell lines were treated with the proteasome inhibitor MG132, we observed accumulation of WT pVHL, P138R, and L163R. Both variants increased their levels in a higher proportion than WT pVHL. Taken together, the above data suggest that the lower protein levels observed for VHL-P138R-Venus and VHL-L163R-Venus are due to proteasomal degradation.

The most studied mechanism for pVHL proteasome-mediated degradation is UCP-mediated polyubiquitination. Other authors have shown that UCP mediates the degradation of V155A, L158Q, and Q164R variants (60). P138R and L163R variants do not involve the substitution of lysine residues (subject to ubiquitination) directly, but they could alter their surroundings, favoring their exposure and thus their ubiquitination. Particularly for L163R variant, lysine 196 appears to be less exposed to the solvent, a result that would not favor polyubiquitination of this residue. Given that the region of interaction of pVHL with UCP has not been determined yet, one could speculate that this region might vary its conformation as a result of changes introduced in the pVHL protein. Therefore, an increase in the affinity of UCP for pVHL variants might explain their increased degradation compared to WT pVHL.

We showed that both pVHL variants maintain their ability to form a VBC complex, although it is apparently formed at a lower rate: P138R appears to bind less Elongin B and C, while L163R appears to bind Elongin C appropriately but less Elongin B. These results are in agreement with other groups' findings, since the majority of inherited *VHL* mutations are defective in Elongin B and C binding (62–65). Other groups have shown that variants close to P138R and L163R such as D121G (66), Q145H (67), F148A (61), V155A (60), Q164R (60), and R167Q (61, 66, 68) form less VBC complex compared to WT pVHL, while L158P (69) and C162F (63, 70) are unable to form this complex and therefore do not have the capacity to downregulate HIF-α subunits (69, 71, 72).

On the other hand, VBC complex formation itself does not ensure its functionality, as it must recognize HIF-α subunits in order to target them for proteasomal degradation. Ding et al. (61) have shown that W117A and F148A mutations form less VBC complex and also lose their ability to interact with HIF-2α. We interrogated the capacity of the P138R and L163R pVHL variants to form a functional VBC complex and therefore accomplish the interaction and proteasome-mediated degradation of HIF-2α. By Western blot, intermediate levels of HIF-2α were observed by the cell lines expressing P138R and L163R; therefore, we decided to evaluate the consequence of these intermediate levels by evaluating the expression (mRNA) of two target genes: *VEGF-A* and *GLUT1*. We showed that under normoxic conditions, these genes exhibit the same regulation in cell lines expressing either the variants or WT pVHL. Nevertheless, after 24 h of pseudohypoxia, significant, though subtle, differences were observed between the cell lines expressing the variants compared to WT pVHL. As a consequence, variants' VBC complexes could not appropriately regulate HIF-2α levels under these experimental conditions. This result suggests that the novel pVHL variants might have a different behavior compared to WT pVHL under more physiologically challenging conditions. The results obtained *in silico* suggest that VBC-HIF-1α complexes formed by the variants are thermodynamically favorable because of their negative ΔG.

In summary, our results indicate that although the protein levels for P138R and L163R pVHL variants are lower compared to WT pVHL, these interact forming a functional VBC complex capable of targeting HIF-2α for proteasome-mediated degradation.

As mentioned before, numerous pVHL HIF-independent mechanisms account for pVHL as a tumor suppressor (18, 19, 73). We decided to explore the relationship of these variants with fibronectin regulation, since it has been explored since 1998 and is the most described HIF-independent function to date (19). Other authors have shown that cell lines with pVHL mutant expression result in a defective fibronectin matrix deposition (19, 71, 74).

Our results indicate that although the novel variants exhibit a different regulation of fibronectin mRNA levels, they both fail in assembling a proper extracellular fibronectin matrix. For the L163R variant, less exposure to solvent of lysine 196 could explain a lower NEDDylation level and therefore the defective interaction with fibronectin, since NEDDylation has been described as a necessary switch for fibronectin interaction (75). These findings are speculative at this point and need to be tested *in vitro* in future studies.

The 786-0 cell line develops tumors when injected into nude mice, while clones of this cell line expressing WT-pVHL do not, or in some cases, they do but in a much smaller proportion of the injected mice compared to 786-0. Our xenograft experiments revealed that P138R-pVHL and L163R-pVHL failed to suppress tumor growth, obtaining 11 tumors out of 20 sites injected with each variant (55% incidence), a similar proportion to the one obtained by parental 786-0 cell line that does not express pVHL (40% incidence). These results confirm the pathogenic role for P138R and L163R pVHL variants, since they are unable to suppress tumor growth such as WT pVHL does. A study conducted by Ding et al. (61) revealed that the amount of a missense-mutated VHL protein (R167Q) could impact its function suppressing tumorigenesis when proteasome is inhibited, and this protein is therefore accumulated. Using the same approach and experimental tools, our pVHL variants were not able to compensate their functional deficiencies and demonstrated tumorigenic capacity, suggesting that there are a variety of mechanisms driving tumor formation. Our work reinforces the importance of studying specific variants to identify their biological impact. This work sets the stage for mechanistic studies exploring the altered mechanisms that explain pathogenesis and could lead to more targeted therapies for specific mutations.

Overall, our results show that P138R and L163R pVHL variants can be classified as pathogenic, since they failed to suppress tumor development in nude mice. Future studies are suggested for the elucidation of the mechanisms underlying their pathogenicity. In the current omics era, our study sets the basis for future proteomic and genomic approaches to compare cell lines expressing these variants with the WT protein to fully understand this missense variants' global effects.

DATA AVAILABILITY STATEMENT

The raw data supporting the conclusions of this article will be made available by the authors without undue reservation.

ETHICS STATEMENT

The animal study was reviewed and approved by Comité de Etica, Hospital de Niños Dr. R. Gutiérrez, Buenos Aires, Argentina.

AUTHOR CONTRIBUTIONS

PP conceived, designed, and directed the experimental research. CM, XL, and EJ designed the experiments. CM and MCF planned and carried out the experiments. AM collected data. AV, GS, and MB performed genetic and clinical characterization of VHL patients. ELC designed and directed the computational component of this work, and JB carried out all the molecular dynamics simulations. CM and MCF took the lead on writing the article under the supervision of PP and ELC (who wrote the *in silico* sections; contact laurac@fcien.edu.uy for direct inquiries). All authors provided critical feedback and helped shape the research, analysis, and article. All authors contributed to the article and approved the submitted version.

FUNDING

This work was supported by Instituto Nacional del Cáncer, Ministerio de Salud, Argentina (Grant 2014-2016, awarded to PP) and Consejo Nacional de Investigaciones Científicas y Técnicas, CONICET, Argentina (PIP#0100214, 2013-2015, awarded to PP).

ACKNOWLEDGMENTS

AM and CM were recipients of doctoral fellowships from CONICET. CM received a Bunge & Born fellowship. MCF is an assistant researcher from CONICET. CM, JB, and ELC are researchers of the Sistema Nacional de Investigadores (SNI, ANII-Uruguay) and PEDECIBA (MEC-UdelaR, Uruguay).
This paper is dedicated to the loving memory of Dr. Alicia Merlino (LQTC, UdelaR) who took part in early stages of this work, prematurely deceased on July 8, 2018.

SUPPLEMENTARY MATERIAL

The Supplementary Material for this article can be found online at: https://www.frontiersin.org/articles/10.3389/fendo.2022.854365/full#supplementary-material

REFERENCES

1. Friedrich, CA. Von Hippel-Lindau Syndrome. A Pleomorphic Condition. *Cancer* (1999) 86:2478–82. doi: 10.1002/(SICI)1097-0142(19991201)86:11+<2478::AID-CNCR4>3.0.CO;2-5
2. Clark, PE, Cookson, MS. The Von Hippel-Lindau Gene: Turning Discovery Into Therapy. *Cancer* (2008) 113:1768–78. doi: 10.1002/cncr.23645
3. Latif, F, Tory, K, Gnarra, J, Yao, M, Duh, FM, Orcutt, ML, et al. Identification of the Von Hippel-Lindau Disease Tumor Suppressor Gene. *Sci (80-)* (1993) 260:1317–20. doi: 10.1126/science.8493574
4. Kim, WY, Kaelin, WG. Role of VHL Gene Mutation in Human Cancer. *J Clin Oncol* (2004) 22:4991–5004. doi: 10.1200/JCO.2004.05.061
5. Cho, HJ, Ki, CS, Kim, JW. Improved Detection of Germline Mutations in Korean VHL Patients by Multiple Ligation-Dependent Probe

Amplification Analysis. *J Korean Med Sci* (2009) 24:77–83. doi: 10.3346/jkms.2009.24.1.77
6. *GTEx Portal* . Available at: https://gtexportal.org/home/gene/VHL#gene-transcript-browser-block (Accessed November 14, 2021).
7. McClellan, AJ, Scott, MD, Frydman, J. Folding and Quality Control of the VHL Tumor Suppressor Proceed Through Distinct Chaperone Pathways. *Cell* (2005) 121:739–48. doi: 10.1016/j.cell.2005.03.024
8. Melville, MW, Mcclellan, AJ, Meyer, AS, Frydman, J, Darveau, A. The Hsp70 and TRiC / CCT Chaperone Systems Cooperate *In Vivo* To Assemble the Von Hippel-Lindau Tumor Suppressor Complex The Hsp70 and TRiC / CCT Chaperone Systems Cooperate *In Vivo* To Assemble the Von Hippel-Lindau Tumor Suppressor Complex. *Mol Cell Biol* (2003) 23:3141–51. doi: 10.1128/MCB.23.9.3141
9. Pause, A, Peterson, B, Schaffar, G, Stearman, R, Klausner, RD. Studying Interactions of Four Proteins in the Yeast Two-Hybrid System: Structural Resemblance of the pVHL/Elongin BC/hCUL-2 Complex With the Ubiquitin Ligase Complex SKP1/cullin/F-Box Protein. *Proc Natl Acad Sci U.S.A.* (1999) 96:9533–8. doi: 10.1073/PNAS.96.17.9533
10. Pause, A, Lee, S, Worrell, RA, Chen, DY, Burgess, WH, Linehan, WM, et al. The Von Hippel-Lindau Tumor-Suppressor Gene Product Forms a Stable Complex With Human CUL-2, a Member of the Cdc53 Family of Proteins. *Proc Natl Acad Sci U.S.A.* (1997) 94:2156–61. doi: 10.1073/pnas.94.6.2156
11. Haase, VH. The VHL/HIF Oxygen-Sensing Pathway and its Relevance to Kidney Disease. *Kidney Int* (2006) 69:1302–7. doi: 10.1038/sj.ki.5000221
12. Chan, DA, Sutphin, PD, Yen, S-E, Giaccia, AJ. Coordinate Regulation of the Oxygen-Dependent Degradation Domains of Hypoxia-Inducible Factor 1 Alpha. *Mol Cell Biol* (2005) 25:6415–26. doi: 10.1128/MCB.25.15.6415-6426.2005
13. Hon, WC, Wilson, MI, Harlos, K, Claridge, TD, Schofield, CJ, Pugh, CW, et al. Structural Basis for the Recognition of Hydroxyproline in HIF-1 Alpha by pVHL. *Nature* (2002) 417:975–8. doi: 10.1038/nature00767nature00767
14. Shen, C, Kaelin, Jr.WG. The VHL/HIF Axis in Clear Cell Renal Carcinoma. *Semin Cancer Biol* (2013) 23:18–25. doi: 10.1016/j.semcancer.2012.06.001
15. Gerez, J, Tedesco, L, Bonfiglio, JJ, Fuertes, M, Barontini, M, Silberstein, S, et al. RSUME Inhibits VHL and Regulates its Tumor Suppressor Function. *Oncogene* (2015) 34:4855–66. doi: 10.1038/onc.2014.407
16. Antico Arciuch, VG, Tedesco, L, Fuertes, M, Arzt, E. Role of RSUME in Inflammation and Cancer. *FEBS Lett* (2015) 589:3330–5. doi: 10.1016/j.febslet.2015.07.048
17. Hergovich, A, Lisztwan, J, Barry, R, Ballschmieter, P, Krek, W. Regulation of Microtubule Stability by the Von Hippel-Lindau Tumour Suppressor Protein pVHL. *Nat Cell Biol* (2003) 5:64–70. doi: 10.1038/ncb899
18. Kuehn, EW, Walz, G, Benzing, T. Von Hippel-Lindau: A Tumor Suppressor Links Microtubules to Ciliogenesis and Cancer Development. *Cancer Res* (2007) 67:4537–40. doi: 10.1158/0008-5472.CAN-07-0391
19. Ohh, M, Yauch, RL, Lonergan, KM, Whaley, JM, Stemmer-Rachamimov, AO, Louis, DN, et al. The Von Hippel-Lindau Tumor Suppressor Protein Is Required for Proper Assembly of an Extracellular Fibronectin Matrix. *Mol Cell* (1998) 1:959–68. doi: 10.1016/S1097-2765(00)80096-9
20. Tang, N, Mack, F, Haase, VH, Simon, MC, Johnson, RS. pVHL Function is Essential for Endothelial Extracellular Matrix Deposition. *Mol Cell Biol* (2006) 26:2519–30. doi: 10.1128/MCB.26.7.2519-2530.2006
21. Stolle, C, Glenn, G, Zbar, B, Humphrey, JS, Choyke, P, Walther, M, et al. Improved Detection of Germline Mutations in the Von Hippel-Lindau Disease Tumor Suppressor Gene. *Hum Mutat* (1998) 12:417–23. doi: 10.1002/(SICI)1098-1004(1998)12:6<417::AID-HUMU8>3.0.CO;2-K
22. Kumar, PS, Venkatesh, K, Srikanth, L, Sarma, PVGK, Reddy, AR, Subramanian, S, et al. Novel Three Missense Mutations Observed in Von Hippel-Lindau Gene in a Patient Reported With Renal Cell Carcinoma. *Indian J Hum Genet* (2013) 19:373–6. doi: 10.4103/0971-6866.120809
23. Maher, ER, Webster, AR, Richards, FM, Green, JS, Crossey, PA, Payne, SJ, et al. Phenotypic Expression in Von Hippel-Lindau Disease: Correlations With Germline VHL Gene Mutations. *J Med Genet* (1996) 33:328–32. doi: 10.1136/jmg.33.4.328
24. McNeill, A, Rattenberry, E, Barber, R, Killick, P, MacDonald, F, Maher, ER. Genotype-Phenotype Correlations in VHL Exon Deletions. *Am J Med Genet A* (2009) 149A:2147–51. doi: 10.1002/ajmg.a.33023
25. Sansó, G, Rudaz, MCG, Levin, G, Barontini, M. Familial Isolated Pheochromocytoma Presenting a New Mutation in the Von Hippel-Lindau Gene. *Am J Hypertens* (2004) 17:1107–11. doi: 10.1016/j.amjhyper.2004.06.013
26. Ding, Z, German, P, Bai, S, Feng, Z, Gao, M, Si, W, et al. Agents That Stabilize Mutated Von Hippel-Lindau (VHL) Protein: Results of a High-Throughput Screen to Identify Compounds That Modulate VHL Proteostasis. *J Biomol Screen* (2012) 17:572–80. doi: 10.1177/1087057112436557
27. Ding, Z, Liang, J, Lu, Y, Yu, Q, Songyang, Z, Lin, S-Y, et al. A Retrovirus-Based Protein Complementation Assay Screen Reveals Functional AKT1-Binding Partners. *Proc Natl Acad Sci U.S.A.* (2006) 103:15014–9. doi: 10.1073/pnas.0606917103
28. Pennisi, PA, Barr, V, Nunez, NP, Stannard, B, Le Roith, D. Reduced Expression of Insulin-Like Growth Factor I Receptors in MCF-7 Breast Cancer Cells Leads to a More Metastatic Phenotype. *Cancer Res* (2002) 62 (22):6529–37.
29. Liu, XD, Yao, J, Tripathi, DN, Ding, Z, Xu, Y, Sun, M, et al. Autophagy Mediates HIF2α Degradation and Suppresses Renal Tumorigenesis. *Oncogene* (2015) 34:2450–60. doi: 10.1038/ONC.2014.199
30. Debnath, J, Muthuswamy, SK, Brugge, JS. Morphogenesis and Oncogenesis of MCF-10A Mammary Epithelial Acini Grown in Three-Dimensional Basement Membrane Cultures. *Methods* (2003) 30:256–68. doi: 10.1016/S1046-2023(03)00032-X
31. Od Nih OO. *GUIDE LABORATORY ANIMALS for the CARE and USE of Eighth Edition Committee for the Update of the Guide for the Care and Use of Laboratory Animals*. Washington, DC: The National Academies Press (2011).
32. Karczewski, KJ, Francioli, LC, Tiao, G, Cummings, BB, Alföldi, J, Wang, Q, et al. The Mutational Constraint Spectrum Quantified From Variation in 141,456 Humans. *Nature* (2020) 581:434–43. doi: 10.1038/S41586-020-2308-7
33. Wheeler, DL, Barrett, T, Benson, DA, Bryant, SH, Canese, K, Chetvernin, V, et al. Database Resources of the National Center for Biotechnology Information. *Nucleic Acids Res* (2007) 35:D5–D12. doi: 10.1093/NAR/GKL1031
34. Landrum, MJ, Lee, JM, Benson, M, Brown, GR, Chao, C, Chitipiralla, S, et al. ClinVar: Improving Access to Variant Interpretations and Supporting Evidence. *Nucleic Acids Res* (2018) 46:D1062–7. doi: 10.1093/NAR/GKX1153
35. Sim, NL, Kumar, P, Hu, J, Henikoff, S, Schneider, G, Ng, PC. SIFT Web Server: Predicting Effects of Amino Acid Substitutions on Proteins. *Nucleic Acids Res* (2012) 40:W452–7. doi: 10.1093/NAR/GKS539
36. Adzhubei, IA, Schmidt, S, Peshkin, L, Ramensky, VE, Gerasimova, A, Bork, P, et al. A Method and Server for Predicting Damaging Missense Mutations. *Nat Methods* (2010) 7:248–9. doi: 10.1038/NMETH0410-248
37. Steinhaus, R, Proft, S, Schuelke, M, Cooper, DN, Schwarz, JM, Seelow, D. Mutationtaster2021. *Nucleic Acids Res* (2021) 49:W446–51. doi: 10.1093/NAR/GKAB266
38. Desmet, FO, Hamroun, D, Lalande, M, Collod-Bëroud, G, Claustres, M, Béroud, C. Human Splicing Finder: An Online Bioinformatics Tool to Predict Splicing Signals. *Nucleic Acids Res* (2009) 37(9):e67. doi: 10.1093/NAR/GKP215
39. Richards, S, Aziz, N, Bale, S, Bick, D, Das, S, Gastier-Foster, J, et al. Standards and Guidelines for the Interpretation of Sequence Variants: A Joint Consensus Recommendation of the American College of Medical Genetics and Genomics and the Association for Molecular Pathology. *Genet Med* (2015) 17:405–23. doi: 10.1038/gim.2015.30
40. Kopanos, C, Tsiolkas, V, Kouris, A, Chapple, CE, Albarca Aguilera, M, Meyer, R, et al. VarSome: The Human Genomic Variant Search Engine. *Bioinformatics* (2019) 35:1978–80. doi: 10.1093/BIOINFORMATICS/BTY897
41. Van Molle, I, Thomann, A, Buckley, DL, So, EC, Lang, S, Crews, CM, et al. Dissecting Fragment-Based Lead Discovery at the Von Hippel-Lindau Protein:Hypoxia Inducible Factor 1α Protein-Protein Interface. *Chem Biol* (2012) 19:1300–12. doi: 10.1016/J.CHEMBIOL.2012.08.015
42. Guex, N, Peitsch, MC. SWISS-MODEL and the Swiss-PdbViewer: An Environment for Comparative Protein Modeling. *Electrophoresis* (1997) 18:2714–23. doi: 10.1002/ELPS.1150181505
43. Waterhouse, A, Bertoni, M, Bienert, S, Studer, G, Tauriello, G, Gumienny, R, et al. SWISS-MODEL: Homology Modelling of Protein Structures and Complexes. *Nucleic Acids Res* (2018) 46:W296–303. doi: 10.1093/NAR/GKY427
44. Olsson, MHM, SØndergaard, CR, Rostkowski, M, Jensen, JH. PROPKA3: Consistent Treatment of Internal and Surface Residues in Empirical pKa Predictions. *J Chem Theory Comput* (2011) 7:525–37. doi: 10.1021/CT100578Z
45. Case, D.A., Cerutti, DS, Cheatham, TE III, Darden, TA, Duke, RE, Kollman, PA, et al. *AMBER 2017*. San Francisco: University of California (2017). Available at: https://ambermd.org/doc12/Amber17.pdf.

46. Ryckaert, J-P, Ciccotti, G, Berendsen, HJC. Numerical Integration of the Cartesian Equations of Motion of a System With Constraints: Molecular Dynamics of N-Alkanes. *J Comput Phys* (1977) 23:327–41. doi: 10.1016/0021-9991(77)90098-5
47. Allen, MP, Tildesley, DJ. *Computer Simulation of Liquids*. New York: Oxford University Press (1991).
48. Åqvist, J, Wennerström, P, Nervall, M, Bjelic, S, Brandsdal, BO. Molecular Dynamics Simulations of Water and Biomolecules With a Monte Carlo Constant Pressure Algorithm. *Chem Phys Lett* (2004) 384:288–94. doi: 10.1016/j.cplett.2003.12.039
49. Essmann, U, Perera, L, Berkowitz, ML, Darden, T, Lee, H, Pedersen, LG. A Smooth Particle Mesh Ewald Method. *J Chem Phys* (1995) 103:8577–93. doi: 10.1063/1.470117
50. Genheden, S, Ryde, U. The MM/PBSA and MM/GBSA Methods to Estimate Ligand-Binding Affinities. *Expert Opin Drug Discovery* (2015) 10:449–61. doi: 10.1517/17460441.2015.1032936
51. Baker, NA, Sept, D, Joseph, S, Holst, MJ, McCammon, JA. Electrostatics of Nanosystems: Application to Microtubules and the Ribosome. *Proc Natl Acad Sci U.S.A.* (2001) 98:10037–41. doi: 10.1073/PNAS.181342398
52. Unni, S, Huang, Y, Hanson, RM, Tobias, M, Krishnan, S, Li, WW, et al. Web Servers and Services for Electrostatics Calculations With APBS and PDB2PQR. *J Comput Chem* (2011) 32:1488–91. doi: 10.1002/JCC.21720
53. Maher, ER, Neumann, HP, Richard, S. Von Hippel-Lindau Disease: A Clinical and Scientific Review. *Eur J Hum Genet* (2011) 19:617–23. doi: 10.1038/ejhg.2010.175
54. Carroll, VA, Ashcroft, M. Role of Hypoxia-Inducible Factor (HIF)-1alpha Versus HIF-2alpha in the Regulation of HIF Target Genes in Response to Hypoxia, Insulin-Like Growth Factor-I, or Loss of Von Hippel-Lindau Function: Implications for Targeting the HIF Pathway. *Cancer Res* (2006) 66:6264–70. doi: 10.1158/0008-5472.CAN-05-2519
55. Nguyen, HC, Yang, H, Fribourgh, JL, Wolfe, LS, Xiong, Y. Insights Into Cullin-RING E3 Ubiquitin Ligase Recruitment: Structure of the VHL-EloBC-Cul2 Complex. *Structure* (2015) 23:441–9. doi: 10.1016/J.STR.2014.12.014
56. Min, JH, Yang, H, Ivan, M, Gertler, F, Kaelin, WG, Pavietich, NP. Structure of an HIF-1alpha -pVHL Complex: Hydroxyproline Recognition in Signaling. *Science* (2002) 296:1886–9. doi: 10.1126/SCIENCE.1073440
57. Bangiyeva, V, Rosenbloom, A, Alexander, AE, Isanova, B, Popko, T, Schoenfeld, AR. Differences in Regulation of Tight Junctions and Cell Morphology Between VHL Mutations From Disease Subtypes. *BMC Cancer* (2009) 9:229. doi: 10.1186/1471-2407-9-229
58. Park, KS, Kim, JH, Shin, HW, Chung, KS, Im, DS, Lim, JH, et al. E2-EPF UCP Regulates Stability and Functions of Missense Mutant pVHL *via* Ubiquitin Mediated Proteolysis. *BMC Cancer* (2015) 15:800. doi: 10.1186/S12885-015-1786-8
59. Lanikova, L, Lorenzo, F, Yang, C, Vankayalapati, H, Drachtman, R, Divoky, V, et al. Novel Homozygous VHL Mutation in Exon 2 is Associated With Congenital Polycythemia But Not With Cancer. *Blood* (2013) 121:3918–24. doi: 10.1182/blood-2012-11-469296
60. Schoenfeld, AR, Davidowitz, EJ, Burk, RD. Elongin BC Complex Prevents Degradation of Von Hippel-Lindau Tumor Suppressor Gene Products. *Proc Natl Acad Sci U.S.A.* (2000) 97:8507–12. doi: 10.1073/PNAS.97.15.8507
61. Ding, Z, German, P, Bai, S, Reddy, AS, Liu, X-D, Sun, M, et al. Genetic and Pharmacological Strategies to Refunctionalize the Von Hippel Lindau R167Q Mutant Protein. *Cancer Res* (2014) 74:3127–36. doi: 10.1158/0008-5472.CAN-13-3213
62. Iliopoulos, O, Kibel, A, Gray, S, Kaelin, WG, Kaelin, WGJr. Tumour Suppression by the Human Von Hippel-Lindau Gene Product. *Nat Med* (1995) 1:822–6. doi: 10.1038/nm0895-822
63. Hansen, WJ, Ohh, M, Moslehi, J, Kondo, K, Kaelin, WG, Welch, WJ. Diverse Effects of Mutations in Exon II of the Von Hippel-Lindau (VHL) Tumor Suppressor Gene on the Interaction of pVHL With the Cytosolic Chaperonin and pVHL-Dependent Ubiquitin Ligase Activity. *Mol Cell Biol* (2002) 22:1947–60. doi: 10.1128/MCB.22.6.1947-1960.2002
64. Lonergan, KM, Iliopoulos, O, Ohh, M, Kamura, T, Conaway, RC, Conaway, JW, et al. Regulation of Hypoxia-Inducible mRNAs by the Von Hippel-Lindau Tumor Suppressor Protein Requires Binding to Complexes Containing Elongins B/C and Cul2. *Mol Cell Biol* (1998) 18:732–41. doi: 10.1128/MCB.18.2.732
65. Kishida, T, Lerman, MI, Zbar, B, Stackhouse, TM, Chen, F. Cellular Proteins That Bind the Von Hippel-Lindau Disease Gene Product: Mapping of Binding Domains and the Effect of Missense Mutations. *Cancer Res* (1995) 55 (20):4544–8.
66. Hacker, KE, Lee, CM, Rathmell, WK. VHL Type 2B Mutations Retain VBC Complex Form and Function. *PloS One* (2008) 3(11):e3801. doi: 10.1371/JOURNAL.PONE.0003801
67. Miller, F, Kentsis, A, Osman, R, Pan, ZQ. Inactivation of VHL by Tumorigenic Mutations That Disrupt Dynamic Coupling of the pVHL.Hypoxia-Inducible Transcription Factor-1alpha Complex. *J Biol Chem* (2005) 280:7985–96. doi: 10.1074/JBC.M413160200
68. Rathmell, WK, Hickey, MM, Bezman, NA, Chmielecki, CA, Carraway, NC, Simon, MC. *In Vitro* and *In Vivo* Models Analyzing Von Hippel-Lindau Disease-Specific Mutations. *Cancer Res* (2004) 64:8595–603. doi: 10.1158/0008-5472.CAN-04-1430
69. Clifford, SC, Cockman, ME, Smallwood, AC, Mole, DR, Woodward, ER, Maxwell, PH, et al. Contrasting Effects on HIF-1alpha Regulation by Disease-Causing pVHL Mutations Correlate With Patterns of Tumourigenesis in Von Hippel-Lindau Disease. *Hum Mol Genet* (2001) 10:1029–38. doi: 10.1093/HMG/10.10.1029
70. Knauth, K, Bex, C, Jemth, P, Buchberger, A. Renal Cell Carcinoma Risk in Type 2 Von Hippel-Lindau Disease Correlates With Defects in pVHL Stability and HIF-1alpha Interactions. *Oncogene* (2006) 25:370–7. doi: 10.1038/SJ.ONC.1209062
71. Hoffman, MA, Ohh, M, Yang, H, Klco, JM, Ivan, M, Kaelin, WGJr., et al. Von Hippel-Lindau Protein Mutants Linked to Type 2C VHL Disease Preserve the Ability to Downregulate HIF. *Hum Mol Genet* (2001) 10:1019–27. doi: 10.1093/HMG/10.10.1019
72. Wiesener, MS, Seyfarth, M, Warnecke, C, Jürgensen, JS, Rosenberger, C, Morgan, NV, et al. Paraneoplastic Erythrocytosis Associated With an Inactivating Point Mutation of the Von Hippel-Lindau Gene in a Renal Cell Carcinoma. *Blood* (2002) 99:3562–5. doi: 10.1182/BLOOD.V99.10.3562
73. Li, M, Kim, WY. Two Sides to Every Story: The HIF-Dependent and HIF-Independent Functions of pVHL. *J Cell Mol Med* (2011) 15:187–95. doi: 10.1111/J.1582-4934.2010.01238.X
74. Stickle, NH, Chung, J, Klco, JM, Hill, RP, Kaelin, WG, Ohh, M. pVHL Modification by NEDD8 is Required for Fibronectin Matrix Assembly and Suppression of Tumor Development. *Mol Cell Biol* (2004) 24:3251–61. doi: 10.1128/MCB.24.8.3251
75. Russell, RC, Ohh, M. NEDD8 Acts as a "Molecular Switch" Defining the Functional Selectivity of VHL. *EMBO Rep* (2008) 9:486–91. doi: 10.1038/EMBOR.2008.19

Conflict of Interest: The authors declare that the research was conducted in the absence of any commercial or financial relationships that could be construed as a potential conflict of interest.

frontiers in Endocrinology

REVIEW
published: 21 March 2022
doi: 10.3389/fendo.2022.840971

Grading Central Diabetes Insipidus Induced by Immune Checkpoint Inhibitors: A Challenging Task

*Agnese Barnabei[1], Lidia Strigari[2], Andrea Corsello[3], Rosa Maria Paragliola[3], Giovanni Maria Iannantuono[4], Roberto Salvatori[5], Salvatore Maria Corsello[3,6] and Francesco Torino[4]**

[1] Endocrinology Unit, Presidio Ospedaliero Santo Spirito in Sassia, Azienda Sanitaria Locale Roma 1, Rome, Italy, [2] Medical Physics Department, Istituto di Ricovero e Cura a Carattere Scientifico (IRCCS) Azienda Ospedaliero-Universitaria di Bologna, Bologna, Italy, [3] Department of Translational Medicine and Surgery, Unit of Endocrinology, Università Cattolica del Sacro Cuore-Fondazione Policlinico "Gemelli" Istituto di Ricovero e Cura a Carattere Scientifico (IRCCS), Rome, Italy, [4] Department of Systems Medicine, Medical Oncology, Tor Vergata University of Rome, Rome, Italy, [5] Division of Endocrinology, Diabetes, and Metabolism and Pituitary Center, Johns Hopkins School of Medicine, Baltimore, MD, United States, [6] UniCamillus Chair of Endocrinology, Saint Camillus International University of Health Sciences, Rome, Italy

Central diabetes insipidus (CDI) is a rare endocrine disease deriving from an insufficient production or secretion of anti-diuretic hormone. Recently, CDI has been reported as a rare side effect triggered by immune checkpoint inhibitors (ICI) in cancer patients. Despite its current rarity, CDI triggered by ICI is expected to affect an increasing number of patients because of the expanding use of these effective drugs in a growing number of solid and hematologic malignancies. An appropriate assessment of the severity of adverse events induced by anticancer agents is crucial in their management, including dosing adjustment and temporary withdrawal or discontinuation treatment. However, assessment of the severity of CDI induced by ICI may be challenging, as its main signs and symptoms (polyuria, dehydration, weight loss, and hypernatremia) can be incompletely graded. Indeed, the current grading system of toxicity induced by anticancer treatments does not include polyuria. Additionally, dehydration in patients affected by diabetes insipidus, including ICI-induced CDI, is different in certain aspects from that due to other conditions seen in cancer patients, such as vomiting and diarrhea. This prompted us to reflect on the need to grade polyuria, and how to grade it, and to consider a specific grading system for dehydration associated with CDI induced by ICI. Here we propose a new grading system for polyuria and dehydration, as critical symptoms of the CDI syndrome occurring in patients on ICI treatment, to obtain better management of both the adverse event and the triggering drugs.

Keywords: central diabetes insipidus, immune checkpoint inhibitors, grading system, CTCAE, endocrine toxicities

OPEN ACCESS

Edited by:
Antonino Belfiore, University of Catania, Italy

Reviewed by:
Giampaolo Papi, Local Health Unit of Modena, Italy
Silvia Martina Ferrari, University of Pisa, Italy

***Correspondence:**
Francesco Torino
torino@med.uniroma2.it

Specialty section:
This article was submitted to Cancer Endocrinology, a section of the journal Frontiers in Endocrinology

Received: *21 December 2021*
Accepted: *08 February 2022*
Published: *21 March 2022*

Citation:
Barnabei A, Strigari L, Corsello A, Paragliola RM, Iannantuono GM, Salvatori R, Corsello SM and Torino F (2022) Grading Central Diabetes Insipidus Induced by Immune Checkpoint Inhibitors: A Challenging Task. Front. Endocrinol. 13:840971. doi: 10.3389/fendo.2022.840971

INTRODUCTION

Anti-diuretic hormone (ADH) (also called Vasopressin) is produced by hypothalamic supraoptic and paraventricular nuclei, stored and secreted at the level of the posterior pituitary. ADH is initially synthesized as a pro-hormone (pre-pro-ADH) that is cleaved generating a 9-amino-acid hormone (ADH) and equimolar amounts of a more stable C-terminus peptide called copeptin. ADH causes water

reabsorption through the V2 receptor-mediated insertion of aquaporin water channels into the luminal membrane in the collecting duct of the kidney (1). Diabetes insipidus (DI) manifests when a decreased activity of ADH occurs. It can be due to partial or complete secretion failure (central DI, CDI), or to renal resistance to its effect (nephrogenic DI, NDI) (2). CDI may derive from injury to the pituitary or the hypothalamus, while NDI is due to insensitivity of the kidney receptor to ADH. The leading causes of CDI and NDI are reported in **Table 1**. The work-up for CDI diagnosis in cancer patients follows the recognition of critical early symptoms, including polyuria, nocturia, excessive thirst, polydipsia, dehydration, weight loss, lethargy, and confusion (44, 45). Once CDI is suspected, endocrinological consultation is recommended (2). As the first diagnostic step, the presence of hypotonic polyuria should be confirmed, then the type of polyuria-polydipsia disorder (central DI vs. nephrogenic DI vs. primary polydipsia) should be identified (44, 45). To this aim, the endocrinologist will opt either to require the water deprivation test (WDT) or the hypertonic saline infusion test, along with serum copeptin measurements (45). Once the disorder is recognized, the underlying etiology needs to be identified among several potential causes, based on an accurate medical history and choosing the appropriate biochemical and imaging tests (44, 45).

The consequence of DI is a variably decreased ability to concentrate urine, leading to polyuria and polydipsia. However, polyuria (arbitrarily defined as a urine volume >3 Liters/day or ≥50 ml/Kg/24 hours) is considered the hallmark of DI and may arise suddenly in CDI, being usually more insidious in NDI (44). The grade of polyuria severity depends on the total solute load, the circulating volume, and the DI severity. Nocturia may be the main symptom in mild DI and the first clue to its diagnosis (2, 44). When DI derives from an injury to the hypothalamus-pituitary (CDI), it may be accompanied by deficiency of anterior pituitary hormones such as adrenocorticotropic hormone (ACTH), resulting in adrenal

TABLE 1 | Causes of central (injury to the pituitary and/or hypothalamus) and nephrogenic diabetes insipidus.

	Central diabetes insipidus	Nephrogenic diabetes insipidus
Autoimmune/ Inflammatory (2–6)	•Lymphocytic hypophysitis •Xanthogranulomatous hypophysitis •IgG4 disease •Anti-vasopressin neuron antibodies •Guillain-Barré syndrome	—
Congenital (genetic) (1, 7–12)	•AVP-neurophysin II gene alterations •Wolfram (DIDMOAD) syndrome •Septo-optic dysplasia •Schinzel-Giedion syndrome •Culler-Jones syndrome •Alstrom syndrome •Hartsfield syndrome •Webb-Dattani syndrome •X-linked defects with subnormal AVP levels	•Aquaporin-2 channel gene alterations •X-linked V-2 receptor gene alterations •PMSE syndrome (polyhydramnios, megalencephaly, and symptomatic epilepsy) •Type 4b Bartter syndrome
Drugs/toxins (4, 13–29)	•Temozolomide •Immune checkpoint inhibitors •Phenytoin •Ethyl alcohol, snake venom	•Lithium •Demeclocycline, Methoxyflurane •Cisplatin, pemetrexed •Aminoglycosides, amphotericin B
Granulomatous or systemic disease (4, 30–33)	•Sarcoidosis •Granulomatous hypophysitis •Langerhans' cell histiocytosis •Erdheim-Chester disease	•Amyloidosis •Sarcoidosis •Sjogren's syndrome
Infectious (2–4, 34)	•Meningitis, encephalitis •Tuberculosis •Pituitary or hypothalamic abscess	—
Neoplastic (4, 35–37)	•Craniopharyngioma, germinoma, meningioma •Invasive pituitary macroadenoma •Pituitary and/or hypothalamus metastasis	•Multiple myeloma
Trauma (38–42)	•Deceleration injury •Intracranial surgery •Transsphenoidal pituitary surgery	—
Vascular (4, 43)	•Hypothalamic infarction/hemorrhage •Cerebral infarction/hemorrhage •Anterior communicating artery ligation/ aneurysm •Sheehan's syndrome •Sickle cell disease	•Renal infarction •Sickle cell disease
Renal disease (1–4)	—	•Chronic kidney disease •Polycystic kidney disease •Obstructive uropathy
Metabolic (1–4)	—	•Hypokalemia •Hypercalcemia

insufficiency, TSH in central hypothyroidism, gonadotropins in hypogonadism, and deficit of growth hormone and prolactin (3, 44). Notably, in mild CDI, polyuria may not be revealed until the adrenal insufficiency is treated since cortisol deficiency increases fluid reabsorption and ADH release and reduces glomerular filtration rate (44). When thirst mechanisms are intact, and access to water is accessible, DI does not result in dehydration and overt hypernatremia (defined as a serum Na >145 mEq/L) (2, 3, 44, 45). Conversely, if thirst or access to water (or both) is somewhat impaired, the persistence of polyuria may cause fluid depletion, leading to hypernatremia and a rapid weight loss (2, 44). This, in turn, may also reduce the effective circulating volume (hypovolemia), causing impairment of tissue and organ perfusion. If severe hypovolemia is not timely corrected, ischemic end-organ damage occurs, leading to life-threatening conditions, up to death if patients are in shock (or affected by other severe comorbidities) (46). Unrecognized or new-onset DI leading to symptomatic hypernatremia in a patient with altered mental status, impaired thirst mechanism, or restricted access to water, may become an emergency condition. In particular, hypothalamic disorders (e.g., tumors, granulomatous disorders, and vascular disease) can result in both DI and impaired thirst sensation ("adipsic DI") (2, 44, 46). Notably, cancer patients may not suffer from any of those conditions, but they may reduce their fluid intake due to nausea, vomiting, fatigue, and malaise, symptoms frequently caused by anticancer treatments and malignancy itself. These conditions may hamper compensating hypernatremia by drinking, leading to a rapid and potentially severe worsening of DI.

Herein, we focused on CDI in cancer patients on treatment with immune checkpoint inhibitors (ICI) and the hurdles of assessing its severity in this subgroup of patients.

CDI IN CANCER PATIENTS

In cancer patients, CDI may arise when local malignancies or metastases compress or infiltrate the posterior pituitary or the supraoptic/paraventricular nuclei of the hypothalamus, or when the function of these structures is impaired by anticancer treatments, such as brain surgery and/or radiotherapy. CDI is rarely diagnosed as a paraneoplastic syndrome (3, 47) or as a side effect of certain anticancer drugs (i.e., temozolomide) (13–16). In recent years, CDI has been reported in a limited number of cancer patients on ICI (17–28). Three classes of ICI are currently available in the clinic: anti-CTLA4 monoclonal antibodies (anti-CTLA4 mAb) and monoclonal antibodies targeting the programmed cell death receptor-1 (PD-1) or its ligands (PD-L1) (anti-PD1 mAb and anti-PDL1 mAb) (48). ICI have demonstrated improvements in survival in patients affected by several malignancies, and their use is expected to increase in the near future with further indications and new agents. ICI act by restoring the immune competence against cancer cells after escaping the control of the immune system (49). However, ICI may trigger several autoimmunity/autoinflammatory adverse events (irAEs) intimately related to their mechanism of action, i.e., the selective stimulation of the host immune system (48, 50). Endocrine irAEs are among the most frequent ICI-related toxicities, being thyroid and pituitary dysfunction prevalent (51–53).

CDI IN PATIENTS ON TREATMENT WITH ICI

CDI induced by ICI is a rare endocrine irAE. Bai et al., in the WHO global database of individual case safety reports (54), in the period between January 2011 and March 2019, found a total of 6,089 ICI-related endocrine side effects. Out of these side effects, 1,144 (18.8%) were pituitary events, including hypophysitis (835 reports), hypopituitarism (268 reports), pituitary enlargement (52), other (18), while CDI was reported in 7 out of 1,072 (0.7%) of the registered hypophysitis/hypopituitarism cases. Recently, we systematically reviewed the literature and found eleven papers reporting on patients who suffered from ICI-induced CDI (Barnabei et al., accepted manuscript; in press). In five of those cases, CDI was diagnosed in the context of a panhypophysitis induced by ipilimumab (an anti-CTLA4 mAb): in three of them, ipilimumab was administered as a single agent (18–20), while in the other two cases, ipilimumab was administered in combination with nivolumab (an anti-PD1 mAb) (21, 22). In four of the 11 cases, CDI was diagnosed as an isolated endocrine irAE: the triggering drug was either avelumab (an anti-PDL1 mAb) (23), nivolumab (an anti-PD1 mAb) (24), or sintilimab (an anti-PD1 mAb) (25), while in the fourth case, CDI was reported in a patient who received a combination treatment (tremelimumab + durvalumab, an anti-CTLA4 mA and an anti-PDL1 mAb, respectively) (26). In another case, CDI occurred in the context of hypothalamitis caused by atezolizumab (an anti-PDL1 mAb) (28). In the last case, CDI was reported in a patient on nivolumab, diagnosed with a concomitant anterior pituitary metastasis (27). The analysis of those case reports did not provide unifying clinical features of the ICI-induced CDI syndrome. Indeed, the work-up that led to the diagnosis and even terms used to describe the CDI syndrome varied. Obviously, once CDI was diagnosed, therapy with vasopressin or its longer acting analog de-amino D-arginine vasopressin (DDAVP or desmopressin) was rapidly started in most cases, and compensation was obtained, but information about how long replacement therapy was continued is unavailable in many reports. Also, the management of the causal drug(s) varied, as in two cases, the anticancer treatment was transiently stopped, in two cases completed, while in the other 9 cases, ICI was permanently discontinued. However, the reasons leading to either maintenance or withdrawal of the triggering ICI(s) were based on clinical judgment, in the absence of specific guidelines for the management of CDI as an irAE induced by ICI.

Studies exploring the pathogenic mechanisms leading to the onset of CDI in patients on ICIs are currently unavailable. It is speculated that autoimmunity triggered by these drugs might impair the anterior pituitary leading to the inflammatory damage of the posterior pituitary or both (51, 55–57). The hypothesis reflects the pathogenesis of other ICI-induced organ damage, including thyroid and other endocrine glands (58, 59). Interestingly, selective injury to the posterior pituitary or the hypothalamus has been

suggested. Specifically, the expression of the PD-L1 on hypothalamic cells of a primate has been recently demonstrated (60), providing the basis for a potential explanation for the onset of hypothalamitis that occurred during treatment with atezolizumab (28). Histological data would be essential in clarifying the pathogenesis of ICI-induced CDI; however, biopsy specimens are difficult to obtain for various reasons, including the unethicality of the procedure in certain clinical conditions. Therefore, studies exploiting autoimmunity antibodies in this subgroup of patients would be essential (61–64).

As in other rare irAEs triggered by ICI (65), with the growing clinical use of these agents, a better knowledge of the CDI syndrome induced by ICI may help oncologists early suspect its onset and early activation endocrinologist consultation. Moreover, a specific grading system capable of adequately assessing the severity of CDI as an irAE triggered by ICI would be helpful in the choice of maintaining, delaying, or withdrawing the causative drug(s). However, some hurdles need to be overcome.

EMERGING PROBLEMS IN GRADING ICI-INDUCED CDI

Anticancer drugs have a narrow therapeutic range. Therefore, their starting dose is carefully assessed in clinical practice, based on the drug schedule, patient's parameters (i.e., performance status, comorbidities, age, organ function impairments, etc.), and, when available, pharmacogenetic factors predicting toxicity (i.e., polymorphisms of dihydropyrimidine dehydrogenase gene if fluoropyrimidines will be used, etc.) (63, 64, 66, 67). After that, the management of anticancer drugs includes the severity of adverse events (level of toxicity) reported after each administration, measured according to the Common Terminology Criteria for Adverse Events (CTCAE) (68). In detail, CTCAE is an updated list of terms describing adverse events (AE) commonly encountered in oncology practice and research, intended to be an agreed-on terminology for the designation, reporting, and grading of AE. Each term indicating an AE is defined, and the severity of AE is classified according to a 5-level scale corresponding to increasing levels of severity (from mild, categorized as grade 1, to patient's death due to toxicity, categorized as grade 5). Laboratory parameters or clinical features are used to grade the severity of each AE (examples in **Table 2**). The CTCAE grading system, through the objective assessment of toxicity experienced by single patients at each treatment administration, informs clinicians if dose adjustments to the treatment plan are needed (CTCAE). Consistently, the management of ICI is based on the level of the reported toxicity, assessed according to the current CTCAE grading system, recently updated including irAEs. Based on CTCAE assessment, the major scientific societies (e.g., ESMO, ASCO, SITC, NCCN) provided detailed guidelines for managing ICI-related toxicities, including endocrine irAEs (69–72). However, recommendations for the management of the causal drug(s) in patients diagnosed with ICI-induced CDI are not yet available, presumably due to the rarity of this irAE. Only the NCCN guidelines suggest "considering workup for diabetes insipidus if a patient complains of polyuria/polydipsia and elevated natremia" (NCCN). However, as CDI is emerging as a new irAe induced by ICI, a reflection on the potential hurdles in assessing the severity of the related symptoms has appeared as timely.

It is widely agreed that polyuria is the hallmark of DI. Similarly, it is well known that polyuria in DI, if not compensated (by adequate fluid intake or vasopressin or desmopressin), may lead to hypernatremia, dehydration, and weight loss. Indeed, the ADH deficit is responsible for pure water loss, leading to elevation in serum osmolality and sodium concentration and, therefore, to the passage of water from the cells into extracellular fluid (due to an osmotic gradient) (3, 46, 47). As in DI approximately two-thirds of the pure water loss derives from the intracellular fluid, the condition is more appropriately defined as "dehydration" than "hypovolemia" (46). Importantly, patients with pure water loss display the symptoms of hypernatremia (produced by the water deficit) before those of marked extracellular fluid depletion (46). Therefore, the assessment of polyuria, dehydration, and hypernatremia are the three critical components of the DI syndrome to consider in evaluating CDI severity. However, in the current CTCAE grading system hypernatremia and dehydration are graded, but not polyuria (**Table 2**) (68). The closer condition to

TABLE 2 | Toxicity level of the main symptoms (dehydration, hypernatremia, weight loss) of diabetes insipidus according to the current CTCAE grading system (version 5.0).

	Grade 1	Grade 2	Grade 3	Grade 4	Grade 5
Dehydration	Increased oral fluids indicated; dry mucous membranes; diminished skin turgor	IV fluids indicated	Hospitalization indicated	Life-threatening consequences; urgent intervention indicated	Death
Definition: A disorder characterized by excessive loss of water from the body. It is usually caused by severe diarrhea, vomiting or diaphoresis.					
Hypernatremia	>ULN - 150 mmol/L	>150 - 155 mmol/L; intervention initiated	>155 - 160 mmol/L; hospitalization indicated	>160 mmol/L; life-threatening consequences	Death
Definition: A disorder characterized by laboratory test results that indicate an elevation in the concentration of sodium in the blood.					
Weight loss	5 to <10% from baseline; intervention not indicated	10 - <20% from baseline; nutritional support indicated	>=20% from baseline; tube feeding or TPN indicated	–	–
Definition: A finding characterized by a decrease in overall body weight; for pediatrics, less than the baseline growth curve.					
Urinary frequency	Present	Limiting instrumental ADL; medical management indicated	–	–	–
Definition: A disorder characterized by urination at short intervals					

ADL, activities of daily living; IV, intravenous; TPN, total parenteral nutrition; ULN, upper limits of normal values.

polyuria categorized in the CTCAE grading system could be "urinary frequency", defined as "a disorder characterized by urination at short intervals" (68). Grade 1 urinary frequency is determined as "present", while grade 2 occurs when urinary frequency limits instrumental ADL and/or medical management is/are indicated (**Table 2**). However, according to its definition, urinary frequency is a synonym of pollakiuria, which describes the frequent elimination of normal volumes of daily urine, while polyuria indicates the urination of larger than normal urine volume. It could be speculated that grading polyuria could not be necessary to assess the severity of ICI-induced CDI, as hypernatremia and dehydration provide enough information about the seriousness of DI. However, in patients affected by CDI, normal natremia or mild hypernatremia, like mild dehydration, may not be informative about the severity of the condition, as patients may compensate through a variably high intake fluid. Notably, the compensation obtained by drinking could mask the severity of DI if polyuria (and polydipsia) are not considered in the evaluation. In other words, the patient on ICI who develops CDI could present with mild hypernatremia or even normal values of natremia and/or mild (or no) dehydration, at the cost of an increased fluid intake. Importantly, the patient's conditions may rapidly worsen if not adequately diagnosed and assessed. Therefore, polyuria seems to be the key symptom to evaluate not only to obtain an early diagnosis of CDI but also to estimate the severity of ICI-induced CDI (essential in the further management of ICI).

Moreover, other symptoms are reported among those that may worsen the "day and night" quality of life of patients affected by DI (e.g., thirst and the compelling need for quick water drinking, urinary frequency, nocturia, and the quality of sleeping, etc.). These symptoms should also be considered in the comprehensive evaluation of ICI-induced CDI and its management.

Finally, the assessment of dehydration related to DI needs careful considerations in cancer patients. In the current CTCAE grading system, the assessment of dehydration severity is not quantitative, based on the need for fluid supplementation and the level of assistance required by the patient (**Table 2**) (68). This is a proper evaluation in patients presenting with loss of fluids due to diarrhea and vomiting. Notably, diarrhea and vomiting, even in their severe forms, may lead to weight loss in a longer time compared with the "rapid" (in a few hours) weight loss induced by polyuria due to DI. This highlights the need for a proper grading system for dehydration in the context of DI, which would be helpful particularly when dehydration occurs in patients with CDI induced by ICI.

CAN ICI-INDUCED CDI BE BETTER ASSESSED?

In our opinion, the assessment of ICI-induced CDI severity would improve if a quantitative evaluation of both polyuria and dehydration/weight loss is considered. In the literature, approaches considering the quantitative assessment of these symptoms are available.

Vedig (73) identified different severity levels of polyuria based on the loss of urine volume/body weight unit/hour and arbitrarily classified polyuria into two grades: mild (<3ml/kg/h) and severe (>7 ml/kg/h for 4-6 h). To respect the standard CTCAE setting, where toxicities are classified into five severity levels, we suggest maintaining the two grades as proposed by Vedig (i.e., mild = grade 1 and severe = grade 3), adding both the grade 2 level, corresponding to moderate polyuria (3-7 ml/kg/h) and grade 4, corresponding to a life-threatening condition (**Table 2**). In the last level, patients with any grade polyuria associated with moderate-severe dehydration and/or moderate-severe hypernatremia should be included (while level 5 toxicity will remain the case of patient death due to treatment toxicity).

Regarding dehydration, it should be noted that the term is often used interchangeably with volume depletion/hypovolemia to indicate a reduction in the circulating volume because of vomiting, diarrhea, diuretics, bleedings, and polyuria as occurring in DI. To better classify the weight loss induced by polyuria due to DI, we considered the yardstick criteria of WDT, and the classification created to define weight loss in the pediatric setting. In infants and children, a quantitative approach is used to assess dehydration based on evaluating signs and symptoms related to volume depletion (74). Hypovolemia is divided into three grades: mild (corresponding to 3-5% volume loss), moderate (6-9% volume loss), and severe (≥10% volume loss). With this premise, to harmonize the scale as mentioned earlier with the standard 5-grade classification used in the CTCAE, we propose to adapt this classification of dehydration to the CTCAE setting by adding the level "mild", indicating a volume/weight loss <3% to the other toxicity levels (considering 3-5% volume loss as moderate, i.e., G2; 6-9% volume loss as sever, i.e., G3; ≥10% volume/weight loss or a shock condition as life-threatening, i.e., G4 (G5 defining death occurring due to treatment toxicity) (**Table 3**). Additionally, considering the time frame in which dehydration ensues may further improve the assessment. This is because dehydration due to loss of water (weight loss) occurring in moderate-severe DI is typically more

TABLE 3 | Suggested classification of polyuria and dehydration in the ICI-induced CDI syndrome.

Grade	1 (mild)	2 (moderate)	3 (severe)	4 (life-threatening)	5
Polyuria	<3 ml/kg/h	3÷7 ml/kg/h	>7 ml/kg/h	Any grade polyuria + moderate-severe dehydration ± moderate-severe hypernatremia	Death
Dehydration	Loss of <3% body weight in 2 hours	Loss of 3 ÷ 5% body weight in 2 hours	Loss of 6 ÷ 9% body weight in 2 hours	Loss of ≥10% body weight in 2 hours or shock	Death

rapid compared to that caused by most other conditions (e.g., diarrhea or vomiting). Therefore, we suggest grading the severity of polyuria-induced dehydration in patients developing ICI-induced CDI, considering weight loss/unit of time (another quantitative assessment) (**Table 3**). This derives from the fact that weight loss/unit of time is used in the WDT, an essential tool in diagnosing DI. WDT measures the capacity of the kidney to concentrate urine in response to dehydration. It can also assess kidney response to desmopressin, verifying if replacement with desmopressin can correct the defect identified in urine concentrating ability. Weight, urine volume, and serum and urine osmolality are measured at baseline and every two hours along with the test. WDT ends if thirst becomes unbearable or if the patient loses >5% initial weight, as measured at each unit of time (two hours) (2, 44, 45). Notably, in older patient excessive fluid loss often presents with nonspecific signs and symptoms, being acute weight loss the most specific sign for hypovolemia. As there is less water in fat than muscle, older individuals have lower total body water (relative to weight). Consequently, for a given degree of fluid loss, those individuals will have a more significant reduction in extracellular fluid volume. Therefore, acute fluid loss reflects body weight loss, so that a two-liter of fluid loss corresponds to two-kilogram weight loss (46).

PRACTICAL MANAGEMENT OF PATIENTS DIAGNOSED WITH ICI-INDUCED CDI

Specific guidelines to properly manage patients who develop ICI-induced CDI are urgently needed. Meanwhile, we suggested managing ICI-induced CDI within a multidisciplinary team, including oncologists and endocrinologists (**Figure 1**). Endocrinology consultation should be required early, as soon as the patients or their caregivers report the onset of polyuria and polydipsia. In case of mild (grade 1 or moderate (grade 2) toxicity, patient hospitalization is not indicated, being recommended in case of grade 3 toxicity and mandatory in case of grade 4 toxicity. Replacement therapy is always indicated in the case of grade 2-4 toxicity, while in grade 1 toxicity, it should be considered by the endocrinologist based on the impact of symptoms (mainly polyuria) on the patient's quality of life. Fluid replacement can be obtained by oral intake in grade 1 polyuria, dehydration/weight loss, or hypernatremia. While vasopressin must be administered parenterally and has a short duration of action (2-8 hours), desmopressin's effect is longer (6-9 hours and possibly longer, often allowing for twice a day administration) and it can also be administered intranasally, sublingually, or orally (75). Oral and sublingual absorption rates are <1%, whereas intranasal is approximately 6% (76). The mean dose ratio of sublingual to intranasal DDAVP is 1:24 (77). Physicians should be familial with different modalities of ADH replacement, their duration of action and equivalencies when transitioning from one therapy to another one. Intravenous fluid replacement becomes recommended when toxicities are graded as 2-4, together with an hourly diuresis monitoring. Finally, in the case of ICI-induced CDI, the causal agent should not be withdrawn unless other life-threatening irAEs have been experienced or persist. This approach is commonly recommended in patients presenting with other endocrine irAEs (69–72). However, it should be noticed that, independently of the severity of CDI symptoms, the ICI administration should be delayed to when the toxicity lessens to G1 (mild) level or symptom(s) disappear, indicating a compensation of the dysfunction. The delay allows testing the efficacy of vasopressin or desmopressin and its dose titration in every patient. This is in the perspective of restarting ICI(s) as soon as clinically indicated, considering the need for cancer control. Importantly, patients on ICI and their caregivers should

	Grade 1	Grade 2	Grade 3	Grade 4	Grade 5
Endocrinological consultation					Death
Hospitalization	Not indicated		Recommended	Mandatory	
DDAVP (*)	Based on patient's QoL	YES (*)			
Liquid replacement	Oral	IV			
Hourly diuresis	No	YES			
ICI(s) management	• Continue ICI + close monitoring of polyuria, body weight loss (dehydration), hypernatremia	• Held ICI until polyuria, body weight loss (dehydration), hypernatremia revert to grade 1 toxicity or lower	• Held ICI until polyuria, body weight loss (dehydration), hypernatremia revert to grade 1 toxicity or lower. • Extreme caution recommended when restarting ICI(s) after grade 3/4 toxicity. • Permanently discontinue ICI only in case of other(s) G4 toxicity.		

DDAVP, desmopressin; * DDAVP dosing is empiric, depending on patient's response to the oral first dose; IV, intravenously; QoL, quality of life.

FIGURE 1 | The suggested management of desmopressin and ICI(s) in patients with ICI-induced CDI.

receive clear information on the importance of alerting the reference care team at the onset of polyuria, polydipsia, and weight loss to timely obtain the appropriate diagnostic work-up and treatment.

CONCLUSIONS

CDI is a rare side effect triggered by ICI, but with the expanding use of these effective drugs, it is expected to be increasingly diagnosed in cancer patients. The current assessment of the severity of ICI-induced CDI may be challenging. We suggested a new grading system of polyuria and dehydration, as critical symptoms of the CDI syndrome occurring in patients on ICI treatment, to obtain better management of both the adverse event and the triggering drugs. Our proposals are attempts to overcome the emerging hurdles in assessing ICI-induced CDI severity. Studies are ongoing to define the reliability of the suggested classifications in clinical practice. At the moment, the evaluation of the severity of ICI-induced CDI should be only based on dehydration and hypernatremia levels, assessed by using the current CTCAE grading system, while the management of patients and ICI(s) treatment should still be based on a case-by-case approach in a multidisciplinary team.

AUTHOR CONTRIBUTIONS

Conceptualization, AB, LS, RS, SC, and FT. Investigation, AB, AC, RP, GI, and FT. Data curation, AB, LS, RS, GI, SC, and FT. Writing—original draft preparation, AB, LS, RS, SC, and FT. Writing—review and editing, AB, LS, RS, SC, and FT. Visualization, AB, LS, GI, and FT. Supervision, AB, SC, and FT. All authors have read and agreed to the published version of the manuscript.

REFERENCES

1. Schrier RW. Vasopressin and Aquaporin 2 (AQP2) in Clinical Disorders of Water Homeostasis. *Semin Nephrol* (2008) 28:289–96. doi: 10.1016/j.semnephrol.2008.03.009
2. Ball S, Feingold KR, Anawalt B, Boyce A, Chrousos G, de Herder WW, et al. *Diabetes Insipidus. Endotext*. South Dartmouth (MA: MDText.com, Inc (2018).
3. Robinson AG, Verbalis JG. Posterior Pituitary. In: S Melmed, K Polonsky, PR Larsen, et al, editors. *Williams Textbook of Endocrinology, 13th ed.* NX Amsterdam, The Netherlands: Elsevier (2015), ISBN: . p. 300–32.
4. Christ-Crain M, Bichet DG, Fenske WK, Goldman MB, Rittig S, Verbalis JG, et al. Diabetes Insipidus. *Nat Rev Dis Primers* (2019) 5:54. doi: 10.1038/s41572-019-0103-2
5. Shikuma J, Kan K, Ito R, Hara K, Sakai H, Miwa T, et al. Critical Review of IgG4-Related Hypophysitis. *Pituitary* (2017) 20:282–91. doi: 10.1007/s11102-016-0773-7
6. Kapoor E, Cartin-Ceba R, Specks U, Leavitt J, Erickson B, Erickson D. Pituitary Dysfunction in Granulomatosis With Polyangiitis: The Mayo Clinic Experience. *J Clin Endocrinol Metab* (2014) 99:3988–94. doi: 10.1210/jc.2014-1962
7. Fujiwara TM, Bichet DG. Molecular Biology of Hereditary Diabetes Insipidus. *J Am Soc Nephrol* (2005) 16:2836–46. doi: 10.1681/ASN.2005040371
8. Hedrich CM, Zachurzok-Buczynska A, Gawlik A, Russ S, Hahn G, Koehler K, et al. Autosomal Dominant Neurohypophyseal Diabetes Insipidus in Two Families. Molecular Analysis of the Vasopressin-Neurophysin II Gene and Functional Studies of Three Missense Mutations. *Horm Res* (2009) 71:111–9. doi: 10.1159/000183900
9. Christensen JH, Rittig S. Familial Neurohypophyseal Diabetes Insipidus-an Update. *Semin Nephrol* (2006) 26:209–23. doi: 10.1016/j.semnephrol.2006.03.003
10. Hansen LK, Rittig S, Robertson GL. Genetic Basis of Familial Neurohypophyseal Diabetes Insipidus. *Trends Endocrinol Metab* (1997) 8:363–72. doi: 10.1016/s1043-2760(97)00157-4
11. Rigoli L, Lombardo F, Di Bella C. Wolfram Syndrome and WFS1 Gene. *Clin Genet* (2011) 79:103–17. doi: 10.1111/j.1399-0004.2010.01522.x
12. Verkman AS. Aquaporins in Clinical Medicine. *Annu Rev Med* (2012) 63:303–16. doi: 10.1146/annurev-med-043010-193843
13. Faje AT, Nachtigall L, Wexler D, Miller KK, Klibanski A, Makimura H. Central Diabetes Insipidus: A Previously Unreported Side Effect of Temozolomide. *J Clin Endocrinol Metab* (2013) 98:3926–31. doi: 10.1210/jc.2013-2435
14. Kuo C, Foon D, Waters K, Cheung C, Margol AS. Central Diabetes Insipidus: A Rare Unreported Side Effect of Temozolomide in Pediatrics. *Pediatr Blood Cancer* (2020) 67:e28516. doi: 10.1002/pbc.28516
15. Mahiat C, Capes A, Duprez T, Whenham N, Duck L, Labriola L. Central Diabetes Insipidus Induced by Temozolomide: A Report of Two Cases. *J Oncol Pharm Pract* (2021) 27:1040–5. doi: 10.1177/1078155220961551
16. Zatelli MC, Ambrosio MR, Bondanelli M, Degli Uberti E. Pituitary Side Effects of Old and New Drugs. *J Endocrinol Invest* (2014) 37:917–23. doi: 10.1007/s40618-014-0133-2
17. Scherbaum WA. Autoimmune Diabetes Insipidus. *Handb Clin Neurol* (2021) 181:193–204. doi: 10.1016/B978-0-12-820683-6.00015-4
18. Dillard T, Yedinak CG, Alumkal J, Fleseriu M. Anti-CTLA-4 Antibody Therapy Associated Autoimmune Hypophysitis: Serious Immune-Related Adverse Events Across a Spectrum of Cancer Subtypes. *Pituitary* (2010) 13:29–38. doi: 10.1007/s11102-009-0193-z
19. Nallapaneni N, Mourya R, Raj Bhatt V, Malhotra S, Kishor Ganti A, Tendulkar KK. Ipilimumab-Induced Hypophysitis and Uveitis in a Patient With Metastatic Melanoma and a History of Ipilimumab-Induced Skin Rash. *J Natl Compr Canc Netw* (2014) 12:1077–81. doi: 10.6004/jnccn.2014.0105
20. Barnabei A, Carpano S, Chiefari A, Bianchini M, Lauretta R, Mormando M, et al. Case Report: Ipilimumab-Induced Panhypophysitis: An Infrequent Occurrence and Literature Review. *Front Oncol* (2020) 1:582394. doi: 10.3389/fonc.2020.582394
21. Gunawan F, George E, Roberts A. Combination Immune Checkpoint Inhibitor Therapy Nivolumab and Ipilimumab Associated With Multiple Endocrinopathies. *Endocrinol Diabetes Metab Case Rep* (2018) 2018:17–0146. doi: 10.1530/EDM-17-0146
22. Grami Z, Manjappachar N, Reddy Dereddi R. Diabetes Insipidus in Checkpoint Inhibitor Treatment and Acute Myeloid Leukemia. *Crit Care Med* (2020) 48(1):144 (abstract 323). doi: 10.1097/01.ccm.0000619648.08126.8f
23. Zhao C, Harsha Tella S, Del Rivero J, Kommalapati A, Ebenuwa I, Gulley J, et al. Anti-PD-L1 Treatment-Induced Central Diabetes Insipidus. *J Clin Endocrinol Metab* (2018) 103:365–9. doi: 10.1210/jc.2017-01905
24. Deligiorgi MV, Siasos G, Vergadis C, Trafalis D. Central Diabetes Insipidus Related to Anti-PD1 Protein Active Immunotherapy. *Int Immunopharm* (2020) 83:106427. doi: 10.1016/j.intimp.2020.106427
25. Yu M, Liu L, Shi P, Zhou H, Qian S, Chen K. Anti-PD-1 Treatment-Induced Immediate Central Diabetes Insipidus: A Case Report. *Immunotherapy* (2021) 13:1255–60. doi: 10.2217/imt-2020-0334
26. Brilli L, Calabrò L, Campanile M, Pilli T, Agostinis C, Cerase A, et al. Permanent Diabetes Insipidus in a Patient With Mesothelioma Treated With Immunotherapy. *Arch Endocrinol Metab* (2020) 64:483–6. doi: 10.20945/2359-3997000000221
27. Fosci M, Pigliaru F, Salcuni AS, Ghiani M, Cherchi MV, Calia MA, et al. Diabetes Insipidus Secondary to Nivolumab-Induced Neurohypophysitis and

Pituitary Metastasis. *Endocrinol Diabetes Metab Case Rep* (2021) 2021:20–0123. doi: 10.1530/EDM-20-0123
28. Tshuma N, Glynn N, Evanson J, Powles T, Drake WM. Hypothalamitis and Severe Hypothalamic Dysfunction Associated With Anti-Programmed Cell Death Ligand 1 Antibody Treatment. *Eur J Cancer* (2018) 104:247–9. doi: 10.1016/j.ejca.2018.09.016
29. Trepiccione F, Christensen BM. Lithium-Induced Nephrogenic Diabetes Insipidus: New Clinical and Experimental Findings. *J Nephrol* (2010) 23 (Suppl 16):S43–48.
30. Leger J, Velasquez A, Garel C, Hassan M, Czernichow P. Thickened Pituitary Stalk on Magnetic Resonance Imaging in Children With Central Diabetes Insipidus. *J Clin Endocrinol Metab* (1999) 84:1954–60. doi: 10.1210/jcem.84.6.5745
31. Stuart CA, Neelon FA, Lebovitz HE. Disordered Control of Thirst in Hypothalamic-Pituitary Sarcoidosis. *N Engl J Med* (1980) 303:1078–82. doi: 10.1056/NEJM198011063031902
32. Garovic VD, Clarke BL, Chilson TS, Specks U. Diabetes Insipidus and Anterior Pituitary Insufficiency as Presenting Features of Wegener's Granulomatosis. *Am J Kidney Dis* (2001) 37(1):E5. doi: 10.1016/s0272-6386(01)90002-2
33. Czarnecki EJ, Spickler EM. MR Demonstration of Wegener Granulomatosis of the Infundibulum, a Cause of Diabetes Insipidus. *AJNR Am J Neuroradiol* (1995) 16(4 Suppl):960–70.
34. Cabuk B, Caklılı M, Anık I, Ceylan S, Celik O, Ustün C. Primary Pituitary Abscess Case Series and a Review of the Literature. *Neuro Endocrinol Lett* (2019) 40:99–104.
35. Andereggen L, Hess B, Andres R, El-Koussy M, Mariani L, Raabe A, et al. A Ten-Year Follow-Up Study of Treatment Outcome of Craniopharyngiomas. *Swiss Med Wkly* (2018) 148:w14521. doi: 10.4414/smw.2018.14521
36. Kimmel DW, O'Neill BP. Systemic Cancer Presenting as Diabetes Insipidus. Clinical and Radiographic Features of 11 Patients With a Review of Metastatic-Induced Diabetes Insipidus. *Cancer* (1983) 52:23552363. doi: 10.1002/1097-0142(19831215)52:12<2355::aid-cncr2820521232>3.0.co;2-j
37. Sun R, Wang C, Zhong X, Wu Y, Tohoku J. Diabetes Insipidus as an Initial Presentation of Myelodysplastic Syndrome: Diagnosis With Single-Nucleotide Polymorphism Array-Based Karyotyping. *Exp Med* (2016) 238:305–10. doi: 10.1620/tjem.238.305
38. Hadjizacharia P, Beale EO, Inaba K, Chan LS, Demetriades D. Acute Diabetes Insipidus in Severe Head Injury: A Prospective Study. *J Am Coll Surg* (2008) 207:477–84. doi: 10.1016/j.jamcollsurg.2008.04.017
39. Tanji M, Mineharu Y, Kikuchi M, Nakagawa T, Sakamoto T, Yamashita M, et al. Intraoperative Cerebrospinal Fluid Leak Graded by Esposito Grade Is a Predictor for Diabetes Insipidus After Endoscopic Endonasal Pituitary Adenoma Resection. *World Neurosurg* (2021) S1878-8750:01802–7. doi: 10.1016/j.wneu.2021.11.090
40. Saldarriaga C, Lyssikatos C, Belyavskaya E, Keil M, Chittiboina P, Sinaii N, et al. Postoperative Diabetes Insipidus and Hyponatremia in Children After Transsphenoidal Surgery for Adrenocorticotropin Hormone and Growth Hormone Secreting Adenomas. *J Pediatr* (2018) 195:169–74. doi: 10.1016/j.jpeds.2017.11.042
41. Kristof RA, Rother M, Neuloh G, Klingmüller D. Incidence, Clinical Manifestations, and Course of Water and Electrolyte Metabolism Disturbances Following Transsphenoidal Pituitary Adenoma Surgery: A Prospective Observational Study. *J Neurosurg* (2009) 111:555–62. doi: 10.3171/2008.9.JNS08191
42. Hannon MJ, Sherlock M, Thompson CJ. Pituitary Dysfunction Following Traumatic Brain Injury or Subarachnoid Haemorrhage. *Best Pract Res Clin Endocrinol Metab* (2011) 25:783–98. doi: 10.1016/j.beem.2011.06.001
43. Kavanagh C, Uy NS. Nephrogenic Diabetes Insipidus. *Pediatr Clin North Am* (2019) 66:227–34. doi: 10.1016/j.pcl.2018.09.006
44. Garrahy A, Moran C, Thompson CJ. Diagnosis and Management of Central Diabetes Insipidus in Adults. *Clin Endocrinol (Oxf)* (2019) 90:23–30. doi: 10.1111/cen.13866
45. Gubbi S, Hannah-Shmouni F, Koch CA, Verbalis JG, Feingold KR, Anawalt B, et al. *Diagnostic Testing for Diabetes Insipidus*. Available at: www.endotext.org (Accessed on 21.10.2021).
46. Sterns RH. *Etiology, Clinical Manifestations, and Diagnosis of Volume Depletion in Adults* (2021). Available at: https://www.uptodate.com/contents/etiology-clinical-manifestations-and-diagnosis-of-volume-depletion-in-adults (Accessed on October 21st).
47. Krol TC, Wood WS. Bronchogenic Carcinoma and Diabetes Insipidus: Case Report and Review. *Cancer* (1982) 49:596–9. doi: 10.1002/1097-0142(19820201)49:3<596::aid-cncr2820490332>3.0.co;2-8
48. Wei SC, Duffy CR, Allison JP. Fundamental Mechanisms of Immune Checkpoint Blockade Therapy. *Cancer Discovery* (2018) 8:1069–86. doi: 10.1158/2159-8290.CD-18-0367
49. Pardoll DM. The Blockade of Immune Checkpoints in Cancer Immunotherapy. *Nat Rev Cancer* (2012) 12:252–64. doi: 10.1038/nrc3239
50. Sullivan RJ, Weber JS. Immune-Related Toxicities of Checkpoint Inhibitors: Mechanisms and Mitigation Strategies. *Nat Rev Drug Discov* (2021). doi: 10.1038/s41573-021-00259-5
51. Chang LS, Barroso-Sousa R, Tolaney SM, Hodi FS, Kaiser UB, Min L. Endocrine Toxicity of Cancer Immunotherapy Targeting Immune Checkpoints. *Endocr Rev* (2019) 40:17–65. doi: 10.1210/er.2018-00006
52. Torino F, Corsello SM, Salvatori R. Endocrinological Side-Effects of Immune Checkpoint Inhibitors. *Curr Opin Oncol* (2016) 4:278–87. doi: 10.1097/CCO.0000000000000293
53. Anderson B, Morganstein DL. Endocrine Toxicity of Cancer Immunotherapy: Clinical Challenges. *Endocr Connect* (2021) 10:R116–24. doi: 10.1530/EC-20-0489
54. Bai X, Chen X, Wu X, Huang Y, Zhuang Y, Chen Y, et al. Immune Checkpoint Inhibitor-Associated Pituitary Adverse Events: An Observational, Retrospective, Disproportionality Study. *J Endocrinol Invest* (2020) 43:1473–83. doi: 10.1007/s40618-020-01226-4
55. Türe U, De Bellis A, Harput MV, Bellastella G, Topcuoglu M, Yaltirik CK, et al. Hypothalamitis: A Novel Autoimmune Endocrine Disease. A Literature Review and Case Report. *J Clin Endocrinol Metab* (2021) 106:e415–29. doi: 10.1210/clinem/dgaa771
56. Di Dalmazi G, Ippolito S, Lupi I, Caturegli P. Hypophysitis Induced by Immune Checkpoint Inhibitors: A 10-Year Assessment. *Expert Rev Endocrinol Metab* (2019) 14:381–98. doi: 10.1080/17446651.2019.1701434
57. Guitar Shaikh M. Hypothalamic Dysfunction (Hypothalamic Syndromes). In: JAH Wass, PM Stewart, SA Amiel, MJ Davies, editors. *Oxford Textbook of Endocrinology and Diabetes*, *2 edn*. Oxford, UK: Oxford University Press (2011), ISBN-13: 9780199235292.
58. Ferrari SM, Fallahi P, Galetta F, Citi E, Benvenga S, Antonelli A. Thyroid Disorders Induced by Checkpoint Inhibitors. *Rev Endocr Metab Disord* (2018) 19:325–33. doi: 10.1007/s11154-018-9463-2
59. Ferrari SM, Fallahi P, Elia G, Ragusa F, Ruffilli I, Patrizio A, et al. Autoimmune Endocrine Dysfunctions Associated With Cancer Immunotherapies. *Int J Mol Sci* (2019) 20:2560. doi: 10.3390/ijms20102560
60. Iervasi E, Strangio A, Saverino D. Hypothalamic Expression of PD-L1: Does it Mediate Hypothalamitis? *Cell Mol Immunol* (2019) 16:625–6. doi: 10.1038/s41423-019-0232-2
61. Lupi I, Brancatella A, Cosottini M, Viola N, Lanzolla G, Sgrò D, et al. Clinical Heterogeneity of Hypophysitis Secondary to PD-1/PD-L1 Blockade: Insights From Four Cases. *Endocrinol Diabetes Metab Case Rep* (2019) 2019:19–0102. doi: 10.1530/EDM-19-0102
62. Bellastella G, Carbone C, Scappaticcio L, Cirillo P, Troiani T, Morgillo F, et al. Hypothalamic-Pituitary Autoimmunity in Patients Treated With Anti-PD-1 and Anti-PD-L1 Antibodies. *Cancers (Basel)* (2021) 13(16):4036. doi: 10.3390/cancers13164036
63. Chiloiro S, Russo F, Tartaglione T, Capoluongo ED. Molecular and Genetic Immune Biomarkers of Primary and Immune-Therapy Induced Hypophysitis: From Laboratories to the Clinical Practice. *J Pers Med* (2021) 11:1026. doi: 10.3390/jpm11101026
64. Bichet DG. *Treatment of Central Diabetes Insipidus. In: UpToDate* . Waltham, MA (Accessed on October 4th, 2021).
65. Schoenfeld SR, Aronow ME, Karp Leaf R, Dougan M, Reynolds KL. Diagnosis and Management of Rare Immune-Related Adverse Events. *Oncologist* (2020) 25:6–14. doi: 10.1634/theoncologist.2019-0083
66. Del Re M, Cinieri S, Michelucci A, Salvadori S, Loupakis F, Schirripa M, et al. DPYD* 6 Plays an Important Role in Fluoropyrimidine Toxicity in Addition to DPYD* 2A and C. 2846A> T: A Comprehensive Analysis in 1254 Patients. *Pharmacogenomics J* (2019) 19:556–63. doi: 10.1038/s41397-019-0077-1

67. Huang RS, Ratain MJ. Pharmacogenetics and Pharmacogenomics of Anticancer Agents. *CA Cancer J Clin* (2009) 59:42–55. doi: 10.3322/caac.20002
68. National Cancer Institute, National Institutes of Health and U.S. Department of Health and Human Services. *Common Terminology Criteria for Adverse Events. Version 5.0* (2017). Bethesda, MD. Available at: https://ctep.cancer.gov/protocoldevelopment/electronic_applications/ctc.htm (Accessed on Sept 14, 2021).
69. Haanen JBAG, Carbonnel F, Robert C, Kerr KM, Peters S, Larkin J, et al. European Society Medical Oncology (ESMO) Guidelines Committee. Management of Toxicities From Immunotherapy: ESMO Clinical Practice Guidelines for Diagnosis, Treatment and Follow-Up. *Ann Oncol* (2017) 28 (suppl 4):iv119–42. doi: 10.1093/annonc/mdx225
70. Brahmer JR, Lacchetti C, Schneider BJ, Atkins MB, Brassil KJ, Caterino JM, et al. Management of Immune-Related Adverse Events in Patients Treated With Immune Checkpoint Inhibitor Therapy: American Society of Clinical Oncology Clinical Practice Guideline. *J Clin Oncol* (2018) 36:1714–68. doi: 10.1200/JCO.2017.77.6385
71. Brahmer JR, Abu-Sbeih H, Ascierto PA, Brufsky J, Cappelli, Cortazar FB, et al. Society for Immunotherapy of Cancer (SITC) Clinical Practice Guideline on Immune Checkpoint Inhibitor-Related Adverse Events. *J Immunother Cancer* (2021) 9:e002435. doi: 10.1136/jitc-2021-002435
72. *NCCN Guidelines® for Management of Immunotherapy-Related Toxicities NCCN Guidelines for Supportive Care. Version 2.2021*. Available at: https://www.nccn.org/professionals/physician_gls/pdf/immunotherapy.pdf (Accessed on October 4th, 2021).
73. Vedig AE. Diabetes Insipidus. In: TE Oh, editor. *Intensive Care Manual*, *4th ed*. Oxford: Butterworth-Heinemann (1997), ISBN: . p. 451–9.
74. Somers MJ. *Clinical Assessment and Diagnosis of Hypovolemia (Dehydration) in Children. In: UpToDate* . Waltham, MA (Accessed on October 4th, 2021).
75. Rembratt A, Graugaard-Jensen C, Senderovitz T, Norgaard JP, Djurhuus JC. Pharmacokinetics and Pharmacodynamics of Desmopressin Administered Orally Versus Intravenously at Daytime Versus Night-Time in Healthy Men Aged 55-70 Years. *Eur J Clin Pharmacol* (2004) 60:397–402. doi: 10.1007/s00228-004-0781-9
76. Oiso Y, Robertson GL, Nørgaard JP, Juul KV. Clinical Review: Treatment of Neurohypophyseal Diabetes Insipidus. *J Clin Endocrinol Metab* (2013) 98:3958–67. doi: 10.1210/jc.2013-2326
77. Arima H, Oiso Y, Juul KV, Nørgaard JP. Efficacy and Safety of Desmopressin Orally Disintegrating Tablet in Patients With Central Diabetes Insipidus: Results of a Multicenter Open-Label Dose-Titration Study. *Endocr J* (2013) 60:1085–109. doi: 10.1507/endocrj.ej13-0165

Conflict of Interest: The authors declare that the research was conducted in the absence of any commercial or financial relationships that could be construed as a potential conflict of interest.

Publisher's Note: All claims expressed in this article are solely those of the authors and do not necessarily represent those of their affiliated organizations, or those of the publisher, the editors and the reviewers. Any product that may be evaluated in this article, or claim that may be made by its manufacturer, is not guaranteed or endorsed by the publisher.

frontiers in Endocrinology

ORIGINAL RESEARCH
published: 30 March 2022
doi: 10.3389/fendo.2022.841118

Methylome Analysis in Nonfunctioning and GH-Secreting Pituitary Adenomas

Giuseppe Giuffrida[1], Valeria D'Argenio[2,3], Francesco Ferraù[1,4], Vito Alessandro Lasorsa[3,5], Francesca Polito[6], Federica Aliquò[1], Marta Ragonese[1], Oana Ruxandra Cotta[4], Ylenia Alessi[4], Rosaria Oteri[6], Federica Di Maggio[3,5], Alessio Asmundo[7], Petronilla Daniela Romeo[1], Federica Spagnolo[4], Lucio Pastore[3,5], Filippo Flavio Angileri[7], Mario Capasso[3,5], Salvatore Cannavò[1,4†] and M'Hammed Aguennouz[6†]*

[1] Department of Human Pathology DETEV, University of Messina, Messina, Italy, [2] Department of Human Sciences and Quality of Life Promotion, San Raffaele Open University, Rome, Italy, [3] CEINGE-Biotecnologie Avanzate, Naples, Italy, [4] Endocrine Unit, "Gaetano Martino" University Hospital, Messina, Italy, [5] Department of Molecular Medicine and Medical Biotechnologies, University of Naples Federico II, Naples, Italy, [6] Department of Clinical and Experimental Medicine, University of Messina, Messina, Italy, [7] Department of Biomedical and Dental Sciences, and Morpho-Functional Imaging, University of Messina, Messina, Italy

OPEN ACCESS

Edited by:
Antonino Belfiore, University of Catania, Italy

Reviewed by:
Elisa Giannetta, Sapienza University of Rome, Italy
Antonio Gomez, University of Vic – Central University of Catalonia (UVic-UCC), Spain

***Correspondence:**
Francesco Ferraù
fferrau@unime.it

†These authors share senior authorship

Specialty section:
This article was submitted to Cancer Endocrinology, a section of the journal Frontiers in Endocrinology

Received: *21 December 2021*
Accepted: *21 February 2022*
Published: *30 March 2022*

Citation:
Giuffrida G, D'Argenio V, Ferraù F, Lasorsa VA, Polito F, Aliquò F, Ragonese M, Cotta OR, Alessi Y, Oteri R, Di Maggio F, Asmundo A, Romeo PD, Spagnolo F, Pastore L, Angileri FF, Capasso M, Cannavò S and Aguennouz M'H (2022) Methylome Analysis in Nonfunctioning and GH-Secreting Pituitary Adenomas. Front. Endocrinol. 13:841118. doi: 10.3389/fendo.2022.841118

Pituitary adenomas (PAs), usually benign lesions, can sometimes present with "aggressive" features (rapid growth, local invasiveness, scarce response to conventional treatments). Despite the fact that a few genetic alterations have been associated to this clinical behavior, the role of epigenetic modifications, mainly methylation and miRNAs activity, is now opening new frontiers in this field. We evaluated the methylation profile of 21 PA (11 GH-omas, 10 nonfunctioning tumors—NFPAs) samples from TNS surgery and 5 normal pituitaries, collected at our neurosurgery between 2015 and 2017. DNA was extracted and sequenced, selecting 184,841 target regions. Moreover, methylation profiles were correlated with demographic, radiological, and clinicopathological features. NFPAs showed higher methylation levels vs. GH-omas, with 178 differentially methylated regions (DMRs) mainly consisting of noncoding and intronic sequences, and mostly localized in the open sea regions. We also found three hypermethylated genes (*C7orf50*, *GNG7*, and *BAHCC1*) involved in tumorigenesis processes and potentially influencing pituitary tumor pathophysiology. Among the clinicopathological features, only the maximum diameter resulted significantly higher in NFPAs. Our data provide further evidence of the complex epigenetic background of pituitary tumors. In line with the current literature, we confirmed a significant prevalence of hypermethylation in NFPAs vs. GH-omas, whose pathophysiological consequence is yet to be defined.

Keywords: GH-OMAs, methylation, pituitary adenomas, NFPAs, pituitary tumors

INTRODUCTION

Pituitary adenomas (PAs) are distinguished by the presence of hormonal secretion and/or the expression of cell line-specific growth factors (1, 2). Although the presence of distant metastases is linked to the definition of pituitary carcinomas, even PAs can show an aggressive biological behavior, being characterized by local invasion, rapid proliferation, and scarce response to conventional treatments in up to 45% of cases (3, 4). In this context, there is a growing amount of data about PA (epi) genetic features predicting their behavior and/or their treatment response/relapse. In terms of genetics, for example, germinal mutations of the AIP (aryl hydrocarbon receptor-interacting protein) gene are associated to the development of familial isolated pituitary adenomas (FIPA), with early onset, higher aggressiveness, and resistance to somatostatin analogs (SSAs) (5). Similarly, the mutations involving the MEN1 oncosuppressor, linked to the homonymous syndrome, are associated with PAs in 15–50% of affected patients and a higher frequency of macroadenomas, that in 1/3 of cases are more invasive than non-MEN1 tumors (6). On the other hand, there is some evidence about somatic changes in sporadic pituitary tumors. These mutations can consist of sequence changes, qualitative alterations of chromosomes, or modification in their copy numbers, but they are often aspecific and infrequent, suggesting an additional oncogenic contribution from nonmutational factors (7, 8). Epigenetic modifications, which take place without altering the DNA sequences, comprehend both the alterations in mRNA transcription (nucleotides methylation, histones acetylation) and the different expression of long noncoding mRNAs (lncmRNAs) and, as also recently described by our group, microRNAs (miRNAs) (9). Methylation, that is, the apposition of methyl groups on DNA chains by specific enzymes—the DNA methyl-n-transferases (DMNTs)—is a physiological mechanism acting to silence specific genes in order to regulate their expression (8). Many DMNT isoforms are known, but DMNT1 and 3A are overexpressed in more aggressive PTs, with the DMNT1 more frequently found in macroadenomas (10). On the contrary, it seems that this DMNT hyperactivity would lead to hypomethylation of other DNA regions, which consequently result to being overtranscripted, as already observed in tumorigenesis processes (7). In such a context, the search for epigenetic changes can be crucial in order to identify potential predictors of clinical behavior and/or treatment response, as well as targets for tailored therapies (8). For example, in the case of GH-secreting PAs causing acromegaly, the presence of parameters predicting treatment response would be useful to avoid potentially inefficacious therapies that could have an impact on other conditions like glucose metabolism, or to guide drug dosing (11–14). Furthermore, even environmental factors, especially pollutants with endocrine disrupting activities, which have been increasingly demonstrated to have a role in PA pathophysiology, could have an impact on tumor epigenetic profile and molecular features, and consequently on their biological behavior (15–18).

This study aimed to assess the methylation status, as compared to normal pituitary tissues, of nonfunctioning pituitary adenomas (NFPAs) and GH-omas, and to correlate the methylation status of NFPAs and GH-omas with their epidemiological and clinicopathological features.

MATERIALS AND METHODS

Tumor Sample Collection and DNA Extraction

Twenty-one PA samples (11 GH-omas, 10 NFPAs) were collected by the Neurosurgery Unit of Messina University Hospital between 2015 and 2017. All patients gave their written informed consent to the study. Demographic information, including sex, age, and clinical data, of the enrolled patients are summarized in **Table 1**. Five nontumor pituitary tissue samples were collected through an autopsy of subjects who died due to non-endocrine causes. The research protocol was approved by the local ethics committee. For DNA methylation analyses (see below), genomic DNA was extracted from each collected tissue using the QIAamp DNA mini kit (Qiagen), according to the manufacturer's instructions.

Whole-Genome DNA Methylation Sequencing

The whole-genome DNA methylation profiling of 11 GH-omas, 10 NFPAs, and 5 normal pituitaries was carried out with the TruSeq Methyl Capture EPIC library preparation protocol followed by next-generation sequencing (NGS) (Illumina). Genomic DNAs underwent picogreen quantification on the Qubit fluorimetric system (dsDNA HS assay, Life Technologies) in order to obtain 1,000 ng of DNA/sample for subsequent library preparation. Libraries were carried out following the manufacturer's instructions. In detail, 1,000 ng of each sample was sonicated (Covaris M220 System) to obtain small DNA fragments (average size 150–200 bp) as assessed by the Tape Station quality check system (High Sensitivity D1000, Agilent). After end repair and adapter ligation, these DNA fragments were enriched by hybridization with specific capture probes. The enriched fragments were bisulfite converted and amplified. These obtained libraries were checked for quantity (Qubit, dsDNA HS assay, Life Technologies) and quality (Tape Station, High Sensitivity D1000, Agilent) before sequencing. NGS was carried out on the Illumina HiSeq1500 System. Up to 12 different DNA libraries, each univocally identified by a specific barcode or index, were pooled in equimolar amounts and sequenced in 4 different lanes in order to avoid analytical biases.

Methylation Sequencing Data Analysis

A multistep bioinformatic pipeline was used to analyze the obtained sequencing data. First, sequencing reads quality check was carried out using the FASTQC software. For the sequence alignment and downstream quantification steps, we used the "QuasR" (version 1.22.1), an R-Bioconductor package installed on R (version 3.5.0) (19). The QuasR package integrates the functionality of several R packages for genomic intervals and alignment files manipulation and external software [e.g., Bowtie (20)] for the real sequence alignment. Sequence mapping was carried out using a BS pre-processed reference genome version (version GRCh37/hg19) that

TABLE 1 | Demographic, radiological, and clinicopathological features of the studied cohort of patients.

ID	Sex	h.r. areas	Age at diagnosis	Micro/macro-adenoma	dmax mm	Cavernous s. invasion*	Ki-67%	p53%	TNS surgeries	*AIP* mutation
GH1	F		27	Macro	22	No	2	0	1	
GH2	F	Yes	76	Macro	15	No	1	0	1	
GH3	F		46	Macro	10	No	2	<1	1	
GH4	M		NA	Macro	NA	No	NA	NA	1	
GH5	M		57	Macro	22.5	No	1		1	
GH7	F		48	Macro	11	No	1	2	1	
GH8	F		28	Macro	18		5	2	1	
GH9	F		22	Micro	5	No	<1		1	Yes
GH10	F		35	Macro	12	No	<1	0	1	
GH11	M	Yes	63	Macro	43	Yes	5	0	2	
GH12	M		57	Macro	11	Yes	<1	0	1	
total	4M, 7F					2/11				
median			47		12		2		1	
SD			17.69		11.13		1.81		0.31	
NFPA1	F		46	Macro	30	Yes	3	1	1	
NFPA5	F		46	Macro	22	No	<1		1	
NFPA6	M		42	Macro	30	No	NA	NA	1	
NFPA8	F		NA	Macro	NA	No	NA	NA	1	
NFPA11	F	Yes	55	Macro	15	No	2		1	
NFPA13	M		68	Macro	30	No	2	<1	1	
NFPA14	F		70	Macro	25	No	<1		1	
NFPA16	M		72	Macro	23	Yes	<1		1	
NFPA18	M		40	Macro	34	Yes	1		2	
NFPA19	F		36	Macro	30	Yes	1	3	3	
total	4M, 6F					4/10				
median			46		30		2		1	
SD			13.94		5.60		0.83		0.70	
P value**	0.78		0.36		***0.02***	0.53	0.48		0.35	

NFPA, nonfunctioning pituitary adenoma; AIP, arhyl hydrocarbon receptor interacting protein (gene); cavernous s., cavernous sinus; h.r. areas, areas classified at high risk for health (highly polluted) by the Italian Government; NA, not available; SD, standard deviation; TNS, trans-nose sphenoidal.

**Cavernous sinus invasion defined by mean of 1.5 T MRI (magnetic resonance imaging) studies.*

***P-value set at <0.05.*

The P-value 0.02 (in bold italic) indicates statistical significance.

was generated exploiting the "QuasR" functions. The tool was run with default parameters. PCR duplicated reads were removed during the alignment. Subsequently, to quantify methylated and unmethylated cytosines in each sample, we used the function qMeth of the QuasR package. We considered a total of 437,792 genomic regions (mean length of 245 bp; from 2 to 8,131 bp) covered in the manifest file of the TruSeq Methyl Capture EPIC Library Prep kit (Illumina). In this step, the tool collapses the information of individual cytosines by query region. Finally, the methylation fraction of each target region for each sample was obtained as the ratio between methylated reads and the total number of aligned reads and ranged between 0 (un-methylated) and 1 (totally methylated). The tools were run with default parameters.

Differential Methylation Analysis

For the differential methylation analysis, we considered GH-oma and NFPAs samples. To improve the consistency of the results, we kept all the target regions (n=184,841) that were covered in all the GH-oma and NFPAs samples and calculated the methylation fold enrichment (as Log2) between NFPAs and GH-omas mean methylation. Statistical significance was calculated with t-test, and P-values were corrected for multiple testing with the Bonferroni method. Significant results were considered if the Bonferroni adjusted P value was less than 0.05 and if the Log2 fold change was above or below 0.5. Functional annotation, to get distances from the nearest genes and other genomic information, of differentially methylated regions was performed with the ANNOVAR software.

The statistical evaluation of demographic and clinicopathological parameters was performed by means of t-test and chi-square test (with Yates' correction), and significance was set at a P value less than 0.05.

RESULTS

Sequencing reads quality evaluation returned good-quality paired-end reads of length between 35 and 101 bp. The percentage of reads with quality scores above 20 (Q20) and above 30 (Q30) was 98.91 and 94.42, respectively (**Supplementary Figure 1A**). The mean base quality was 36.20 (**Supplementary Figure 1B**). The overall mapping rate ranged between 71.3% and 78.95%, as reported in **Supplementary Figure 1C**.

The methylation quantification step was performed by restricting the analysis to the genomic regions covered in the TruSeq Methyl Capture EPIC manifest file provided by Illumina. A total of 437,792 regions with a mean length of 245 bp (from 2 to 8,131 bp), being equivalent to 301,525 non-CpGs, 61,703 CpG

islands, 18,707 N_shelf, 19,038 N_shore, 19,201 S_shelf, and 17,618 S_shore regions, were analyzed. The general positioning of these sequences in the human genome is summarized in **Figure 1A**.

For the differential methylation analysis, we compared GH-oma and NFPAs samples. To improve the consistency of the results, we kept all the target regions (n=184,841) that were covered in all the GH-oma and NFPAs samples. As reported in **Figure 1B** and **Supplementary Figure 1D**, globally, NFPAs showed higher methylation levels (median=0.68) compared to GH-secreting pituitary tumors (median=0.48) ($P<2.2x10^{-16}$; Mann–Whitney test). Moreover, we evaluated the methylation levels of CpG-related regions and found that NFPAs were hypermethylated, as compared to GH-secreting pituitary tumors. In particular, we found hypermethylation in Open sea (median=0.7210 vs median=0.5236, respectively); in N Shelfs (median=0.7707 vs median=0.5786, respectively); in N Shores (median=0.6534 vs median=0.4517, respectively); in Islands (median=0.04584 vs median=0.030993, respectively); in S Shores (median=0.6526 vs median=0.4569, respectively), and in S Shelfs (median=0.7748 vs median=0.5855, respectively) (**Figure 1C**; $P<2.2x10^{-16}$; Mann–Whitney test).

Next, we calculated the methylation fold enrichment (as Log2) between NFPA and GH-oma samples to identify the differentially methylated regions (DMRs).

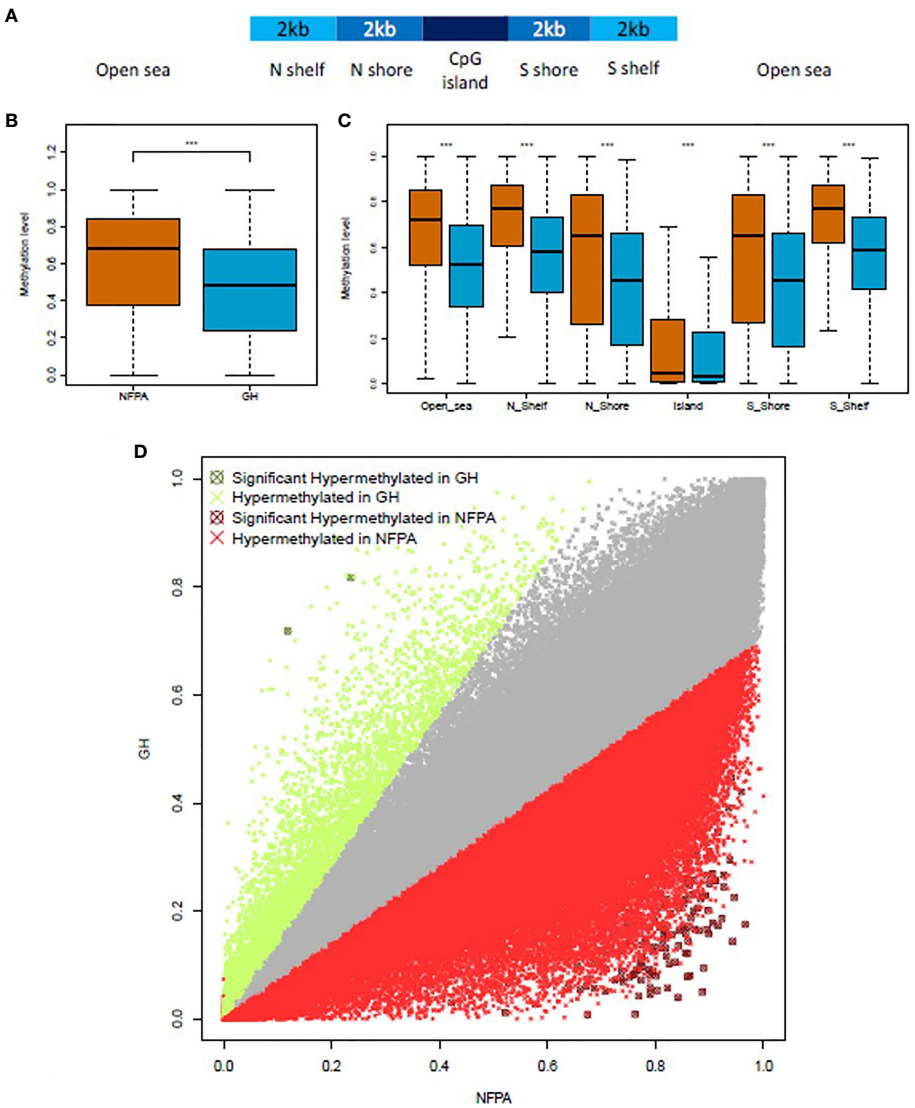

FIGURE 1 | NFPAs are hypermethylated when compared to GH-secreting tumors. **(A)** Schematic representation of the CpG-related region annotation. **(B)** Boxplot showing the global level of methylation in nonfunctioning pituitary adenomas (NFPAs—brown) and GH-secreting (blue) tumors. **(C)** Methylation levels in CpG-related regions. **(D)** The scatterplot compares the methylation levels of 184,841 regions in NFPAs (x-axis) and GH-omas (y-axis). Data points in gray did not pass the Log_2 fold change cutoffs. Points in red or green passed the Log_2 fold change cutoffs. Points in dark red or dark green were significantly hypermethylated in NFPAs or GH, respectively. Mann–Whitney test was used in **(B, C)** t-test was used in **(D)**. $P < 0.0001$ (***).

NFPAs showed a distinct methylation profile as compared to GH-omas. In particular, we obtained 178 target regions that were differentially methylated (corrected P-value ≤0.05; Log2 Fold Change ± 0.5) between the two tumor types (**Figure 1D** and **Supplementary Table 1**). Of note, only two regions resulted significantly hypermethylated in GH-omas compared to NFPAs (**Figure 1D**).

We classified as H-DMRs (high differentially methylated regions) those regions having Log2 FC above 2 or below -2. This category counted a total of 111 DMRs (62.36%), one of which was hypomethylated in NFPAs as compared to GH-oma. DMRs with Log2 FC values between 2 and -2 were deemed as L-DMRs (low differentially methylated regions). This class included a total of 67 DMRs (37.64%), one of which was hypermethylated in NFPAs as compared to GH-oma.

Subsequently, we functionally annotated the list of DMRs and found that the majority of them mapped in noncoding regions (92.7%), of which 64.85% were intronic sequences (**Figure 2A**). Moreover, we found that DMRs within the coding regions were significantly hypermethylated in NFPAs (median beta value=0.83 and 0.25 for NFPAs and GH-oma, respectively; P = $1.92x10^{-07}$). Accordingly, also noncoding sequences were significantly hypermethylated in NFPAs (median beta value=0.81 and 0.16 for NFPAs and GH-oma, respectively; P = $4.38x10^{-53}$) (**Figure 2B**, and **Supplementary Table 1**).

The CpG-centric annotation of DMRs (see **Figure 1A**) highlighted that the large majority of DMRs were annotated as Open sea (82.02%) (**Figure 2C**). These DMRs were significantly hypermethylated in NFPAs (median beta value=0.82 and 0.17 for NFPAs and GH-oma, respectively; P = $4.60x10^{-47}$). Overall, as reported in **Figures 2B, D**, we observed generalized hypermethylation in NFPAs as compared to GH-oma ($P < 4.38x10^{-53}$).

To assess if the DMR-related genes were involved in specific pathways, we conducted a Gene Ontology Biological Process Enrichment Analysis using the web app ShinyGO (v0.741) (PMID: 31882993) and set the FDR cutoff to 0.05. Of note, among the significantly enriched GO terms, we found biological

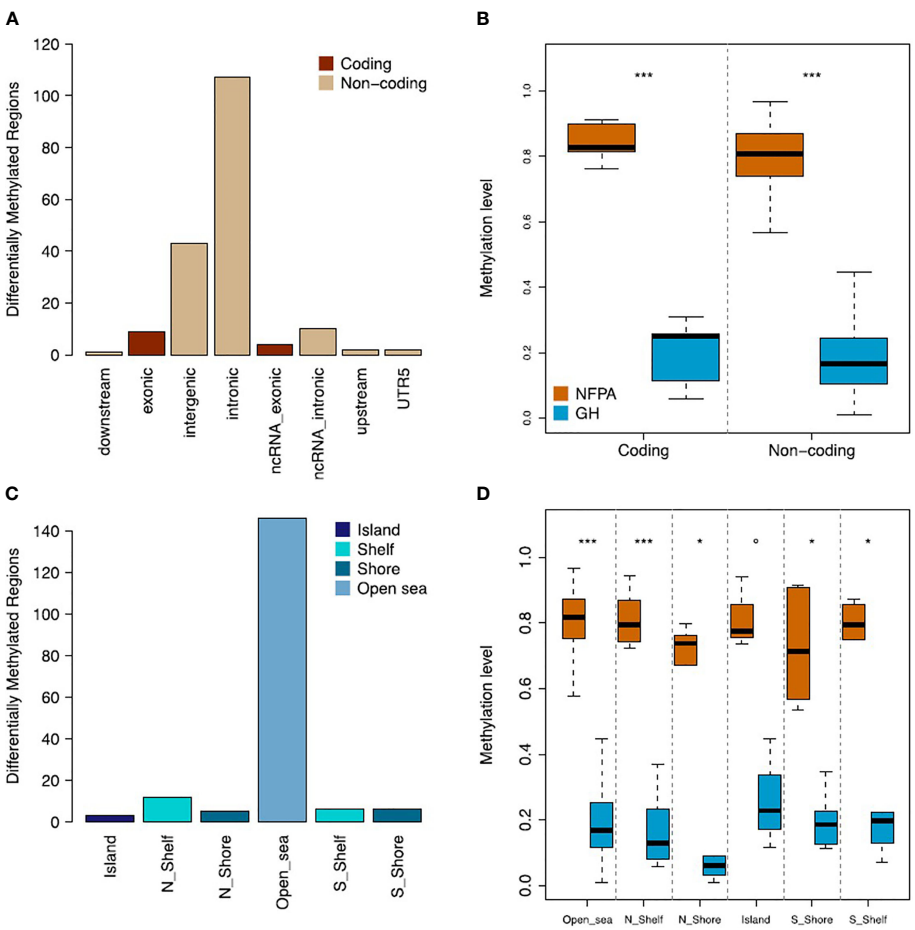

FIGURE 2 | NFPAs and GH tumors are differentially methylated. **(A)** Barplot showing the gene annotation of the 178 DMRs. **(B)** Boxplot reporting the comparison of methylation levels of coding and noncoding regions between nonfunctioning pituitary adenomas (NFPAs) and GH tumors. **(C)** Barplot showing the CpG-related annotation of the 178 DMRs. **(D)** Boxplot reporting the comparison of methylation levels of CpG-related regions between NFPAs and GH tumors. Mann–Whitney test was used in **(B, D)** P = 0.1 (°), P < 0.01 (*), P < 0.0001 (***).

processes related to cell and neuron development (**Figure 3** and **Supplementary Table 2**).

With regard to the correlation between methylation profile and demographic (including the degree of pollution of the residence area) or clinicopathological features of pituitary tumors, no statistically significant differences were observed between GH-omas and NFPAs, except for the maximum tumor diameter (**Table 1**), which resulted significantly higher in the latter group (median ± SD: 30 ± 5.6 vs 12 ± 11.13 mm; P = 0.02). Of note, 4 out of 10 (40%) patients with NFPAs presented with a neuroradiologically documented invasion of cavernous sinus vs 2 out of 11 (18.2%) in the GH-oma group, but this difference was not statistically significant (**Table 1**).

Finally, we found three hypermethylated genes (*C7orf50*, *GNG7*, and *BAHCC1*), involved in tumorigenesis processes, whose role could be related to pituitary tumor pathophysiology.

DISCUSSION

The role of epigenetic modifications, especially methylation, has increased its importance in the genetic background of sporadic pituitary tumors in the last few years. In fact, only a few somatic mutations with significant effects are known, such as *GNAS* alterations (this gene codifies for the α stimulatory subunit of G proteins) in GH-omas or *USP8* mutations in ACTH-omas causing *EGFR* overexpression and promoting corticotroph cells growth and ACTH hypersecretion (21). Also, our group recently demonstrated a novel somatic deletion in exon 10 of the *AHR* (aryl hydrocarbon receptor) gene in patients affected by GH-omas, whose role could be related to an altered AHR/AIP pathway favoring tumorigenesis (22). On the other hand, in pituitary tumors, it has been observed that methylation is preferentially concentrated in the so-called CpG islands, sequences of about 500 bp strictly connected to promoter regions, leading to the silencing of genes often involved in cell cycle regulation (23). Of note, a lot of oncosuppressors can be found among these genes, as for the couple *CDKN2A/Rb1*, whose deregulation can cause altered apoptosis regulation (8). In fact, methylation of *CDNK2A* leads to a reduced expression of p16, which, in turn, determines pRb phosphorylation and cell cycle progression through the activation of E2F transcription factors (24). However, the hardest challenge in the assessment of pituitary tumor methylation profile is to find a consistent "signature," potentially useful as biological/prognostic/therapeutic marker. As it emerges from many studies—also confirmed by our findings—NFPAs tend to present with a higher degree of methylation compared to GH-omas, although some invasive NFPAs can even be characterized by hypomethylation (7, 23, 25, 26). Besides, NFPAs more frequently harbor *CDKN2A/p16* alterations, inversely from what were observed in GH-secreting pituitary tumors, which often do not express pRb (8). *CDKN2A* methylation has been related to the pituitary tumor volume, grade, and patients' age, with higher methylation levels in macroadenomas (8). Furthermore, p27 hypermethylation was found in ACTH-omas, while *EML2*, *HOXB1*, and *RHOD* epigenetic modifications have been reported in NFPAs, GH-omas, and PRL-omas, respectively (7, 8). Gu et al. demonstrated that methylation would lead to the downregulation of genes like *GALNT9*, *CDH1*, and *CDH13* (E-cadherin and H-cadherin, respectively), involved into cellular adhesion processes, and potentially linked to the development of invasiveness (26). The same study observed that DMRs were located not only in CpG islands but also in the gene body in 40% of the cases (26). Accordingly, in our study, only 3 DMRs were found in known CpG islands, while the remaining alterations were found in genome open sea regions. Other genome elements prone to methylation are lncRNAs, RNA fragments of about 200 nucleotides functionally similar to the respective coding RNAs (27). In this regard, the downregulation following the hypermethylation of *MEG3*, which interacts with p53 and acts as oncosuppressor, has been found in gonadotropinomas (8, 27, 28). Another lncRNA, called C5orf66-AS1, regulates several genes, including *PAQR7*, a progesterone receptor that causes a progesterone A-B receptor-independent reduction in GnRH, whose expression has been found to have a role in progression and invasion of null-cell pituitary adenomas (24, 29).

With regard to our findings, DMR analysis revealed a prevalence of methylation of noncoding sequences, including lncRNAs (**Figure 2A**). Most of the methylation profile alterations were localized in open-sea regions more than involving promoters, with an inverse trend if compared to the literature (**Figure 2C**). Anyway, the prevalence of hypermethylation in NFPAs vs GH-omas has been confirmed (**Figures 2B, D**). Interestingly, we found hypermethylation of 3 known CpG islands belonging to genes

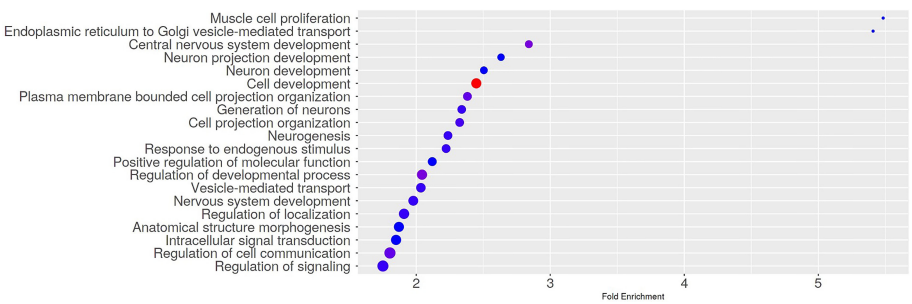

FIGURE 3 | Gene Ontology Biological Process Enrichment results. The dotplot shows the top 20 significantly enriched GO terms. The Gene Ontology Biological Process Enrichment Analysis was run using the web app ShinyGO (v0.741) with the FDR cutoff set to 0.05.

thought to have a role in tumorigenesis processes: *C7orf50*, *GNG7*, and *BAHCC1*.

C7orf50 is a ubiquitarian gene whose product is implicated in the assembling of ribosomal RNA to the nucleus, even if part of its sequences could also originate some regulatory miRNAs. Its full function is still unknown, although some evidence suggests it could bind the Sp1 transcriptional factor, which has several regulatory functions (i.e., cell cycle, apoptosis, etc.) including an interaction with *AHR* favoring the ubiquitination and consequent degradation of the estrogenic receptor α (ERα) in murine breast and uterine cancer (30).

GNG7 is a gene located on chromosome 19 codifying for the γ7 subunit of guanin-binding G proteins, which is involved in contact-mediated cell growth blockade and acts as an oncosuppressor (31), whose promoter methylation has been found in many cases of head/neck cancer and associated with higher tumor volume and lesser metastatic potential (31). Similarly, Xu et al. observed methylation-mediated, reduced expression of *GNG7* in renal clear cell carcinoma. In this case, methylation, not present in normal tissue, led to the impairment of the mTOR1 signaling pathway and was linked to a higher stadium/grade of the disease and a reduced overall survival (32).

BAHCC1 is a chromatin transcriptional silencer, implied into cell replication and transcriptional regulation mechanisms. Amplifications and deletions of this gene would make it potentially part of aberrant cell regeneration processes linked to the development of liver cancer, according to still-not-well-known mechanisms, but possibly due to downstream alterations in the signaling pathways (33). However, there are few data about epigenetic modifications of *BAHCC1*, although an experimental study by Gitik et al. found an increase in its methylation in the dorsal hippocampus of mice treated with nicotine before adolescence, in an animal model correlating substance abuse in the age of adolescence (or alcohol exposure *in utero*) with addiction. These chromatin modifications were linked to the development of cognitive deficits in the adult age, otherwise preventable by the simultaneous administration of choline (34).

With regards to the correlation between methylation profile and clinicopathological features, the higher maximum diameter of NFPAs could hypothetically be linked to a higher proliferative potential in this subtype of pituitary tumors. The same could apply to the higher frequency of cavernous sinus invasion—although not statistically significant—in the NFPA group. These findings are in line with the study by Gu et al. in which hypermethylation altered the expression profile of cell adhesion proteins (26). Finally, no relationship was observed between the methylation status and the degree of pollution of the residence area of our patients, but the number of pituitary tumors evaluated in this study is very small. Furthermore, the hypermethylation of *C7orf50*, a gene interacting with *AHR*, should be investigated in larger cohorts of patients. In fact, better defining such an interaction could add new information to the complex role played by *AHR*, which along the years we demonstrated to significantly influence morphology, secretion, and therapeutic response in GH-omas (16–18, 35).

In conclusion, our data provide further evidence on the complexity of the epigenetic background of pituitary tumors. We found a significant prevalence of hypermethylation in NFPAs, as compared to GH-omas, whose pathophysiological consequence is yet to be defined. Further studies are needed to clarify the role and relevance of *C7orf50*, *GNG7*, and *BAHCC1* genes—which have been found to be methylated—in pituitary tumor biology, oncogenesis, and clinical expression.

DATA AVAILABILITY STATEMENT

The data presented in the study are available on the European Nucleotide Archive (ENA) repository. Accession nr: PRJEB50807.

ETHICS STATEMENT

The studies involving human participants were reviewed and approved by the Ethics Committee of The Province of Messina. The patients/participants provided their written informed consent to participate in this study.

AUTHOR CONTRIBUTIONS

GG and FF wrote the paper and organized research data. GG, MR, OC, FS, and YA contributed to the gathering of clinical data. FP, FAl, PR, RO, and M'HA (Messina) and VD'A, FM, LP, VL, and MC (Naples) performed DNA sequencing and methylome analysis. FAn provided samples from patients by means of TNS surgery, while AA provided healthy pituitary samples from autopsies. FF, SC, M'HA, and MC conceived the entire study and revised the final paper version. All authors contributed to the article and approved the submitted version.

FUNDING

This work was supported by the following grants of the Italian government: Ricerca Finalizzata 2013: "Role of environment-gene interaction in etiology and promotion of pituitary tumours" (code: RF-2013-02356201); Programma di Ricerca di Interesse Nazionale 2015: "Epidemiological determinants, molecular mechanisms and clinical criteria of treatment outcome and resistance in pituitary disease syndromes" (code: PRIN-2015-2015ZHKFTA); and Progetto Rilevante di Interesse Nazionale 2017: "Identification of new biomarkers and clinical determinants for management improvement of patients with pituitary tumor related syndromes" (code: PRIN 2017S55RXB).

SUPPLEMENTARY MATERIAL

The Supplementary Material for this article can be found online at: https://www.frontiersin.org/articles/10.3389/fendo.2022.841118/full#supplementary-material

Supplementary Figure 1 | Evaluation of sequencing, mapping, and methylation analysis data. **(A)** Boxplot reporting the percentage of reads with quality scores above 20 (Q20) and above 30 (Q30). **(B)** Boxplot reporting the mean base quality of sequencing reads. **(C)** Summary of the mapping rates. **(D)** Boxplot of the global methylation level of the 437,792 regions analyzed.

REFERENCES

1. Melmed S. Pituitary-Tumor Endocrinopaties. *N Engl J Med* (2020) 382:937–50. doi: 10.1056/NEJMra1810772
2. Trouillas J, Jaffrain-Rea ML, Vasiljevic A, Raverot G, Roncaroli F, Villa C. How to Classify Pituitary Neuroendocrine Tumors (PitNETs) in 2020. *Cancers* (2020) 12:514. doi: 10.3390/cancers12020514
3. Raverot G, Burman P, McCormack A, Heaney A, Petersenn S, Popovic V, et al. Clinical Practice Guidelines for the Management of Aggressive Pituitary Tumors and Carcinomas. *Eur J Endocrinol* (2018) 178:G1–24. doi: 10.1530/EJE-17-0796
4. Giuffrida G, Ferraù F, Laudicella R, Cotta OR, Messina E, Granata F, et al. Peptide Receptor Radionuclide Therapy for Aggressive Pituitary Tumors: A Monocentric Experience. *Endocr Connect* (2019) 8:528–35. doi: 10.1530/EC-19-0065
5. Korbonits M, Kumar AV. AIP Familial Isolated Pituitary Adenomas. In: MP Adam, HH Ardinger, RA Pagon, SE Wallace, LJH Bean, K Stephens, A Amemiya, editors. *GeneReviews®*. Seattle (WA: University of Washington, Seattle (2012). p. 1993–2020. updated 2020 Apr 16.
6. Thakker RV, Newey PG, Walls GV, Bilezikian J, Dralle H, Ebeling PR, et al. Clinical Practice Guidelines for Multiple Endocrine Neoplasia Type 1 (Men1). *J Clin Endocrinol Metab* (2012) 97:2990–3011. doi: 10.1210/jc.2012-1230
7. Hauser BM, Lau A, Gupta S, Bi WL, Dunn IF. The Epigenomics of Pituitary Adenoma. *Front Endocrinol* (2019) 10:290. doi: 10.3389/fendo.2019.00290
8. Pease M, Ling C, Mack WJ, Wang K, Zada G. The Role of Epigenetic Modification in Tumorigenesis and Progression of Pituitary Adenomas: A Systematic Review of the Literature. *PloS One* (2013) 8:e82619. doi: 10.1371/journal.pone.0082619
9. Vicchio TM, Aliquò F, Ruggeri RM, Ragonese M, Giuffrida G, Cotta OR, et al. MicroRNAs Expression in Pituitary Tumors: Differences Related to Functional Status, Pathological Features, and Clinical Behavior. *J Endocrinol Invest* (2020) 43:947–58. doi: 10.1007/s40618-019-01178-4
10. Ma HS, Wang EL, Xu WF, Yamada S, Yoshimoto K, Qian ZR, et al. Overexpression of DNA (Cytosine-5)-Methyltransferase 1 (DNMT1) and DNA (Cytosine-5)-Methyltransferase 3A (DNMT3A) Is Associated With Aggressive Behavior and Hypermethylation of Tumor Suppressor Genes in Human Pituitary Adenomas. *Med Sci Monit* (2018) 24:4841–50. doi: 10.12659/MSM.910608
11. Cozzolino A, Feola T, Simonelli I, Puliani G, Pozza C, Giannetta E, et al. Somatostatin Analogs and Glucose Metabolism in Acromegaly: A Meta-Analysis of Prospective Interventional Studies. *J Clin Endocrinol Metab* (2018) 41(5):575–81. doi: 10.1210/jc.2017-02566
12. Feola T, Cozzolino A, Simonelli I, Sbardella E, Pozza C, Giannetta E, et al. Pegvisomant Improves Glucose Metabolism in Acromegaly: A Meta-Analysis of Prospective Interventional Studies. *J Clin Endocrinol Metab* (2019) 104 (7):2892–902. doi: 10.1210/jc.2018-02281
13. Cozzolino A, Feola T, Simonelli I, Puliani G, Hasenmajer V, Minnetti M, et al. Metabolic Complications in Acromegaly After Neurosurgery: A Meta-Analysis. *Eur J Endocrinol* (2020) 183(6):597–606. doi: 10.1530/EJE-20-0497
14. Ragonese M, Grottoli S, Maffei P, Alibrandi A, Ambrosio MR, Arnaldi G, et al. How to Improve Effectiveness of Pegvisomant Treatment in Acromegalic Patients. *J Endocrinol Invest* (2018) 41:575–81. doi: 10.1007/s40618-017-0773-0
15. Diamanti-Kandarakis E, Bourguignon JP, Giudice LC, Hauser R, Prins GS, Soto AS, et al. Endocrine-Disrupting Chemicals: An Endocrine Society Scientific Statement. *Endocrine Rev* (2009) 30:293–342. doi: 10.1210/er.2009-0002
16. Cannavò S, Ferraù F, Ragonese M, Curtò L, Torre ML, Magistri M, et al. Increased Prevalence of Acromegaly in a Highly Polluted Area. *Eur J Endocrinol* (2010) 163:509–13. doi: 10.1530/EJE-10-0465
17. Cannavò S, Ferrau F, Ragonese M, Romeo PD, Torre ML, Puglisi S, et al. Increased Frequency of the Rs2066853 Variant of Aryl Hydrocarbon Receptor Gene in Patients With Acromegaly. *Clin Endocrinol* (2014) 81(2):249–53. doi: 10.1111/cen.12424
18. Cannavò S, Ragonese M, Puglisi S, Romeo PD, Torre ML, Alibrandi A, et al. Acromegaly is More Severe in Patients With AHR or AIP Gene Variants Living in Highly Polluted Areas. *J Clin Endocr Metab* (2016) 101:1872–9. doi: 10.1210/jc.2015-4191
19. Gaidatzis D, Lerch A, Hahne F, Stadler MB. QuasR: Quantification and Annotation of Short Reads in R. *Bioinformatics* (2015) 31:1130–2. doi: 10.1093/bioinformatics/btu781
20. Langmead B, Salzberg SL. Fast Gapped-Read Alignment With Bowtie 2. *Nat Methods* (2012) 9(4):357–9. doi: 10.1038/nmeth.1923
21. Nadhamuni VS, Korbonits M. Novel Insights Into Pituitary Tumorigenesis: Genetic and Epigenetic Mechanisms. *Endocr Rev* (2020) 41:bnaa006. doi: 10.1210/endrev/bnaa006
22. Re A, Ferraù F, Cafiero C, Spagnolo F, Barresi V, Romeo DP, et al. Somatic Deletion in Exon 10 of Aryl Hydrocarbon Receptor Gene in Human GH-Secreting Pituitary Tumors. *Front Endocrinol* (2020) 12(11):591039. doi: 10.3389/fendo.2020.591039
23. Duong CV, Emes RD, Wessely F, Yacub-Usman K, Clayton RN, Farrell WE. Quantitative, Genome-Wide Analysis of the DNA Methylome in Sporadic Pituitary Adenomas. *Endocr Relat Cancer* (2012) 19:805–16. doi: 10.1530/ERC-12-0251
24. Chang M, Yang C, Bao X, Wang R. Genetic and Epigenetic Causes of Pituitary Adenomas. *Front Endocrinol* (2021) 11:596554. doi: 10.3389/fendo.2020.596554
25. Ling C, Pease M, Shi L, Punj V, Shiroishi MS, Commins D, et al. A Pilot Genome-Scale Profiling of DNA Methylation in Sporadic Pituitary Macroadenomas: Association With Tumor Invasion and Histopathological Subtype. *PloS One* (2014) 9:e96178. doi: 10.1371/journal.pone.0096178
26. Gu Y, Zhou X, Hu F, Yu Y, Xie T, Huang Y, et al. Differential DNA Methylome Profiling of Nonfunctioning Pituitary Adenomas Suggesting Tumour Invasion is Correlated With Cell Adhesion. *J Neurooncol* (2016) 129:23–31. doi: 10.1007/s11060-016-2139-4
27. Beylerli O, Gareev I, Pavlov V, Chen X, Zhao S. The Role of Long Noncoding RNAs in the Biology of Pituitary Adenomas. *World Neurosurg* (2020) 137:252–6. doi: 10.1016/j.wneu.2019.10.137
28. Gejman R, Batista DL, Zhong Y, Zhou Y, Zhang X, Swearingen B, et al. Selective Loss of MEG3 Expression and Intergenic Differentially Methylated Region Hypermethylation in the MEG3/DLK1 Locus in Human Clinically Nonfunctioning Pituitary Adenomas. *J Clin Endocrinol Metab* (2008) 93:4119–25. doi: 10.1210/jc.2007-2633
29. Yu G, Li C, Xie W, Wang Z, Gao H, Cao L, et al. Long non-Coding RNA C5orf66-AS1 Is Downregulated in Pituitary Null Cell Adenomas and is Associated With Their Invasiveness. *Oncol Rep* (2017) 38:1140–8. doi: 10.3892/or.2017.5739
30. Wormke M, Stoner M, Saville B, Walker K, Abdelrahim M, Burghardt R, et al. The Aryl Hydrocarbon Receptor Mediates Degradation of Estrogen Receptor Alpha Through Activation of Proteasomes. *Mol Cell Biol* (2003) 23(6):1843–55. doi: 10.1128/MCB.23.6.1843-1855.2003
31. Hartmann S, Szaumkessel M, Salaverria I, Simon R, Sauter G, Kiwerska K, et al. Loss of Protein Expression and Recurrent DNA Hypermethylation of the GNG7 Gene in Squamous Cell Carcinoma of the Head and Neck. *J Appl Genet* (2012) 53:167–74. doi: 10.1007/s13353-011-0079-4
32. Xu S, Zhang H, Liu T, Chen Y, He D, Li L. G Protein γ Subunit 7 Loss Contributes to Progression of Clear Cell Renal Cell Carcinoma. *J Cell Physiol* (2019) 234:20002–12. doi: 10.1002/jcp.28597
33. Nalesnik MA, Tseng G, Ding Y, Xiang GS, Zheng Z, Yu YP, et al. 2012 Gene Deletions and Amplifications in Human Hepatocellular Carcinomas. *Am J Pathol* (2012) 180:1496–508. doi: 10.1016/j.ajpath.2011.12.021
34. Gitik M, Holliday ED, Leung M, Yuan Q, Logue SF, Tikkanen R, et al. Choline Ameliorates Adult Learning Deficits and Reverses Epigenetic Modification of Chromatin Remodeling Factors Related to Adolescent Nicotine Exposure. *Neurobiol Learn Mem* (2018) 155:239–48. doi: 10.1016/j.nlm.2018.08.009
35. Cannavò S, Trimarchi F, Ferraù F. Acromegaly, Genetic Variants of the Aryl Hydrocarbon Receptor Pathway and Environmental Burden. *Mol Cell Endocrinol* (2017) 457:81–8. doi: 10.1016/j.mce.2016.12.019

Conflict of Interest: The authors declare that the research was conducted in the absence of any commercial or financial relationships that could be construed as a potential conflict of interest.

this article, or claim that may be made by its manufacturer, is not guaranteed or endorsed by the publisher.

frontiers in Endocrinology

REVIEW
published: 31 March 2022
doi: 10.3389/fendo.2022.844575

BRCA1: An Endocrine and Metabolic Regulator

*Haim Werner**

Department of Human Molecular Genetics and Biochemistry, Sackler School of Medicine, Tel Aviv University, Tel Aviv, Israel

The breast and ovarian cancer susceptibility gene (BRCA1) is a tumor suppressor whose mutation has been associated with the development of breast, ovarian and, probably, other malignancies at young ages. The BRCA1 gene product participates in multiple biological pathways including the DNA damage response, transcriptional control, cell growth and apoptosis. Inactivating germline mutations of the *BRCA1* gene can be detected in a substantial portion of families with inherited breast and/or ovarian cancer. While the genomic and cancer-related actions of BRCA1 have been extensively investigated, not much information exists regarding the cellular and circulating factors involved in regulation of *BRCA1* expression and action. The present review article dissects the emerging role of BRCA1 as an important regulator of various endocrine and metabolic axes. Experimental and clinical evidence links BRCA1 with a number of peptide and steroid hormones. Furthermore, comprehensive analyses identified complex interactions between the insulin/insulin-like growth factor-1 (IGF1) signaling axis and BRCA1. The correlation between metabolic disorders, including diabetes and the metabolic syndrome, and *BRCA1* mutations, are discussed in this article.

Keywords: BRCA1, tumor suppressors, p53, insulin-like growth factor-1 (IGF1), estrogen receptor, transcription

OPEN ACCESS

Edited by:
Claire Perks,
University of Bristol, United Kingdom

Reviewed by:
Patricia Alejandra Pennisi,
Centro de Investigaciones Endocrinológicas "Dr. César Bergadá" (CEDIE)(CONICET), Argentina
Katia Scotlandi,
Rizzoli Orthopedic Institute (IRCCS), Italy

***Correspondence:**
Haim Werner
hwerner@post.tau.ac.il

Specialty section:
This article was submitted to Cancer Endocrinology, a section of the journal Frontiers in Endocrinology

Received: *28 December 2021*
Accepted: *07 March 2022*
Published: *31 March 2022*

Citation:
Werner H (2022) BRCA1: An Endocrine and Metabolic Regulator. Front. Endocrinol. 13:844575. doi: 10.3389/fendo.2022.844575

DISCOVERY AND EARLY CHARACTERIZATION OF BRCA1

The race for the identification of the gene responsible for inherited breast and ovarian cancer ended in 1994 with the cloning of the *BRCA1* gene by Miki and colleagues (1, 2). Positional cloning methodology allowed identification of a 17q-linked gene whose mutation affected susceptibility to breast and ovarian cancer. The *BRCA1* gene encodes a predicted protein of 1863 amino acids, containing a distinct ring finger element in its N-terminal domain. The high penetrance of the *BRCA1* gene was recognized early on in the course of *BRCA1* characterization by analyses showing that mutation carriers have an increased lifetime risk of developing breast (40–85%) and/or ovarian (16–64%) cancers (3–8). In classical terms, *BRCA1* fits the criteria of a candidate tumor suppressor gene and some of its archetypal biological activities are described in the next section.

While inactivating *BRCA1* germline mutations are linked to a small portion of the total number of breast tumor cases worldwide, the cloning and subsequent characterization of the *BRCA1* gene had an unprecedented impact on our understanding of breast cancer etiology (9). In fact, lessons learned from molecular and genetic analyses of *BRCA1* transcended the area of familial breast and ovarian cancer and are regarded as universal biological paradigms in cancer (10). In addition to its genomic and cancer-related activities, more recent evidence revealed that BRCA1 displays a number of metabolic and hormone-like types of action. The present review article focuses on the

involvement of tumor suppressor BRCA1 in endocrine system control. Our assay attempts to shed new light on the rapidly expanding spectrum of actions of BRCA1. Their potential clinical ramifications are discussed in detail.

BRCA1 DEVELOPS ITS IDENTITY

Early studies identified BRCA1 as a critical player in the maintenance of genomic stability (11–13). Consistent with this role, cells with a defective *BRCA1* gene exhibit a series of typical anomalies, including impaired DNA damage response, defects in homologous recombination with ensuing low efficiency DNA repair, and faulty cell cycle checkpoints (14–16). BRCA1 was shown to interact with a wide range of molecules, including BARD1 (*via* its N-terminal ring finger domain), DNA repair enzymes (mainly *via* its central domain), and transcriptional activators (primarily *via* two tandem BRCA1 C-terminal, or BRCT, motifs) (17–19) (**Figure 1**). A number of excellent review articles focusing on the physical and functional interactions of BRCA1 have been published (18, 20).

The involvement of BRCA1 in transcriptional regulation is supported by solid experimental evidence (21, 22). Specifically: (i) BRCA1 is predominantly found within the nucleus (23, 24), albeit DNA damage as well as viral infection can alter its subcellular distribution (25); (ii) BRCA1 has been identified as a component of the RNA polymerase II holoenzyme by a number of biochemical criteria (19); (iii) the C-terminal domain of BRCA1 is highly acidic and exhibits a potent transcriptional transactivation activity (21, 26); and (iv) the N-terminal ring finger element resembles a similar motif described in several DNA-binding proteins, including the Wilms' tumor suppressor, WT1 (1). Finally, a novel transcriptional mechanism responsible for autoregulation of *BRCA1* gene transcription has been described (27). This regulatory loop involves the formation of a multimeric complex that contains, in addition to BRCA1, nuclear proteins E2F1 and RB. This complex displays a constitutive repressive activity pattern that leads to inhibition of *BRCA1* transcription. Disruption of the complex by various genotoxic stresses results in displacement of the BRCA1 protein from the *BRCA1* promoter region with subsequent upregulation of *BRCA1* transcription.

BRCA1 INHIBITS IGF1 RECEPTOR GENE EXPRESSION AND ACTION

The insulin-like growth factors (IGF1, IGF2) have an important role in the development and maturation of the mammary gland. In addition, IGFs are key players in breast cancer initiation and progression (28–31). Epidemiological analyses conducted over the past twenty-five years identified IGF1 as a risk factor for breast cancer (32–34). These population studies are in agreement with IGF1 function as a progression factor during the cell cycle (35, 36). Furthermore, studies reflect the well-established pro-survival role of IGF1 as well as its involvement in metabolic and nutritional control. The cell-surface IGF1 receptor (IGF1R), which mediates the biological actions of both IGF1 and IGF2, is regarded as a central player in breast cancer (31, 37–39). Constitutive activation of the IGF1R tyrosine kinase domain is a common event in cancer cells, although the prognostic significance of IGF1R levels and activation status in clinical settings remain unsettled (40).

Molecular, genetic and biochemical analyses identified complex physical and functional interactions between BRCA1 and the IGF1 signaling pathway (41, 42). Consistent with its tumor suppressor role, wild-type BRCA1 was shown to repress *IGF1R* gene transcription and promoter activity as well as endogenous IGF1R levels in breast cancer cells (43, 44). In contrast, a truncated form of BRCA1 (185delAG, a mutation

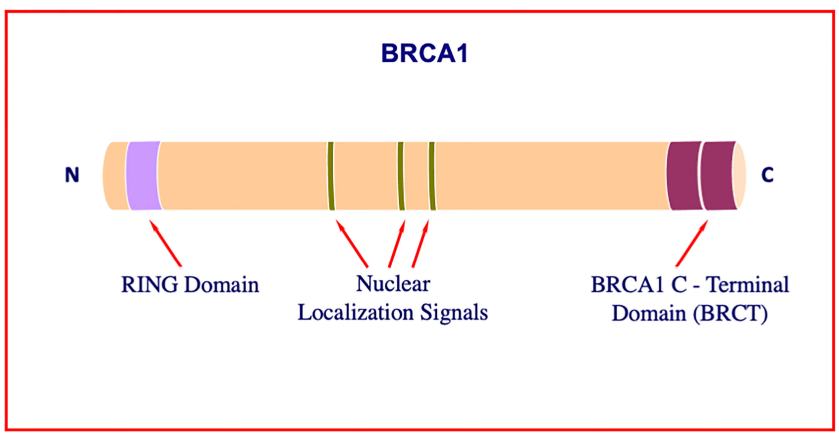

FIGURE 1 | Structure of BRCA1. The *BRCA1* gene encodes a 1863-amino acid protein with tumor suppressor activity. BRCA1 plays a critical role in DNA damage sensing and it forms a complex that repairs double-strand breaks. The N-terminal portion of the molecule includes a particular type of zinc finger element, termed RING motif. Among other roles, this domain interacts with proteins involved in BRCA1 ubiquitination. The central portion of the molecule includes a number of nuclear localization signals. The tandem C-terminal BRCT domain has important roles in DNA repair, transcription regulation and tumor suppressive functions.

with a high incidence among Ashkenazi Jews) was unable to inhibit *IGF1R* promoter activity (45, 46). The mechanism of action of BRCA1 involves interaction with Sp1, a zinc-finger transactivator of the *IGF1R* gene (**Figure 2**). Specifically, binding of BRCA1 to Sp1 prevents Sp1 from binding the *IGF1R* promoter region, leading to reduction in IGF1R levels and ensuing decrease in IGF1-mediated proliferation. In agreement with the inability of mutant BRCA1 to suppress *IGF1R* transcription, primary breast tumors derived from *BRCA1* mutation carrier patients expressed significantly higher levels of IGF1R than sporadic breast tumors (47).

Of importance, the transcriptional activity of BRCA1 is strongly dependent on the cellular status of tumor suppressor p53. Thus, BRCA1 was capable of repressing *IGF1R* transcription in both p53-expressing and p53-null cellular backgrounds, but not in mutant p53-containing cells (48). As a corollary, *loss-of-function* mutation of the *p53* gene in human cancer may affect the capacity of BRCA1 to repress *IGF1R* gene expression, with major clinical implications (49). In addition to breast cancer, BRCA1 was identified as a transcriptional repressor of the *IGF1R* gene in prostate and endometrial cancer cells (50–53).

Besides the *IGF1R* gene, BRCA1 was shown to target other components of the insulin-IGF1 axis. Intratumoral IGF1 concentrations were elevated in tumors from *BRCA1* or *BRCA2* mutation carriers compared with matched sporadic tumors (54). In addition, BRCA1 was shown to interact with the insulin receptor substrate-1 (*IRS-1*) promoter and to inhibit its activity (55). This effect at the promoter level was associated with epigenetic modifications of histone H3 and H4, leading to a transcriptional repressive chromatin configuration. Consistent with this inhibitory role, *BRCA1*-deficient mammary tumor cells exhibited high levels of IRS-1. Furthermore, suppression of *IRS-1* using RNA interference markedly inhibited cell growth. **Table 1** summarizes key concepts on the interaction between BRCA1 and the IGF1 axis.

DEVELOPMENTAL AND HORMONAL REGULATION OF *BRCA1* EXPRESSION

Ontogenetic analysis of *BRCA1* gene expression in the normal mouse showed that BRCA1 is highly expressed in rapidly proliferating cells (56). In addition, *BRCA1* expression is

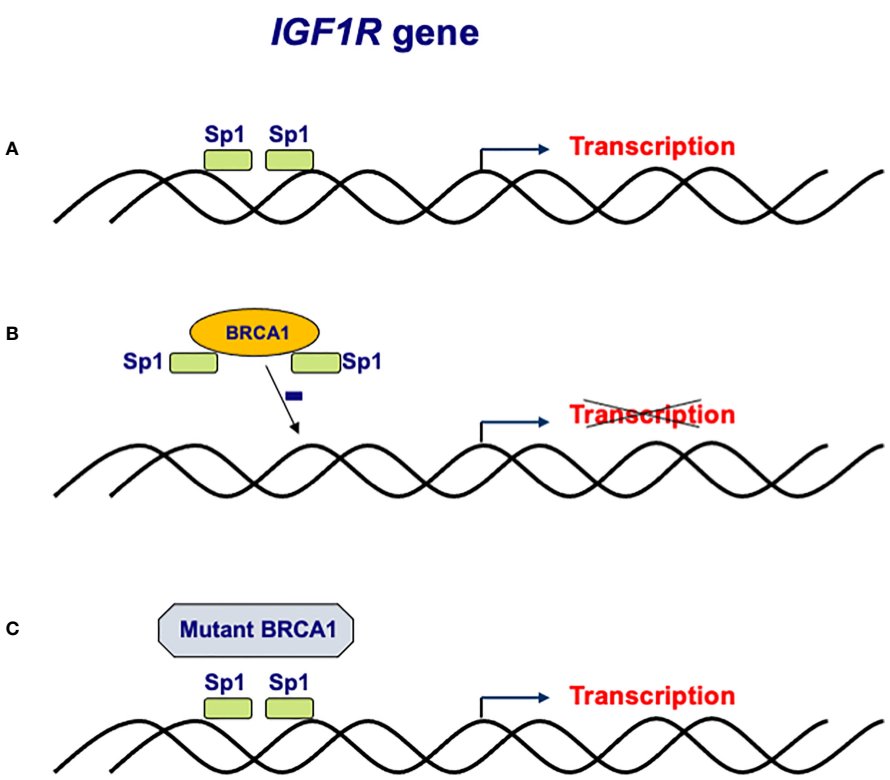

FIGURE 2 | Regulation of *IGF1R* gene expression by BRCA1. **(A)** The *IGF1R* gene promoter includes a number of high affinity binding sites for transcription factor Sp1 in its proximal region. **(B)** The mechanism of action of BRCA1 involves binding to, and sequestration of, Sp1, thus preventing its binding to *cis*-elements in the promoter region. Lack of Sp1 binding leads to a reduction in *IGF1R* promoter activity and IGF1R levels. **(C)** *Loss-of-function* mutation of BRCA1 in familial and, potentially, sporadic breast cancer may lead to inactivation of BRCA1. Mutant BRCA1 is unable to bind Sp1 and suppress *IGF1R* gene transcription. Enhanced IGF1R levels are usually associated with augmented cell proliferation.

TABLE 1 | Interactions between BRCA1, steroid hormones and the IGF1 signaling pathway.

The *IGF1R* gene is a *bona fide* downstream target for BRCA1 action
Wild-type, but not mutant, BRCA1 suppresses *IGF1R* promoter activity
IGF1R levels are higher in tumors from *BRCA1* mutation carriers than in sporadic tumors
IGF1 and IGF2 enhance *BRCA1* gene expression
IGF1 levels are upregulated in tumors from *BRCA1/BRCA2* mutation carriers
BRCA1 inhibits *IRS-1* promoter activity
BRCA1 inhibits the estradiol-inducible transcriptional activity of ERα
The stress hormone hydrocortisone represses *BRCA1* gene expression
The glucocorticoid receptor physically interacts with the *BRCA1* gene promoter

induced by positive growth signals at the cell cycle point where cells become committed to replicate their DNA and undergo cell division (57, 58). Maximal *BRCA1* expression was detected during the pre-replicative (G_1) phase of the cell cycle (59), and it was proved that BRCA1 is involved in the control of the G_1-S and G_2-M transition checkpoints (12, 16, 60). Finally, structure-function analyses have demonstrated that the tandem BRCT domain is essential in cell cycle checkpoint control by interacting in a phosphorylation-dependent fashion with specific DNA damage-induced proteins (61).

While BRCA1 has an important role in regulating *IGF1R* gene expression, as described in the previous section, experimental evidence indicates that both IGF1 and IGF2 stimulate *BRCA1* expression in a dose-dependent fashion (62). The effect of the growth factors was mediated at the transcriptional level, as revealed by transfection experiments using *BRCA1* promoter-luciferase reporter constructs. Given the fact that IGFs regulate cell division by controlling events that occur mainly during G_1, it is reasonable to assume that at least part of the bioactivities of the IGFs are mediated by BRCA1. This concept is supported by experiments showing that BRCA1 silencing was associated with a two-fold increase in the IGF1-induced portion of cells that arrested at SubG0, and with a ~33% reduction in the portion of cells at the M-phase. In view of the fact that IGF1 is mainly produced by stromal cells whereas IGF2 biosynthesis occurs directly in breast tumor cells, data indicate that *BRCA1* gene expression is potentially regulated by both autocrine (IGF2) and paracrine/endocrine (IGF1) stimuli (54).

Finally, AKT, a downstream IGF1 target, was shown to regulate BRCA1 stability independent of new protein synthesis (63). Hence, IGF1 signaling is capable of modulating BRCA1 abundance at various levels of regulation. Taken together, studies suggest that a feedback loop controls expression and action of the IGF1 and BRCA1 signaling pathways in a synchronized manner. Deregulated expression of *BRCA1* as a result of aberrant IGF signaling might bear consequences in breast cancer development (41).

METABOLIC ROLES OF BRCA1

The impact of obesity and diabetes on cancer risk in *BRCA1* mutation carriers has been the topic of major clinical concern (64–66). While obesity and hyperinsulinemia are well established risk factors for breast cancer, and given the fact that BRCA1 exhibits a number of metabolic types of action, it is of medical relevance to explore the effects of a defective BRCA1 pathway on the linkage between diabetes and breast pathologies. The BRCA1-induced metabolic reprogramming of breast cancer cells was examined using global metabolomics and transcriptomics platforms (67). Wild-type BRCA1 induced numerous metabolic modifications, including a marked inhibition of glycolysis. Thus, all glycolysis indicators were largely (~50%) decreased in BRCA1wild-type, in comparison to BRCA1 mutant, cells. Five major enzymes of this pathway, including HK2 and PFKFB3, and both pyruvate and lactate were down-regulated by BRCA1 transfection. On the other hand, the tricarboxylic acid (TCA) cycle and oxidative phosphorylation were activated in BRCA1-expressing cells. In addition, BRCA1 induced a decrease of ketone bodies and free fatty acids, which were probably employed to supply Acetyl-CoA for the TCA cycle. Furthermore, BRCA1-transfected cells displayed enhanced activity of antioxidative pathways, most likely as a result of ROS production by oxidative phosphorylation. The overall implication of these analyses is that BRCA1 is capable or reversing the Warburg effect (see **Table 2**). The impact of this novel mechanism on tumor suppression has yet to be assessed.

A recent study examined the impact of reduced BRCA1 expression on metabolic reprogramming of ovarian cancer cells (68). Authors showed that BRCA1 depletion led to diminished mitochondrial respiration and reduced ATP concentrations. Of interest, these metabolic alterations sensitized the cells to agents that inhibit mitochondrial activity and glucose import. Hence, inhibition of energy metabolism might constitute a useful strategy to target BRCA1-deficient high grade serous ovarian cancer, a type of tumor characterized by frequent BRCA1 loss (69).

Bordeleau et al. examined the medical histories of 6,052 women with *BRCA1* or *BRCA2* mutations, half of whom had been diagnosed with breast cancer (70). Authors reported that there was no excess of diabetes among patients with breast cancer in the period before diagnosis, compared with control individuals without cancer. However, there was a doubling in the risk of diabetes among *BRCA1* or *BRCA2* mutation carriers in the 15-year period after diagnosis of breast cancer. Importantly, the risk was even higher for women with a BMI higher than 25. Authors suggested that the enhanced risk might be linked to weight gain after tumor therapy. Finally, Oliverio et al. examined the risk of metabolic exposures with respect to a number of BRCA1/2 variants in a cohort of 438 women carriers of *BRCA1/2* mutations (71). Authors reported that *loss-of-function* variant

TABLE 2 | Metabolic actions of BRCA1.

BRCA1 induces several metabolic modifications, including inhibition of glycolysis
BRCA1 activates the TCA cycle and oxidative phosphorylation
BRCA1 induces a decrease of ketone bodies and free fatty acids
BRCA1-transfected cells display enhanced activity of antioxidative pathways
Mutant BRCA1 leads to increased lipogenesis
BRCA1 depletion leads to reduced mitochondrial respiration and reduced ATP levels

carriers had significantly higher levels of plasma glucose and serum insulin than nonsynonymous variant carriers. Given that *BRCA* mutations confer a lower ability to repair DNA damage, authors suggested that mutation carriers may be more sensitive to the proliferative effects of insulin.

INVOLVEMENT OF BRCA1 IN LIPOGENESIS

Given the connection between obesity and cancer risk, as described above, studies investigated the potential role of BRCA1 in regulation of lipogenesis and energy metabolism. Mutant *BRCA1* has been associated with increased lipogenesis due to relaxation of the repressive action of wild-type BRCA1 on acetyl-CoA carboxylase, a key enzyme in fatty acid synthesis (72). Furthermore, *BRCA1* mutation carriers seem to have decreased blood IGF-binding proteins concentrations and, sometimes, lack an allele containing cytosine–adenine repeats in the *IGF1* gene promoter, which has been linked to decreased insulin sensitivity (7).

A recent study by Koobotse et al. reported that loss of BRCA1 in breast cancer cells led to downregulation of a phosphorylated and inactive form of acetyl CoA carboxylase-α (ACCA) (73). This effect was linked to a concomitant increase in levels of fatty acid synthase (FASN). In addition, IGF1 stimulated dephosphorylation of ACCA by inhibiting the interaction between BRCA1 and phospho-ACCA. In consequence, deficit of BRCA1 increased the non-genomic effects of IGF1 as well as the mitogenic response of cells to IGF1. Furthermore, the effect of high glucose, as compared to physiological concentrations, on the tumor suppressive role of BRCA1 was investigated (74). Normal glucose levels blocked ACCA dephosphorylation by enhancing the association between BRCA1 and phospho-ACCA. The mitogenic response of breast cancer cells to IGF1 was decreased under physiological glucose values whereas no differences were seen in normal mammary epithelial cells. Hence, it is reasonable to assume that normal glucose concentrations facilitate the role of BRCA1 as a metabolic restraint of IGF1 actions. As a corollary, maintaining physiological levels of glucose may improve BRCA1 function and delay breast cancer progression.

In conclusion, the association between metabolic disorders, including diabetes and the metabolic syndrome, and *BRCA1* and *BRCA2* mutations is of major clinical relevance and warrants further investigation.

INTERACTIONS BETWEEN BRCA1 AND STEROID HORMONES

Early studies have identified functional interactions between BRCA1 and a number of steroid hormones, including the estrogen receptor-α (ERα) and androgen receptor (AR). BRCA1 inhibited the estradiol-inducible transcriptional activity of ERα in breast and prostate cancer cells whereas cancer-associated *BRCA1*-mutant cells did not exhibit depressed ERα activity (75, 76). On the other hand, estrogens are capable of enhancing *BRCA1* expression, probably as a result of the mitogenic activity of estrogens. In addition, a direct effect of estrogens was suggested by studies showing that estradiol directly stimulates *BRCA1* promoter activity.

Rosen et al. suggested that BRCA1 regulation of ERα signaling might be important in sporadic carcinogenesis given that this type of breast cancer, unlike *BRCA1*-associated tumors, are usually ERα-positive and often exhibit loss of BRCA1 expression. Loss of BRCA1 could result in unopposed estrogen stimulation of mammary epithelial cell proliferation (77). The impact of *BRCA1/2* mutations on steroid hormone activity was assessed by examining endometrial thickness for each menstrual cycle day as an index of hormone regulation in a cohort of 228 women in the UK Familial Ovarian Cancer Screening Study (78). In addition, estradiol and progesterone titers for the same days were measured. Authors reported that *BRCA1/2* mutation carriers were exposed to enhanced levels of both steroid hormones. Higher values of estradiol in mutation carriers are consistent with a potential carcinogenic role of this hormone in the ovary.

Evidence for functional interactions between BRCA1 and androgens was suggested by experiments showing differential regulation of the *IGF1R* gene by BRCA1 in androgen receptor (AR) positive, as compared to AR negative, prostate cancer cells (50). BRCA1 was expressed at relatively high levels in prostate cancer compared with a low BRCA1 immunostaining in normal prostate epithelium. In addition, there was a negative correlation between IGF1R and BRCA1 expression levels in AR-negative prostate cancer cells whereas in cells with an active AR there was a positive correlation. Finally, cotransfection experiments revealed that BRCA1 expression enhanced AR transcriptional activity. Taken together, analyses identified a new mechanism for IGF1R and AR stimulation of prostate cancer, and further support the relevance of targeting AR and IGF1R in this type of tumors with BRCA1 serving as a marker for defining the target activity.

BRCA1 MUTATIONS AND REPRODUCTION

The potential impact of *BRCA1* mutations on reproduction and fertility has been the focus of major interest (79). However, despite many efforts involved data remain controversial. A study by Kwiatkowski et al. suggested that *BRCA1* mutations increase fertility in families at hereditary breast/ovarian cancer risk (80). Authors evaluated the following hypothesis: if mutations that favor cancer development have survived selection pressure through generations, it is reasonable to assume that these mutations must provide clear advantages that compensate for the reduction in life expectancy. Analyses were conducted on 2,150 families with hereditary cancer, including approximately 96,000 individuals. Authors reported that fertility advantages were seen in a subgroup of 746 *BRCA1* mutation carriers and 483 non-carriers from *BRCA1* mutated families. Female carriers were less often nulliparous (9.1% of carriers in comparison to 16.0% of

non-carriers) and had more children (1.8 ± 1.4 *vs* 1.5 ± 1.3). Likewise, male carriers had more children (1.7 ± 1.3 *vs* 1.4 ± 1.3). While moderate, this increase in fertility in both male and female carriers is suggestive of a mechanism that compensates for shortening of the reproductive phase of life.

An additional report based on two longitudinal studies provides evidence that female *BRCA1/2* mutation carriers had more children, shorter birth intervals and reproduced later in life when compared to matched controls (81). Authors suggested that the positive correlation between *BRCA1/2* mutations and fertility can probably be explained by reported associations between *BRCA* mutations and telomere length and between telomere length and fertility.

In contrast, a negative impact of *BRCA1/2* mutations on fertility was suggested by studies showing that these mutations negatively affect ovarian reserve through accumulated DNA damage (82). Ovarian stimulation was performed in 126 women with breast cancer by using letrozole and gonadotropins for the purpose of fertility preservation by embryo or oocyte cryopreservation. Compared to controls, *BRCA1*, but not *BRCA2*, mutation positive women produced lower numbers of eggs (7.4 *vs* 12.4) and had very high chances of low response to ovarian stimulation. Therefore, authors suggested that *BRCA1* mutations are associated with occult primary ovarian insufficiency. Finally, a study by Shapira et al. shows no evidence of an association between *BRCA1/2* mutations with a lower ovarian response in IVF treatment (83).

INTERACTIONS BETWEEN BRCA1 AND STRESS HORMONES

The stress hormone hydrocortisone (cortisol) was shown to repress *BRCA1* gene expression in a mouse mammary cell line (84). Furthermore, hydrocortisone was also demonstrated to inhibit the stimulatory effect of estrogen on *BRCA1* expression, hence interfering with estrogen-related signaling in mammary epithelial cells. Hence, down-regulation of BRCA1 by cortisol may constitute a distinct pathological mechanism for involvement of stress hormones in breast carcinogenesis.

In addition, studies have identified a direct role for the unliganded glucocorticoid receptor (GR) in BRCA1 upregulation in the absence of hydrocortisone (85). GR was shown to physically interact with the *BRCA1* gene promoter in the absence of hydrocortisone, whereas the positive effect of GR was lost upon addition of the ligand. Given the fact that low levels of BRCA1 have been correlated with the initiation and progression of sporadic breast cancer, this molecular mechanism may explain the finding that prolonged stress signaling increases breast cancer risk.

CONCLUSIONS

Studies summarized in the present review article emphasize the emerging role of BRCA1 as an important player in metabolic and endocrine regulation. While BRCA1 was discovered by virtue of its roles in cancer biology and its genomic activities, accumulating evidence indicates that BRCA1 displays a spectrum of actions that do not fall within the classical cancer-related types of action.

Among other physiological activities, BRCA1 was shown to induce the metabolic reprogramming of breast cancer cells with ensuing reversal of the Warburg effect. BRCA1 governs important steps of the lipogenetic pathway and has a key role in energy metabolism. BRCA1 interacts with several hormones, including IGF1, estrogens and androgens, cortisol, etc. In addition, BRCA1 seems to be involved in the process of reproduction.

In conclusion, a better understanding of the complex physical and functional interactions between BRCA1 and hormonal and metabolic pathways will have major basic and translational relevance.

AUTHOR CONTRIBUTIONS

The author confirms being the sole contributor of this work and has approved it for publication.

ACKNOWLEDGMENTS

HW is the incumbent of the Lady Davis Chair in Biochemistry.

REFERENCES

1. Miki Y, Swensen J, Shattuck-Eidens D, Futreal PA, Harshman K, Tavtigian S, et al. A Strong Candidate for the Breast and Ovarian Cancer Susceptibility Gene BRCA1. *Science* (1994) 266:66–71. doi: 10.1126/science.7545954
2. Hall JM, Lee MK, Newman B, Morrow JE, Anderson LA, Huey B, et al. Linkage of Early-Onset Familial Breast Cancer to Chromosome 17q21. *Science* (1990) 250:1684–9. doi: 10.1126/science.2270482
3. Castilla LH, Couch FJ, Erdos MR, Hoskins KF, Calzone K, Garber JE, et al. Mutations in the BRCA1 Gene in Families With Early-Onset Breast and Ovarian Cancer. *Nat Genet* (1994) 8:387–91. doi: 10.1038/ng1294-387
4. Futreal PA, Liu Q, Shattuck-Eidens D, Cochran C, Harshman K, Tavtigian S, et al. BRCA1 Mutations in Primary Breast and Ovarian Carcinomas. *Science* (1994) 266:120–2. doi: 10.1126/science.7939630
5. Szabo CI, King MC. Population Genetics of BRCA1 and BRCA2. *Am J Hum Genet* (1997) 60:1013–20.
6. King MC, Marks JH, Mandell JB. Breast and Ovarian Cancer Risks Due to Inherited Mutations in BRCA1 and BRCA2. *Science* (2003) 302:643–6. doi: 10.1126/science.1088759
7. Berstein LM. Endocrinology of the Wild and Mutant BRCA1 Gene and Types of Hormonal Carcinogenesis. *Future Oncol* (2008) 4:23–39. doi: 10.2217/14796694.4.1.23
8. Barcellos-Hoff MH, Kleinberg DL. Breast Cancer Risk in BRCA1 Mutation Carriers: Insights From Mouse Models. *Ann Oncol* (2013) 24:Viii8–viii12. doi: 10.1093/annonc/mdt305
9. Narod SA, Foulkes WD. BRCA1 and BRCA2: 1994 and Beyond. *Nat Rev Cancer* (2004) 4:665–76. doi: 10.1038/nrc1431
10. Turner NC, Reis-Filho JS, Russell AM, Springall RJ, Ryder K, Steele D, et al. BRCA1 Dysfunction in Sporadic Basal-Like Breast Cancer. *Oncogene* (2007) 26:2126–32. doi: 10.1038/sj.onc.1210014
11. Roy R, Chun J, Powell SN. BRCA1 and BRCA2: Different Roles in a Common Pathway of Genome Protection. *Nat Rev Cancer* (2012) 12:68–78. doi: 10.1038/nrc3181

12. Xu B, Kim S, Kastan MB. Involvement of Brca1 in s-Phase and G2-Phase Checkpoints After Ionizing Radiation. *Mol Cell Bio* (2001) 21:3445–50. doi: 10.1128/MCB.21.10.3445-3450.2001
13. Deng CX. BRCA1: Cell Cycle Checkpoint, Genetic Instability, DNA Damage Response and Cancer Evolution. *Nucleic Acids Res* (2006) 34:1416–26. doi: 10.1093/nar/gkl010
14. Gudas JM, Li T, Nguyen H, Jensen D, Rauscher FJIII, Cowan KH. Cell Cycle Regulation of BRCA1 Messenger RNA in Human Breast Epithelial Cells. *Cell Growth Diff* (1996) 7:717–23.
15. Kerr P, Ashworth A. New Complexities for BRCA1 and BRCA2. *Curr Biol* (2001) 11:R668–676. doi: 10.1016/S0960-9822(01)00389-X
16. Yarden RI, Pardo-Reoyo S, Sgagias M, Cowan KH, Brody LC. BRCA1 Regulates the G2/M Checkpoint by Activating Chk1 Kinase Upon DNA Damage. *Nat Genet* (2002) 30:285–9. doi: 10.1038/ng837
17. Rosen EM, Fan S, Ma Y. BRCA1 Regulation of Transcription. *Cancer Lett* (2006) 236:175–85. doi: 10.1016/j.canlet.2005.04.037
18. Mullan PB, Quinn JE, Harkin DP. The Role of BRCA1 in Transcriptional Regulation and Cell Cycle Control. *Oncogene* (2006) 25:5854–63. doi: 10.1038/sj.onc.1209872
19. Scully R, Anderson SF, Chao DM, Wei W, Ye L, Young RA, et al. BRCA1 is a Component of the RNA Polymerase II Holoenzyme. *Proc Natl Acad Sci USA* (1997) 94:5605–10. doi: 10.1073/pnas.94.11.5605
20. Silver DP, Livingston DM. Mechanisms of BRCA1 Tumor Suppression. *Cancer Discovery* (2012) 2:679–84. doi: 10.1158/2159-8290.CD-12-0221
21. Chapman MS, Verma IM. Transcriptional Activation by BRCA1. *Nature* (1996) 382:678–9. doi: 10.1038/382678a0
22. Welcsh PL, Lee MK, Gonzalez-Hernandez RM, Black DJ, Mahadevappa M, Swisher EM, et al. BRCA1 Transcriptionally Regulates Genes Involved in Breast Tumorigenesis. *Proc Natl Acad Sci USA* (2002) 99:7560–5. doi: 10.1073/pnas.062181799
23. Jin Y, Xu XL, Yang MC, Wei F, Ayi TC, Bowcock AM, et al. Cell Cycle-Dependent Colocalization of BARD1 and BRCA1 Proteins in Discrete Nyclear Domains. *Proc Natl Acad Sci USA* (1997) 94:12075–80. doi: 10.1073/pnas.94.22.12075
24. Scully R, Chen J, Ochs RL, Keegan K, Hoekstra M, Feunteun J, et al. Dynamic Changes of BRCA1 Subnuclear Location and Phosphorylation State are Initiated by DNA Damage. *Cell* (1997) 90:425–35. doi: 10.1016/S0092-8674(00)80503-6
25. Maul GG, Jensen DE, Ishov AM, Herlyn M, Rauscher FJ. III. Nuclear Redistribution of BRCA1 During Viral Infection. *Cell Growth Diff* (1998) 9:743–55.
26. Monteiro ANA, August A, Hanafusa H. Evidence for a Transcriptional Activation Function of BRCA1 C-Terminal Region. *Proc Natl Acad Sci USA* (1996) 93:13595–9. doi: 10.1073/pnas.93.24.13595
27. De Siervi A, De Luca P, Byun JS, Di LJ, Fufa T, Haggerty CM, et al. Transcriptional Autoregulation by BRCA1. *Cancer Res* (2010) 70:532–42. doi: 10.1158/0008-5472.CAN-09-1477
28. Lann D, LeRoith D. The Role of Endocrine Insulin-Like Growth Factor-I and Insulin in Breast Cancer. *J Mamm Gland Biol Neoplasia* (2008) 13:371–9. doi: 10.1007/s10911-008-9100-x
29. Farabaugh S, Boone D, Lee A. Role of IGF1R in Breast Cancer Subtypes, Stemness, and Lineage Differentiation. *Front Endocrinol (Lausanne)* (2015) 6:59. doi: 10.3389/fendo.2015.00059
30. Rota L, Wood T. Crosstalk of the Insulin-Like Growth Factor Receptor With the Wnt Signaling Pathway in Breast Cancer. *Front Endocrinol (Lausanne)* (2015) 6:92. doi: 10.3389/fendo.2015.00092
31. Yee D, Lee AV. Crosstalk Between the Insulin-Like Growth Factors and Estrogens in Breast Cancer. *J Mamm Gland Biol Neoplasia* (2000) 5:107–15. doi: 10.1023/a:1009575518338
32. Hankinson SE, Willett WC, Colditz GA, Hunter DJ, Michaud DS, Deroo B, et al. Circulating Concentrations of Insulin-Like Growth Factor-I and Risk of Breast Cancer. *Lancet* (1998) 351:1393–6. doi: 10.1016/S0140-6736(97)10384-1
33. Pollak M. The Insulin and Insulin-Like Growth Factor Receptor Family in Neoplasia: An Update. *Nat Rev Cancer* (2012) 12:159–69. doi: 10.1038/nrc3215
34. Renehan AG, Zwahlen M CM, O'Dwyer ST, Shalet SM, Egger M. Insulin-Like Growth Factor-I, IGF Binding Protein-3, and Cancer Risk: Systematic Review and Meta-Regression Analysis. *Lancet* (2004) 363:1346–53. doi: 10.1016/S0140-6736(04)16044-3
35. Baserga R, Peruzzi F, Reiss K. The IGF-1 Receptor in Cancer Biology. *Int J Cancer* (2003) 107:873–7. doi: 10.1002/ijc.11487
36. Dupont J, Pierre A, Froment P, Moreau C. The Insulin-Like Growth Factor Axis in Cell Cycle Pregression. *Horm Metab Res* (2003) 35:740–50. doi: 10.1055/s-2004-814162
37. LeRoith D, Roberts CTJr. The Insulin-Like Growth Factor System and Cancer. *Cancer Lett* (2003) 195:127–37. doi: 10.1016/S0304-3835(03)00159-9
38. Werner H. The Pathophysiological Significance of IGF-I Receptor Overexpression: New Insights. *Ped Endocrinol Rev* (2009) 7:2–5.
39. Werner H, Laron Z. Role of the GH-IGF1 System in Progression of Cancer. *Mol Cell Endocrinol* (2020) 518:111003. doi: 10.1016/j.mce.2020.111003
40. Yerushalmi R, Gelmon KA, Leung S, Gao D, Cheang M, Pollak M, et al. Insulin-Like Growth Factor Receptor (IGF-IR) in Breast Subtypes. *Breast Cancer Res Treat* (2012) 132:131–42. doi: 10.1007/s10549-011-1529-8
41. Werner H, Bruchim I. IGF-1 and BRCA1 Signalling Pathways in Familial Cancer. *Lancet Oncol* (2012) 13:e537–44. doi: 10.1016/S1470-2045(12)70362-5
42. Werner H. Tumor Suppressors Govern Insulin-Like Growth Factor Signaling Pathways: Implications in Metabolism and Cancer. *Oncogene* (2012) 31:2703–14. doi: 10.1038/onc.2011.447
43. Maor SB, Abramovitch S, Erdos MR, Brody LC, Werner H. BRCA1 Suppresses Insulin-Like Growth Factor-I Receptor Promoter Activity: Potential Interaction Between BRCA1 and Sp1. *Mol Gen Metab* (2000) 69:130–6. doi: 10.1006/mgme.1999.2958
44. Abramovitch S, Glaser T, Ouchi T, Werner H. BRCA1-Sp1 Interactions in Transcriptional Regulation of the IGF-IR Gene. *FEBS Lett* (2003) 541:149–54. doi: 10.1016/s0014-5793(03)00315-6
45. Abeliovich D, Kaduri L, Lerer I, Weinberg N, Amir G, Sagi M, et al. The Founder Mutations 185delag and 5382insc in BRCA1 and 6174delt in BRCA2 Appear in 60% of Ovarian Cancer and 30% of Early-Onset Breast Cancer Patients Among Ashkenazi Women. *Am J Hum Genet* (1997) 60:505–14.
46. Shiri-Sverdlov SR, Oefner P, Green L, Baruch RG, Wagner T, Kruglikova A, et al. Mutational Analysis of BRCA1 and BRCA2 in Ashkenazi and Non-Ashkenazi Jewish Women With Familial Breast and Ovarian Cancer. *Hum Mutat* (2000) 16:491–501. doi: 10.1002/1098-1004(200012)16:6<491::AID-HUMU6>3.0.CO;2-J
47. Maor S, Yosepovich A, Papa MZ, Yarden RI, Mayer D, Friedman E, et al. Elevated Insulin-Like Growth Factor-I Receptor (IGF-IR) Levels in Primary Breast Tumors Associated With BRCA1 Mutations. *Cancer Lett* (2007) 257:236–43. doi: 10.1016/j.canlet.2007.07.019
48. Abramovitch S, Werner H. Functional and Physical Interactions Between BRCA1 and P53 in Transcriptional Regulation of the IGF-IR Gene. *Horm Metab Res* (2003) 35:758–62. doi: 10.1055/s-2004-814154
49. Werner H, Sarfstein R, LeRoith D, Bruchim I. Insulin-Like Growth Factor 1 Signaling Axis Meets P53 Genome Protection Pathways. *Front Oncol* (2016) 6:159. doi: 10.3389/fonc.2016.00159
50. Schayek H, Haugk K, Sun S, True LD, Plymate SR, Werner H. Tumor Suppressor BRCA1 is Expressed in Prostate Cancer and Control IGF1-R Gene Transcription in an Androgen Receptor-Dependent Manner. *Clin Cancer Res* (2009) 15:1558–65. doi: 10.1158/1078-0432.CCR-08-1440
51. Amichay K, Kidron D, Attias-Geva Z, Schayek H, Sarfstein R, Fishman A, et al. BRCA1 is Expressed in Uterine Serous Carcinoma and Controls Insulin-Like Growth Factor I Receptor Gene Expression in USC Cell Lines. *Int J Gynecol Cancer* (2012) 22:748–54. doi: 10.1097/IGC.0b013e31825011f
52. Bruchim I, Amichay K, Kidron D, Attias Z, Biron-Shental T, Drucker L, et al. BRCA1/2 Germline Mutations in Jewish Patients With Uterine Serous Carcinoma. *Int J Gynecol Cancer* (2010) 20:1148–53. doi: 10.1111/IGC.0b013e3181ef622d
53. Pennington KP, Walsh T, Lee M, Pennil C, Novetsky AP, Agnew KJ, et al. BRCA1, TP53, and CHEK2 Germline Mutations in Uterine Serous Carcinoma. *Cancer* (2013) 119:332–8. doi: 10.1002/cncr.27720
54. Hudelist G, Wagner T, Rosner M, Fink-Retter A, Gschwantler-Kaulich D, Czerwenka K, et al. Intratumoral IGF-I Protein Expression is Selectively Upregulated in Breast Cancer Patients With BRCA1/2 Mutations. *Endocr Related Cancer* (2007) 14:1053–62. doi: 10.1677/ERC-06-0075
55. Shukla V, Coumoul X, Cao L, Wang RH, Xiao C, Xu X, et al. Absence of the Full-Length Breast Cancer-Associated Gene-1 Leads to Increased Expression of Insulin-Like Growth Factor Signaling Axis Members. *Cancer Res* (2006) 66:7151–7. doi: 10.1158/0008-5472.CAN-05-4570

56. Marquis ST, Rajan JV, Wynshaw-Boris A, Xu J, Yin G-Y, Abel KJ, et al. The Developmental Pattern of BRCA1 Expression Implies a Role in Differentiation of the Breast and Other Tissues. *Nat Genet* (1995) 11:17–26. doi: 10.1038/ng0995-17
57. Satterwhite DJ, Matsunami N, White RL. TGF-Beta1 Inhibits BRCA1 Expression Through a Pathway That Requires Prb. *Biochem Biophys Res Comm* (2000) 276:686–92. doi: 10.1006/bbrc.2000.3510
58. Thomas JE, Smith M, Tonkinson JL, Rubinfeld B, Polakis P. Induction of Phosphorylation on BRCA1 During the Cell Cycle and After DNA Damage. *Cell Growth Diff* (1997) 8:801–9.
59. Vaughn JP, Davis PL, Jarboe MD, Huper G, Evans AC, Wiseman RW, et al. BRCA1 Expression is Induced Before DNA Synthesis in Both Normal and Tumor-Derived Breast Cells. *Cell Growth Diff* (1996) 7:711–5.
60. Somasundaram K, Zhang H, Zeng YX, Houvras Y, Peng Y, Zhang H, et al. Arrest of the Cell Cycle by the Tumour-Suppressor BRCA1 Requires the CDK-Inhibitor $P21^{waf1/Cip1}$. *Nature* (1997) 389:187–90. doi: 10.1038/38291
61. Varma AK, Brown RS, Birrane G, Ladias JAA. Structural Basis for Cell Cycle Checkpoint Control by the BRCA1-Ctip Complex. *Biochemistry* (2005) 44:10941–6. doi: 10.1021/bi0509651
62. Maor S, Papa MZ, Yarden RI, Friedman E, Lerenthal Y, Lee SW, et al. Insulin-Like Growth Factor-I Controls BRCA1 Gene Expression Through Activation of Transcription Factor Sp1. *Horm Metab Res* (2007) 39:179–85. doi: 10.1055/s-2007-970415
63. Nelson AC, Lyons TR, Young CD, Hansen KC, Anderson CM, Holt JT. Akt Regulates BRCA1 Stability in Response to Hormone Signaling. *Mol Cell Endocrinol* (2010) 319:129–42. doi: 10.1016/j.mce.2010.01.019
64. Clayton P, Banerjee I, Murray PG, Renehan AG. Growth Hormone, the Insulin-Like Growth Factor Axis, Insulin and Cancer Risk. *Nat Rev Endocrinol* (2011) 7:11–24. doi: 10.1038/nrendo.2010.171
65. Antoniou A, Pharoah PD, Narod S, Risch HA, Eyfjord JE, Hopper JL, et al. Average Risks of Breast and Ovarian Cancer Associated With BRCA1 or BRCA2 Mutations Detected in Case Series Unselected for Family History: A Combined Analysis of 22 Studies. *Am J Hum Genet* (2003) 72:1117–30. doi: 10.1086/375033
66. Narod SA. BRCA Mutations in the Management of Breast Cancer: The State of the Art. *Nat Rev Clin Oncol* (2010) 7:702–7. doi: 10.1038/nrclinonc.2010.166
67. Privat M, Radosevic-Robin N, Aubel C, Cayre A, Penault-Llorca F, Marceau G, et al. BRCA1 Induces Major Energetic Metabolism Reprogramming in Breast Cancer Cells. *PloS One* (2014) 9:e102438. doi: 10.1371/journal.pone.0102438
68. Kanakkanthara A, Kurmi K, Ekstrom TL, Hou X, Purfeerst ER, Heinzen EP, et al. BRCA1 Deficiency Upregulates NNMT, Which Reprograms Metabolism and Sensitizes Ovarian Cancer Cells to Mitochondrial Metabolic Targeting Agents. *Cancer Res* (2019) 79:5920–9. doi: 10.1158/0008-5472.CAN-19-1405
69. Bruchim I, Fishman A, Friedman E, Goldberg I, Chetrit A, Barshack I, et al. Analyses of P53 Expression Pattern and BRCA Mutations in Patients With Double Primary Breast and Ovarian Cancer. *Int J Gynecol Cancer* (2004) 14:251–8. doi: 10.1111/j.1048-891X.2004.014208.x
70. Bordeleau L, Lipscombe L, Lubinski J, Ghadirian P, Foulkes WDN, Neuhausen S, et al. Diabetes and Breast Cancer Among Women With BRCA1 and BRCA2 Mutations. *Cancer* (2011) 117:1812–8. doi: 10.1002/cncr.25595
71. Oliverio A, Bruno E, Colombo M, Paradiso A, Tommasi S, Daniele A, et al. BRCA1/2 Variants and Metabolic Factors: Results From a Cohort of Italian Female Carriers. *Cancers (Basel)* (2020) 12:3584. doi: 10.3390/cancers12123584
72. Moreau K, Dizin E, Ray H, Luquain C, Lefai E, Foufelle F, et al. BRCA1 Affects Lipid Synthesis Through its Interaction With Acetyl-Coa Carboxylase. *J Biol Chem* (2006) 281:3172–81. doi: 10.1074/jbc.M504652200
73. Koobotse M, Holly J, Perks C. Elucidating the Novel BRCA1 Function as a Non-Genomic Metabolic Restraint in ER-Positive Breast Cancer Cell Lines. *Oncotarget* (2018) 9:33562–76. doi: 10.18632/oncotarget.26093
74. Koobotse MO, Schmidt D, Holly JMP, Perks CM. Glucose Concentration in Cell Culture Medium Influences the BRCA1-Mediated Regulation of the Lipogenic Action of IGF-I in Breast Cancer Cells. *Int J Mol Sci* (2020) 21:8674. doi: 10.3390/ijms21228674
75. Fan S, Ma YX, Wang C, Yuan R, Meng Q, Wang J-A, et al. Role of Direct Interaction in BRCA1 Inhibition of Estrogen Receptor Activity. *Oncogene* (2001) 20:77–87. doi: 10.1038/sj.onc.1204073
76. Xu J, Fan S, Rosen EM. Regulation of the Estrogen-Inducible Gene Expression Profile by the Breast Cancer Susceptibility Gene BRCA1. *Endocrinology* (2005) 146:2031–47. doi: 10.1210/en.2004-0409
77. Rosen EM, Fan S, Pestell RG, Goldberg ID. BRCA1 in Hormone-Responsive Cancers. *Trends Endocrinol Metab* (2003) 14:378–85. doi: 10.1016/j.tem.2003.08.001
78. Widschwendter M, Rosenthal AN, Philpott S, Rizzuto I, Fraser L, Hayward J, et al. The Sex Hormone System in Carriers of BRCA1/2 Mutations: A Case-Control Study. *Lancet Oncol* (2013) 14:1226–32. doi: 10.1016/S1470-2045(13)70448-0
79. Daum H, Peretz T, Laufer N. BRCA Mutations and Reproduction. *Fertil Steril* (2018) 109:33–8. doi: 10.1016/j.fertnstert.2017.12.004
80. Kwiatkowski F, Arbre M, Bidet Y, Laquet C, Uhrhammer N, Bignon YJ. BRCA Mutations Increase Fertility in Families at Hereditary Breast/Ovarian Cancer Risk. *PloS One* (2015) 10:e0127363. doi: 10.1371/journal.pone.0127363
81. Smith KR, Hanson HA, Mineau GP, Buys SS. Effects of BRCA1 and BRCA2 Mutations on Female Fertility. *Proc Biol Sci* (2012) 279:1389–95. doi: 10.1098/rspb.2011.1697
82. Oktay K, Kim JY, Barad D, Babayev SN. Association of BRCA1 Mutations With Occult Primary Ovarian Insufficiency: A Possible Explanation for the Link Between Infertility and Breast/Ovarian Cancer Risks. *J Clin Oncol* (2010) 28:240–4. doi: 10.1200/JCO.2009.24.2057
83. Shapira M, Raanani H, Feldman B, Srebnik N, Dereck-Haim S, Manela D, et al. BRCA Mutation Carriers Show Normal Ovarian Response in *In Vitro* Fertilization Cycles. *Fertil Steril* (2015) 104:1162–7. doi: 10.1016/j.fertnstert.2015.07.1162
84. Antonova L, Mueller CR. Hydrocortisone Down-Regulates the Tumor Suppressor Gene BRCA1 in Mammary Cells: A Possible Molecular Link Between Stress and Breast Cancer. *Genes Chrom Cancer* (2008) 47:341–52. doi: 10.1002/gcc.20538
85. Ritter HD, Antonova L, Mueller CR. The Unliganded Glucocorticoid Receptor Positively Regulates the Tumor Suppressor Gene BRCA1 Through GABP Beta. *Mol Cancer Res* (2012) 10:558–69. doi: 10.1158/1541-7786.MCR-11-0423-T

Conflict of Interest: The author declares that the research was conducted in the absence of any commercial or financial relationships that could be construed as a potential conflict of interest.

frontiers | Frontiers in Endocrinology

MINI REVIEW
published: 05 April 2022
doi: 10.3389/fendo.2022.861434

New Insights in PRRT: Lessons From 2021

Giulia Puliani[1,2], *Alfonsina Chiefari*[1], *Marilda Mormando*[1], *Marta Bianchini*[1], *Rosa Lauretta*[1] *and Marialuisa Appetecchia*[1]*

[1] Oncological Endocrinology Unit, Scientific Institute for Research, Hospitalization and Healthcare (IRCCS) Regina Elena National Cancer Institute, Rome, Italy, [2] Department of Experimental Medicine, Sapienza University of Rome, Rome, Italy

Peptide receptor radionuclide therapy (PRRT) using radiolabeled somatostatin analogs has been used for over two decades for the treatment of well-differentiated neuroendocrine tumors (NETs), and the publication of the NETTER-1 trials has further strengthened its clinical use. However, many aspects of this treatment are still under discussion. The purpose of this review is to collect and discuss the new available evidence, published in 2021, on the use of ^{177}Lu-Oxodotreotide (DOTATATE) or ^{90}Y-Edotreotide (DOTATOC) in adult patients with NETs focusing on the following hot topics: 1) PRRT use in new clinical settings, broaden its indications; 2) the short- and long-term safety; and 3) the identification of prognostic and predictive factors. The review suggests a possible future increase of PRRT applications, using it in other NETs, as a neoadjuvant treatment, or for rechallenge. Regarding safety, available studies, even those with long follow-up, supported the low rates of adverse events, even though 1.8% of treated patients developed a second malignancy. Finally, there is a lack of prognostic and predictive factors for PRRT, with the exception of the crucial role of nuclear imaging for both patient selection and treatment response estimation.

Keywords: peptide receptor radionuclide therapy, radioligand therapy, predictive factors, prognostic factors, neuroendocrine tumors, neuroendocrine neoplasms, safety

OPEN ACCESS

Edited by:
Antonino Belfiore, University of Catania, Italy

Reviewed by:
Krystallenia I. Alexandraki, National and Kapodistrian University of Athens, Greece

***Correspondence:**
Marialuisa Appetecchia
marialuisa.appetecchia@ifo.it

Specialty section:
This article was submitted to Cancer Endocrinology, a section of the journal Frontiers in Endocrinology

Received: *24 January 2022*
Accepted: *07 March 2022*
Published: *05 April 2022*

Citation:
Puliani G, Chiefari A, Mormando M, Bianchini M, Lauretta R and Appetecchia M (2022) New Insights in PRRT: Lessons From 2021. Front. Endocrinol. 13:861434. doi: 10.3389/fendo.2022.861434

1 INTRODUCTION

Peptide receptor radionuclide therapy (PRRT) with radiolabeled somatostatin analogs has been used for two decades for the treatment of well-differentiated neuroendocrine tumors (NETs) expressing somatostatin receptor (SSTR) type 2. The two most commonly used peptides are ^{177}Lutetium (^{177}Lu)-DOTATATE and ^{90}Yttrium (^{90}Y)-DOTATOC, respectively, beta- or gamma-emitting radionuclides (1). The publication of the NETTER-1 trial in 2017 has further confirmed the efficacy of this kind of therapy in NETs, also considering that the control arm of the study was represented by above label doses of somatostatin analogs, a very effective treatment (2). This study led to the approval of ^{177}Lu-oxodotreotide (®Lutathera) by the European Medicines Agency and thus facilitated access to this treatment. However, this treatment is actually recommended only for progressive grade 1–2 gastroenteropancreatic (GEP) NETs. European Society for Medical Oncology (ESMO) guidelines recommend considering PRRT also in carcinoid syndrome (CS) and functional pancreatic (Pan) NETs refractory to somatostatin analogs and in selected cases of NET G3 (3).

Although PRRT represents a major cornerstone of treatment of well-differentiated low-grade GEP-NETs, some important aspects such as additional clinical indications, long-term safety, and predictive markers are not well established, and great attention is paid to these topics in recent literature.

This review aims to collect the evidence published in 2021 on the use of 177Lu-DOTATATE or 90Y-DOTATOC in adult patients with NETs in order to summarize the new evidence in 3 main research fields: 1) the use of PRRT in new settings, to broaden clinical indications; 2) short- and long-term safety assessment; and 3) the identification of prognostic and predictive factors.

2 METHODS

We searched the PubMed database for articles in English on PRRT published in 2021. The search strategies used were "peptide receptor radionuclide therapy" and "radioligand therapy." The latest search was carried out on November 18, 2021. We have selected all the articles concerning the use of PRRT in human patients affected by neuroendocrine neoplasms of any origin regarding one of three reported topics. Articles not on humans, not using ^{177}Lu or ^{90}Y compounds, or on children were excluded from this review. Excluding duplicate articles, from the original number of 531 articles, 453 were excluded after abstract screening and 33 after full-text evaluation. Ultimately, 45 studies were included, as reported in **Supplementary Figure S1**.

3 RESULTS

3.1 New Indications and Settings for Peptide Receptor Radionuclide Therapy

3.1.1 Expanding the Clinical Indication

The overexpression of SSTRs in NETs other than GEP has led PRRT to be used in these neoplasms even if not actually approved.

A retrospective study evaluated the long-term outcome of ^{177}Lu-DOTATATE in patients with paragangliomas (PGLs), demonstrating a disease control rate (DCR) of 67%. At 40 months, the observed progression-free survival (PFS) rate was 63% (95% CI: 30–96) and the overall survival (OS) rate was 65% (95% CI: 32–97) (4). These data were confirmed in a prospective phase II clinical trial (5), in which an overall DCR of 80% was observed (95% CI: 68.9–91.9) after a mean of five cycles of PRRT. Patients treated with ^{177}Lu-DOTATATE showed a better OS compared with those treated with ^{90}Y-DOTATOC (143 vs. 92 months). No high-grade renal and hematological toxicities occurred in both studies. Regarding the risk of PRRT-induced acute catecholamine crisis, premedication combining alpha- and beta-adrenergic blocking agents was effective in preventing this complication in a series of 5 patients (6).

A retrospective multicenter study aimed at evaluating the role of ^{68}Ga-DOTATATE PET/CT in metastatic medullary thyroid cancer (MTC) and for patients' selection for PRRT. Twenty-one of 71 patients, with tumor expressing SSTR, were treated with PRRT, with ^{177}Lu-DOTATATE or ^{90}Y-DOTATOC or both (median number of treatment cycles, 3; range, 1–4). At baseline, 10 patients had radiological and 3 had biochemical progression. After a median follow-up of 12 months, 12 patients had radiological progression, 1 had biochemical progression, and 3 patients died. The median time to treatment failure (including radiological or biochemical progression or death) was 14 months (95% CI: 8–25) without difference in terms of age, type of radionuclide, calcitonin serum level, or gallium avidity (7).

Bronchopulmonary NETs expressing SSTR may also benefit from PRRT. A retrospective study evaluated the role of combined ^{68}Ga-DOTATATE and ^{18}F-FDG PET/CT imaging to guide the choice of PRRT treatment in patients with typical and atypical carcinoids (TC and AC). About half of the patients (46% TC, 53% AC) were unsuitable for PRRT. In 16 patients who were treated with PRRT, DCR at 3 months was 85% with an OS of 54.6 months (95% CI 44–70). Patients with all lesions ^{68}Ga-DODATATE positive and ^{18}FDG PET/CT negative were less likely to develop disease progression (8).

Finally, patients with functioning tumors can benefit from PRRT. A retrospective cohort study that included patients with refractory CS, without evidence of disease progression, demonstrated a reduction in bowel movement frequency of more than 30% with PRRT in 47% of patients, also with a benefit on flushing. Importantly, no carcinoid crisis occurred with the use of short-acting octreotide subcutaneously between cycles (9).

3.1.2 Peptide Receptor Radionuclide Therapy in the Neoadjuvant Setting

Promising evidence is emerging on the use of PRRT as a neoadjuvant treatment. In an open-label retrospective study, enrolling patients with unresectable GEP-NET, ^{177}Lu-DOTATATE resulted in a significant tumor shrinkage, allowing primary tumor resection in 26.3% of the patients. Baseline significant response predictors were primary duodenal tumor site, the size of the primary tumor (<5 cm), absence of regional lymph node involvement, the size (≤1.5 cm) and number (≤3) of liver metastases, and ^{18}F-FDG uptake (SUV_{max} <5) in the primary tumor (10).

3.1.3 Retreatment With Peptide Receptor Radionuclide Therapy

Several uncontrolled studies have evaluated the outcome and feasibility of retreatment after an initial response to the first single course of PRRT followed by later disease progression (rechallenge with PRRT).

A retrospective study on 40 patients with advanced GEP-NETs with progressive disease after the first PRRT course demonstrated that the second PRRT course determined partial remission in 5% of patients, stable disease in 52.5% of patients, and disease progression in 42.5% of patients. The median OS was 122.1 months and was significantly longer in patients without uptake at ^{18}F-FDG-PET CT (145.50 vs. 95.06 months, respectively) (11).

In a large Danish retrospective study, progression after the first PRRT course was seen in 62% of patients. Thirty-two patients were submitted to a second series of PRRT, and progression was observed in 64% of patients. The median PFS was 19 (range, 10–32) months. Interestingly, this study also included 8 patients who underwent a third PRRT series, with a PFS of 12 (range, 8–15) months (12).

Two meta-analyses have been published on the rechallenge with PRRT (the term "salvage treatment" was used in some articles included in the meta-analyses). A meta-analysis on 13 studies involving 560 patients evaluated the efficacy and safety of PRRT retreatment in patients with GEP-NETs, with encouraging results. Median pooled PFS was 12.52 months (95% CI: 9.82–15.22), and pooled DCR was 71% (95% CI: 66–75). The safety profile for retreatment was comparable to the initial PRRT, with grade 3–4 adverse events occurring in 5% (95% CI: 2–8) of patients (13).

Similar results emerged from another meta-analysis, including 9 studies on 426 patients. After PRRT retreatment, pooled DCR was 76.9% (95% CI: 72.3–81.0) months, pooled PFS was 14.1 (95% CI: 12.2–15.9) months, and pooled median OS of 26.8 (95% CI: 18.8–34.9) months. As expected, PRRT showed a significantly lower DCR and shorter PFS compared to initial PRRT, without significant differences in hematologic and renal toxicities (14).

3.1.4 Positioning Peptide Receptor Radionuclide Therapy in the Treatment Sequence

Until now, the optimal treatment sequence for NETs is not well established. A retrospective study in patients with metastatic G2 Pan-NETs, treated with more than one systemic therapy, showed that patients who received PRRT in the treatment sequence (most frequently as third or fourth line) had significantly prolonged survival compared with those who did not receive PRRT [median, 84 vs. 56 months; hazard ratio (HR), 0.55; 95% CI: 0.31–0.98] (15).

Parghane et al. (16) evaluated the long-term outcome of a combined chemotherapy and PRRT protocol with a "sandwich" regimen in the treatment of metastatic progressive NETs with both ^{18}F-FDG and ^{68}Ga-DODATOC avid lesions. In 38 patients analyzed, DCR of 84%, PFS of 72.5%, and OS of 80.4% at 36 months were observed. A longer PFS and higher DCR were noted in patients without metastatic bone involvement. Only low-grade and transient toxicities were registered, without renal toxicities of any grade (16).

The features of the main articles on the new indications and settings and safety of PRRT are summarized in **Table 1**.

3.2 Short- and Long-Term Safety of Peptide Receptor Radionuclide Therapy

The critical organs to consider before PRRT are the kidney and bone marrow. Until now, the accepted upper limit doses have been adapted by external radiotherapy (23 Gy for kidneys and 2 Gy for bone marrow) (28). Data from a retrospective study including 37 patients receiving ^{177}Lu-DOTATATE showed that only 5.5% reached 2 Gy to the bone marrow and the threshold value of 23 Gy for kidney was reached in 21% of patients receiving 4 cycles and in 37.5% in case of more than 4 cycles. However, no long-term renal dysfunction occurred with a kidney dose of 23–29 Gy, suggesting a possible increase of kidney threshold levels (17). Accordingly, an open-label, prospective, phase II study showed the absence of grade 3–4 hematological toxicities and renal impairment using ^{177}Lu-DOTATATE at two different doses (18.5 and 27.5 GBq in 5 cycles) (18). Globally, PRRT was safe, with a low incidence of severe nephrotoxicity and hematotoxicity. Notably, in the majority of the studies, a protocol of amino acid infusion was used in order to reduce renal injury. A large study described an impairment in kidney function and hemoglobin in 20.6% of patients 1 year after the start of the treatment. Age over 65 years seems to be a risk factor for the development of anemia. Leukocyte and platelet count reduction was 14.7% and 10.8% of patients, respectively (19). Another retrospective study did not confirm any significant change in glomerular filtrate after PRRT (20). Considering the late effects of PRRT, in a large series of 1,631 treated patients, only 1.8% developed therapy-related myeloid neoplasm, including myelodysplastic syndrome and acute myeloid leukemia, after a median time of 43 months (range, 6–123) (21). A case series on 5 patients with bone marrow infiltration of NETs and myelosuppression demonstrated that PRRT could be safe also in these patients when prophylactic peripheral blood stem cell collection was performed before PRRT (29). In another study, grade 1–2 hematological toxicities were observed in 60.3% of patients and grade 3–4 toxicities were observed in 25 patients (32.1%), without the development of myelodysplasia or the need for dialysis or liver failure (27).

Two studies have evaluated the effect of PRRT on pituitary function, as normal pituitary tissue expresses SSTRs. Comparing patients treated or not with PRRT, after a long follow-up (68 months), the prevalence of hypopituitarism was the same in the two groups (22). Another study evaluated pituitary function at baseline and 1 year after high-dose PRRT. The study demonstrated a significant decrease in insulin like growth factor 1 (IGF1) levels, which was related to the number of cycles and the absorbed radiation dose, without changes in the adrenal and thyroid axes (23).

Strosberg et al. (30) reported a 3% incidence of risk of bowel obstruction within 3 months in patients receiving PRRT. All patients had a mesenteric or peritoneal disease and responded to high doses of corticosteroid (30). PRRT-related cardiotoxicity has been investigated in 13 patients affected by NETs. No significant change in serum troponin I was demonstrated after PRRT (24).

The safety of ^{177}Lu-DOTATATE was also confirmed in patients with advanced PanNET heavily pretreated with chemotherapy. Grade 3–4 bone marrow toxicities occurred in 10.8% and were unrelated to the type and duration of previous chemotherapy, amount of activity administered, and dose absorbed from the bone marrow. One patient (1.0%) developed acute myeloid leukemia (25). In older patients (≥70 years) treated with PRRT, the most common adverse events were fatigue and grade 1–2 gastrointestinal disturbances, occurring in 98.3% of patients. The most common hematological adverse

TABLE 1 | List of the main studies published in 2021 on **(A)** additional indications, **(B)** neoadjuvant role, **(C)** rechallenge, and **(D)** safety of PRRT treatment in patients affected by NETs.

Authors (ref)	Design	Patients[a] total (M/F) number	Age Median (range) years	NET type	NET Grade	Prior treatment n (%)	PRRT Scheme Radionuclide, median dose, median n cycles	Main inclusion criteria	Aim of the study	Follow-up Median (range) months
A) Additional indications of PRRT										
Parghane RV (4)	R	10 (5/5)	49 (33–61)	Metastatic PGLs	–	RT: 6 (60%) CHT: 1 (10%)	**^{177}Lu:** 10 (100%) 24.42 GBq (range 7.4–37) in 4 (1–6) cycles	Negative ^{131}I-MIBG SPECT positive ^{68}Ga-PET	PFS OS	40 (NA)
Severi S (5)	P (Ph 2)	46 (20/26)	52 (NA)	Progressive locally advanced or metastatic PGLs	–	NA	**^{90}Y**: 12 (26%) 9.2 GBq in 5 cycles **^{177}Lu**: 34 (74%) 24.42 GBq in 5 cycles	SSTR2 positive	Activity and safety	73 (5–146)
Hayes AR (7)	R	21 (14/7)	50 (27–74)	MTC	–	NA	**^{90}Y**: 5 (24%) **^{177}Lu**: 12 (57%) **Both**: 4 (19%) in 3 cycles (1–4)	SSTR2 positive evaluated by ^{68}Ga-PET	Role of ^{68}Ga- PET in MTC	12 (2–47)
Zidan L (8)	R	56 (24/32) (*only 16 treated by PRRT*)	TC: 63(21–81) AC: 68.5 (33–83)	Lung carcinoids	TC: 22 (39%) AC: 34 (61%)	Surgery ± SSA: 25 (44.6%) CHT: 3 (5.4%)	**^{177}Lu**: 14 (87.5%) in 4 cycles (3–4) **Both**: 2 (12.5%)	Progression or uncontrolled symptoms	Role of ^{68}Ga- PET and ^{18}F-FDG PET for treatment selection	TC: 37 (NA) AC: 38 (NA)
Zandee WT (9)	R	22 (12/10)	62.7 ± 8.2[b]	Metastatic midgut NET with CS	G1: 7 (32%) G2: 7 (32%) UK: 8 (36%)	CHT: 2 (9%) Other: 8 (37%)	**^{177}Lu:** 22 (100%) 27.8-29.6 GBq 4 cycles	Non-progressive and SSA refractory CS	Efficacy for symptoms reduction	>1 year
B) PRRT as neoadjuvant treatment										
Parghane RV (10)	R	57 (33/24)	51.5 (30–78)	unresectable GEP-NET P: 32 (56.1%) GI: 25 (43.9%)	G1: 26 (45.6%) G2: 30 (52.6%) G3: 1 (1.7%)	CHT: 15 (26%) SSA: 12 (21%)	**^{177}Lu**: 57 (100%) 22.2-27.5 GBq (14.8–40.7) in 4 cycles (2–5)	Unresectable GEP NET with or without liver metastasis	Efficacy of neoadjuvant PRRT	24 (NA)
C) Rechallenge with PRRT										
Rodrigues M (11)	R	40 (26/14)	54.6 (29–83)	Advanced GEP P: 18 (45%) GI: 22 (55%)	G1: 2 (5%) G2: 29 (72.5%) G3: 8 (20%) UK: 1 (2.5%)	LRT: 16 (40%)	**^{177}Lu**: 40 (100%) cumulative 48.8 ± 11.8[b] GBq	At least two courses of PRRT	Efficacy of a second PRRT	NA
Zacho MD (12)	R	133 (72/61)	70 (64–76)	P: 31 (23.3%) GI: 82 (61.6%) Lung: 14 (10.5%) Oth: 6 (4.5%)	G1: 24 (20%) G2: 78 (63%) G3: 21 (17%)	SSA: 113 (85%) IFN: 42 (37%) CHT: 67 (51%) LRT: 11 (8%)	***First series*** **^{177}Lu:** 60 (45%) **^{90}Y**: 66 (50%) **Both**: 7 (5%) ***Second series*** **^{177}Lu**: 25 (69%) **^{90}Y**: 8 (23%) **Both**: 3 (8%) ***Third series*** **^{177}Lu:** 6 (75%) **^{90}Y:** 2 (25%)	Patients treated at least one course PRRT	Treatment response	NA
D) Safety of PRRT										
Kovan B (17)	R	36 (18/18)	54.7 ± 12.9[b]	P: 8 (22.2%) GI: 2 (5.5%) MTC: 6 (16.7%) Lung: 2 (5.5%) UK: 18 (50%)	NA	NA	**^{177}Lu**: 36 (100%) 691 ± 257[b] mCi in 3.91 ± 1.33[b] cycles	NET patient treated with PRRT	Evaluating critical organ threshold values	20 (2–61)
Paganelli G (18)	P (Ph 2)	43 (28/15)	65 (44–82)	GI NETs	G1: 13 (30%) G2: 18 (42%) UK: 12 (28%)		**^{177}Lu**: 43 (100%) 27.5 GBq (25 pts) 18.5 GBq (18 pts) in 5 cycles	Positive octreoscan or ^{68}Ga- PET	DCR and Toxicity	118 (12.6–139.6)
Nilica B (19)	R	102 (67/35)	44 pts ≥65 years	GI: 47 (46.1%) P: 24 (23.5%) Lung: 5 (4.9%) PGLS: 3 (2.9%) MTC: 1 (1%) FTC: 3 (2.9%) UK: 6 (5.9%) NA: 13 (12.7%)	NA	NA	**^{177}Lu**: 86 (84%) 29.6 GBq in 4 cycles[d] **^{90}Y**: 16 (16%) 16 GBq in 4 cycles[d]	≥4 PRRT cycles No concomitant oncologic treatment (excl. SSA) ≥52 weeks FU	Long-term safety	>52 weeks
Guhne F (20)	R	32 (16/16)	64.2 ± 11.1[b]	For: 16 (50%) Mid: 6 (18.7%) UK: 4 (12.5%)	NA	NA	**^{177}Lu**: 32 (100%) 20.7 ± 3.7 GBq in 3 cycles	Availability of ^{68}Ga-PET after third cycle	Safety	NA

(Continued)

TABLE 1 | Continued

Authors (ref)	Design	Patients[a] total (M/F) number	Age Median (range) years	NET type	NET Grade	Prior treatment n (%)	PRRT Scheme Radionuclide, median dose, median n cycles	Main inclusion criteria	Aim of the study	Follow-up Median (range) months
				Others: 6 (18.7%)						
Chantadisai M (21)	R	1631 [30 pts developed t-MN 15/15)]	59 (32-70)	GI: 11 (37%) P: 13 (43%) Lung: 1 (3%) UK: 2 (7%) Oth: 3 (10%)	G1: 8 (27%) G2: 10 (33%) NET G3: 1 (3%) UK: 11 (37%)	SSA: 12 (40%) 1-line CHT: 8 (27%) >1-line CHT: 3 (10%) Others 11 (37%) No: 5 (17%)	**^{90}Y:** 3 (10%) 10.5 GBq in 4 cycles **^{177}Lu**: 8 (27%) 22.1 GBq in 3.5 cycles **Both**: 18 (60%) 25 Gbq in 5 cycles[c]	Development of therapy-related hematologic neoplasms	OS	55 (17–145)
Elston MS (22)	Cohort	34 PRRT (23/11)	65.1 (56.1–71.7)	GI: 13 (38.2%) P: 18 (52.9%) Lung: 1 (2.9%) UK: 2 (5.9%)	NA	CHT: 17 (50%)	NA 31.8 (31.2–35.0) in 4 cycles (4–4.25)	Unresectable NET without pituitary disease	Prevalence of hypopituitarism	68 (NA)
		32 no PRRT (15/17)	61.6 (54.9–68.7)	GI: 18 (56.2%) P: 10 (31.2%) Lung: 1 (3.1%) UK: 3 (9.4%)	NA	CHT: 1 (3.1%)	–			
Sundlov A (23)	P (Ph 2)	68 (37/31)	66 (41–80)	GI: 40 (59%) P: 14 (21%) Lung: 5 (7%) Oth: 9 (13%)	G1–G2	1-line CHT: 4 (6%) 2 lines CHT: 2 (3%) 3 lines CHT: 2 (3%) SSA: 55 (81%) LRT: 27 (40%) Others: 11 (16%)	**^{177}Lu:** 68 (100%) 37 Gbq (14.8–66.6) in 5 cycles (2–9)	Progressive NET with SSRT expression	Evaluate long –term pituitary function after PRRT	30 (11–39)
Jafari E (24)	R	13 (9/4)	52 (27–71)	NA	NA	NA	**^{177}Lu**: 13 (100%) 14.8 GBq (6–44) in 2 cycles (1–6)	NET treated by PRRT	Evaluating PRRT cardiotoxicity	21 (4–28)
Fross-Baron K (25)	R	102 (64/38)	57.1 (29–79)	P: 102 (100%)	G1: 2 (1.9%) G2: 76 (74.5%) G3: 7 (6.9%) UK: 17 (16.7%)	1-line CHT: 68 (66.7%) 2-lines CTH: 29 (28.4%) 3-lines CHT: 5 (4.9%) Other: 16 (15.7%) LRT: 39 (38.2%) RT: 4 (3.9%)	**^{177}Lu:** 102 (100%) 32 ± 10.9 GBq, in 4 cycles (44 patients >4 cycles)	Patients had previously received one (67%) or multiple (33%) chemotherapy lines prior to ^{177}LuPRRT	PFS OS	34 (4–160)
Chen L (26)	R	71 (42/29)	70 (55–80)	GI: 55 (77.5%) P: 8 (11.3%) Lung: 3 (4.2%) UK: 5 (7%)	G1 or TC: 38 (53.5%) G2 or AC: 29 (40.8%) G3: 2 (2.8%) UK: 5 (7%)	SSA: 66 (93%) CHT: 10 (14.1%) 90Y: 3 (4.2%)	**^{177}Lu**: 71 (100%) 29.6 GBq (78.9% of patients completed 4 cycles)	>70 years	Safety QOL Efficacy	29 (NA)
Kipnis ST (27)	R	78 (39/39)	59.8 (53.5–69.2)	GI: 34 (43.6%) P: 22 (28.2%) Oth: 22 (28.2%)	G1: 27 (34.6%) G2: 35 (44.9%) G3: 8 (10.3%) UK: 8 (10.3%)	SSA: 49 (62.8%) LRT: 49 (62.8%)	**^{177}Lu:** 78 (100%) 29.6 GBq in 4 cycles[d]	Metastatic NETs with at least 1 dose of PRRT	PFS OS	15.5 (8.7–19.8)

R, retrospective; LRT, locoregional therapy; OS, overall survival; PFS, progression-free survival; PGL, paraganglioma; CS, carcinoid syndrome; SSA, somatostatin analogs; SI, small intestine; NA, not available in the article; UK, unknown; P, pancreas; CHT, chemotherapy; G, grade; GI, gastrointestinal; MTC, medullary thyroid cancer; LRT, locoregional treatment; Pts, patients; FU, follow-up; FTC, follicular thyroid cancer; for, forgut; mid, midgut; t-MN, therapy-related myeloid neoplasm; RT, radiotherapy; Oth, other; DCR, disease control rate. ref, reference; M, males; F, females; NET, neuroendocrine tumor; ph, phase; PRRT, peptide receptor radioligand therapy; n, number; QOL, quality of life; PET, positron emission tomography; SSTR, somatostatin analogs receptor.

[a]referred to patients treated by PRRT, unless otherwise stated; [b]mean ± standard deviation; [c]1 patient received 36.5 GBq; [d]reported protocol.

events were grade 1–2 lymphocytopenia and anemia. An increase in creatinine values after PRRT occurred in 12.7% of patients (grade 1–2) (26). In a small study evaluating the combination of ^{177}Lu-DOTATATE and ^{90}Y-DOTATOC therapy in 9 patients affected by NETs with a large bulky lesion (≥5 cm), posttreatment imaging showed excellent uptake of the radionuclides in the lesions in almost all patients, and only mild-grade adverse events were observed (31).

The frequencies of adverse events described in the main studies are summarized in **Supplementary Table S1**.

3.3 Prognostic and Predictive Factors

Many studies have focused on the role of factors that could predict prognosis or response to PRRT, including circulating biomarkers, clinical parameters, and imaging.

Starting from the role of inflammation in NET progression, Ohlendorf et al. (32), in a study on 33 patients with advanced GEP-NETs treated with PRRT, evaluated the predictive role of inflammatory markers. C-reactive protein (CRP), composite index as Platelet × CRP multiplier (PCM), CPR/albumin ratio, and absolute neutrophil count were all significantly higher in patients who were non-responders to PRRT. Interestingly, in this study, the first ^{68}Ga-DOTATATE PET/CT was performed early (after two cycles of treatment); at this time point, CRP and neutrophil-to-lymphocyte ratio were predictors of change in tumor burden (32). Another inflammatory biomarker, platelet-to-lymphocyte ratio (PLR), was evaluated in a retrospective study on a heterogeneous population of 42 patients affected by NET (all grades and sites) and treated by ^{177}Lu-DOTATATE. Patients with PLR greater than 173.1 had significantly reduced PFS, with a univariate HR for progression or death of 3.82 (95% CI: 1.21–12.03) (33).

The predictive role of the classical neuroendocrine markers is debated. A study by Papantoniou et al. (34) demonstrated that changes in chromogranin A and 5-hydroxyindoleacetic acid during treatment were not predictors of PRRT response (34), although baseline values correlated to PFS (34, 35).

In the field of biochemical markers, growing attention is paid to NETest, an application of liquid biopsy in the field of NET, which has also demonstrated a prognostic role (36). In a larger study on the personalized approach to patients affected by neuroendocrine neoplasms, Frilling et al. (37) described that NETest scores decreased after 6 months in 9/9 patients with metastatic small bowel NETs treated with a combination of surgery and PRRT, and NETest values directly correlated with tumor volume. On the contrary, cell-free DNA levels, although higher in patients with NETs than those in healthy controls, were unable to predict OS and response to PRRT (38).

Many clinical parameters have been proposed as prognostic markers. Factors associated with a reduction in PFS and OS in PRRT-treated patients were ascites (35), marked liver metastasis burden (18, 25, 35), unusual metastatic sites (35), and age >65 years at the time of PRRT (18). Other factors such as interim ascites, the presence of ≥5 bone metastases, and NETs other than GEP were predictors of worse OS (35). The importance of bone metastasis is also confirmed by the evidence that an increase in baseline alkaline phosphatase is associated with poorer PFS and OS (25, 26). Das et al. (39) developed an interesting clinical score that included 5 elements, availability of treatments other than ^{177}Lu-DOTATATE, prior systemic treatments, symptoms, tumor burden of critical organs, and peritoneal carcinomatosis, that was able to predict PFS only in patients treated with PRRT. One study failed in demonstrating the role of sarcopenia and myosteatosis in predicting PFS in 49 patients with NET (any grade) treated by PRRT (40). Finally, one study confirmed that resection of the primary tumor had a beneficial effect in increasing OS after PRRT (41).

Morphological and functional imaging has been proposed for treatment response prediction. In a study on 66 patients with PanNET undergoing PRRT, the authors evaluated the tumor growth rate (TGR), expressed as change/month. TGR decreases significantly during PRRT with ^{177}Lu-DOTATATE, and patients with TGR ≥0.5%/month had shorter PFS (HR, 2.82; 95% CI: 1.05–7.57) (42). Many studies focused on the prognostic role of ^{18}F-FDG PET/CT status even in the setting of PRRT-treated patients (18, 43, 44). An interesting prospective 10-year follow-up study of 166 patients demonstrated that ^{18}F-FDG PET/CT is more effective than grading in predicting OS and PFS. In the subgroup of 78 patients who received PRRT, ^{18}F-FDG PET/CT negative cases had significantly longer survival. Interestingly, PRRT increased OS in patients with positive ^{18}F-FDG PET/CT when compared with non-treated patients, while no difference in OS was found between treated and not-treated subgroup of patients with negative ^{18}F-FDG PET/CT (43). A recent meta-analysis on 12 studies and 1,492 patients evaluated the prognostic role of pretreatment ^{18}F-FDG PET/CT in patients affected by any grade NETs treated with PRRT. Positive uptake at ^{18}F-FDG PET/CT was associated with a higher risk of worse outcome [odds ratio (OR), 4.85; 95% CI: 2.27–10.36]. Regarding PFS, the pooled HR for progression was higher in case of positive ^{18}F-FDG PET/CT (HR, 2.45; 95% CI: 1.48–4.04), and likewise, OS was lower (HR, 2.25; 95% CI: 1.55–3.28) (44). SSTR2 expression assessment by nuclear imaging is mandatory for selecting patients for PRRT. However, its prognostic value is less clear. Two studies evaluated the role of standardized uptake value (SUV) parameters at ^{68}Ga-DOTATATE PET/CT in predicting PFS and response to treatment (45, 46). The mean SUV_{max} was significantly higher in responders than that in non-responders (45, 46) and was higher in patients with PFS >18 months (46). In a subset of 36 patients, another ^{68}Ga-DOTATATE PET/CT scan was performed before the second cycle of PRRT, and SUV_{max} correlated to therapy response (45). Accordingly, another study demonstrated that the evaluation after two cycles can predict further response. With stable disease after 2 cycles, patients with PanNET were more likely than patients with other NETs to achieve a response (0.60 vs. 0.11) after 4 cycles. In patients with a response after two cycles, all PanNETs demonstrated a continuous response after 4 cycles compared with only 66% of other NETs (47).

PRRT absorbed dose may play a role in predicting the response. Both for small intestine and PanNETs, a dose–

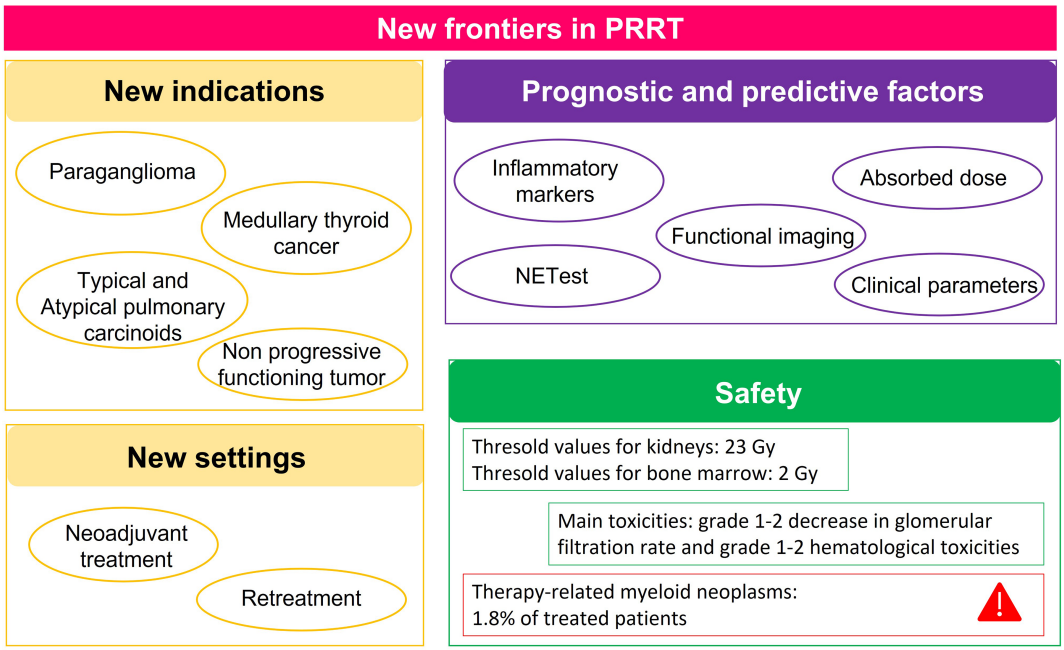

FIGURE 1 | Summary of the main findings of articles published in 2021 on the 3 hot topics of peptide receptor radionuclide therapy (PRRT) in neuroendocrine tumors (NETs): new indications and settings, prognostic and predictive factors, and safety.

response relationship was found between the absorbed dose and tumor shrinkage, which was more pronounced in PanNET (48). Histological parameters have also been proposed as predictors of treatment response. The expression of SSTR2, assessed by immunohistochemistry in tumor samples, was not a predictive factor for PRRT response in a study on 42 patients with small intestine NETs (49). It has also been proposed that in unresponsive patients, PRRT may result in a clonal selection of resistant cells. In a case series on 7 patients with metastatic PanNET treated by PRRT and with evidence of progressive disease within 6 months from treatment, 3 patients underwent a new biopsy. In 2 cases, Ki 67 labeling index increased significantly, and in one patient morphology changed to poorly differentiated. The hypothesis of initial tumor heterogeneity was also supported by the positivity of both gallium and ^{18}F-FDG PET/CT (50).

4 CONCLUSIONS

In 2021, many articles have been published on three hot topics of PRRT treatment in NETs: new clinical indications, safety, and prognostic and predictive markers. The main findings are summarized in **Figure 1**. Considering the evidence that this treatment has been used in PGLs, MTC, pulmonary carcinoids, and uncontrolled CS and in the neoadjuvant or salvage settings, PRRT indications are likely to increase in the near future. Despite the concern of the kidney and bone marrow toxicities of PRRT, available studies, including long follow-up studies, demonstrated the safety of this treatment, with the worse complication, the development of second neoplasia, appearing in 1.8% of treated patients. Finally, as in other aspects of NETs, prognostic and predictive factors are also lacking for PRRT. New evidence confirmed the crucial role of nuclear imaging not only for the selection of the patients but also for estimating treatment response.

AUTHOR CONTRIBUTIONS

Conceptualization: GP and MA. Data curation: GP, AC, MM, MB, and RL. Methodology and validation: GP. Writing—original draft: GP, AC, MM, MB, and RL. Writing—review and editing and supervision: MA. All authors contributed to the article and approved the submitted version.

SUPPLEMENTARY MATERIAL

The Supplementary Material for this article can be found online at: https://www.frontiersin.org/articles/10.3389/fendo.2022.861434/full#supplementary-material

Supplementary Table 1 | Frequency of adverse events of PRRT reported in main studies.

Supplementary Figure 1 | PRISMA flow diagram of the search strategy.

REFERENCES

1. Kwekkeboom DJ, Krenning EP, Lebtahi R, Komminoth P, Kos-Kudla B, de Herder WW, et al. Enets Consensus Guidelines for the Standards of Care in Neuroendocrine Tumors: Peptide Receptor Radionuclide Therapy With Radiolabeled Somatostatin Analogs. *Neuroendocrinology* (2009) 90(2):220–6. doi: 10.1159/000225951
2. Strosberg J, El-Haddad G, Wolin E, Hendifar A, Yao J, Chasen B, et al. Phase 3 Trial of (177)Lu-Dotatate for Midgut Neuroendocrine Tumors. *N Engl J Med* (2017) 376(2):125–35. doi: 10.1056/NEJMoa1607427
3. Pavel M, Oberg K, Falconi M, Krenning EP, Sundin A, Perren A, et al. Gastroenteropancreatic Neuroendocrine Neoplasms: Esmo Clinical Practice Guidelines for Diagnosis, Treatment and Follow-Up. *Ann Oncol* (2020) 31 (7):844–60. doi: 10.1016/j.annonc.2020.03.304
4. Parghane RV, Talole S, Basu S. (131)I-Mibg Negative Progressive Symptomatic Metastatic Paraganglioma: Response and Outcome With (177)Lu-Dotatate Peptide Receptor Radionuclide Therapy. *Ann Nucl Med* (2021) 35(1):92–101. doi: 10.1007/s12149-020-01541-z
5. Severi S, Bongiovanni A, Ferrara M, Nicolini S, Di Mauro F, Sansovini M, et al. Peptide Receptor Radionuclide Therapy in Patients With Metastatic Progressive Pheochromocytoma and Paraganglioma: Long-Term Toxicity, Efficacy and Prognostic Biomarker Data of Phase Ii Clinical Trials. *ESMO Open* (2021) 6(4):100171. doi: 10.1016/j.esmoop.2021.100171
6. Tsang ES, Funk G, Leung J, Kalish G, Kennecke HF. Supportive Management of Patients With Advanced Pheochromocytomas and Paragangliomas Receiving Prrt. *Curr Oncol* (2021) 28(4):2823–9. doi: 10.3390/curroncol28040247
7. Hayes AR, Crawford A, Al Riyami K, Tang C, Bomanji J, Baldeweg SE, et al. Metastatic Medullary Thyroid Cancer: The Role of 68gallium-Dota-Somatostatin Analogue Pet/Ct and Peptide Receptor Radionuclide Therapy. *J Clin Endocrinol Metab* (2021) 106(12):e4903–e16. doi: 10.1210/clinem/dgab588
8. Zidan L, Iravani A, Kong G, Akhurst T, Michael M, Hicks RJ. Theranostic Implications of Molecular Imaging Phenotype of Well-Differentiated Pulmonary Carcinoid Based on (68)Ga-Dotatate Pet/Ct and (18)F-Fdg Pet/Ct. *Eur J Nucl Med Mol Imaging* (2021) 48(1):204–16. doi: 10.1007/s00259-020-04915-7
9. Zandee WT, Brabander T, Blazevic A, Minczeles NS, Feelders RA, de Herder WW, et al. Peptide Receptor Radionuclide Therapy With 177lu-Dotatate for Symptomatic Control of Refractory Carcinoid Syndrome. *J Clin Endocrinol Metab* (2021) 106(9):e3665–e72. doi: 10.1210/clinem/dgab289
10. Parghane RV, Bhandare M, Chaudhari V, Ostwal V, Ramaswamy A, Talole S, et al. Surgical Feasibility, Determinants, and Overall Efficacy of Neoadjuvant (177)Lu-Dotatate Prrt for Locally Advanced Unresectable Gastroenteropancreatic Neuroendocrine Tumors. *J Nucl Med* (2021) 62 (11):1558–63. doi: 10.2967/jnumed.120.258772
11. Rodrigues M, Winkler KK, Svirydenka H, Nilica B, Uprimny C, Virgolini I. Long-Term Survival and Value of (18)F-Fdg Pet/Ct in Patients With Gastroenteropancreatic Neuroendocrine Tumors Treated With Second Peptide Receptor Radionuclide Therapy Course With (177)Lu-Dotatate. *Life (Basel)* (2021) 11(3). doi: 10.3390/life11030198
12. Zacho MD, Iversen P, Villadsen GE, Baunwall SMD, Arveschoug AK, Gronbaek H, et al. Clinical Efficacy of First and Second Series of Peptide Receptor Radionuclide Therapy in Patients With Neuroendocrine Neoplasm: A Cohort Study. *Scand J Gastroenterol* (2021) 56(3):289–97. doi: 10.1080/00365521.2021.1872095
13. Strosberg J, Leeuwenkamp O, Siddiqui MK. Peptide Receptor Radiotherapy Re-Treatment in Patients With Progressive Neuroendocrine Tumors: A Systematic Review and Meta-Analysis. *Cancer Treat Rev* (2021) 93:102141. doi: 10.1016/j.ctrv.2020.102141
14. Kim YI. Salvage Peptide Receptor Radionuclide Therapy in Patients With Progressive Neuroendocrine Tumors: A Systematic Review and Meta-Analysis. *Nucl Med Commun* (2021) 42(4):451–8. doi: 10.1097/MNM.0000000000001350
15. Hayes AR, Mak IYF, Evans N, Naik R, Crawford A, Khoo B, et al. Understanding the Treatment Algorithm of Patients With Metastatic Pancreatic Neuroendocrine Neoplasms: A Single-Institution Retrospective Analysis Comparing Outcomes of Chemotherapy, Molecular Targeted Therapy, and Peptide Receptor Radionuclide Therapy in 255 Patients. *Neuroendocrinology* (2021) 111(9):863–75. doi: 10.1159/000511662
16. Parghane RV, Ostwal V, Ramaswamy A, Bhandare M, Chaudhari V, Talole S, et al. Long-Term Outcome of "Sandwich" Chemo-Prrt: A Novel Treatment Strategy for Metastatic Neuroendocrine Tumors With Both Fdg- and Sstr-Avid Aggressive Disease. *Eur J Nucl Med Mol Imaging* (2021) 48(3):913–23. doi: 10.1007/s00259-020-05004-5
17. Kovan B, Ozkan ZG, Demir B, Tuncman D, Isik EG, Simsek DH, et al. An Analysis for Therapeutic Doses of Patients With Neuroendocrine Tumor Treated With Lutetium-177-Dotatate. *Cancer Biother Radiopharm* (2021) 37 (1):17–22. doi: 10.1089/cbr.2021.0071
18. Paganelli G, Sansovini M, Nicolini S, Grassi I, Ibrahim T, Amadori E, et al. (177)Lu-Prrt in Advanced Gastrointestinal Neuroendocrine Tumors: 10-Year Follow-Up of the Irst Phase Ii Prospective Study. *Eur J Nucl Med Mol Imaging* (2021) 48(1):152–60. doi: 10.1007/s00259-020-04873-0
19. Nilica B, Svirydenka A, Fritz J, Bayerschmidt S, Kroiss AS, Gruber L, et al. Nephrotoxicity and Hematotoxicity One Year After Four Cycles of Peptide Receptor Radionuclide Therapy (Prrt) and Its Impact on Future Treatment Planning. A Retrospective Analysis. *Rev Esp Med Nucl Imagen Mol (Engl Ed)* (2021). doi: 10.1016/j.remn.2021.03.004
20. Guhne F, Heinzig A, Seifert P, Drescher R, Freesmeyer M. The Dependence of Renal (68)Ga[Ga]-Dotatoc Uptake on Kidney Function and Its Relevance for Peptide Receptor Radionuclide Therapy With (177)Lu [Lu]-Dotatoc. *Diagnostics (Basel)* (2021) 11(7):1216–27. doi: 10.3390/diagnostics11071216
21. Chantadisai M, Kulkarni HR, Baum RP. Therapy-Related Myeloid Neoplasm After Peptide Receptor Radionuclide Therapy (Prrt) in 1631 Patients From Our 20 Years of Experiences: Prognostic Parameters and Overall Survival. *Eur J Nucl Med Mol Imaging* (2021) 48(5):1390–8. doi: 10.1007/s00259-020-05127-9
22. Elston MS, Love A, Kevat D, Carroll R, Siow ZR, Pattison S, et al. Pituitary Function Following Peptide Receptor Radionuclide Therapy for Neuroendocrine Tumours. *Cancer Med* (2021) 10(23):8405–11. doi: 10.1002/cam4.4345
23. Sundlov A, Sjogreen-Gleisner K, Tennvall J, Dahl L, Svensson J, Akesson A, et al. Pituitary Function After High-Dose 177lu-Dotatate Therapy and Long-Term Follow-Up. *Neuroendocrinology* (2021) 111(4):344–53. doi: 10.1159/000507761
24. Jafari E, Amini AL, Ahmadzadehfar H, Bagheri D, Assadi M. Cardiotoxicity and Cardiac Monitoring Following the Use of Radiotheranostics Agents Including 177lu-Psma for Prostate Cancer and 177lu-Dotatate for Neuroendocrine Tumors. *Nuklearmedizin* (2021) 60(2):99–105. doi: 10.1055/a-1332-8230
25. Fross-Baron K, Garske-Roman U, Welin S, Granberg D, Eriksson B, Khan T, et al. 177lu-Dotatate Therapy of Advanced Pancreatic Neuroendocrine Tumors Heavily Pretreated With Chemotherapy: Analysis of Outcome, Safety, and Their Determinants. *Neuroendocrinology* (2021) 111(4):330–43. doi: 10.1159/000506746
26. Chen L, Navalkissoor S, Quigley AM, Gnanasegaran G, Mandair D, Toumpanakis C, et al. (177)Lu-Dotatate in Older Patients With Metastatic Neuroendocrine Tumours: Safety, Efficacy and Health-Related Quality of Life. *Eur J Nucl Med Mol Imaging* (2021) 48(11):3582–94. doi: 10.1007/s00259-021-05332-0
27. Kipnis ST, Hung M, Kumar S, Heckert JM, Lee H, Bennett B, et al. Laboratory, Clinical, and Survival Outcomes Associated With Peptide Receptor Radionuclide Therapy in Patients With Gastroenteropancreatic Neuroendocrine Tumors. *JAMA Netw Open* (2021) 4(3):e212274. doi: 10.1001/jamanetworkopen.2021.2274
28. Emami B, Lyman J, Brown A, Coia L, Goitein M, Munzenrider JE, et al. Tolerance of Normal Tissue to Therapeutic Irradiation. *Int J Radiat Oncol Biol Phys* (1991) 21(1):109–22. doi: 10.1016/0360-3016(91)90171-y
29. Sabet A, Mader N, Bittenbring JT, Khreish F, Grunwald F, Biersack HJ, et al. Prophylactic Peripheral Blood Stem Cell Collection in Patients With Extensive Bone-Marrow Infiltration of Neuroendocrine Tumours Prior to Peptide Receptor Radionuclide Therapy With (177)Lu-Dotatate. *Pharmaceuticals (Basel)* (2021) 14(10):1022–8. doi: 10.3390/ph14101022
30. Strosberg JR, Al-Toubah T, Pelle E, Smith J, Haider M, Hutchinson T, et al. Risk of Bowel Obstruction in Patients With Mesenteric or Peritoneal Disease

Receiving Peptide Receptor Radionuclide Therapy. *J Nucl Med* (2021) 62 (1):69–72. doi: 10.2967/jnumed.120.242875
31. Parghane RV, Mitra A, Bannore TU, Rakshit S, Banerjee S, Basu S. Initial Clinical Evaluation of Indigenous (90)Y-Dotatate in Sequential Duo-Prrt Approach ((177)Lu-Dotatate and (90)Y-Dotatate) in Neuroendocrine Tumors With Large Bulky Disease: Observation on Tolerability, (90)Y-Dotatate Post- Prrt Imaging Characteristics (Bremsstrahlung and Petct) and Early Adverse Effects. *World J Nucl Med* (2021) 20(1):73–81. doi: 10.4103/wjnm.WJNM_52_20
32. Ohlendorf F, Werner RA, Henkenberens C, Ross TL, Christiansen H, Bengel FM, et al. Predictive and Prognostic Impact of Blood-Based Inflammatory Biomarkers in Patients With Gastroenteropancreatic Neuroendocrine Tumors Commencing Peptide Receptor Radionuclide Therapy. *Diagnostics (Basel)* (2021) 11(3):504–15. doi: 10.3390/diagnostics11030504
33. Satapathy S, Bhattacharya A, Sood A, Kapoor R, Gupta R, Sood A, et al. Hematological Markers as Predictors of Treatment Outcomes With Lu-177 Dotatate in Patients With Advanced Neuroendocrine Tumors. *Cancer Biother Radiopharm* (2021) 37(1):23–9. doi: 10.1089/cbr.2021.0053
34. Papantoniou D, Gronberg M, Landerholm K, Welin S, Ziolkowska B, Nordvall D, et al. Assessment of Hormonal Levels as Prognostic Markers and of Their Optimal Cut-Offs in Small Intestinal Neuroendocrine Tumours Grade 2. *Endocrine* (2021) 72(3):893–904. doi: 10.1007/s12020-020-02534-8
35. Swiha MM, Sutherland DEK, Sistani G, Khatami A, Abazid RM, Mujoomdar A, et al. Survival Predictors of (177)Lu-Dotatate Peptide Receptor Radionuclide Therapy (Prrt) in Patients With Progressive Well-Differentiated Neuroendocrine Tumors (Nets). *J Cancer Res Clin Oncol* (2022) 148(1):225–36. doi: 10.1007/s00432-021-03672-w
36. Puliani G, Di Vito V, Feola T, Sesti F, Centello R, Pandozzi C, et al. Netest: A Systematic Review Focusing on the Prognostic and Predictive Role. *Neuroendocrinology* (2021). doi: 10.1159/000518873
37. Frilling A, Clift AK, Frampton AE, Bomanji J, Kaemmerer D, Al-Nahhas A, et al. A Combination of Surgery, Theranostics, and Liquid Biopsy - a Personalised Oncologic Approach to Treatment of Patients With Advanced Metastatic Neuroendocrine Neoplasms. *Int J Med Sci* (2021) 18(10):2166–75. doi: 10.7150/ijms.51740
38. Oversoe SK, Sorensen BS, Tabaksblat EM, Gronbaek H, Kelsen J. Cell-Free DNA and Clinical Characteristics in Patients With Small Intestinal or Pancreatic Neuroendocrine Tumors. *Neuroendocrinology* (2022) 112(1):43–50. doi: 10.1159/000514457
39. Das S, Du L, Schad A, Jain S, Jessop A, Shah C, et al. A Clinical Score for Neuroendocrine Tumor Patients Under Consideration for Lu-177-Dotatate Therapy. *Endocr Relat Cancer* (2021) 28(3):203–12. doi: 10.1530/ERC-20-0482
40. Chan DL, Clarke SJ, Engel A, Diakos CI, Pavlakis N, Roach PJ, et al. Computed Tomography (Ct)-Defined Sarcopenia and Myosteatosis Are Prevalent in Patients With Neuroendocrine Neoplasms (Nens) Treated With Peptide Receptor Radionuclide Therapy (Prrt). *Eur J Clin Nutr* (2022) 76(1):143–9. doi: 10.1038/s41430-021-00915-4
41. Kaemmerer D, Twrznik M, Kulkarni HR, Horsch D, Sehner S, Baum RP, et al. Prior Resection of the Primary Tumor Prolongs Survival After Peptide Receptor Radionuclide Therapy of Advanced Neuroendocrine Neoplasms. *Ann Surg* (2021) 274(1):e45–53. doi: 10.1097/SLA.0000000000003237
42. Pettersson OJ, Fross-Baron K, Crona J, Sundin A. Tumor Growth Rate in Pancreatic Neuroendocrine Tumor Patients Undergoing Prrt With 177lu-Dotatate. *Endocr Connect* (2021) 10(4):422–31. doi: 10.1530/EC-21-0027
43. Binderup T, Knigge U, Johnbeck CB, Loft A, Berthelsen AK, Oturai P, et al. (18)F-Fdg Pet Is Superior to Who Grading as a Prognostic Tool in Neuroendocrine Neoplasms and Useful in Guiding Prrt: A Prospective 10-Year Follow-Up Study. *J Nucl Med* (2021) 62(6):808–15. doi: 10.2967/jnumed.120.244798
44. Alevroudis E, Spei ME, Chatziioannou SN, Tsoli M, Wallin G, Kaltsas G, et al. Clinical Utility of (18)F-Fdg Pet in Neuroendocrine Tumors Prior to Peptide Receptor Radionuclide Therapy: A Systematic Review and Meta-Analysis. *Cancers (Basel)* (2021) 13(8):1813–27. doi: 10.3390/cancers13081813
45. Ortega C, Wong RKS, Schaefferkoetter J, Veit-Haibach P, Myrehaug S, Juergens R, et al. Quantitative (68)Ga-Dotatate Pet/Ct Parameters for the Prediction of Therapy Response in Patients With Progressive Metastatic Neuroendocrine Tumors Treated With (177)Lu-Dotatate. *J Nucl Med* (2021) 62(10):1406–14. doi: 10.2967/jnumed.120.256727
46. Teker F, Elboga U. Is Suvmax a Useful Marker for Progression-Free Survival in Patients With Metastatic Gep-Net Receiving (177)Lu-Dotatate Therapy? *Hell J Nucl Med* (2021) 24(2):122–31. doi: 10.1967/s002449912352
47. Vaghaiwalla T, Ruhle B, Memeh K, Angelos P, Kaplan E, Liao CY, et al. Response Rates in Metastatic Neuroendocrine Tumors Receiving Peptide Receptor Radionuclide Therapy and Implications for Future Treatment Strategies. *Surgery* (2021) 169(1):162–7. doi: 10.1016/j.surg.2020.04.001
48. Jahn U, Ilan E, Sandstrom M, Lubberink M, Garske-Roman U, Sundin A. Peptide Receptor Radionuclide Therapy (Prrt) With (177)Lu-Dotatate; Differences in Tumor Dosimetry, Vascularity and Lesion Metrics in Pancreatic and Small Intestinal Neuroendocrine Neoplasms. *Cancers (Basel)* (2021) 13(5):962–76. doi: 10.3390/cancers13050962
49. Elf AK, Johanson V, Marin I, Bergstrom A, Nilsson O, Svensson J, et al. Evaluation of Sstr2 Expression in Si-Nets and Relation to Overall Survival After Prrt. *Cancers (Basel)* (2021) 13(9):2035–47. doi: 10.3390/cancers13092035
50. Assi HA, Hornbacker K, Shaheen S, Wittenberg T, Silberman R, Kunz PL. Rapid Progression After 177lu-Dotatate in Patients With Neuroendocrine Tumors. *Pancreas* (2021) 50(6):890–4. doi: 10.1097/MPA.0000000000001841

Conflict of Interest: MA does consultancy and has received research grants from Bayer, Eisai, and Eli-Lilly.

The remaining authors declare that the research was conducted in the absence of any commercial or financial relationships that could be construed as a potential conflict of interest.

Publisher's Note: All claims expressed in this article are solely those of the authors and do not necessarily represent those of their affiliated organizations, or those of the publisher, the editors and the reviewers. Any product that may be evaluated in this article, or claim that may be made by its manufacturer, is not guaranteed or endorsed by the publisher.

frontiers | Frontiers in Endocrinology

ORIGINAL RESEARCH
published: 27 April 2022
doi: 10.3389/fendo.2022.866572

Is Encapsulated Medullary Thyroid Carcinoma Associated With a Better Prognosis? A Case Series and a Review of the Literature

Andrea Contarino[1], Alessia Dolci[2], Marco Maggioni[3], Francesca Maria Porta[3], Gianluca Lopez[3], Uberta Verga[2], Francesca Marta Elli[2], Elisabetta Francesca Iofrida[4], Gianmaria Cantoni[5], Giovanna Mantovani[1,2] and Maura Arosio[1,2]*

[1] Department of Clinical Sciences and Community Health, University of Milan, Milan, Italy, [2] Endocrinology Unit, Fondazione Istituto di Ricovero e Cura a Carattere Scientifico (IRCCS) Ca' Granda Ospedale Maggiore Policlinico, Milan, Italy, [3] Pathology Unit, Fondazione Istituto di Ricovero e Cura a Carattere Scientifico (IRCCS) Ca' Granda Ospedale Maggiore Policlinico, Milan, Italy, [4] Otolaryngology and Head and Neck Surgery Unit, Fondazione Istituto di Ricovero e Cura a Carattere Scientifico (IRCCS) Ca' Granda Ospedale Maggiore Policlinico, Milan, Italy, [5] Endocrine Surgery Unit, Fondazione Istituto di Ricovero e Cura a Carattere Scientifico (IRCCS) Ca' Granda Ospedale Maggiore Policlinico, Milan, Italy

OPEN ACCESS

Edited by:
Antonino Belfiore, University of Catania, Italy

Reviewed by:
Friedhelm Raue, University of Heidelberg, Germany
Valeriano Leite, Instituto Português de Oncologia Francisco Gentil, Portugal
Maria Alevizaki, National and Kapodistrian University of Athens, Greece
Takahiro Okamoto, Tokyo Women's Medical University, Japan

***Correspondence:**
Andrea Contarino
andrea.contarino@unimi.it

Specialty section:
This article was submitted to Cancer Endocrinology, a section of the journal Frontiers in Endocrinology

Received: *31 January 2022*
Accepted: *23 March 2022*
Published: *27 April 2022*

Citation:
Contarino A, Dolci A, Maggioni M, Porta FM, Lopez G, Verga U, Elli FM, Iofrida EF, Cantoni G, Mantovani G and Arosio M (2022) Is Encapsulated Medullary Thyroid Carcinoma Associated With a Better Prognosis? A Case Series and a Review of the Literature. Front. Endocrinol. 13:866572. doi: 10.3389/fendo.2022.866572

Context: Medullary thyroid carcinoma (MTC) is a malignant neuroendocrine neoplasm that may spread to lymph nodes before the primary tumor is diagnosed; moreover, distant metastases are already present in about 10% of patients at diagnosis. Serum calcitonin (Ctn) usually reflects the spread of disease, thus orienting the extent of surgery and predicting the possibility of biochemical remission. Tumor size and vascular invasion are important prognostic factors, but little is known on the relationship between other histopathological features, such as the presence of a tumor capsule, and long term outcome of MTC.

Purpose: To evaluate the prevalence of encapsulated tumors among MTCs and the association of tumor capsule with a favorable outcome after surgery.

Methods: A retrospective observational single-center study was conducted together with a narrative review of the available literature.

Results: Among 44 patients (27 female, 17 male; median age: 56 years) with MTC (6 hereditary, 37 sporadic) followed up at our center in the last four years (median follow-up: 29.2 months), seven (15.9%) showed an encapsulated tumor at histology and a clinical remission after surgery. None of them had nodal metastases and median preoperative Ctn (398 pg/mL, IQR 126.5–7336) did not differ significantly from that of the 14 patients (31.8%) with persistent disease after surgery (787 pg/mL, IQR 340.5–2905.5; p=0.633), although their tumor size was significantly higher (median 33 mm versus 16 mm respectively, p=0.036). Among patients with preoperative Ctn levels above 500 pg/mL (n=11), only two (18.2%) showed undetectable Ctn levels during follow-up, both having an encapsulated MTC (OR 0.000, p=0.02). Notably, they were two similar cases of large MTC (> 3 cm) with extensive hyalinization and calcification, associated with very high Ctn levels (> 13'500 and 1'100 pg/mL, respectively) but no nodal nor distant metastases,

in complete remission after surgery although one of them carried the aggressive M918T somatic *RET* mutation.

Conclusion: MTC rarely shows a tumor capsule, which seems to correlate with a better prognosis and absence of nodal metastases, regardless of *RET* or *RAS* mutational status. Among encapsulated MTCs (E-MTC), Ctn levels and tumor size are not predictive of persistence of disease after surgery.

Keywords: thyroid tumors, medullary thyroid carcinoma, tumor encapsulation, capsular invasion, calcitonin, desmoplastic stromal reaction

INTRODUCTION

Medullary thyroid carcinoma (MTC) is a rare neuroendocrine tumor originating from calcitonin-secreting thyroid C-cells (1). It accounts for 3-5% of all primary thyroid malignancies and occurs sporadically in 75-80% of cases. Activating germline mutations of the *RET* proto-oncogene are responsible for remaining hereditary forms, which include multiple endocrine neoplasia (MEN) syndromes type 2A and 2B (2). MTC shows variable clinical course but an overall more aggressive behavior, for different tumor cell lymphovascular dissemination compared to well-differentiated papillary and follicular thyroid carcinomas, and it is more prone to have lymph node and distant metastases at diagnosis (50-75% and 10%, respectively) (3).

Calcitonin (Ctn) serum concentration is a sensitive and specific biomarker useful for early detection of MTC (4). Furthermore, preoperative Ctn levels in MTC may be indicative of tumor burden, as with every increment of basal Ctn levels (above 20, 50 and 200 pg/mL, respectively) there is a successive involvement of the ipsilateral, contralateral paratracheal and bilateral laterocervical lymph node compartments, with upper mediastinal and distant metastases becoming more common above a basal Ctn threshold of 500 pg/mL (5). Therefore, Ctn is very useful for orienting the locoregional extent of surgery (after proper preoperative radiological staging) and predicting postoperative biochemical cure of patients with MTC (6). A similar relation with tumor size, number of lymph nodes metastases and outcome was seen for carcinoembryonic antigen (CEA) levels and, recently, also for procalcitonin (PCT) levels (5, 7).

Patients with intrathyroidal disease have a 10-year survival rate of 95.6%, whereas the presence of locoregional involvement or distant metastases at the time of diagnosis are associated with overall survival rates of 75.5% and 40%, respectively (8). Therefore, radical neck (thyroid and involved cervical lymph nodes) surgery represents the first-line therapy to achieve MTC cure (9). Systemic treatment is to be considered for those patients with progressive advanced disease (10). Current available drugs for MTC include multikinase inhibitors (MKIs) Vandetanib and Cabozantinib and new selective RET inhibitors Selpercatinib and Pralsetinib, but none of these have been shown to improve patients' overall survival (OS) (11). Moreover, numerous side effects have frequently been reported and primary or acquired resistance mechanisms may be present (12).

Some histological features of the primary tumor have been proposed for predicting the outcome of MTC (13). Among these, lymphovascular invasion, intense desmoplastic stromal reaction (DSR), evidence of infiltrative tumor margins and extrathyroidal extension (ETE) (14, 15) significantly correlate with the presence of node metastases which is, in turn, the most relevant predictor of distant metastatic disease in MTC (16). On the contrary, the presence of a complete tumor capsule is a strong predictor of the absence of lymphatic spreading of the disease (17).

To date, just over a dozen published studies have described patients with encapsulated MTC (E-MTC) and correlated the presence and infiltration of the tumor capsule with the presence of lymph node metastases or disease remission after surgery, respectively. Very recently, Machens et al. (18) proposed the possibility of avoiding lymph node dissection in the case of well-encapsulated tumors without associated desmoplastic reaction, tested at intraoperative examination. Considering this interesting hypothesis, in the present article we have retrospectively researched cases of encapsulated tumors within the series of MTC patients in follow-up at our Institution to assess their staging at diagnosis and subsequent response to therapy. In addition, previously published research studies focusing on this histopathological issue have been reviewed and discussed.

MATERIAL AND METHODS

A total of 53 consecutive patients with MTC underwent one or more follow-up visits at our Institution between January 2017 and January 2022. From this cohort, 44 patients with sufficiently detailed histopathological examination were selected, and samples of 26 MTCs diagnosed at Fondazione IRCCS Ca' Granda Ospedale Maggiore Policlinico, Milan, Italy between 2010 and 2021 were identified and independently reviewed by three pathologists with experience of endocrine pathology, blinded to the patient lymph nodes status and clinical outcome. The study was conducted in accordance with the World Medical Association's Declaration of Helsinki and approved by the local ethics committee.

All patients with a preoperative diagnosis of MTC underwent total thyroidectomy (except for one subject who was submitted to lobo-isthmectomy for surgical contraindications) and systematic central neck compartment lymphadenectomy. Patients with clinical evidence or suspicion of laterocervical metastases also underwent dissection of lateral neck

compartments (ipsilateral or bilateral, as appropriate). Preoperative assessment of distant metastases was performed with total body CT or CT/PET in patients with Ctn levels above 500 pg/mL. The diagnosis of MTC was confirmed histologically and the following common pathological features were assessed: primary tumor size and extension (single focus or multifocal tumor), tumor margins, intratumoral gross calcifications, extrathyroid extension (ETE), vascular invasion, number of removed lymph nodes metastases, total removed lymph nodes. Tumoral encapsulation was defined as the presence of a fibrous rim of tissue enveloping the tumor and capsular invasion was defined as full-thickness tumor infiltration of the capsule into the adjacent thyroid tissue. DSR was defined as newly formed collagen-rich stroma into a peritumoral circumferential area of 0.5 cm from the tumor margins; it was evaluated semi-quantitatively by visually estimating the presence or absence of fibrosis. The TNM classification and tumor staging were performed according to the criteria described in the 8th Edition of American Joint Committee on Cancer (AJCC) TNM Classification of MTC (19).

The selected patients' medical records were retrospectively assessed up until the last follow-up (January 2022). Pre- and postoperative serum levels of Ctn and CEA, when available, were determined using chemoluminescent (CLIA) and electrochemiluinescent (ECLIA) assays. Patients diagnosed at Fondazione IRCCS Ca' Granda Ospedale Maggiore Policlinico, Milan, Italy between 2018 and 2021 also performed PCT dosage with ECLIA method (Elecsys BRAHMS PCT, normal values between 0.02 and 0.06 ng/mL). The follow-up was based on regular clinical examination, neck ultrasound imaging and serum Ctn and CEA measurement every 3 to 12 months, depending on the patient's response to treatment. Further radiological investigations, such as neck-torax-abdomen CT and total body CT/PET were performed to assess any distant metastases in patients with permanently elevated or progressively increasing Ctn values after surgery. Of the patients with persistent disease after the first surgery, three underwent a second surgery on the neck lymph nodes. At last control, patients were considered in remission when there was neither biochemical (basal Ctn levels < 2 pg/mL) nor structural evidence of disease.

Molecular genetics investigations to discover the presence of germline *RET* mutations on peripheral blood of all MTC patients were performed by targeted Sanger or NGS (in the last 5 years) sequencing. Somatic *RET* and *RAS* pathogenetic variants were tested on the genomic DNA extracted from FFPE samples of surgically resected E-MTCs. DNA was obtained with the MagMAX FFPE DNA/RNA Ultra Kit (Applied Biosystems, US) according to the manufacturer's instructions and the analysis was performed by targeted NGS sequencing on the Illumina MiSeq platform, using the HaloPlex Target Enrichment System kit (Agilent Technologies, Santa Clara, CA) for the library preparation; data analysis, including alignment, categorization and annotation of variants, was done with the SureCall application (Agilent Technologies, Santa Clara, CA). Some extremely degraded FFPE-derived DNAs were pre-amplified with the SsoAdvanced PreAmp Supermix (BioRad, US) to obtain amplicons of sufficient quality for subsequent Sanger sequencing (BigDye Terminator v3.1, Applied Biosystems, US); target sequences were previously amplified with the high fidelity polymerase Takara Taq HS polymerase (Takara, Japan).

Statistical analysis was performed with GraphPad Prism (version 9.3.1). Quantitative variables were expressed as medians with interquartile ranges (IQR) and complete ranges (from minimum to maximum) and were compared with the two-tailed Mann-Whitney U test. Qualitative variables were presented as absolute and relative (percentage) frequencies and were tested with a Chi-square test or Fisher's exact test. Odds ratios (OR) were expressed together with their 95% confidence interval (95%CI). Correlations between quantitative variables were assessed by calculating Pearson's correlation coefficient. The level of statistical significance (two-tailed) was set at $p < 0.05$.

RESULTS

Between January 2017 and January 2022, a total of 53 patients with MTC underwent a follow-up visit at our Institution. Among them, we retrieved complete pre- and postoperative medical records for 44 patients (female to male ratio: 27/17) who were diagnosed with MTC between February 1996 and August 2021 (median age at thyroidectomy of 56 years, IQR 46.5–66 years).

As shown in **Table 1**, preoperative serum Ctn was available for 37 of 44 patients of the study cohort and its median level was 184 pg/mL (IQR 75 – 720.5 pg/mL). Ctn was significantly correlated with tumor size ($r = 0.723$, 95%CI 0.521–0.848, $p < 0.001$) but not with the number of positive lymph nodes ($r = 0.272$, $p = 0.109$). DNA analysis for germline *RET* mutations showed 4 cases of hereditary MTC in the context of a MEN2A syndrome and 2 cases of FMTC (belonging to four different families).

After histopathological examination, median primary tumor size was 14 mm (IQR 8–21 mm) and multifocality was present in 6 (13.6%) cases, five of whom showed bilateral tumor foci. We found that 7 of 44 MTCs had a tumor capsule (**Figure 1**). Among the non-encapsulated (NE-MTC) tumors (84.1%), defined by the total absence of a capsule surrounding the tumor, infiltrative margins were reported in 14 and expansive or well-defined margins in 14 out of 28 cases. Concerning other histopathological findings, 6 out of 44 (13.6%) exhibited diffuse (50%) or focal (50%) intratumoral gross calcifications, vascular invasion was observed in 10 (22.7%) and ETE in 4 (9.1%) of 44 cases. Fifteen (34.1%) patients had histologically confirmed lymph node metastases (pN1) at initial surgery, in all cases involving the central compartment (VI level) of the neck and in 60% of cases also the laterocervical compartment. Peritumoral desmoplasia was present in 18 of the 26 (69.2%) reviewed MTC specimen at our Institution. Half of these were associated with lymph node metastases (positive predictive value of 50%), whereas no DSR-negative cases had lymph node metastases (negative predictive value of 100%, $p = 0.023$) neither at primary surgery nor during the follow-up. According to the 8th edition AJCC TNM Staging System, 22 (50%) patients had a Stage I tumor after surgery, 7 (15.9%) patients were at Stage II, 6 (13.6%) at Stage III and 9 (20.5%) at

TABLE 1 | Clinical and histopathological characteristics of the study cohort.

No. of patients	44
Age at thyroidectomy, years [median, (IQR), range]	56 [46.5–66] (7–78)
Gender, no. of female/male patients	27/17
Hereditary/sporadic MTC	6/38
Preoperative Ctn level, pg/mL [median, (IQR), range]*	184 [75–720.5] (12.6–13540)
Primary tumor size, mm [median, (IQR), range]	14 [8–21] (1–65)
Single focus/multifocal tumor	38/6
No. of patients with intratumoral gross calcifications (%)	6 (13.6)
No. of patients with desmoplastic stromal reaction, DSR (%)**	18/26 (69.2)
No. of patients with extrathyroid extension, ETE (%)	4 (9.1)
No. of patients with vascular invasion (%)	10 (22.7)
No. of patients with nodal disease, N+ (%)	15 (34.1)
N+ in the central compartment, N1a	15 (100)
N+ in the laterocervical compartment, N1b	9 (60)
No. of node metastases removed, total [median, (IQR), range]***	147 (0) [0–2] (0–39)
No. of nodes removed, total [median, (IQR), range]***	544 (7) [1–22] (0–82)
AJCC TNM 8th edition clinical staging (%)	
Stage I	22 (50)
Stage II	7 (15.9)
Stage III	6 (13.6)
Stage IVA	9 (20.5)
Stage IVB	0 (0)
Stage IVC	0 (0)
No. of patients with biochemical cure (%)	30 (68.2)
Follow-up, months [median, (IQR), range]	29.2 [15.9–80.7] (0.3–350.6)

AJCC TNM, American Joint Committee on Cancer Tumor-Node-Metastases; Ctn, calcitonin; IQR, interquartile range.
**Preoperative Ctn levels were available for 37 of 44 patients of the study cohort.*
***DSR was evaluated on the 26 samples of MTCs diagnosed at Fondazione IRCCS Ca' Granda Ospedale Maggiore Policlinico, Milan, Italy.*
****Number of removed and metastatic node was available for 43 of 44 patients of the study cohort.*

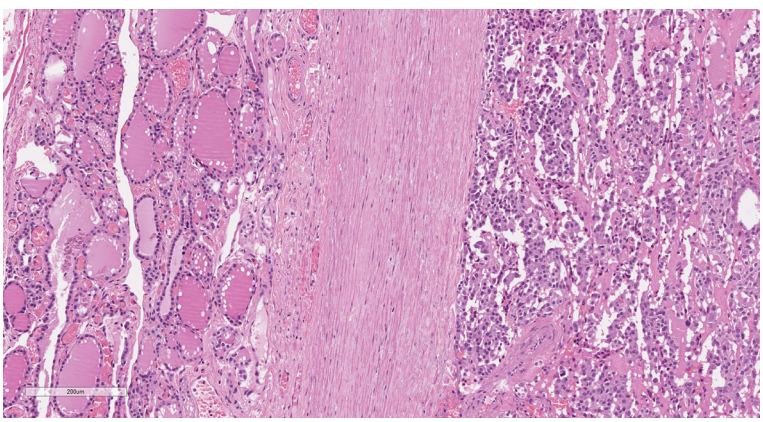

FIGURE 1 | Medullary thyroid carcinoma showing a tumor capsule. The neoplastic cells (right) are demarcated from the normal thyroid parenchima (left) by a fibrous capsule (center). (Hematoxylin and eosin, original magnification 10x).

stage IVA. At diagnosis, as well as at the last outpatient visit, no radiologically proven distant metastases were detected.

At the last follow-up (median follow-up period of 29.2 months, IQR 15.9–80.7), 30 (68.2%) patients (including 3 of the 15 pN1 patients) achieved biochemical cure, 13 (29.5%) showed a biochemical incomplete response and a single patient (2.3%) had a structural incomplete response with stable disease. Statistically significant predictive factors of persistence of disease after primary surgery were vascular invasion (OR infinity, 95%CI 12.3–infinity, $p < 0.0001$), lymph nodes involvement (OR 54, 95%CI 6.99–279.2, $p < 0.0001$) and ETE (OR infinity, 95%CI 2.29–infinity, $p = 0.007$).

Non-Encapsulated MTCs

Clinical and pathological features of NE-MTC patients (84.1%) were reported in the right side of **Table 2**, subgrouping them according to the presence or absence of biochemical remission at last visit (23 'cured' and 14 'non-cured' patients).

TABLE 2 | Clinical and histopathological characteristics of encapsulated (all cured) and non-encapsulated MTC (cured and not cured).

Tumor capsule	Present	Absent	
No. of patients (%)	7 (15.9)	37 (84.1)	
Biochemical cure	**Cured (n = 30, 68.2%)**		**Not cured (n = 14, 31.8%)**
No. of patients (%)	7 (100)	23 (62.2)	14 (31.8)
Age at thyroidectomy, years [median, (IQR), range]	57 [34–60] (27–65)	56 [48–69] (7–78)	55 [45.3–66] (31–77)
Gender, no. of female/male patients	3/4	19/4	5/9
Hereditary/sporadic MTC	0/7	2/21	4/10
Preoperative Ctn level, pg/mL [median, (IQR), range]	398 [126.5–7336] (102–13540)	75 [42.2–127] (12.6–337)	787 [340.5–2905.5] (90.2–9916)
Primary tumor size, mm [median, (IQR), range]	33 [20–38] (14–65)	8.6 [6–15] (1–35)	16 [12–22.3] (7–41)
No. of patients with multifocal MTC (%)	0 (0)	2 (8.7)	4 (28.6)
No. of patients with intratumoral gross calcifications (%)	3 (42.9)	0 (0)	3 (21.4)
No. of patients with desmoplastic stromal reaction, DSR (%)	2/6 (33.3)	7/11 (63.6)	9/9 (100)
No. of patients with extrathyroid extension, ETE (%)	0 (0)	0 (0)	4 (28.6)
No. of patients with vascular invasion (%)	0 (0)	0 (0)	10 (71.4)
No. of patients with nodal disease, N+ (%)	0 (0)	3 (13)	12 (85.7)
N+ in the central compartment, N1a	0 (0)	3 (100)	12 (100)
N+ in the laterocervical compartment, N1b	0 (0)	0 (0)	9 (60)
No. of node metastases removed, total [median, (IQR), range]	0 (0)	7 (0) [0] (0–3)	140 (7) [2–15.5] (0–39)
No. of nodes removed, total [median, (IQR), range]	72 (7) [1–13] (0–39)	92 (1) [0–7] (0–22)	380 (31) [15.5–48] (6–82)
AJCC TNM 8th edition clinical staging (%)			
Stage I	2 (28.6)	18 (78.3)	2 (14.3)
Stage II	5 (71.4)	2 (8.7)	0 (0)
Stage III	0 (0)	3 (13)	3 (21.4)
Stage IVA	0 (0)	0 (0)	9 (64.3)
Stage IVB	0 (0)	0 (0)	0 (0)
Stage IVC	0 (0)	0 (0)	0 (0)
Follow-up, months [median, (IQR), range]	18.9 [16.1–23.9] (11–132.8)	54.8 [19.6–112] (3.5–350.6)	20.9 [6.3–47.1] (0.3–158.3)

AJCC TNM, American Joint Committee on Cancer Tumor-Node-Metastases; Ctn, calcitonin; IQR, interquartile range.

There were no significant differences in term of germline *RET* mutations (p = 0.174) and patients' age when comparing patients in remission and those not in remission, whereas a statistically significant difference was noted concerning the preponderance of males among those non-cured (64.3% versus 17.4% among cured patients, p = 0.006).

Higher preoperative serum Ctn (p < 0.0001), greater tumor size (p = 0.008) and presence of ETE (p = 0.015) were significantly associated with lack of biochemical cure after surgery. Multifocality was not different between the two groups of NE-MTC patients. Vascular invasion was observed only in non-cured MTCs (p < 0.0001) and lymph nodes involvement was significantly more frequent in this subgroup of patients (12/15 positive nodes in non-cured versus 3/25 in cured patients, p < 0.0001). DSR was detected in 9 out of 9 (100%) non-cured NE-MTCs, almost always associated with lymph node metastases (88.9%), and in 63.6% (7/11) of cured NE-MTCs, only in one case (14.3%) associated with lymph node metastases.

Among all NE-MTCs, a significant correlation was found between serum Ctn at diagnosis and the number of node metastases removed (r = 0.515, 95%CI 0.197–0.735, p = 0.003).

Encapsulated MTCs

Prevalence of encapsulated tumors in the present cohort of patients with histologically proven MTC was 15.9% (95%CI 5.1– 26.7%). Full-thickness invasion of the capsule was detected in 3 (42.9%) cases but such invasion was observed only in a single focus per case. No E-MTC was associated with nodal or distant metastases and all seven patients achieved biochemical and structural remission after neck surgery (excellent response).

All E-MTCs were sporadic tumors and concerned male patients in 57.1% and female in 42.9%, with a median age at thyroidectomy comparable with that of the entire study cohort (57 years, IQR 34–60 years).

Comparing E-MTCs with non-cured NE-MTCs (**Table 2**), there were no significant differences in term of preoperative Ctn levels (median 398 pg/mL, IQR 126.5–7336 pg/mL versus median 787 pg/mL, IQR 340.5–2905.5 pg/mL respectively, p = 0.633) but there were for primary tumor size (median 33 mm, IQR 20–38 mm versus median 16 mm, IQR 12–22.3 mm respectively, p = 0.036), as shown in **Figure 2**. However, E-MTCs did not show multifocality, extrathyroidal extension nor vascular invasion (p = 0.004). One case had a large central cystic component, whereas intratumoral gross calcifications were detected in 3 out of 7 E-MTCs (42.9%). DSR was significantly more present among the NE-MTCs examined (76.9%) compared to the E-MTCs (23.1%, p = 0.029). Among the latter, the two cases associated with peritumoral desmoplasia (only mild grade) both showed focal capsular invasion. Unlike non-cured NE-MTCs, in which AJCC/TNM stages III and IV prevailed (p = 0.003), E-MTCs were only stage I (28.6%) and Stage II (71.4%) tumors, depending exclusively on their size.

Tumor tissue mutational status was known for four (57.1%) of the E-MTCs: one case was positive for the two *RET* polymorphisms Gly691Ser (rs1799939) and Arg982Cys (rs17158558), other two cases showed the previous two *RET* variants combined with the somatic Met918Thr mutation (p.G691S/M918T/R982C compound

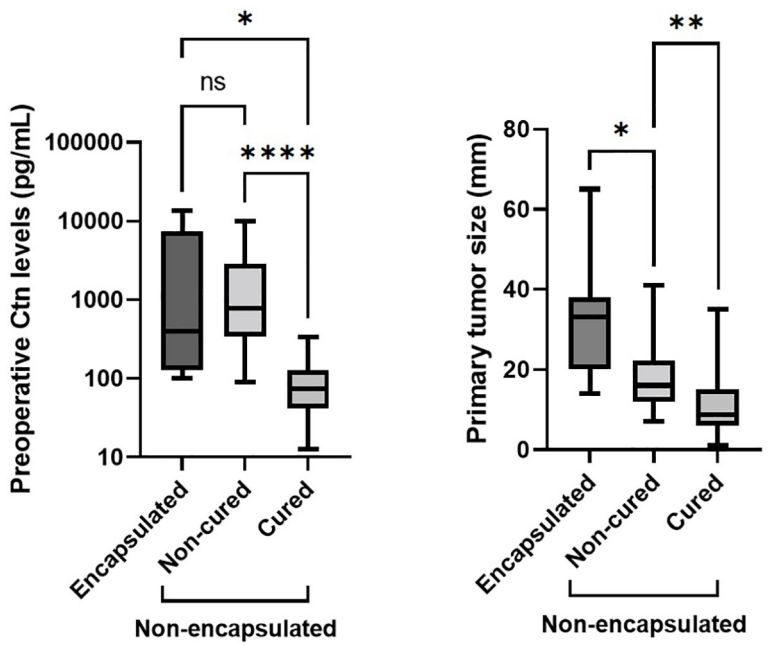

FIGURE 2 | Comparing E-MTCs with non-cured NE-MTCs (**Table 2**), there were no significant differences in term of preoperative Ctn levels (p = 0.633, left side) but there were for primary tumor size (p = 0.036, right side), which was higher in the former (median 33 mm versus median 16 mm, respectively). Among NE-MTCs, higher preoperative serum Ctn (p < 0.0001) and greater tumor size (p = 0.008) were seen in non-cured patients than those cured. Ctn, calcitonin; ns, not significant. The asterisks refer to the different p values indicated in the caption of the figure (*p = 0.036, **p = 0.008, ****p < 0.0001).

genotype), whereas the last one was both *RET* and *RAS* wild-type. The remaining samples were not analyzable despite appropriate DNA amplification techniques.

MTCs With Preoperative Ctn > 500 pg/mL

Eleven of 37 (29.7%) MTCs of the present study were associated to preoperative serum Ctn levels higher than 500 pg/mL (median 1730 pg/mL, IQR 787–3145 pg/mL), with a median CEA of 44.2 ng/mL (IQR 29–120 ng/mL) and a median PCT of 45.9 ng/mL (IQR 10.9–65.9 ng/mL). Their clinical and histopathological characteristics as well as response to surgery were reported in **Table 3**.

Median primary tumor size was 21 mm (IQR 14–35 mm), vascular invasion and lymph node metastases were observed in 7 (63.6%) and ETE in 2 (18.2%) of 11 cases. Biochemical cure was reported only in two of the high preoperative Ctn-associated

TABLE 3 | Clinical and histopathological characteristics and response to surgery of MTCs presenting with preoperative serum Ctn levels above 500 pg/mL.

ID	Sex	Age (yrs)	Preoperative markers		Tumor size (mm)	Tumor capsule	ETE	Vascular invasion	Lymph nodes involvement	AJCC TNM 8th ed. staging	Clinical setting	Postoperative markers		Cured
			Ctn (pg/mL)	CEA (ng/mL)								Ctn (pg/mL)	CEA (ng/mL)	
#29	F	77	535	52.4	11	No	No	No	No	pT1b, N0, M0	sMTC	8.7	2.5	No
#23	F	77	654	*N/A*	20	No	No	Yes	No	pT1b, N0, M0	sMTC	348	34.3	No
#24	M	55	787	41.1	35	No	Yes	Yes	Yes	pT4a(m), N1b, M0	sMTC	92.6	16.3	No
#30	M	31	996	18.1	8	No	No	Yes	Yes	pT1a(m), N1b, M0	sMTC	320	6.9	No
#21	M	59	1132	88.0	33	Yes	No	No	No	pT2, N0, M0	sMTC	< 2	3.8	Yes
#10	M	66	1730	39.9	14	No	Yes	Yes	Yes	pT1b, N1b, M0	sMTC	88.3	1.8	No
#20	F	49	2815	44.2	41	No	No	Yes	Yes	pT3a, N1b, M0	FMTC	375	5.0	No
#4	M	55	2996	13.0	19	No	No	Yes	Yes	pT1b, N1b, M0	MEN2A	485	4.2	No
#39	F	61	3145	*N/A*	26	No	No	No	Yes	pT2, N1a, M0	sMTC	16.1	2.7	No
#3	M	46	9916	339	21	No	No	Yes	Yes	pT2, N1b, M0	sMTC	184	7.5	No
#40	M	60	13540	152	65	Yes	No	No	No	pT3a, N0, M0	sMTC	< 2	4.3	Yes

AJCC TNM, American Joint Committee on Cancer Tumor-Node-Metastases; CEA, carcinoembrion antigen; Ctn, calcitonin; ETE, extrathyroid extension; FMTC, familial medullary thyroid carcinoma; MEN2A, multiple endocrine neoplasia type 2A; N/A not assessed; sMTC, sporadic medullary thyroid carcinoma; Yrs, years.

MTCs and both were encapsulated, so the presence of a tumor capsule was predictive of disease remission in this specific subgroup (OR 0.000, 95%CI 0–0.3, p = 0.02) but not in the entire MTC cohort (OR 0.000, 95%CI 0–1.185, p = 0.078). Notably, both E-MTCs were largely replaced by sclero-hyaline tissue with abundant intratumoral calcifications at the histological examination.

DISCUSSION

Tumoral encapsulation is a well-known important, if not fundamental, element for the pathological definition of follicular cell-derived thyroid tumors. According to the 4th edition WHO Classification of Tumors of Endocrine Organs, published in 2017 (20), the detection of a whole and preserved tumor capsule in thyroid lesions allows to define benign tumors such as follicular adenoma and new borderline tumors such as the "follicular tumor of uncertain malignant potential" (FT-UMP) and the "non-invasive follicular thyroid neoplasm with papillary-like nuclear features" (NIFTP), which share a more indolent behavior and a favorable prognosis (21). Among malignant tumors, the presence of an encapsulated nodule, without evidence of the invasion of the tumor capsule, seems to be an independent prognostic factor for a good prognosis also in the classical variant of papillary thyroid carcinomas (encapsulated non-invasive CV-PTC), according to recent studies (22). Furthermore, it is known that follicular thyroid carcinomas (FTC) showing limited capsular infiltration, but not foci of vascular invasion (so called minimally invasive FTC), have a low recurrence risk after surgery (23).

Against so many evidences regarding both the diagnostic and prognostic value of tumoral encapsulation in differentiated thyroid tumors of follicular origin, only a limited number of studies (including several not recent case reports) have investigated the possible correlation between the presence of a complete tumor capsule with the clinical behavior and outcome in the setting of MTC. As shown in **Table 4**, so far fifteen studies on the pathological features of MTCs have described the presence of about 30% grossly and/or microscopically encapsulated tumors, of which at least half surrounded by a continuous and/or invasion-free capsule. Five (2.9%) cases were reported to have an extra-thyroidal involvement, exclusively limited to neck lymph nodes, but it was not known whether tumor capsule was intact or infiltrated or neither. Only ten (66.7%) of the 15 selected studies also analyzed clinical data on the follow-up and treatment response of patients with E-MTC. Where available, these studies showed biochemical remission of disease in almost all cases (98.9%).

According to their apparent more benign prognosis (than typical MTC), these encapsulated thyroid lesions have been named "C-cell adenomas" by some Authors (25, 26, 32) for the lack of malignant morphological features commonly found in MTC (mainly infiltrative growth pattern). However, they did not better define a reproducible pathological or molecular profile typical of this entity. A possible shared element between these cases could be the association with low serum CEA levels. Although less sensitive and specific than Ctn, CEA levels tend to increase with the disease stage in MTC. However, MTC associated with normal CEA values have been described both at diagnosis (some of which with ascertained lymph node metastases) and at the time of relapse (34), so that negativity to CEA can hardly be considered as a marker of benign behavior.

These promising albeit limited data have led some Authors (Miccoli et al.) to hypothesize the possibility of reconsider the extension of MTC surgical treatment on the basis of the lack of a preserved tumor capsule, that may be intraoperatively revealed by a frozen section analysis (17).

Other morphological parameters have been proposed as useful intraoperative markers to exclude node involvement and thereby to modulate the extent of the surgery in MTC patients, such as DSR (35). Peritumoral desmoplasia is defined as the presence of a newly formed fibrotic stroma surrounding the invasive epithelial tumor cells and can be demonstrated in the majority of MTCs (approximately 80%). In the remaining 20% of sporadic MTCs, as well as in a number of hereditary MTCs, DSR is completely lacking; these cases, which are usually well circumscribed but not necessarily enveloped by a tumor capsule, are typically associated with a very low metastatic potential (36). Combining both the favorable features of tumor encapsulation and absence of peritumoral desmoplasia, very recently Machens et al. proved that patients with E-MTC without associated DSR (or minimal/low desmoplasia), if confirmed on frozen section analysis by experienced pathologists, could avoid even routine central compartment lymph node dissection (18).

In the present study, we have retrospectively researched cases of encapsulated tumors within a series of MTC patients in follow-up at our Institution to assess their staging at diagnosis and subsequent response to therapy. To this purpose, we studied 44 cases of MTC, both hereditary (13.6%) and sporadic (86.4%) cases, and found that prevalence of E-MTC was 15.9%.

Within the entire cohort, preoperative Ctn significantly correlated with tumor size but not with the number of positive lymph nodes; excluding encapsulated tumors from these, however, a significant correlation was found between serum Ctn levels and the number of node metastases. This is because, although Ctn levels of E-MTCs were not significantly different from those of non-cured NE-MTCs (**Table 2**), none of the E-MTCs was associated with nodal or distant metastases, so they were only Stage I-II tumors. Furthermore, they did not show ETE nor vascular invasion, both histological features known to be associated with lymph node involvement in MTC, and all affected patients achieved clinical remission after the first surgical treatment. In the present study (**Table 2**), vascular invasion, lymph nodes involvement and ETE were statistically significant predictive factors of persistence of disease after primary surgery.

Peritumoral desmoplasia was a frequent finding among the reviewed MTC of the present study, always but not exclusively detected in non-cured NE-MTC, where it was almost invariably associated with lymph node metastases. DSR-negative MTCs did not involve lymph nodes neither at primary surgery nor during the follow-up, confirming the negative predictive value already described by various Authors. In support of this evidence, in a large retrospective study of 360 patients with MTC who

TABLE 4 | Review of previously published reports and series of E-MTCs.

Author, year [reference]	Description of reported E-MTCs (with definition of encapsulation when available)	E-MTC (%)	Capsule integrity (%)	Tumor size (mm)	Metastatic MTC (%), site	Biochemical Cure (%)
Williams et al., 1966 (24)	MTC sharply demarcated from the surrounding thyroid tissue by a complete or partial fibrous capsule	9/67 (13.4)	2/9 (22.2)	*NR*	*NR*	*NR*
Beskid, 1979 (25)	"C cell adenoma" surrounded by a thick hyaline capsule with no infiltration of the capsule by the nodule cells	1/1 (100)	1/1 (100)	40	0	1/1 (100)
Kodama et al., 1988 (26)	"C cell adenomas" (one with incomplete very thin capsule without infiltrative growth) with positive Ctn and no CEA staining; low serum CEA	1/2 (50)	0/1 (0)	40 (both)	0	2/2 (100)
Driman et al., 1991 (27)	MTC surrounded by a distinct fibrous capsule with weak Ctn, CEA and CgA staining; normal-high serum Ctn and low serum CEA	1/1 (100)	*NR*	20	0	1/1 (100)
Ozkara et al., 2002 (28)	Encapsulated (intact capsule) papillary variant MTC with extensive cystic degeneration and positive Ctn, CEA, CgA staining	1/1 (100)	1/1 (100)	40	0	1/1 (100)
Miccoli et al., 2007 (17)	MTCs divided in completely encapsulated and non-encapsulated	18/70 (34.6)	18/18 (100)	*NR*	0	18/18 (100)
Santosh et al., 2011 (29)	Well-encapsulated HTA-like variant MTC with positive Ctn staining	1/1 (100)	1/1 (100)	30	0	1/1 (100)
Bhat and Jena, 2012 (30)	Well-encapsulated HTA-like variant MTC with positive Ctn staining	1/1 (100)	1/1 (100)	30	0	*NR*
Aubert et al., 2018 (14)	MTCs with or without tumor capsule (*not otherwise specified*)	21/54 (38.9)	*NR*	*NR*	3 (14.3), N	18/18 (100)
Cipri et al., 2019 (31)	Encapsulated microMTC with positive Ctn and CgA staining; undetectable serum Ctn	1/1 (100)	*NR*	≤ 10	0	1/1 (100)
Censi et al., 2019 (32)	Well-encapsulated "borderline tumor" (between adenoma and carcinoma) with weak CEA and no CgA staining; low serum CEA	1/1 (100)	1/1 (100)	70	0	1/1 (100)
Alzumaili et al., 2020 (13)	MTCs divided in completely encapsulated/well circumscribed, partially encapsulated or totally lacking a capsule; capsular invasion defined as complete tumoral penetration of the capsule	26/143 (18.2)	8/26 (30.8)	*NR*	*NR*	*NR**
Singh et al., 2020 (33)	Encapsulated papillary variant MTC with extensive cystic degeneration and positive Ctn and CgA staining	1/1 (100)	*NR*	80	1 (100), N	*NR*§§
Moura et al., 2021 (15)	Collateral reporting of encapsulated MTC (*not otherwise specified*)	8/65 (12.3)	*NR*	*NR*	1 (12.5), N	*NR*
Machens et al., 2021 (18)	Tumor capsule integrity was classed into 5 subgroups: tumor capsule evenly demarcated; tumor capsule irregular but intact, with or without invasion; breach of the tumor capsule with ≤3 tumor extensions measuring ≤3 mm in width; breach of the tumor capsule with >3 tumor extensions or one tumor extension measuring >3 mm in width; diffuse tumor growth without tumor capsule.	81/139 (58.3)	47§/81 (58)	Between 7 and 12§§ (median)	0	45/46§§§ (97.8)
Sum of published cases		172/548 (31.4)	80/140 (57.1)	–	5 (2.9), N	89/90 (98.9)
Present series		7/44 (15.9)	4**/7 (57.1)		0	7/7 (100)
Total cases		179/592 (30.2)	84/147 (57.1)	–	5 (2.8), N	96/97 (98.9)

E-MTC, encapsulated medullary thyroid carcinoma; CEA, carcinoembrion antigen; CgA, cromogranin A; Ctn, calcitonin; HTA, hyalinizing trabecular adenoma; N, nodal metastases; NR, not reported.

**Tumor encapsulation improved loco-regional free survival but had no effect on disease specific survival and distant metastasis free survival.*

§ Included cases with tumor capsule evenly demarcated, irregular but intact, or with less than 3 tumor extensions < 3 mm in width.

§§Only tumors with size ≤ 25 mm on histopathologic evaluation were included in the entire study.

***Only encapsulated tumors without full-thickness capsular invasion (albeit focal).*

§§§One patient lost at follow-up.

underwent intraoperative frozen-section analysis before surgery, patients with DSR-negative tumor (18%) did not undergo lateral lymph nodes dissection and all maintained biochemical remission for up to 100 months after surgery. Patients with an intraoperative diagnosis of a DSR in the MTC specimen (82%) underwent total thyroidectomy and bilateral central and functional lateral neck dissection; in this group, lymph node and distant metastases were present in 31% and 6% of patients, respectively. As no patient in the DSR-negative group presented with LN metastases in any compartment (negative predictive value of 100%) and each of them had an excellent long-term prognosis, Authors proposed to avoid lateral neck surgery in MTC patients with intraoperative frozen-section negative for DSR (37). Among the E-MTCs of the present study, only two cases showed a mild grade DSR, and both were associated with focal capsular invasion.

Among NE-MTCs, male gender was significantly associated with lymph nodes metastases (but not with larger primary tumor size) and with persistence of disease after surgery. According to the current literature, men with MTC present with larger tumors and are less likely to have localized disease (38), since male sex was recognized as a possible risk factor for lateral neck lymph node metastasis (39). Male gender independently predicts worse overall survival in MTC, even if both disease burden at initial surgery and biochemical response to surgery appear to be stronger prognostic factors (40). Gender differences in term of MTC presentation and outcome could be attributed to a later diagnosis in men, for behavioral reasons and possibly for the lower tendency to perform thyroid tests compared to women, although an underlying biological explanation has been proposed recently but not yet confirmed in larger studies (41). Notably, men and women were almost numerically equal among E-MTC patients in the present study.

Primary tumor size was higher for E-MTCs than non-cured NE-MTCs, so neither serum Ctn nor tumor diameter were predictive of persistence of disease when tumor encapsulation was present (**Figure 2**). It was hypothesized that tumor lymphatic dissemination might be correlated with an infiltrative behavior, depending on the ability of the tumor cells to invade lymphatic vessels located in surrounding normal thyroid tissue (42). Conversely, encapsulated tumors are prevented from loco-regional dissemination due to the containing effect exerted by the capsule itself, and tend to reach much larger size as a result of their expansive growth pattern.

The different predictive value of preoperative Ctn between E- and NE-MTC is particularly evident in the patients subgroup with serum Ctn levels higher than 500 pg/mL (**Table 3**). Above this threshold, distant metastases become very common while biochemical cure rate is progressively reduced (6). No distant metastases were detected in the present series and tumor encapsulation was a statistically significant predictive factor of biochemical remission in this specific subgroup, but not in the entire MTC cohort. Among high preoperative Ctn-associated MTCs, only the two E-MTCs showed undetectable postoperative Ctn levels during a mean follow-up period of 17.4 months (versus 20.1 months in MTCs with persistent disease). It is noteworthy that they were two similar cases of large MTC characterized by extensive tumoral hyalinization and calcification, associated with very high preoperative Ctn and CEA levels, in complete remission after surgery although one of them carried the aggressive M918T somatic *RET* mutation.

Somatic *RET* mutations are present in 40-50% of sporadic MTC (sMTC), with the most common occurring in codon M918 (which is present in up to 90% of *RET*-positive cases) and in codon C634 (43). Recently, activating point mutations in *RAS* genes (H-, K-, and NRAS) have been described predominantly in *RET*-negative sMTC, with a percentage ranging from 10 to 60% depending on the different series (44) but a better prognosis than those harboring *RET* mutations or presenting no mutations. Trying to define a genotype–phenotype correlation in MTC, tumors with somatic p.Met918Thr *RET* mutation and those having no detectable *RET* or *RAS* mutations have been typically associated with lymphovascular invasion, extrathyroidal extension and more advanced stages of disease (15). It is not known whether this more aggressive behavior is maintained even in the presence of more favorable pathological features, such as the tumor capsule. So far only two studies (15, 32), in addition to the present one, have analyzed the mutational status of sporadic E-MTC (**Table 5**). Overall, four cases (30.8%) carried pathogenic mutations in *RET* exons 10 and 11 (C620S and C630S) and three (23.1%) the aggressive somatic M918T mutation (isolated or in combination with other polymorphic variants), while in two cases (15.4%) there were only *RET* polymorphisms (G691S variant alone or combined G619S/R982C variant). *RAS* mutations emerged in two *RET* wild-type cases and no mutations of either *RET* or *RAS* were detected in other two. Therefore, E-MTCs seem to be genetically heterogeneous, with a relative low prevalence of M918T somatic mutations (3 out of 7 *RET* mutated E-MTCs), but retain a more benign behavior regardless of the presence and type of underlying driver molecular alteration.

In conclusion, the current research, along with previously published findings here reviewed, provides support for the idea that tumor encapsulation may represent a valid tissue biomarker of node-negative MTC, even in the setting of focal full-thickness capsular invasion, and thus be predictive of a better prognosis, similar to what is well established in follicular-derived thyroid carcinomas. We cannot say how much and in what way this can change the surgical approach to MTC, with the aim of limiting the number of unnecessary lymph node dissections for achieving disease remission with fewer side effects, as proposed by Machens and colleagues (18). From the literature review presented here, some E-MTCs with lymph node metastases have been described, although univocal definitions and shared criteria for the evaluation of tumor capsule, its continuity and integrity have not been provided.

TABLE 5 | *RET* and *RAS* genes mutational status in encapsulated MTC samples from previously published studies and present series.

Somatic mutations	Censi et al., 2019 (32)	Moura et al., 2021 (15)	Present series	Total cases
RET (%)	0/1 (0)	5/8 (62.5)	4/4 (100)	9/13 (69.2)
C620S	0	1	0	1
C630S	0	3	0	3
G691S or G691S/R982C	0	0	2	2
G691S/M918T/R982C	0	0	2	2
M918T	0	1	0	1
HRAS (%)	0/1 (0)	2/8 (25)	0/4 (0)	2/13 (15.4)
RET+RAS wild type (%)	1/1 (100)	1/8 (12.5)	0/4 (0)	2/13 (15.4)

Further studies would be also necessary to clarify the possible correlation of the presence of a complete capsule with other histological characteristics and with the molecular profile of the tumor, as well as larger longitudinal studies to better understand the outcome of patients with E-MTC on longer follow-up periods. Therefore, our proposal is to always describe the tumor capsule when present at the histopathological examination of a MTC, specifying its integrity and possible tumor invasion. Although this is not a necessary element for the diagnosis, as in other histotypes of thyroid cancer, this could be the first step in recognizing a standalone variant of MTC.

DATA AVAILABILITY STATEMENT

The raw data supporting the conclusions of this article will be made available by the authors, without undue reservation.

ETHICS STATEMENT

The studies involving human participants were reviewed and approved by Milan Area 2 ethics committee. The patients/participants provided their written informed consent to participate in this study.

AUTHOR CONTRIBUTIONS

MA and AC designed the present study. AC conducted the literature research, collected clinical data and prepared the manuscript. MA, AD, UV, GC, EI, and AC performed clinical diagnosis and patient treatment and follow-up. MM, GL, and FP performed histopathological review of available samples at Fondazione IRCCS Ca' Granda Ospedale Maggiore Policlinico, Milan, Italy. FE and GM were responsible for DNA analysis and *RET* and *RAS* mutations detection. MA, GM, and AD performed the critical revision of the manuscript. All authors read and approved the submitted version.

FUNDING

This work was supported by Ricerca Corrente Funds from the Italian Ministry of Health to Fondazione IRCCS Ca' Granda Ospedale Maggiore Policlinico.

REFERENCES

1. Chernock RD, Hagemann IS. Molecular Pathology of Hereditary and Sporadic Medullary Thyroid Carcinomas. *Am J Clin Pathol* (2015) 143 (6):768–77. doi: 10.1309/AJCPHWACTTUYJ7DD
2. Elisei R, Tacito A, Ramone T, Ciampi R, Bottici V, Cappagli V, et al. Twenty-Five Years Experience on RET Genetic Screening on Hereditary MTC: An Update on The Prevalence of Germline RET Mutations. *Genes (Basel)* (2019) 10(9):698. doi: 10.3390/genes10090698
3. Machens A, Lorenz K, Dralle H. Prediction of Biochemical Cure in Patients With Medullary Thyroid Cancer. *Br J Surg* (2020) 107(6):695–704. doi: 10.1002/bjs.11444
4. Costante G, Meringolo D. Calcitonin as a Biomarker of C Cell Disease: Recent Achievements and Current Challenges. *Endocrine* (2020) 67(2):273–80. doi: 10.1007/s12020-019-02183-6
5. Machens A, Dralle H. Biomarker-Based Risk Stratification for Previously Untreated Medullary Thyroid Cancer. *J Clin Endocrinol Metab* (2010) 95 (6):2655–63. doi: 10.1210/jc.2009-2368
6. Machens A, Schneyer U, Holzhausen HJ, Dralle H. Prospects of Remission in Medullary Thyroid Carcinoma According to Basal Calcitonin Level. *J Clin Endocrinol Metab* (2005) 90(4):2029–34. doi: 10.1210/jc.2004-1836
7. Machens A, Lorenz K, Dralle H. Utility of Serum Procalcitonin for Screening and Risk Stratification of Medullary Thyroid Cancer. *J Clin Endocrinol Metab* (2014) 99(8):2986–94. doi: 10.1210/jc.2014-1278
8. Roman S, Lin R, Sosa JA. Prognosis of Medullary Thyroid Carcinoma: Demographic, Clinical, and Pathologic Predictors of Survival in 1252 Cases. *Cancer* (2006) 107(9):2134–42. doi: 10.1002/cncr.22244
9. Wells SA Jr, Asa SL, Dralle H, Elisei R, Evans DB, Gagel RF, et al. American Thyroid Association Guidelines Task Force on Medullary Thyroid Carcinoma. Revised American Thyroid Association Guidelines for the Management of Medullary Thyroid Carcinoma. *Thyroid* (2015) 25(6):567–610. doi: 10.1089/thy.2014.0335
10. Schlumberger M, Bastholt L, Dralle H, Jarzab B, Pacini F, Smit JW, et al. 2012 European Thyroid Association Guidelines for Metastatic Medullary Thyroid Cancer. *Eur Thyroid J* (2012) 1(1):5–14. doi: 10.1159/000336977
11. Koehler VF, Adam P, Frank-Raue K, Raue F, Berg E, Hoster E, et al. Real-World Efficacy and Safety of Cabozantinib and Vandetanib in Advanced Medullary Thyroid Cancer. *Thyroid* (2021) 31(3):459–69. doi: 10.1089/thy.2020.0206
12. Jager EC, Broekman KE, Kruijff S, Links TP. State of the Art and Future Directions in the Systemic Treatment of Medullary Thyroid Cancer. *Curr Opin Oncol* (2022) 34(1):1–8. doi: 10.1097/CCO.0000000000000798
13. Alzumaili B, Xu B, Spanheimer PM, Tuttle RM, Sherman E, Katabi N, et al. Grading of Medullary Thyroid Carcinoma on the Basis of Tumor Necrosis and High Mitotic Rate is an Independent Predictor of Poor Outcome. *Mod Pathol* (2020) 33(9):1690–701. doi: 10.1038/s41379-020-0532-1
14. Aubert S, Berdelou A, Gnemmi V, Behal H, Caiazzo R, D'herbomez M, et al. Large Sporadic Thyroid Medullary Carcinomas: Predictive Factors for Lymph Node Involvement. *Virchows Arch* (2018) 472(3):461–68. doi: 10.1007/s00428-018-2303-7
15. Moura MM, Cabrera RA, Esteves S, Cavaco BM, Soares P, Leite V. Correlation of Molecular Data With Histopathological and Clinical Features in a Series of 66 Patients With Medullary Thyroid Carcinoma. *J Endocrinol Invest* (2021) 44 (9):1837–46. doi: 10.1007/s40618-020-01456-6
16. Machens A, Lorenz K, Weber F, Dralle H. Exceptionality of Distant Metastasis in Node-Negative Hereditary and Sporadic Medullary Thyroid Cancer: Lessons Learned. *J Clin Endocrinol Metab* (2021) 106(8):e2968–79. doi: 10.1210/clinem/dgab214
17. Miccoli P, Minuto MN, Ugolini C, Molinaro E, Basolo F, Berti P, et al. Clinically Unpredictable Prognostic Factors in the Outcome of Medullary Thyroid Cancer. *Endocr Relat Cancer* (2007) 14(4):1099–105. doi: 10.1677/ERC-07-0128
18. Machens A, Kaatzsch P, Lorenz K, Horn LC, Wickenhauser C, Schmid KW, et al. Abandoning Node Dissection for Desmoplasia-Negative Encapsulated Unifocal Sporadic Medullary Thyroid Cancer. *Surgery* (2022) 171(2):360–67. doi: 10.1016/j.surg.2021.07.035
19. Amin MB, Edge SB, Greene FL, Byrd DR, Brookland RK, Washington MK, et al. eds. *AJCC Cancer Staging Manual. 8th ed*. Cham, Switzerland: Springer (2017) 1032 p.
20. Lloyd RV, Osamura RY, Klöppel GRJ. *WHO Classification of Tumours of Endocrine Organs* (2017). WHO–OMS. Available at: https://apps-who-int.pros2.lib.unimi.it/bookorders/anglais/detart1.jsp?codlan=1&codcol=70&codcch=4010#%0Ahttp://apps.who.int/bookorders/anglais/detart1.jsp?codlan=1&codcol=70&codcch=4010 (Accessed February 15, 2021).

21. Ito Y, Hirokawa M, Hayashi T, Kihara M, Onoda N, Miya A, et al. Clinical Outcomes of Follicular Tumor of Uncertain Malignant Potential of the Thyroid: Real-World Data. *Endocr J* (2022). doi: 10.1507/endocrj.EJ21-0723
22. Giani C, Torregrossa L, Ramone T, Romei C, Matrone A, Molinaro E, et al. Whole Tumor Capsule Is Prognostic of Very Good Outcome in the Classical Variant of Papillary Thyroid Cancer. *J Clin Endocrinol Metab* (2021) 106(10): e4072–83. doi: 10.1210/clinem/dgab396
23. Xu B, Ghossein R. Encapsulated Thyroid Carcinoma of Follicular Cell Origin. *Endocr Pathol* (2015) 26(3):191–9. doi: 10.1007/s12022-015-9376-5
24. Williams ED, Brown CL, Doniach I. Pathological and Clinical Findings in a Series of 67 Cases of Medullary Carcinoma of the Thyroid. *J Clin Pathol* (1966) 19(2):103–13. doi: 10.1136/jcp.19.2.103
25. Beskid M. C Cell Adenoma of the Human Thyroid Gland. *Oncology* (1979) 36 (1):19–22. doi: 10.1159/000225312
26. Kodama T, Okamoto T, Fujimoto Y, Obara T, Ito Y, Aiba M, et al. C Cell Adenoma of the Thyroid: A Rare But Distinct Clinical Entity. *Surgery* (1988) 104(6):997–1003. doi: 10.5555/uri:pii:0039606088901602
27. Driman D, Murray D, Kovacs K, Stefaneanu L, Higgins HP. Encapsulated Medullary Carcinoma of the Thyroid. A Morphologic Study Including Immunocytochemistry, Electron Microscopy, Flow Cytometry, and *in Situ* Hybridization. *Am J Surg Pathol* (1991) 15(11):1089–95. doi: 10.1097/00000478-199111000-00009
28. Ozkara SK, Gürbüz Y, Müezzinoğlu B, Yumbal Z. Encapsulated Cystic Papillary Variant of Medullary Carcinoma of Thyroid Gland. *Endocr Pathol* (2002) 13(2):167–71. doi: 10.1385/EP:13:2:167
29. Santosh KV, Raychaudhuri S, Subramanya H, Naveen Kumar BJ. Cytology of Hyalinising Trabecular Adenoma-Like Variant of Medullary Thyroid Carcinoma. *J Cancer Res Ther* (2011) 7(2):189–91. doi: 10.4103/0973-1482.82916
30. Bhat V, Jena M. Medullary Carcinoma of the Thyroid - An Unusual Case of Hyalinizing Trabecular Adenoma-Like Variant (Encapsulated). *Internet J Med Update* (2012) 7(2):54–6.
31. Cipri C, Vescini F, Torresan F, Pennelli G, Pelizzo MR, Triggiani V, et al. An Unusual Case of Medullary Thyroid Carcinoma and A Revision of Current Literature. *Endocr Metab Immune Disord Drug Targets* (2019) 19(2):226–29. doi: 10.2174/1871530319666181220165350
32. Censi S, Cavedon E, Watutantrige-Fernando S, Barollo S, Bertazza L, Manso J, et al. Unique Case of a Large Indolent Medullary Thyroid Carcinoma: Time to Reconsider the Medullary Thyroid Adenoma Entity? *Eur Thyroid J* (2019) 8 (2):108–12. doi: 10.1159/000494675
33. Singh M, Ahuja A, Rahar S, Bhardwaj M. Encapsulated Papillary Variant of Medullary Carcinoma of Thyroid With Extensive Cystic Change: An Extremely Rare Presentation. *Med Pharm Rep* (2021) 94(3):372–76. doi: 10.15386/mpr-1570
34. Kim J, Park H, Choi MS, Park J, Jang HW, Kim TH, et al. Serum Carcinoembryonic Antigen as a Biomarker for Medullary Thyroid Cancer. *Int J Thyroidol* (2021) 14(2):143–51. doi: 10.11106/ijt.2021.14.2.143
35. Scheuba C, Kaserer K, Kaczirek K, Asari R, Niederle B. Desmoplastic Stromal Reaction in Medullary Thyroid Cancer-an Intraoperative "Marker" for Lymph Node Metastases. *World J Surg* (2006) 30(5):853–9. doi: 10.1007/s00268-005-0391-4
36. Koperek O, Scheuba C, Cherenko M, Neuhold N, De Micco C, Schmid KW, et al. Desmoplasia in Medullary Thyroid Carcinoma: A Reliable Indicator of Metastatic Potential. *Histopathology* (2008) 52(5):623–30. doi: 10.1111/j.1365-2559.2008.03002.x
37. Niederle MB, Riss P, Selberherr A, Koperek O, Kaserer K, Niederle B, et al. Omission of Lateral Lymph Node Dissection in Medullary Thyroid Cancer Without a Desmoplastic Stromal Reaction. *Br J Surg* (2021) 108(2):174–81. doi: 10.1093/bjs/znaa047
38. Cox C, Chen Y, Cress R, Semrad AM, Semrad T, Gosnell JE, et al. Are There Disparities in the Presentation, Treatment and Outcomes of Patients Diagnosed With Medullary Thyroid Cancer? An Analysis of 634 Patients From the California Cancer Registry. *Gland Surg* (2016) 5(4):398–404. doi: 10.21037/gs.2016.04.02
39. Zhou TH, Zhao LQ, Zhang Y, Wu F, Lu KN, Mao LL, et al. The Prediction of Metastases of Lateral Cervical Lymph Node in Medullary Thyroid Carcinoma. *Front Endocrinol (Lausanne)* (2021) 12:741289. doi: 10.3389/fendo.2021.741289
40. Kotwal A, Erickson D, Geske JR, Hay ID, Castro MR. Predicting Outcomes in Sporadic and Hereditary Medullary Thyroid Carcinoma Over Two Decades. *Thyroid* (2021) 31(4):616–26. doi: 10.1089/thy.2020.0167
41. Costa C, Souteiro P, Paredes S, Bettencourt-Silva R, Pedro J, Ferreira MJ, et al. Male Gender as a Poor Prognostic Factor in Medullary Thyroid Carcinoma: Behaviour or Biological Difference? *Minerva Endocrinol (Torino)* (2022). doi: 10.23736/S2724-6507.22.03692-2
42. Pereira F, Pereira SS, Mesquita M, Morais T, Costa MM, Quelhas P, et al. Lymph Node Metastases in Papillary and Medullary Thyroid Carcinoma Are Independent of Intratumoral Lymphatic Vessel Density. *Eur Thyroid J* (2017) 6(2):57–64. doi: 10.1159/000457794
43. Ciampi R, Romei C, Ramone T, Prete A, Tacito A, Cappagli V, et al. Genetic Landscape of Somatic Mutations in a Large Cohort of Sporadic Medullary Thyroid Carcinomas Studied by Next-Generation Targeted Sequencing. *iScience* (2019) 20:324–36. doi: 10.1016/j.isci.2019.09.030
44. Moura MM, Cavaco BM, Leite V. RAS Proto-Oncogene in Medullary Thyroid Carcinoma. *Endocr Relat Cancer* (2015) 22(5):R235–52. doi: 10.1530/ERC-15-0070

Conflict of Interest: The authors declare that the research was conducted in the absence of any commercial or financial relationships that could be construed as a potential conflict of interest.

Publisher's Note: All claims expressed in this article are solely those of the authors and do not necessarily represent those of their affiliated organizations, or those of the publisher, the editors and the reviewers. Any product that may be evaluated in this article, or claim that may be made by its manufacturer, is not guaranteed or endorsed by the publisher.

frontiers | Frontiers in Endocrinology

ORIGINAL RESEARCH
published: 25 May 2022
doi: 10.3389/fendo.2022.853623

Burden of Prostate Cancer in China, 1990–2019: Findings From the 2019 Global Burden of Disease Study

Fuquan Wang[1,2†], *Chenchen Wang*[1,2†], *Haifa Xia*[1,2], *Yun Lin*[1,2], *Dingyu Zhang*[1,2,3*], *Peng Yin*[4*] and *Shanglong Yao*[1,2*]

[1] Department of Anesthesiology, Union Hospital, Tongji Medical College, Huazhong University of Science and Technology, Wuhan, China, [2] Institute of Anesthesia and Critical Care Medicine, Union Hospital, Tongji Medical College, Huazhong University of Science and Technology, Wuhan, China, [3] Jinyintan Hospital,Tongji Medical College, Huazhong University of Science and Technology, Wuhan, China, [4] National Center for Chronic and Noncommunicable Disease Control and Prevention, Chinese Center for Disease Control and Prevention, Beijing, China

Our study is the first to illustrate the age and geographic distribution differences in the epidemiology of prostate cancer from 1990 to 2019 in China.

Prostate cancer (PC) is a malignant tumor derived from prostate epithelial cells and is one of the most commonly diagnosed cancers in men. In recent years, the global incidence and the annual deaths number of PC showed a continuous increase, which has caused a huge disease burden on human health. In terms of the global average, the incidence and mortality of PC in China are relatively low. However, the age-standardized incidence rate of PC was 17.3/100,000 in 2019 in China, with a 95.2% rise compared to 1990, while the global growth rate of incidence rate over the same period is 13.2%. This showed that the development trend of PC in China is not optimistic. There are few precise studies on the epidemiology of PC in China. After the general analysis strategy used in the Global Burden of Diseases, Injuries and Risk Factors Study (GBD) 2019, we elaborated on the incidence, mortality, and disability-adjusted life-years (DALYs) and the corresponding age-standardized rate of the Chinese PC population from 1990 to 2019 according to different ages and provinces. We used joinpoint regression analysis to estimate the incidence and mortality trends. Our analysis shows that elderly people over 80 are still the main focus of incidence and death. The epidemiology and disease burden of PC of different provinces in China show obvious regional differences, and some certain provinces such as HongKong, Macao, and Zhejiang should be paid more attention. More targeted and effective strategies should be developed to reduce the burden of PC in China.

Keywords: burden of disease, disability-adjusted life-years, public health, epidemiology, prostate cancer

OPEN ACCESS

Edited by:
Claire Perks,
University of Bristol, United Kingdom

Reviewed by:
Dimas Bayu,
Hasanuddin University, Indonesia
Noorwati Sutandyo,
Dharmais Hospital National Cancer Center, Indonesia

***Correspondence:**
Dingyu Zhang
1813886398@qq.com
Shanglong Yao
shanglong_yao@sina.com
Peng Yin
yinpengcdc@163.com

[†]These authors have contributed equally to this work and share first authorship

Specialty section:
This article was submitted to Cancer Endocrinology, a section of the journal Frontiers in Endocrinology

Received: *02 February 2022*
Accepted: *11 April 2022*
Published: *25 May 2022*

Citation:
Wang F, Wang C, Xia H, Lin Y, Zhang D, Yin P and Yao S (2022) Burden of Prostate Cancer in China, 1990–2019: Findings From the 2019 Global Burden of Disease Study. Front. Endocrinol. 13:853623. doi: 10.3389/fendo.2022.853623

INTRODUCTION

Prostate cancer (PC) ranks second in the current global incidence of male malignant tumors and is the fifth leading cause of cancer deaths in male patients (1). In 2019, there were an estimated 1410451 new cases of PC worldwide, and about 486836 patients died of PC. The age-standardized incidence rate and age-standardized death rate were 38.6/100,000 and 15.3/100,000. In terms of the global average (2), the incidence of PA in China is still at a relatively low level, but it has shown a significant upward trend in recent years. With the increasing aging of the Chinese population, the continuous westernization of diet and lifestyle, etc., the development of PA in China is even less optimistic (3–5).

Considering the major threat that PC poses to human health, there is an urgent need to accurately assess the epidemiological trends of PC. PC is particularly common in developed countries (6), so previous epidemiological studies mainly focus on the PC disease burden among different countries (2, 7), and more concentrated on European and American countries (8, 9). Currently, few targeted studies are focusing on the burden of PC in China. Due to the differences in important factors such as economic development level and medical level, the incidence, and death of PC have large spatial distribution differences (10, 11). China is made up of many provinces and there are varying degrees of differences in the economy, medical level, lifestyle, and the degree of population aging among different provinces. Therefore, there are bound to be differences in the epidemiological characteristics of PC among these provinces. Regrettably, there is no comparison of the epidemiological characteristics and disease burden of PC among different provinces in China. Our research is beneficial to the adjustments to the medical strategy by governments and medical institutions according to the development level and regional characteristics of PC. Clarifying the epidemiological distribution and trend of the incidence and death of PC in different provinces of China can make public health resources more reasonable distribution so that PC patients can obtain more balanced medical resources, which is beneficial for them to receive better treatment.

Based on the epidemiological data related to PC from the Global Burden of Diseases, Injuries and Risk Factors Study (GBD) 2019, our research clarified the current status, the spatial patterns, and temporal trends of PC in China according to age and region. Our research can help the public and policymakers assess the current PC disease burden, coordinate resource allocation, and improve the efficiency of PC prevention and treatment.

MATERIALS AND METHODS

Data Sources

The GBD 2019 includes more than 3.5 billion estimates of 286 causes of death, 369 diseases and injuries, and 87 risk factors in 204 countries and regions (12, 13). Input data were extracted from various sources were extracted from censuses, including household surveys, civil registration and vital statistics, disease registries, health service use, air pollution monitors, and so on. It is the largest and most comprehensive quantification of health loss across regions and times research. We obtained the related data on PC from the Global Health Data Exchange (GHDX, http://ghdx.healthdata.org/gbd-results-tool). Data of China were mainly obtained from the following sources: the Maternal and Child Surveillance System, the Chinese Center for Disease Control and Prevention cause-of-death reporting system, cancer registries, the Disease Surveillance Point system, and reports from Hong Kong and Macao (14). The data included the annual case data and the age-standardized rates of the incidence, the deaths, the years of life lost (YLLs), the years of life lived with disability (YLDs), the disability-adjusted life-years (DALYs) of PC in 204 countries, and regions around the world from 1990 to 2019. International Classification of Diseases (ICD),10th revision codes C61-C61.9, D29.1, and D40.0 were used to represent PC.

Estimates of Disease Burden

GBD 2019 provides a standardized approach for estimating the prevalence, incidence, mortality, YLDS, YLLS, and DALYs of each disease (13). The general approach of GBD2019 to estimate causes of death and incidence is the same as GBD2017 (15, 16). In short, it is to first analyze data from different sources to generate a specific cause of mortality (17), then use the linear-step mixed-effects model, sociodemographic index, and general spatiotemporal Gaussian process regression to analyze the incidence and mortality data from multiple sources to obtain mortality-to-incidence ratios (MIRs) (18). The final estimated incidence of PC is obtained by dividing the estimated mortality by MIRs. YLDs are estimated as the product of the disability weight in the Bayesian regression model and the prevalence. YLLs were estimated by multiplying the estimated number of deaths with the life loss value for the corresponding age. Disability-adjusted life years (DALYs) were generated by summing of the YLLs and the YLDs.

As in the previous studies (19), we use Joinpoint regression analysis to assess the trend in the disease burden of PC by Joinpoint software (4.5.0.1). Annual percentage change (APC) and 95% confidence interval (CI) were calculated.

RESULTS

Overall Findings

Table 1 showed the overall age-standardized rate, number, and percentage change of PC from 1990 to 2019 at the global and China levels, respectively. In 1990, the incidence numbers of PC were 26,440 (20103-31,916.887) in China, and the age-standardized incidence rate was 8.9 (7.1-10.9) per 100,000. In 2019, the values of the above two indicators are 153,448 (118,400-204,943) and 17.3 (13.6-22.7) per 100,000. The death numbers and the DALYs number of PC in China in 1990 were 20,382 (15,817-24,679) and 403,112 (606,178-488,113), respectively. By 2019, it has grown to 54,391 (42,904-71,307) and 1,002,594 (794,010-1,322,635) respectively. The age-standardized DALYs rate has dropped from

Abbreviations: 95% CI, the 95% confidence interval; 95% UI, the 95% uncertainty interval; DALYs, disability-adjusted life-years; GBD, the Global Burden of Diseases, Injuries and Risk Factors Study; ICD, International Classification of Diseases; MI: mortality-to-incidence; YLDs, years lived with disability; YLLs, years of life lost

TABLE 1 | The age-standardized rate, numbers and percent change for PC globally and for China, 1990–2019.

Variables	Global			China		
	1990	2019	Change (%)	1990	2019	Change (%)
Incidence Rate	34.1(26.8-39.7)	38.6 (33.6-49.8)	13.2	8.9(7.1-10.9)	17.3 (13.6-22.7)	95.2
Incidence Numbers	524,110 (409,133-613,005)	1,410,452 (1,227,900-1,825,766)	169.1	26,440 (20,103-31,917)	153,448 (118,400-204,943)	480.4
Deaths Rate	18.1(14.7-21.2)	15.3 (13.0-18.6)	-15.7	8.2 (6.6-10.3)	7.8 (6.2-9.9)	-5.3
Deaths Numbers	232,999 (191,398-268,882)	486,836(420,498-593,689)	108.9	20,382 (15,817-24,679)	54,391 (42,904-71,307)	166.9
DALYs Rate	286.3 (232.8-326.2)	244.1 (211.8-297.7)	-0.1	125.9 (99.5-151.8)	118.9 (95.1-154.1)	-5.6
DALYs Numbers	4,360,506(3,528,030-4,951,007)	8,644,870 (7,548,020-10,559,866)	98.3	403,112 (606,178-488,113)	1,002,595 (794,010-1,322,635)	148.7

125.9 (99.5-151.8) per 100,000 in 1990 to 118.9 (95.1-154.1) per 100,000 in 2019. The global average of the indicators mentioned above is higher than that of China. From 1990 to 2019, the growth rate of China's PC incidence rate and the decline rate of DALYs rate were higher than the world level, and the decline rate of deaths rate was lower than the world average.

Temporal Trends of Burden of Prostate Cancer From 1990 to 2019

Figure 1 shows the related epidemiological indicators of the age-standardized rate of PC in China from 1990 to 2019. **Table 2** showed the APC of the age-standardized rate. The age-standardized incidence rate of PC increased from 1990-1997 in China (**Figure 1A**), during this period, the APC during 1990-1994 was 1.3 (0.7,1.8), 1994 to 2001 was 2.1 (1.9,2.4), 2001 to 2007 was 2.9 (2.5,3.3), 2007 to 2010 was 4.2 (2.5,6.0) and 2010 to 2019 was 1.9 (1.7,2.0), respectively.

The age-standardized death rate and the age-standardized DALYs rate from 1990 to 2019 of PC in China showed an overall downward trend (**Figures 1B, C**). The two important parts of the DALYs rate, YLDs, and YLLs, show opposite trends (**Figure 2D, E**). The age-standardized YLLs rate gradually decreases, while the age-standardized YLDs rate increases year by year.

Age Distribution Pattern

We compared the incidence numbers and the deaths numbers of PC patients in different age groups in China in 1990 and 2019 (**Table 3**). We found that the incidence numbers of PC in all age bands in 2019 were higher than the corresponding age range in 1990. In 2019, the incidence numbers of PC is mainly concentrated in the age bands above 60 years old, and the age group with the largest number of cases is 80 plus.

As for the number of deaths of PC, although the total number of deaths from PC in 2019 was significantly higher than that in 1990, the number of deaths from PC in the age group under 40 in 2019 was lower than in 1990. In 2019, the death numbers in each age group increased with age, reaching a peak in the 80 plus age group. In 1990, the deaths numbers in each age group showed the same trend as in 2019 and peaked in the 80 plus age group.

The incidence, death, and DALYs rate of PC in 1990 and 2019 were compared by age groups (**Figures 2A–C**). In 2019, the incidence rate of each age group was significantly higher than that in 1990, but the 80 plus group of death and DALYs rate showed a difference from other groups. The PC death and DALYs rate of people under 80 years old in 2019 showed a downward trend compared with 1990, but the above two indicators of people over 80 years old are opposite.

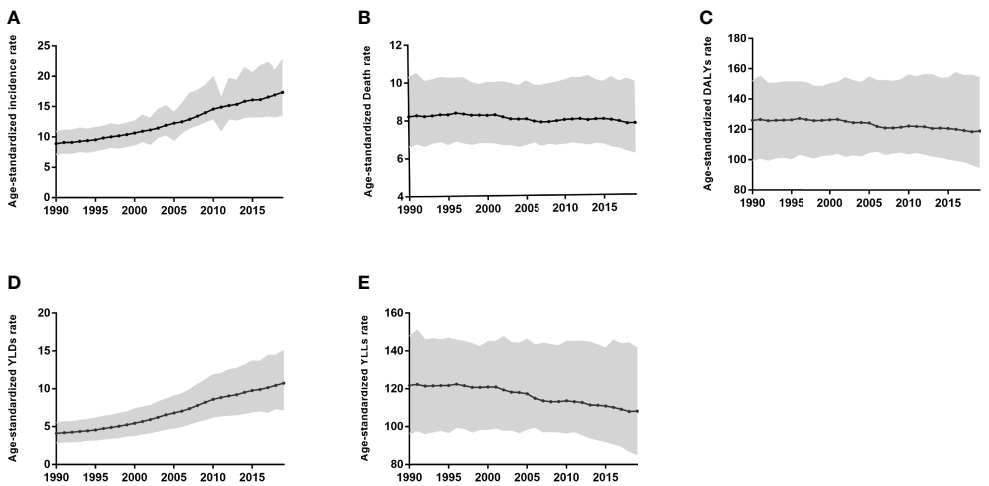

FIGURE 1 | Age-standardized incidence **(A)**, Death **(B)**, DALYs **(C)**, YLDs **(D)**, and YLLs **(E)** rate for Prostate Cancer in China from 1990 to 2019.

TABLE 2 | Trends in age-standardized incidence rate, death rate and DALYs rate for China, 1990–2019.

Measure	Trend	Years	Annual Percentage Change (95% CI)
DALYs rate	1	1990-2001	0.0 (-0.1,0.1)
	2	2001-2008	-0.6* (-0.8,-0.4)
	3	2008-2011	0.3 (-0.8,1.5)
	4	2011-2019	-0.4* (-0.5,-0.2)
Deaths Rate	1	1990-1997	0.3* (0.1,0.5)
	2	1997-2007	-0.6* (-0.7,-0.4)
	3	2007-2015	0.2 (-0.0,0.4)
	4	2015-2019	-0.9* (-1.3,-0.4)
Incidence rate	1	1990-1994	1.3* (0.7,1.8)
	2	1994-2001	2.1* (1.9,2.4)
	3	2001-2007	2.9* (2.5,3.3)
	4	2007-2010	4.2* (2.5,6.0)
	5	2010-2019	1.9* (1.7,2.0)

**p-value < 0.05.*

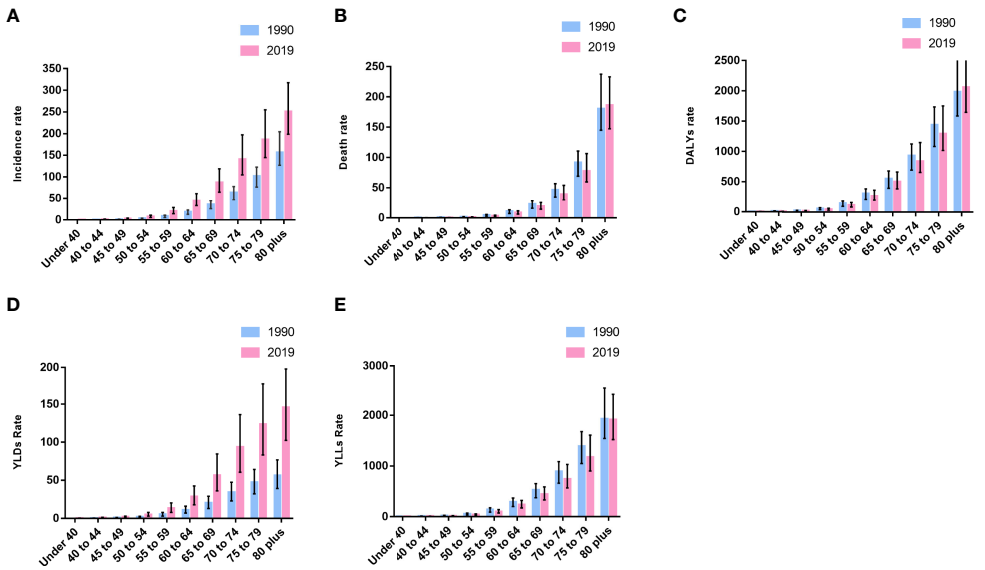

FIGURE 2 | Incidence **(A)**, death **(B)**, DALYs **(C)**, YLDs **(D)**, and YLLs **(E)** rate by age for prostate cancer in China in 2019.

TABLE 3 | The incidence and death numbers for Prostate Cancer by age bands a in 1990 and 2019.

Age Bands	1990		2019	
	Incidence numbers	Death numbers	Incidence numbers	Death numbers
Under 40	354 (248-433)	160 (113-194)	1,068 (843-1,424)	141 (112-189)
40 to 44	149 (105-188)	79 (55-98)	599 (449-830)	93 (69-126)
45 to 49	283 (186-362)	144 (97-184)	1,702 (1,227-2,435)	257 (188-361)
50 to 54	743 (493-950)	371 (247-480)	4,624 (3,329-6,638)	677 (483-973)
55 to 59	1,885 (1,257-2,458)	967 (639-1,241)	9,482 (6,747-13,565)	1,476 (1,075-2,077)
60 to 64	3,300 (2,335-4,147)	1,910 (1,311-2,407)	17,569 (13,007-24,057)	3,301 (2,459-4,542)
65 to 69	4,777 (3,468-5,974)	3,036 (2,158-3,773)	29,882 (22,282-40,959)	6,515 (4,926-8,730)
70 to 74	5,542 (4,086-6,763)	4,073 (3,026-4,970)	32,692 (24,396-45,960)	9,066 (6,944-12,600)
75 to 79	4,957 (3,739-6,006)	4,494 (3,392-5,435)	26,301 (20,423-36,011)	10,952 (8,443-15,066)
80 plus	4,450 (3,619-5,834)	5,149 (4,142-6,781)	29,528 (23,376-37,374)	21,912 (17,360-27,453)

Both YLLs and YLDs rates increase with age, and the 80plus group has the highest YLDs and YLLs rate (**Figures 2D, E**). However, the comparison of the YLDs and YLLs rates in 2019 and 1990 shows that the YLLs rate of each age group in 2019 is lower than in 1990, while the YLDs rate is just the opposite.

Geographic Differences in China

From 1990 to 2019, the incidence of PC in different provinces of China has undergone significant changes (**Figures 3A–C**). In 2019, the top three provinces with age-standardized incidence rate per 100,000 were Hong Kong 28.7 (19.6,39.8), Macao 25.2 (17.1,36.0) and Zhejiang 25.0 (17.4,36.8). The age-standardized incidence rate of Xizang was 8.1 (5.6,11.1) per 100,000 in 2019, which was the lowest among the provinces. By 2019, the age-standardized incidence rate of PC in 23 provinces in China exceeded 15. In 1990, only Hong Kong had an age-standardized incidence rate of PC exceeding 15.

In 2019, the top three provinces with the highest DALYs rate of PC in China are Xinjiang 145.2 (101.5,192.2), Shanghai 130.6 (80.5,179.6), Yunnan 130.2 (102.1,173.2) (**Figure 3E**). In 1990, the three provinces with the highest DALYs rate were Shanghai 163.7 (112.7,206.2), Tianjin 146.2 (113.6,188.3), and Zhejiang 142.7 (98.1,183.5) (**Figure 3D**). From 1990 to 2019, the highest growth rate of PC disease burden was Xinjiang 20.7%, and the lowest was Tianjin -21.6% (**Figure 3F**).

DISCUSSION

In 1990, the incidence numbers of PC in China accounted for 5.0% of the incidence numbers of PC in the world. By 2019, the incidence of PC in China has accounted for 10.8% of the total number of incidences of PC in the world. The proportion of China PC death numbers in the world is also increasing, respectively 8.8% in 1990 and 11.2% in 2019. These indicated that Chinese PC accounts for an increasing proportion of PC patients in the world, and we need to pay more attention to the epidemiology of PC in China.

Our research found that from 1990 to 2019, one of the most obvious epidemiological features of PC in China was the continuous increase of the incidence. Moreover, the rate of increase in the incidence of PC in China is much higher than the world average. The year-on-year increase in the incidence of PC in China may be mainly due to the continuous progress of the aging of the population, the westernization of the diet and lifestyle, the active development of PSA screening, and so on.

PC is a typical senile disease, and age is one of the definite risk factors (20). The aging population in China is a particularly noteworthy issue. The proportion of the population aged 65 and over in China has increased from 5.6% in 1990 to 12.0% in 2020, and this proportion is still rising. It is estimated that the proportion of the population aged 65 and over will reach 23.7% by 2040 (21). Our research found the incidence, the mortality and the DALYs rate of PC are positively correlated with age in China. The elderly not only have a high incidence of PC but also have a high degree of malignancy and a low survival rate (22). This may be related to the weakening of body functions such as the function of important organs and immunity due to aging. The elderly over 65 should still be the focus of attention.

It is worth noting that although the incidence numbers of PC population under the age of 40 have increased, the death numbers have decreased. This phenomenon reflects the progress of medical standards in China, but it also implies that

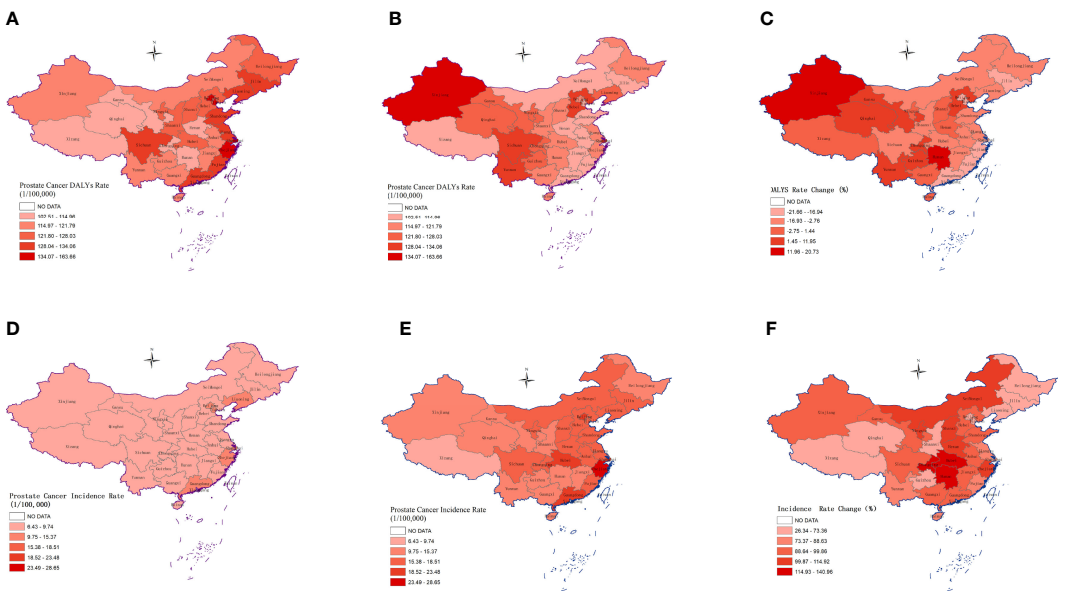

FIGURE 3 | The age-standardized incidence rate of Prostate Cancer in 33 provinces of China in 1990 **(A)**, 2019 **(B)**, and the percentage change of incidence **(C)**. The age-standardized DALYs rate of Prostate Cancer in 33 provinces of China in 1990 **(D)**, 2019 **(E)** and the percentage change of incidence **(F)**.

the overall age of onset of PC in China is moving forward, and it is necessary to further explore PC prevention and treatment strategies suitable for national conditions. More attention should be paid to the status of PC among young people.

Our analysis showed that the incidence of PC increased significantly from 2007 to 2010 (APC=4.21), which may be related to the 2007 Chinese Urology Guidelines that added recommendations for annual PSA testing for men over 55 years of age (23). Before 2007, there was no standard guideline for PSA testing in China. PSA testing is provided based on the experience of clinicians. The early detection and treatment of PC are of great significance to improve the duration and quality of life of the PC patients. However, PSA is not a specific indicator of PC, so PSA is still controversial in the early screening of PC.

The China Statistical Yearbook showed that Chinese residents' consumption expenditures on meat and dairy products are increasing rapidly, and residents' nutritional diets consume excessive amounts of protein, fat, and sugar. Chinese population's malnutrition is becoming more and more serious. Studies have shown that increased dietary intake of animal fat, meat, and dairy products may increase the risk of PC (24–26). Unhealthy eating habits have continued to increase the rate of overweight and obesity in China. The obesity prevalence rose from 3.1% in 2004 to 8·1% in 2018 (27). Obesity is positively correlated with the incidence and mortality of high-grade advanced PC (28). Therefore, the construction of a reasonable dietary structure is of great significance in reducing the incidence of PC.

One of the exciting news is that from 1990 to 2019, the age-standardized death rate and DALYs rate showed a relatively steady decline. The main components of DALYs, YLDs, and YLLs show opposite time trends, YLLs increase year by year while YLDs decrease. It shows that with the improvement of medical standards, the overall disease burden caused by PC is on a downward trend. YLDs account for an increasing proportion of the disease burden of PC.

Previous studies have shown that there are large differences in the incidence of PC between different geographic regions (29). There are many reasons for the regional differences in the epidemiology of PC. For example, the incidence of PC in Asian populations in European and American developed countries is quite different from other ethnic groups (11), indicating that genetic background plays a certain role in the occurrence and development of PC in different ethnic groups. In addition to race and family history, which are two relatively clear risk factors for PC (30–32), diet and lifestyle among different regions may also play an important role in it. Our research showed that there are significant differences in the spatial distribution and temporal changes of PC among different provinces in China. China has a vast territory with 34 provincial-level administrative regions. There are obvious differences in environment, diet, climate, economic development level, and medical level among different regions. The severity of population aging in different provinces is different, which may be another important reason for the difference in the burden of PC disease in different provinces. In 2018, six provinces including Liaoning, Shanghai, Shandong, Sichuan, Jiangsu and Chongqing all crossed the 14.0% deep aging standard.

With the global PC incidence rate increasing year by year, the incidence of PC in China is increasing rapidly, especially in the western and central provinces of China. China has entered a society with an aging population, and the disease burden of PC will further increase. Therefore, PC should be paid more attention to cancer prevention and control in the future.

A certain degree of limitation exists in our research. On the one hand, our data is mainly based on GBD 2019, but the data may not fully represent the real situation in different provinces in China, which may lead to inaccurate estimates of disease burden. On the other hand, our research only uses age as a grouping factor and has not conducted an in-depth exploration of many factors that are closely related to the evolution of the disease burden of PC, such as the lifestyles of people in different regions.

CONCLUSION

In summary, our studies suggested that PC has caused a huge health burden on the Chinese population and has obvious geographical differences. More effective strategies and policies are urgently needed to reduce the disease burden of PC and improve the quality of life of people, especially older men.

DATA AVAILABILITY STATEMENT

The original contributions presented in the study are included in the article/**Supplementary Material**. Further inquiries can be directed to the corresponding authors.

ETHICS STATEMENT

This is an observational, non-interventional database study, re-utilizing the data from the Global Burden of Diseases, Injuries, and Risk Factors 2019 study for the purpose of addressing a research question. The need for ethics approval and consent was waived.

AUTHOR CONTRIBUTIONS

FW and CW wrote this article and analysed the data. YL and HX prepared the figures. PY, SY and DZ designed the study and revised the article. All authors contributed to the article and approved the submitted version.

FUNDING

The study was supported by Major Technological Innovation Special Project of Hubei Province of China (2019ACA167).

SUPPLEMENTARY MATERIAL

The Supplementary Material for this article can be found online at: https://www.frontiersin.org/articles/10.3389/fendo.2022.853623/full#supplementary-material

REFERENCES

1. Bray F, Ferlay J, Soerjomataram I, Siegel RL, Torre LA, Jemal A. Global Cancer Statistics 2018: GLOBOCAN Estimates of Incidence and Mortality Worldwide for 36 Cancers in 185 Countries. *CA Cancer J Clin* (2018) 68 (6):394–424. doi: 10.3322/caac.21492
2. Zhai Z, Zheng Y, Li N, Deng Y, Zhou L, Tian T, et al. Incidence and Disease Burden of Prostate Cancer From 1990 to 2017: Results From the Global Burden of Disease Study 2017. *Cancer* (2020) 126(9):1969–78. doi: 10.1002/cncr.32733
3. Gu XY, Zheng RS, Zhang SW, Zeng HM, Sun KX, Zou XN, et al. [Analysis on the Trend of Prostate Cancer Incidence and Age Change in Cancer Registration Areas of China, 2000 to 2014]. *Zhonghua Yu Fang Yi Xue Za Zhi* (2018) 52(6):586–92. doi: 10.3760/cma.j.issn.0253-9624.2018.06.006
4. Qi D, Wu C, Liu F, Gu K, Shi Z, Lin X, et al. Trends of Prostate Cancer Incidence and Mortality in Shanghai, China From 1973 to 2009. *Prostate* (2015) 75(14):1662–8. doi: 10.1002/pros.23046
5. Chen W, Zheng R, Baade PD, Zhang S, Zeng H, Bray F, et al. Cancer Statistics in China, 2015. *CA Cancer J Clin* (2016) 66(2):115–32. doi: 10.3322/caac.21338
6. Pernar CH, Ebot EM, Wilson KM, Mucci LA. The Epidemiology of Prostate Cancer. *Cold Spring Harb Perspect Med* (2018) 8(12). doi: 10.1101/cshperspect.a030361
7. Pishgar F, Ebrahimi H, Saeedi Moghaddam S, Fitzmaurice C, Amini E. Global, Regional and National Burden of Prostate Cancer, 1990 to 2015: Results From the Global Burden of Disease Study 2015. *J Urol* (2018) 199 (5):1224–32. doi: 10.1016/j.juro.2017.10.044
8. Kelly SP, Anderson WF, Rosenberg PS, Cook MB. Past, Current, and Future Incidence Rates and Burden of Metastatic Prostate Cancer in the United States. *Eur Urol Focus* (2018) 4(1):121–7. doi: 10.1016/j.euf.2017.10.014
9. Smith-Palmer J, Takizawa C, Valentine W. Literature Review of the Burden of Prostate Cancer in Germany, France, the United Kingdom and Canada. *BMC Urol* (2019) 19(1):19. doi: 10.1186/s12894-019-0448-6
10. Rebbeck TR. Prostate Cancer Genetics: Variation by Race, Ethnicity, and Geography. *Semin Radiat Oncol* (2017) 27(1):3–10. doi: 10.1016/j.semradonc.2016.08.002
11. Ito K. Prostate Cancer in Asian Men. *Nat Rev Urol* (2014) 11(4):197–212. doi: 10.1038/nrurol.2014.42
12. Zhu N, Zhang D, Wang W, Li X, Yang B, Song J, et al. A Novel Coronavirus From Patients With Pneumonia in China, 2019. *N Engl J Med* (2020) 382 (8):727–33. doi: 10.1056/NEJMoa2001017
13. GBD 2019 Diseases and Injuries Collaborators. Global Burden of 369 Diseases and Injuries in 204 Countries and Territories, 1990-2019: A Systematic Analysis for the Global Burden of Disease Study 2019. *Lancet (London England)* (2020) 396(10258):1204–22. doi: 10.1016/S0140-6736(20)30925-9
14. Zhou M, Wang H, Zeng X, Yin P, Zhu J, Chen W, et al. Mortality, Morbidity, and Risk Factors in China and its Provinces, 1990-2017: A Systematic Analysis for the Global Burden of Disease Study 2017. *Lancet* (2019) 394(10204):1145–58. doi: 10.1016/S0140-6736(19)30427-1
15. GBD 2019 Diseases and Injuries Collaborators. Global, Regional, and National Incidence, Prevalence, and Years Lived With Disability for 354 Diseases and Injuries for 195 Countries and Territories, 1990-2017: A Systematic Analysis for the Global Burden of Disease Study 2017. *Lancet* (2018) 392(10159):1789–858. doi: 10.1016/S0140-6736(18)32279-7
16. GBD 2019 Diseases and Injuries Collaborators. Global, Regional, and National Age-Sex-Specific Mortality for 282 Causes of Death in 195 Countries and Territories, 1980-2017: A Systematic Analysis for the Global Burden of Disease Study 2017. *Lancet* (2018) 392(10159):1736–88. doi: 10.1016/S0140-6736(18)32203-7
17. Zhou M, Wang H, Zhu J, Chen W, Wang L, Liu S, et al. Cause-Specific Mortality for 240 Causes in China During 1990-2013: A Systematic Subnational Analysis for the Global Burden of Disease Study 2013. *Lancet* (2016) 387(10015):251–72. doi: 10.1016/S0140-6736(15)00551-6
18. Huang C, Huang L, Wang Y, Li X, Ren L, Gu X, et al. 6-Month Consequences of COVID-19 in Patients Discharged From Hospital: A Cohort Study. *Lancet (London England)* (2021) 397(10270):220–32. doi: 10.1016/S0140-6736(20)32656-8
19. Clegg LX, Hankey BF, Tiwari R, Feuer EJ, Edwards BK. Estimating Average Annual Per Cent Change in Trend Analysis. *Stat Med* (2009) 28(29):3670–82. doi: 10.1002/sim.3733
20. Cooperberg MR, Broering JM, Carroll PR. Risk Assessment for Prostate Cancer Metastasis and Mortality at the Time of Diagnosis. *J Natl Cancer Inst* (2009) 101(12):878–87. doi: 10.1093/jnci/djp122
21. Zhao B, Lu R, Chen J, Xie M, Zhao X, Kong L. S100A9 Blockade Prevents Lipopolysaccharide-Induced Lung Injury *via* Suppressing the NLRP3 Pathway. *Respir Res* (2021) 22(1):45. doi: 10.1186/s12931-021-01641-y
22. Perdana NR, Mochtar CA, Umbas R, Hamid AR. The Risk Factors of Prostate Cancer and Its Prevention: A Literature Review. *Acta Med Indones* (2016) 48 (3):228–38.
23. Na R, Jiang H, Kim ST, Wu Y, Tong S, Zhang L, et al. Outcomes and Trends of Prostate Biopsy for Prostate Cancer in Chinese Men From 2003 to 2011. *PloS One* (2012) 7(11):e49914. doi: 10.1371/journal.pone.0049914
24. Venkateswaran V, Klotz LH. Diet and Prostate Cancer: Mechanisms of Action and Implications for Chemoprevention. *Nat Rev Urol* (2010) 7(8):442–53. doi: 10.1038/nrurol.2010.102
25. Aronson WJ, Barnard RJ, Freedland SJ, Henning S, Elashoff D, Jardack PM, et al. Growth Inhibitory Effect of Low Fat Diet on Prostate Cancer Cells: Results of a Prospective, Randomized Dietary Intervention Trial in Men With Prostate Cancer. *J Urol* (2010) 183(1):345–50. doi: 10.1016/j.juro.2009.08.104
26. Arab L, Su J, Steck SE, Ang A, Fontham ET, Bensen JT, et al. Adherence to World Cancer Research Fund/American Institute for Cancer Research Lifestyle Recommendations Reduces Prostate Cancer Aggressiveness Among African and Caucasian Americans. *Nutr Cancer* (2013) 65(5):633–43. doi: 10.1080/01635581.2013.789540
27. Wang L, Zhou B, Zhao Z, Yang L, Zhang M, Jiang Y, et al. Body-Mass Index and Obesity in Urban and Rural China: Findings From Consecutive Nationally Representative Surveys During 2004-18. *Lancet (Lond Engl)* (2021) 398(10294):53–63. doi: 10.1016/S0140-6736(21)00798-4
28. Parekh N, Lin Y, Dipaola RS, Marcella S, Lu-Yao G. Obesity and Prostate Cancer Detection: Insights From Three National Surveys. *Am J Med* (2010) 123(9):829–35. doi: 10.1016/j.amjmed.2010.05.011
29. Ferlay J, Shin HR, Bray F, Forman D, Mathers C, Parkin DM. Estimates of Worldwide Burden of Cancer in 2008: GLOBOCAN 2008. *Int J Cancer* (2010) 127(12):2893–917. doi: 10.1002/ijc.25516
30. Platz EA, Rimm EB, Willett WC, Kantoff PW, Giovannucci E. Racial Variation in Prostate Cancer Incidence and in Hormonal System Markers Among Male Health Professionals. *J Natl Cancer Inst* (2000) 92(24):2009–17. doi: 10.1093/jnci/92.24.2009
31. Mucci LA, Hjelmborg JB, Harris JR, Czene K, Havelick DJ, Scheike T, et al. Familial Risk and Heritability of Cancer Among Twins in Nordic Countries. *Jama* (2016) 315(1):68–76. doi: 10.1001/jama.2015.17703
32. Benafif S, Kote-Jarai Z, Eeles RA. A Review of Prostate Cancer Genome-Wide Association Studies (GWAS). *Cancer Epidemiol Biomarkers Prev* (2018) 27 (8):845–57. doi: 10.1158/1055-9965.EPI-16-1046

Conflict of Interest: The authors declare that the research was conducted in the absence of any commercial or financial relationships that could be construed as a potential conflict of interest.

frontiers | Frontiers in Endocrinology

ORIGINAL RESEARCH
published: 03 June 2022
doi: 10.3389/fendo.2022.867822

DRD2 Agonist Cabergoline Abolished the Escape Mechanism Induced by mTOR Inhibitor Everolimus in Tumoral Pituitary Cells

Federica Mangili[1], Emanuela Esposito[1], Donatella Treppiedi[1], Rosa Catalano[1], Giusy Marra[1], Genesio Di Muro[1], Anna Maria Barbieri[1], Marco Locatelli[2,3], Andrea G. Lania[4,5], Alessandra Mangone[1,6], Anna Spada[1], Maura Arosio[1,6], Erika Peverelli[1] and Giovanna Mantovani[1,6]*

[1] Department of Clinical Sciences and Community Health, University of Milan, Milan, Italy, [2] Neurosurgery Unit, Fondazione Istituto di Ricovero e Cura a Carattere Scientifico (IRCCS) Ca' Granda Ospedale Maggiore Policlinico, Milan, Italy, [3] Department of Pathophysiology and Transplantation, University of Milan, Milan, Italy, [4] Department of Biomedical Sciences, Humanitas University, Pieve Emanuele, Italy, [5] Endocrinology and Diabetology Unit, Istituto di Ricovero e Cura a Carattere Scientifico (IRCCS) Humanitas Research Hospital, Rozzano, Italy, [6] Endocrinology Unit, Fondazione Istituto di Ricovero e Cura a Carattere Scientifico (IRCCS) Ca' Granda Ospedale Maggiore Policlinico, Milan, Italy

OPEN ACCESS

Edited by:
Antonino Belfiore, University of Catania, Italy

Reviewed by:
Teresa Gagliano, University of Udine, Italy
Federica Barbieri, University of Genoa, Italy
Filippo Ceccato, University of Padua, Italy

***Correspondence:**
Erika Peverelli
erika.peverelli@unimi.it

Specialty section:
This article was submitted to Cancer Endocrinology, a section of the journal Frontiers in Endocrinology

Received: *01 February 2022*
Accepted: *04 April 2022*
Published: *03 June 2022*

Citation:
Mangili F, Esposito E, Treppiedi D, Catalano R, Marra G, Di Muro G, Barbieri AM, Locatelli M, Lania AG, Mangone A, Spada A, Arosio M, Peverelli E and Mantovani G (2022) DRD2 Agonist Cabergoline Abolished the Escape Mechanism Induced by mTOR Inhibitor Everolimus in Tumoral Pituitary Cells. Front. Endocrinol. 13:867822. doi: 10.3389/fendo.2022.867822

The mammalian target of rapamycin (mTOR) inhibitor everolimus has been shown to display antiproliferative effects on a wide spectrum of tumors. *In vitro* studies demonstrated that everolimus inhibited pituitary neuroendocrine tumor (PitNET) cell growth in a subset of patients. Sensitivity to everolimus is reduced by an escape mechanism that increases AKT phosphorylation (p-AKT), leading to pro-survival pathway activation. Dopamine receptor type 2 (DRD2) mediates a reduction of p-AKT in a subgroup of non-functioning PitNETs (NF-PitNETs) and in prolactin-secreting tumor cells (MMQ cells) through a β-arrestin 2-dependent mechanism. The aim of this study was to investigate the efficacy of everolimus combined with DRD2 agonist cabergoline in reducing NF-PitNET primary cells and MMQ cell proliferation and to evaluate AKT phosphorylation and a possible role of β-arrestin 2. We found that 9 out of 14 NF-PitNETs were resistant to everolimus, but the combined treatment with cabergoline inhibited cell proliferation in 7 out of 9 tumors (-31.4 ± 9.9%, $p < 0.001$ vs. basal) and reduced cyclin D3 expression. In the everolimus-unresponsive NF-PitNET group, everolimus determined a significant increase of p-AKT/total-AKT ratio (2.1-fold, $p < 0.01$, vs. basal) that was reverted by cabergoline cotreatment. To investigate the molecular mechanism involved, we used MMQ cells as a model of everolimus escape mechanism. Indeed everolimus did not affect MMQ cell proliferation and increased the p-AKT/total-AKT ratio (+1.53 ± 0.24-fold, $p < 0.001$ vs. basal), whereas cabergoline significantly reduced cell proliferation (-22.8 ± 6.8%, $p < 0.001$ vs. basal) and p-AKT. The combined treatment of everolimus and cabergoline induced a reduction of both cell proliferation (-34.8 ± 18%, $p < 0.001$ vs. basal and $p < 0.05$ vs. cabergoline alone) and p-AKT/total-AKT ratio (-34.5 ± 14%, $p < 0.001$ vs. basal and $p < 0.05$ *vs*. cabergoline alone). To test β-arrestin 2 involvement, silencing experiments were performed in MMQ cells. Our

data showed that the lack of β-arrestin 2 prevented the everolimus and cabergoline cotreatment inhibitory effects on both p-AKT and cell proliferation. In conclusion, this study revealed that cabergoline might overcome the everolimus escape mechanism in NF-PitNETs and tumoral lactotrophs by inhibiting upstream AKT activation. The co-administration of cabergoline might improve mTOR inhibitor antitumoral activity, paving the way for a potential combined therapy in β-arrestin 2-expressing NF-PitNETs or other PitNETs resistant to conventional treatments.

Keywords: pituitary neuroendocrine tumors, mTOR inhibitors, everolimus, AKT phosphorylation, dopamine receptor type 2, cabergoline

INTRODUCTION

In recent years, PI3K–AKT–mTOR inhibitors have been proposed as an alternative therapeutic strategy for tumors resistant to conventional drugs. Indeed mTOR inhibitors, like everolimus, torin-1, or rapamycin, displayed successful results in a wide spectrum of tumors. Specifically, everolimus showed a promising perspective in tumors such as HER2/neu negative advanced breast cancer, bronchial and renal cell carcinoma, unresectable or metastatic neuroendocrine pancreatic tumors, or nonfunctional gastrointestinal and lung-originating ones (1).

The PI3K–AKT–mTOR pathway is known to have a fundamental role in regulating cell proliferation, survival, and metabolism. In particular, this pathway has been found overactivated in pituitary neuroendocrine tumors (PitNETs) compared with normal pituitary (2–4), supporting its contribution to PitNET progression (5).

Non-functioning (NF)-PitNETs cause visual field deficits and neurologic manifestations due to mass spread effects, and even if generally benign, they may invade surrounding structures and present resistance to medical treatments. Surgical tumor debulking is currently considered the first-line approach, and to date, NF-PitNETs are still orphans of effective medical therapy (6, 7).

In vitro studies displayed that mTOR inhibitors induced a reduction of cell growth and viability in primary cultured NF-PitNET cells (8–11). On the other hand, several different mechanisms have been demonstrated in literature to explain how sensitivity to mTOR inhibitors could be reduced in different kinds of tumors (12).

Among these, one of the most outlined is an escape mechanism that induces an upstream increase of AKT phosphorylation levels (p-AKT) through insulin receptor substrate-1 (IRS-1) triggering, leading to pro-survival pathway activation (13). Indeed the PI3K–AKT–mTOR pathway activation results in a negative feedback loop, mediated by the mTOR/S6K-dependent loss of IRS-1 expression (14). This mechanism of negative feedback is lost when mTOR activity is inhibited with everolimus, flowing into an increase of p-AKT levels and thereby in an enhancement of cell proliferation (13, 15).

The inhibition of mTORC1 has been reported to induce AKT activation in numerous cell types (16–18), unveiling the fact that mTOR inhibitors block mTORC1 activity but do not alter mTORC2 assembly, accordingly with the direct phosphorylation of AKT at Ser 473 (19). In this regard, an increase of AKT activity has been shown to be one of the major contributors that diminished mTOR inhibitors' anticancer activity (20).

This limited efficacy of everolimus due to p-AKT re-activation could be overcome by upstream AKT phosphorylation inhibition.

In this connection, a new molecular mechanism that contributes to confer sensitivity or resistance to dopamine agonists (DAs) in PitNETs was recently revealed (21). More specifically, it was demonstrated that, in a subset of NF-PitNETs and in rat prolactin (PRL)-secreting tumoral cells (MMQ), the treatment with a DRD2-selective agonist (BIM53097) leads to p-AKT inhibition, flowing into a reduction of cell proliferation through a β-arrestin 2-dependent mechanism. Briefly, in this work, it was demonstrated that β-arrestin 2 transfection in NF-PitNETs lacking its expression restored the ability of the dopamine agonist to exert its antimitotic action (21). Moreover, in MMQ cells silenced for β-arrestin 2, an opposite effect of BIM53097 on p-AKT was observed, together with a complete loss of its antiproliferative activity. These data unveiled a new molecular mechanism that contributes to confer sensitivity or resistance to DAs in pituitary tumors. In tumoral lactotrophs and NF-PitNETs, the lack of β-arrestin 2 prevents the inhibitory effect of DRD2 on AKT pathway activation with a consequent resistance to the antimitotic action of DAs.

Based on the above-mentioned premises, the aim of this study was to test the efficacy of cabergoline in increasing the sensitivity of human primary cultured NF-PitNET cells to the antiproliferative effects of everolimus and to investigate the contribution of β-arrestin 2.

MATERIALS AND METHODS

Cell Cultures

The local ethics committee previously approved the study, and each patient involved gave informed consent to the use of his/her tumor sample. A brief description of the patient and tumor characteristics is reported in **Table 1**. Human pituitary cells were obtained by trans-sphenoidal surgery from patients with NF-PitNET. The tissues were partially frozen for subsequent molecular analysis and partially enzymatically dissociated as

TABLE 1 | Radiological pre- and post-surgery information of NF-PitNET patient's derived samples.

NF-PitNET samples	Gender	Age at surgery (years)	Radiology information			Pre-surgery information			Post-surgery information	
			Macroadenoma	Tumor's maximum dimension (mm)	Cavernous sinus invasion	Pre-surgery therapy	Hypopituitarism	Number of deficits	Hypopituitarism	Number of deficits
1	F	44	Yes	27.5	Yes	No	Yes	1	Yes	2
2	F	74	Yes	23	Yes	No	Yes	1	No	0
3	F	35	Yes	33	Yes	No	Yes	1	Yes	1
4	F	54	Yes	19	Yes	No	Yes	2	Yes	2
5	F	72	Yes	25	Yes	No	No	0	No	0
6	F	54	Yes	26	Yes	No	No	0	Yes	3
7	M	83	Yes	30	Yes	No	Yes	1	No	0
8	F	43	Yes	27	No	No	No	0	No	0
9	M	72	Yes	26	No	Yes[a]	Yes	3	Yes	3
10	M	53	Yes	26	Yes	No	Yes	1	Yes	1
11	M	68	Yes	27	Yes	No	Yes	1	No	0
12	F	62	Yes	24	Yes	No	No	0	Yes	1
13	M	68	Yes	25	Yes	No	Yes	3	Yes	4
14	M	68	Yes	14	No	No	No	0	No	0

[a]*Cabergoline, 1 mg/week for 2 years.*

A summary of the characteristics of the patients from whom the samples are derived is shown. The gender and age at surgery of the patients are shown, together with the radiological characteristics of the tumor (presence of macroadenomas, its maximum dimension, and if cavernous sinus was invaded). Details about the presence of hypopituitarism and deficits before and after the surgery are reported

previously described (22). The dispersed cells were cultured in Dulbecco's modified Eagle's medium supplemented with 10% fetal bovine serum (FBS), 2 mM glutamine, and antibiotics (Gibco, Invitrogen, Life Technologies Inc., Carlsbad, CA, USA). Rat tumoral pituitary MMQ cells (ATCC CRL-10609) were grown in RPMI medium (Life Technologies, Thermo Fisher, Carlsbad, CA, USA) supplemented with 15% horse serum, 2.5% FBS, 2 mM glutamine, and antibiotics.

Chemicals

Everolimus and cabergoline were both purchased from Sigma-Aldrich. The powders were suspended in sterile dimethyl sulfoxide, stocked at -80°C, and diluted immediately before use in complete culture medium.

Proliferation Assay

Cell proliferation was determined by the colorimetric measurement of 5-bromo-2′-deoxyuridine (BrdU) incorporation during DNA synthesis in proliferating cells as previously described (23). MMQ and NF-PitNET cells were seeded in starved medium in a 96-well polylysine-coated plate at a density of 2 or 5 × 10^4 cells/well, respectively. The cells were incubated for 72 h in complete medium with cabergoline, everolimus, or their combination. BrdU incorporation in newly synthesized DNA was then allowed at 37° C for 24 h (NF-PitNETs) or 2 h (MMQ). Therefore, the assay was performed in accordance with the instruction of the manufacturer (Cytiva, Life Science, Marlborough, MA, USA).

Western Blot Analysis

MMQ and NF-PitNETs cells were seeded at a density of 3 × 10^5 cells/well in a 6-well plate for western blot analysis. After 24 h, the cells were treated with cabergoline and everolimus, alone or in combination, for 3 h at 37°C. Total proteins were quantified by bicinchoninic acid assay; 60 µg were separated on SDS/polyacrylamide gels and transferred to a nitrocellulose filter. Total-AKT and cyclin D3 antibodies were used at 1:1,000, phospho-AKT (Ser473) and β-arrestin 2 antibodies at 1:2,000 (Cell Signaling, Danvers, MA, USA). Primary antibodies were incubated overnight at 4°C; secondary antibodies anti-rabbit or anti-mouse (Cell Signaling, Danvers, MA, USA) was used at 1:2,000 at room temperature for 1 h. Anti-GAPDH antibody (Invitrogen, Thermo Fisher, CA, USA) were used at 1:4,000 for 1 h at room temperature. Chemiluminescence was detected using ChemiDOC-IT Imaging System (UVP, Upland, CA, USA) and analyzed with NIH ImageJ software. β-arrestin 2 expression level analysis was performed on frozen samples of human NF-PitNETs.

β-Arrestin 2 Silencing

MMQ cells were silenced with rat β-arrestin 2 smart pool siRNAs and Dharmafect transfection agent 4 (Dharmacon, GE Healthcare Life Sciences, Chicago, IL, USA) as previously described (21). In each experiment, a negative control siRNA (non-targeting sequence without a significant homology to the sequence of human, mouse, or rat transcripts) was used. For each experiment, the silencing efficiency was tested by western blot analysis, and only experiments with at least 70% silencing efficiency were considered.

Transcription Factor Analysis

Total RNA was extracted from human NF-PitNET frozen tissues conserved at -80°C with Trizol Reagent (Life Technologies, Carlsbad, CA, USA) using standard methods. Moreover, 2 µg of total RNA were reverse-transcribed with RevertAid H Minus First Strand cDNA Synthesis Kit (Thermo Fisher Scientific,

Whaltam, MA, USA). Then, 1 µl of cDNA was used for PCR with a specific primer amplifying human SF-1 (Fw: 5′-AGCTGCAAGGGCTTCTTCAA-3′; Rw: 5′-GAATCTGTGCCTTCTTCTGC-3′) and DRD2 (Fw: 5′-AGACCAGAACGAGTGCATCA-3′; Rw: 5′-CGCCAAACCAGAGAAGAATG-3′). A GAPDH transcript was used as the housekeeping standard.

Statistical Analysis

The results are expressed as mean ± SD. A paired two-tailed Student's *t*-test was used to detect the significance between two series of data. Two-way ANOVA test was used to analyze the significance between two different groups of data. In addition, $p < 0.05$ was accepted as statistically significant.

RESULTS

In Vitro Responsiveness of NF-PitNET Primary Cultures to Cabergoline, Everolimus, and Their Cotreatment

The everolimus treatment was effective in reducing cell proliferation in 5 out of 14 NF-PitNET primary cultured cells (-39.2 ± 25.8% at 1 nM, $p < 0.01$ vs. basal) (**Figure 1A**). An everolimus dose was chosen based on literature data (8), and preliminary dose–response experiments were performed in NF-PitNET cultured cells (**Supplementary Figure S1A**). In unresponsive tumors, no reduction of cell proliferation was observed even at higher doses of everolimus (10 nM, 100 nM, and 1 µM) (**Supplementary Figure S1B**). Cabergoline incubation determined a reduction of NF-PitNET primary cell proliferation in 5 out of 14 samples (-32 ± 21.2% at 100 nM, $p < 0.01$ vs. basal, **Figure 1B**). In total, 4 out of these 5 tumors were responsive to both drugs. In responsive tumors, the cotreatment of everolimus and cabergoline did not enhance the efficacy of the drugs administered singularly (**Figures 1A, B**). Moreover, 8 out of 14 NF-PitNETs were resistant to both cabergoline and everolimus (**Table 2**).

Interestingly, in NF-PitNETs resistant to everolimus, the coadministration of cabergoline was effective in inhibiting cell proliferation in 7 out of 9 tumors (-31.4 ± 9.9%, $p < 0.001$ vs. basal) (**Figure 1C** and **Table 2**). Similarly, the combined treatment exerted a strong reduction of cyclin D3 expression (-52 ± 18%, mean of 3 different tumors, $p < 0.01$ vs. basal, **Figure 1D**).

In order to establish if NF-PitNET lineage derivation might affect the responsiveness to cabergoline, everolimus, or both, the expression of transcription factor steroidogenic factor-1 (SF-1), marker of a gonadotrophic lineage (24), was evaluated by RT-PCR analysis. Our results showed a positive expression of SF-1 in all tumor samples (**Figure 1E**). Moreover, all tumors expressed both the long (D2L) and short (D2S) isoforms of DRD2 (**Figure 1E**).

Everolimus and Cabergoline Effects on AKT Phosphorylation in NF-PitNETs

We then evaluated the AKT activity, testing its phosphorylation status on Ser473 (p-AKT). Our data unveiled that in 6 out of 7 everolimus-unresponsive NF-PitNET group, the 3h everolimus treatment determined a significant increase of the p-AKT/total-AKT ratio (2.1-fold, $p < 0.01$ vs. basal), and this effect was reverted by cabergoline cotreatment (**Figure 1F**).

Interestingly, cabergoline was unable to revert the increase of AKT phosphorylation in one everolimus-resistant sample that was also resistant to the antiproliferative effects of the everolimus-and-cabergoline combined treatment, suggesting that the ability to reduce everolimus-dependent AKT phosphorylation is required for the antiproliferative effect (**Figures 1G, H**).

Cabergoline and Everolimus Cotreatment Reduced Cell Proliferation and AKT Phosphorylation in Everolimus-Resistant MMQ Cells

In MMQ cells, everolimus administration did not affect cell proliferation in a range of doses from 0.1 to 100 nM (**Supplementary Figure S1C**), while cabergoline inhibited cell growth (-22.8 ± 6.8%, $p < 0.001$ vs. basal), and a greater inhibition was reached after cabergoline and everolimus coincubation (-34.8 ± 18%, $p < 0.001$ vs. basal and $p < 0.05$ vs. cabergoline) (**Figure 2A**).

In order to test everolimus' effects on AKT activity, the AKT phosphorylation levels on Ser473 were evaluated by western blot analysis after 3 h of incubation with everolimus and/or cabergoline. As shown in **Figure 3B**, everolimus significantly increased the p-AKT/total-AKT ratio (+1.53 ± 0.24-fold, $p < 0.001$ vs. basal), while cabergoline induced a reduction (-18.6 ± 5.6%, $p < 0.001$ vs. basal). Cotreatment with cabergoline and everolimus resulted in a strong decrease of p-AKT/total-AKT ratio (-34.5 ± 14%, $p < 0.001$ vs. basal) (**Figure 2B**).

β-Arrestin 2 Silencing Prevented Everolimus and Cabergoline Cotreatment Inhibitory Effects on Both p-AKT and Cell Proliferation in MMQ Cells

To test a possible involvement of β-arrestin 2 in mediating cabergoline's inhibition of everolimus-induced AKT phosphorylation, genetic silencing experiments were performed in MMQ cells. Our data show that cell proliferation inhibition induced by cabergoline, both alone and in combination with everolimus, was reverted by β-arrestin 2 silencing (**Figure 3A**). Accordingly, the lack of β-arrestin 2 prevented the ability of cabergoline to reduce the p-AKT/total-AKT ratio after 3 h of exposure to everolimus (**Figure 3B**).

In addition, in cells silenced for β-arrestin 2, cabergoline induced a stimulatory effect on AKT according to the observed increase in cell proliferation (**Figures 3A, B**).

DISCUSSION

This study demonstrated that the cotreatment with the mTOR inhibitor everolimus and DRD2 agonist cabergoline is able to overcome the resistance of a consistent subgroup of NF-PitNETs to everolimus' antiproliferative effects by preventing the upstream activation of AKT.

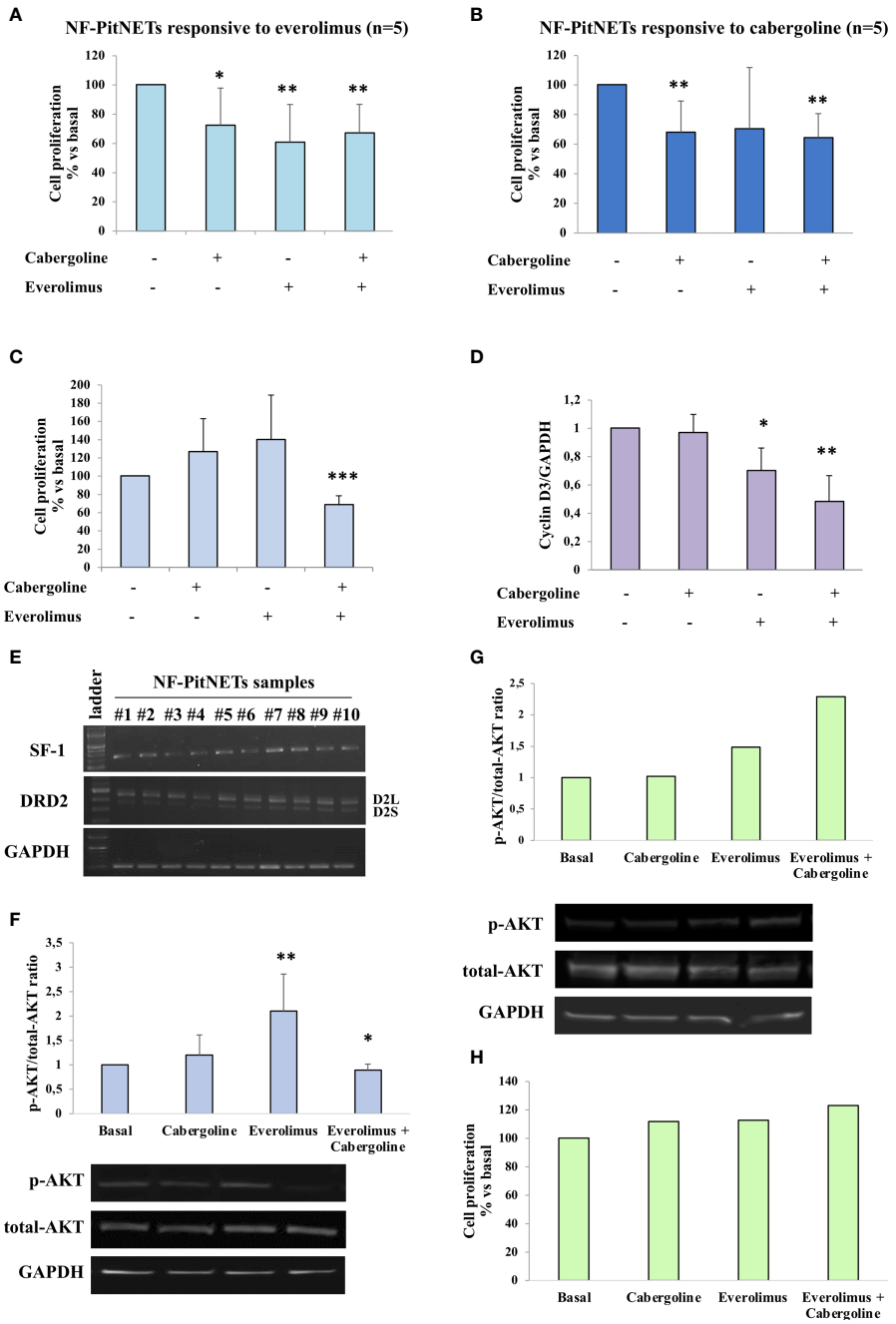

FIGURE 1 | NF-PitNET cell primary culture response to everolimus, cabergoline, and cotreatment on AKT phosphorylation and cell proliferation. Primary cultured of NF-PitNET cells **(A–H)** were treated with 100 nM cabergoline and 1 nM everolimus for 72 h **(A–C**, **H)** or 3 h **(D, F, G)** at 37°C, administered singularly or in combination. **(A–C)** BrdU incorporation in newly synthesized DNA was measured. Data represent the mean ± SD normalized vs. respective basal of 14 different NF-PitNETs primary cultures: $n = 5$ responsive to everolimus **(A)**, $n = 5$ responsive to cabergoline **(B)**, $n = 7$ resistant to both drugs but responsive to the cotreatment **(C)**. Each determination was done in triplicate. $^{*}p < 0.05$, $^{**}p < 0.01$, $^{***}p < 0.001$ *vs*. corresponding basal. **(D)** The graph shows the quantification of cyclin D3 normalized to GAPDH (mean value ± SD from 3 primary cultures of NF-PitNETs cells). $^{*}p < 0.05$, $^{**}p < 0.01$ vs. corresponding basal. **(E)** RT-PCR analysis of NF-PitNET samples ($n = 10$) in order to detect SF-1, D2L, and D2S DRD2 isoform expression. GAPDH expression was analyzed as control. Representative images are shown. **(F)** The graph shows the quantification of p-AKT/total AKT normalized to the basal. Data represent mean ± SD of 6 different NF-PitNET samples. Representative immunoblots are shown. $^{*}p < 0.05$; $^{**}p < 0.01$, vs. corresponding basal. **(G, H)** NF-PitNET primary cultured cells resistant to cabergoline, everolimus, and cotreatment were analyzed. **(G)** The graph shows the quantification of p-AKT/total AKT normalized to the basal and representative immunoblots. **(H)** Measurement of BrdU incorporation in newly synthesized DNA.

TABLE 2 | NF-PitNETs primary cultured responsiveness to everolimus, cabergoline, and their cotreatment.

NF-PitNET sample	Cabergoline	Everolimus	Cabergoline + everolimus
1			
2			
3			
4			
5			
6			
7			
8			
9			
10			
11			
12			
13			
14			

[a]*Primary cultures (n = 14) of NF-PitNET cells were treated with 100 nM cabergoline and 1 nM everolimus for 72 h at 37°C, administered singularly or in combination, and BrdU incorporation in newly synthesized DNA was measured. The table presents the responsiveness, in terms of proliferation reduction, of each sample to each treatment. Responsive NF-PitNETs are indicated in green color and the unresponsive ones in red.*

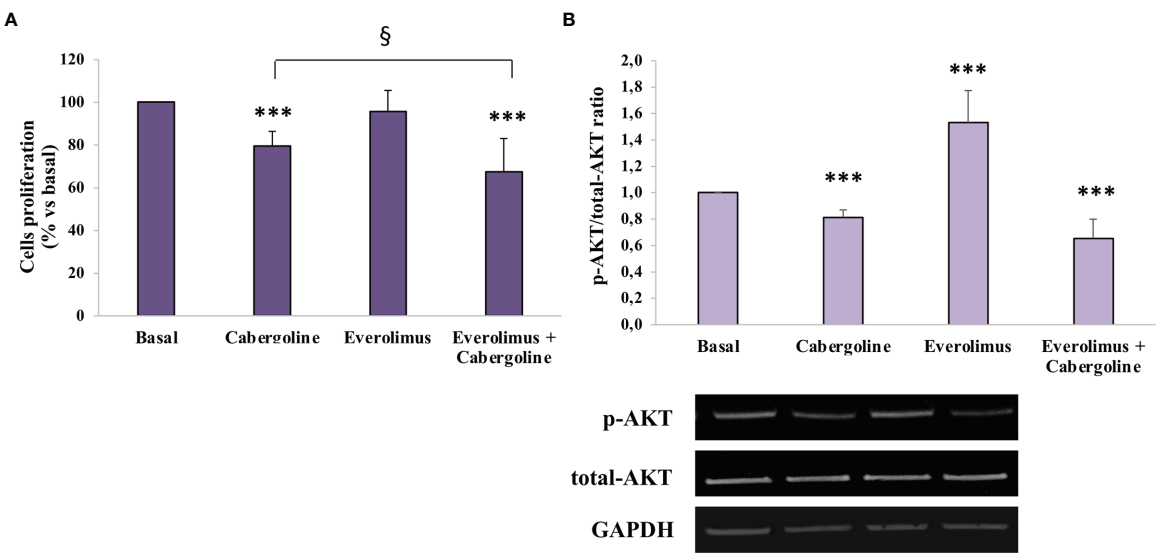

FIGURE 2 | Cabergoline and everolimus cotreatment reduced both cell proliferation and AKT phosphorylation in MMQ cells. MMQ cells were cultured with 100 nM cabergoline and 1 nM everolimus for 72 h **(A)** or 3 h **(B)**, administered singularly or in combination. **(A)** BrdU incorporation in newly synthesized DNA was measured. The experiments were repeated 4 times, and each determination was done in quadruplicate. Values represent mean (± SD) normalized vs. respective basal. *** $p < 0.001$ vs. corresponding basal; § $p < 0.05$ vs. cabergoline administered alone. **(B)** The graph shows the quantification of p-AKT on Ser473 normalized to total AKT (mean value ± SD from 4 independent experiments). Representative immunoblots are shown. *** $p < 0.001$ vs. corresponding basal.

This work's results highlighted that about two-thirds of NF-PitNETs were resistant to everolimus treatment in terms of cell proliferation inhibition, and almost all tumors of this subgroup were also resistant to cabergoline. However, the coadministration of everolimus and cabergoline was able to significantly reduce cell proliferation, while it did not potentiate the effects of each agent singularly administered in responsive tumors.

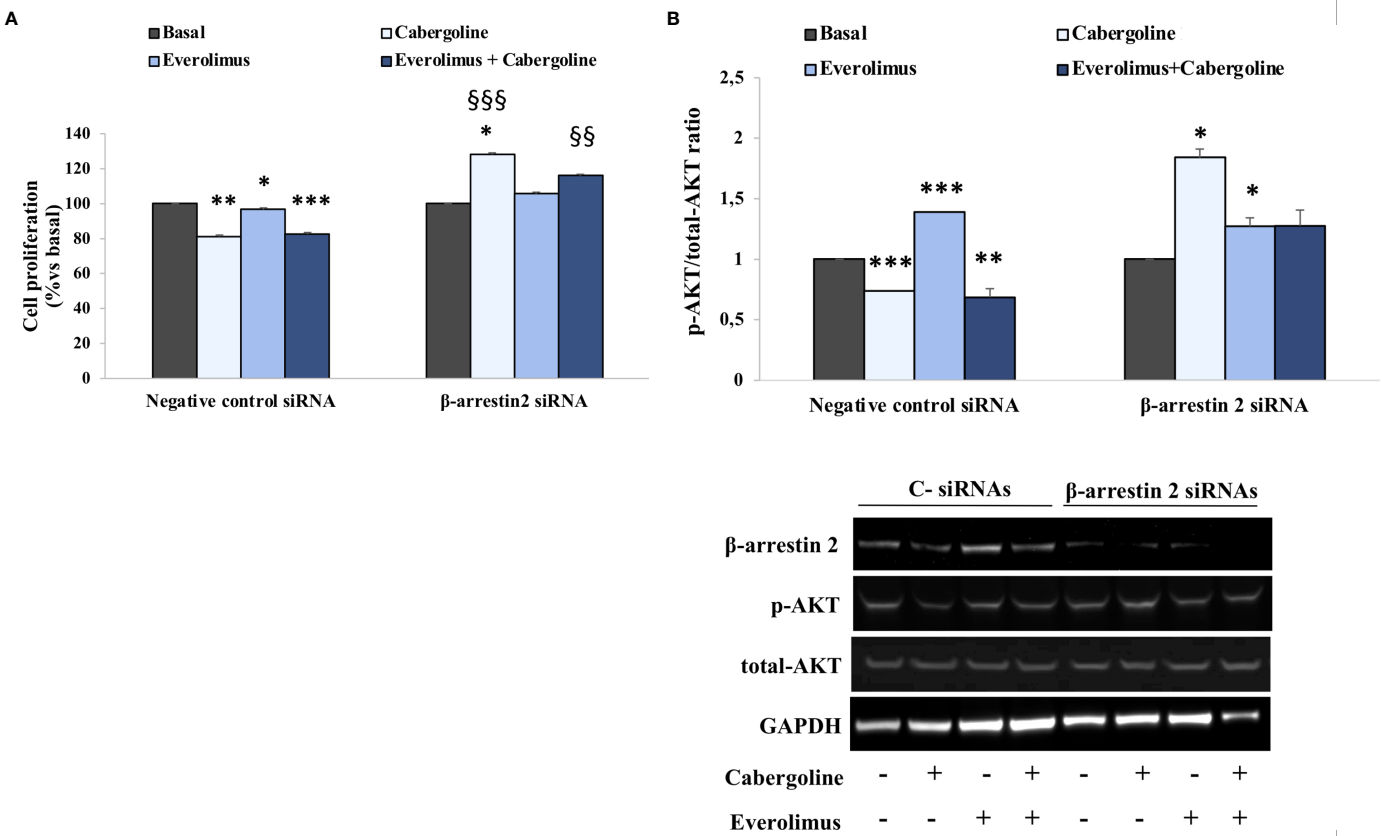

FIGURE 3 | β-arrestin 2 lack reverted everolimus and cabergoline cotreatment ability in reducing both p-AKT and cell proliferation in MMQ cells. The MMQ cells were transiently transfected with β-arrestin 2 siRNAs or negative control siRNAs (C-) for 72 h and then incubated with 100 nM cabergoline and 1 nM everolimus for 72 h **(A)** or 3 h **(B)**, administered singularly or in combination. **(A)** BrdU incorporation in newly synthesized DNA was measured. The experiments were repeated 4 times, and each determination was done in quadruplicate. Values represent mean ± SD normalized vs. respective basal. $^{*}p < 0.05$, $^{***}p < 0.001$ vs. corresponding basal, $^{§§}p < 0.01$; $^{§§§}p < 0.001$ vs. corresponding treated negative control. **(B)** Densitometrical analysis of p-AKT (Ser473)/total AKT ratio normalized vs. respective basal (mean ± SD from 3 independent experiments), and representative immunoblots are shown. The equal amount of proteins was confirmed by stripping and reprobing with an anti-GAPDH antibody. $^{*}p < 0.05$, $^{**}p < 0.01$, $^{***}p < 0.001$ vs. corresponding basal.

In agreement, it has been previously shown that a subset of NF-PitNETs is resistant to the antiproliferative *in vitro* effects of everolimus (8, 11) or rapamycin (10). In particular, Zatelli and co-authors demonstrated that everolimus, used at a higher concentration compared to the present investigation, was effective in reducing cell proliferation in about 70% of NF-PitNETs, and cabergoline did not potentiate the effect of everolimus in responsive tumors (8). Moreover, a study by Rubinfeld et al. unveiled that the limited tumoral responsiveness to mTOR inhibitors in human-derived NF-PitNET cells could be overtaken by combining different kinds of drug or targeting multiple players of the PI3K–AKT–mTOR pathway, emphasizing the cell type-specific effects of these treatments (11). Another work suggested that mTOR inhibitors' efficacy could be improved by cotreatment with other drugs. Particularly, it was shown that, in NF-PitNETs, octreotide cotreatment potentiated the effects of rapamycin and conferred responsiveness to resistant NF-PitNETs (10).

A lot of potential mechanisms leading to mTOR inhibitor resistance have been described in literature in various kinds of tumors (12)—for instance, earlier studies suggested that tumors with PTEN, FKBP-12, or FKB domain mutations or constitutive PI3K activity displayed scarce responses to mTOR inhibitors. Alterations in protein translation (decreased 4E-BP1 or increased eIF4E) have also been demonstrated to interfere with the effects of mTOR inhibitors on protein synthesis. The stimulation of autophagy and the increased levels of anti-apoptotic molecules, such as Bcl-2, represent additional mechanisms of resistance. Moreover, non-functional apoptotic pathways have been highlighted to potentially confer resistance together with modulation of apoptotic regulators' stimulation of autophagy and enhanced angiogenesis. In addition, another way can be addressed to the increase in ERK/MAPK signaling, activation of the serin/threonine PIM kinases, the activation status of PDK1, or the altered expression levels of 4E-BP1, a downstream substrate of

mTOR, which suppresses eIF4E activity. Furthermore, it was demonstrated that preventing the downregulation of p27Kip1 levels can lead to a less response to this kind of drugs (12). Nevertheless, the increase in AKT activation has been shown to be one of the major contributors that diminished everolimus' anticancer activity effectiveness, which was induced by an escape mechanism.

Specifically, in different human-derived tumoral cell lines, everolimus blocked mTOR's ability in inhibiting the ribosomal protein S6 kinase (p706SK), determining an activation of IRS-1 that leads to AKT phosphorylation. This cascade of events flows into an increase of AKT activity and, consequently, into an enhancement of cell proliferation (13).

This suggests that a combined therapy that inhibits mTOR function and prevents AKT activation might have improved the antitumoral activity.

A possible therapeutic potential of DRD2 as a target in PitNETs has been also reported in a previous study in which it was stated that, in ACTH-secreting PitNET cell model, an association of 9-cis retinoic acid and the DRD2 agonist bromocriptine modulates the receptor's signaling in terms of hormone secretion and cell viability (25).

We have recently demonstrated that the DRD2 agonist cabergoline was effective in inhibiting AKT phosphorylation through a β-arrestin 2-dependent mechanism in tumoral lactotrophs and NF-PitNETs (21). Here we showed that cabergoline improved everolimus' efficacy by blocking the AKT upstream reactivation.

The AKT phosphorylation levels were analyzed in order to study its activation status after everolimus and cabergoline treatment, singularly and in combination. Our data demonstrated that everolimus-unresponsive NF-PitNETs showed a substantial enhancement of the p-AKT/total-AKT ratio when incubated with everolimus alone, in agreement with the escape mechanism mentioned above. On the other side, the combined treatment with cabergoline strongly reduced this increase of AKT activity, and this ability is correlated with its antimitotic effect. In order to test the relevance of DRD2 expression for NF-PitNETs' responsiveness to cabergoline and to evaluate the different expressions in DRD2 or its isoforms, long (D2L) and short (D2S), RT-PCR was performed. From our analysis, it emerged that all tumors positively expressed both isoforms of DRD2, regardless of responsiveness to dopamine agonist, ruling out a possible a role of both specific DRD2 isoforms in mediating opposite effects on the everolimus escape mechanism. Our results are in accordance with the observation that the clinical sensitivity to DAs was not associated with the expression of DRD2 or its isoforms (26).

In this sense, we might assume that everolimus' poor efficacy in NF-PitNETs might be caused by the loss of the negative upstream feedback on AKT, thereby determining the resistance to treatment.

An effect of cabergoline in potentiating the effect of everolimus administration by a reduction of the mTOR inhibitor-induced escape mechanisms was previously reported in lung carcinoid tumoral cells (27).

In PRL-secreting PitNET MMQ cells, cabergoline determined a significant reduction of both cell proliferation and the p-AKT/total-AKT ratio as previously reported (21). On the contrary, everolimus was unable to reduce cell proliferation due to a significant increase of AKT phosphorylation. This effect was reverted by the combined treatment with cabergoline. The co-incubation with everolimus and cabergoline significantly induced a reduction of both cell proliferation and the p-AKT/total-AKT ratio with respect to cabergoline treatment alone, suggesting a possible synergic effect. These observations allow us to consider MMQ cells as a model of "everolimus escape". Conversely, in rat somatolactotroph tumoral GH3 cells that are responsive to everolimus' antiproliferative effects, no increase of AKT activity was detected after the everolimus treatment (28). With regard to this, a previous study demonstrated that, in aggressive PRL-PitNETs, everolimus exhibited an antiproliferative action *in vitro*, suggesting it as a novel therapeutic option in PRL-PitNETs resistant to conventional therapy with cabergoline. Moreover, they demonstrated how the everolimus and cabergoline combination determined *in vivo* tumor size reduction and PRL level normalization (29).

In addition, we demonstrated the involvement of β-arrestin 2 in mediating cabergoline's inhibition of AKT activity and cell proliferation after everolimus cotreatment.

Genetic silencing experiments in MMQ cells revealed that the lack of β-arrestin 2 reverted the antimitotic effect induced by the combined treatment with everolimus and cabergoline as well as the inhibition of AKT. It should be noted that MMQ cells only express D2L (21, 30), and studies in literature seem to attribute the postsynaptic phenomena to D2L, such as AKT regulation (31).

However, a specific role of DRD2 isoforms in β-arrestin 2 recruitment has not yet been specifically investigated.

In conclusion, the present study revealed that cabergoline might overcome the everolimus escape mechanism in NF-PitNETs and tumoral lactotrophs by inhibiting the upstream AKT activation. The coadministration of cabergoline might improve mTOR inhibitors' antitumoral activity, paving the way for a potential combined therapy in β-arrestin 2-expressing NF-PitNETs or other PitNETs resistant to conventional treatments.

DATA AVAILABILITY STATEMENT

The raw data supporting the conclusions of this article will be made available by the authors without undue reservation.

AUTHOR CONTRIBUTIONS

FM: conceptualization, methodology, investigation, data curation, writing—original draft, writing—review and editing, and formal analysis. EE, DT, RC, GM, GDM, and AMB: investigation. ML and AL: resources, review, and editing; AM, AS, and MA: review and editing. EP: conceptualization, validation, data curation, funding acquisition, supervision, writing—original draft, writing—review and editing, project administration, and formal analysis. GM:

conceptualization, supervision, funding acquisition, project administration, and writing—review and editing.

FUNDING

This work was supported by Associazione Italiana Ricerca Cancro grant to GM (IG 2017-20594), Italian Ministry of Health grant to GM (PE-2016-02361797), and Ricerca Corrente Funds from the Italian Ministry of Health and Progetti di Ricerca di Interesse Nazionale grant to EP (2017N8CK4K).

SUPPLEMENTARY MATERIAL

The Supplementary Material for this article can be found online at: https://www.frontiersin.org/articles/10.3389/fendo.2022.867822/full#supplementary-material

REFERENCES

1. Hasskarl J. Everolimus. *Recent Results Cancer Res* (2018) 211:101–23. doi: 10.1007/978-3-319-91442-8_8
2. Musat M, Korbonits M, Kola B, Borboli N, Hanson MR, Nanzer AM, et al. Enhanced Protein Kinase B/AKT Signalling in Pituitary Tumours. *Endocr Relat Cancer* (2005) 2):423–33. doi: 10.1677/erc.1.00949
3. Xu M, Ahorts-Cary L, Knox AJ, Kleinsmidt-DeMasters B, Lillehei K, Wierman ME. Epidermal Growth Factor Receptor Pathway Substrate 8 Is Ovexpressed in Human Pituitary Tumors: Role in Proliferation and Survival. *Endocrinology* (2009) 150:2064–71. doi: 10.1210/en.2008-1265
4. Noh TW, Jeong HJ, Lee MK, Kim TS, Kim SH, Lee EJ. Predicting Recurrence of Nonfunctioning Pituitary Adenomas. *J Clin Endocrinol Metab* (2009) 94 (11):4406–13. doi: 10.1210/jc.2009-0471
5. Monsalves E, Juraschka K, Tateno T, Agnihotri S, Asa SL, Ezzat S, et al. The PI3K/AKT/mTOR Pathway in the Pathophysiology and Treatment of Pituitary Adenomas. *Endocr Relat Cancer* (2014) 21(4):R331–344. doi: 10.1530/ERC-14-0188
6. Esposito D, Olsson DS, Ragnarsson O, Buchfelder M, Skoglund T, Johannsson G. Non-Functioning Pituitary Adenomas: Indications for Pituitary Surgery and Post-Surgical Management. *Pituitary* (2019) 22 (4):422–34. doi: 10.1007/s11102-019-00960-0
7. Ntali G, Wass JA. Epidemiology, Clinical Presentation and Diagnosis of non-Functioning Pituitary Adenomas. *Pituitary* (2018) 21(2):111–8. doi: 10.1007/s11102-018-0869-3
8. Zatelli MC, Minoia M, Filieri C, Tagliati F, Buratto M, Ambrosio MR, et al. Effect of Everolimus on Cell Viability in Nonfunctioning Pituitary Adenomas. *J Clin Endocrinol Metab* (2010) 95(2):968–76. doi: 10.1210/jc.2009-1641
9. Lee M, Wiedemann T, Gross C, Leinhäuser I, Roncaroli F, Braren R, et al. Targeting PI3K/mTOR Signaling Displays Potent Antitumor Efficacy Against Nonfunctioning Pituitary Adenomas. *Clin Cancer Res* (2015) 21(14):3204–15. doi: 10.1158/1078-0432.CCR-15-0288
10. Cerovac V, Monteserin-Garcia J, Rubinfeld H, Buchfelder M, Losa M, Florio T, et al. The Somatostatin Analogue Octreotide Confers Sensitivity to Rapamycin Treatment on Pituitary Tumor Cells. *Cancer Res* (2010) 70 (2):666–74. doi: 10.1158/0008-5472.CAN-09-2951
11. Rubinfeld H, Cohen O, Kammer A, Yang G, Cohen ZR, Hadani M, et al. Combination of mTOR Inhibitors Augments Potency While Activating PI3K Signaling in Pituitary Tumors. *Neuroendocrinology* (2016) 103(5):592–604. doi: 10.1159/000442205
12. Carew JS, Kelly KR, Nawrocki ST. Mechanisms of mTOR Inhibitor Resistance in Cancer Therapy. *Target Oncol* (2011) 6(1):17–27. doi: 10.1007/s11523-011-0167-8
13. O'Reilly KE, Rojo F, She QB, Solit D, Mills GB, Smith D, et al. mTOR Inhibition Induces Upstream Receptor Tyrosine Kinase Signaling and Activates Akt. *Cancer Res* (2006) 66(3):1500–8. doi: 10.1158/0008-5472
14. Oldham S, Hafen E. Insulin/IGF and Target of Rapamycin Signaling: A TOR De Force in Growth Control. *Trends Cell Biol* (2003) 13(2):79–85. doi: 10.1016/s0962-8924(02)00042-9
15. Shi Y, Yan H, Frost P, Gera J, Lichtenstein A. Mammalian Target of Rapamycin Inhibitors Activate the AKT Kinase in Multiple Myeloma Cells by Up-Regulating the Insulin-Like Growth Factor Receptor/Insulin Receptor Substrate-1/Phosphatidylinositol 3-Kinase Cascade. *Mol Cancer Ther* (2005) 4 (10):1533–40. doi: 10.1158/1535-7163.MCT-05-0068
16. Bhatt AP, Bhende PM, Sin SH, Roy D, Dittmer DP, Damania B. Dual Inhibition of PI3K and mTOR Inhibits Autocrine and Paracrine Proliferative Loops in PI3K/Akt/mTOR-Addicted Lymphomas. *Blood* (2010) 115(22):4455–63. doi: 10.1182/blood-2009-10-251082
17. Kharas MG, Janes MR, Scarfone VM, Lilly MB, Knight ZA, Shokat KM, et al. Ablation of PI3K Blocks BCR-ABL Leukemogenesis in Mice, and a Dual PI3K/mTOR Inhibitor Prevents Expansion of Human BCR-ABL+ Leukemia Cells. *J Clin Invest* (2017) 127(6):2438. doi: 10.1172/JCI95182
18. Tamburini J, Chapuis N, Bardet V, Park S, Sujobert P, Willems L, et al. Mammalian Target of Rapamycin (mTOR) Inhibition Activates Phosphatidylinositol 3-Kinase/Akt by Up-Regulating Insulin-Like Growth Factor-1 Receptor Signaling in Acute Myeloid Leukemia: Rationale for Therapeutic Inhibition of Both Pathways. *Blood* (2008) 111(1):379–82. doi: 10.1182/blood-2007-03-080796
19. Sarbassov DD, Guertin DA, Ali SM, Sabatini DM. Phosphorylation and Regulation of Akt/PKB by the rictor-mTOR Complex. *Science* (2005) 307 (5712):1098–101. doi: 10.1126/science.1106148
20. Gupta M, Ansell SM, Novak AJ, Kumar S, Kaufmann SH, Witzig TE. Inhibition of Histone Deacetylase Overcomes Rapamycin-Mediated Resistance in Diffuse Large B-Cell Lymphoma by Inhibiting Akt Signaling Through Mtorc2. *Blood* (2009) 114(14):2926–35. doi: 10.1182/blood-2009-05-220889
21. Mangili F, Giardino E, Treppiedi D, Barbieri AM, Catalano R, Locatelli M, et al. Beta-Arrestin 2 Is Required for Dopamine Receptor Type 2 Inhibitory Effects on AKT Phosphorylation and Cell Proliferation in Pituitary Tumors. *Neuroendocrinology* (2021) 111(6):568–79. doi: 10.1159/000509219
22. Peverelli E, Olgiati L, Locatelli M, Magni P, Fustini MF, Frank G, et al. The Dopamine-Somatostatin Chimeric Compound BIM-23A760 Exerts Antiproliferative and Cytotoxic Effects in Human non-Functioning Pituitary Tumors by Activating ERK1/2 and P38 Pathways. *Cancer Lett* (2010) 288(2):170–6. doi: 10.1016/j.canlet.2009.06.034
23. Peverelli E, Giardino E, Treppiedi D, Meregalli M, Belicchi M, Vaira V, et al. Dopamine Receptor Type 2 (DRD2) and Somatostatin Receptor Type 2 (SSTR2) Agonists are Effective in Inhibiting Proliferation of Progenitor/Stem-Like Cells Isolated From Nonfunctioning Pituitary Tumors. *Int J Cancer* (2017) 140(8):1870–80. doi: 10.1002/ijc.30613
24. Lopes MBS. The 2017 World Health Organization Classification of Tumors of the Pituitary Gland: A Summary. *Acta Neuropathol* (2017) 134(4):521–35. doi: 10.1007/s00401-017-1769-8
25. Occhi G, Regazzo D, Albiger NM, Ceccato F, Ferasin S, Scanarini M, et al. Activation of the Dopamine Receptor Type-2 (DRD2) Promoter by 9-Cis Retinoic Acid in a Cellular Model of Cushing's Disease Mediates the Inhibition of Cell Proliferation and ACTH Secretion Without a Complete Corticotroph-To-Melanotroph Transdifferentiation. *Endocrinology* (2014) 155(9):3538–49. doi: 10.1210/en.2013-1820
26. Greenman Y, Cooper O, Yaish I, Robenshtok E, Sagiv N, Jonas-Kimchi T, et al. Treatment of Clinically Nonfunctioning Pituitary Adenomas With Dopamine Agonists. *Eur J Endocrinol* (2016) 175(1):63–72. doi: 10.1530/EJE-16-0206
27. Pivonello C, Rousaki P, Negri M, Sarnataro M, Napolitano M, Marino FZ, et al. Effects of the Single and Combined Treatment With Dopamine Agonist, Somatostatin Analog and mTOR Inhibitors in a Human Lung Carcinoid Cell Line: An *In Vitro* Study. *Endocrine* (2017) 56(3):603–20. doi: 10.1007/s12020-016-1079-2

28. Gorshtein A, Rubinfeld H, Kendler E, Theodoropoulou M, Cerovac V, Stalla GK, et al. Mammalian Target of Rapamycin Inhibitors Rapamycin and RAD001 (Everolimus) Induce Anti-Proliferative Effects in GH-Secreting Pituitary Tumor Cells In Vitro. *Endocr Relat Cancer* (2009) 16(3):1017–27. doi: 10.1677/ERC-08-0269
29. Zhang D, Way JS, Zhang X, Sergey M, Bergsneider M, Wang MB, et al. Effect of Everolimus in Treatment of Aggressive Prolactin-Secreting Pituitary Adenomas. *J Clin Endocrinol Metab* (2019) 104(6):1929–36. doi: 10.1210/jc.2018-02461
30. Ventra C, Meucci O, Grimaldi M, Scorziello A, Porcellini A, Schettini G. Absence of D2S Dopamine Receptor in the Prolactin-Secreting MMQ Pituitary Clone: Characterization of a Wild D2L Receptor Coupled to Native Transduction Mechanisms. *J Mol Endocrinol* (1995) 14(3):375–89. doi: 10.1038/onc.2016.264
31. Beaulieu JM, Tirotta E, Sotnikova TD, Masri B, Salahpour A, Gainetdinov RR, et al. Regulation of Akt Signaling by D2 and D3 Dopamine Receptors *In Vivo*. *J Neurosci* (2007) 27(4):881–5. doi: 10.1523/JNEUROSCI.5074-06.2007

Conflict of Interest: The authors declare that the research was conducted in the absence of any commercial or financial relationships that could be construed as a potential conflict of interest.

frontiers | Frontiers in Endocrinology

REVIEW
published: 16 June 2022
doi: 10.3389/fendo.2022.877537

Fertility Preservation and Restoration Options for Pre-Pubertal Male Cancer Patients: Current Approaches

Elena Eugeni[1,2*†], *Iva Arato*[1†], *Rachele Del Sordo*[3], *Angelo Sidoni*[3], *Andrea Garolla*[4], *Alberto Ferlin*[4], *Riccardo Calafiore*[1], *Stefano Brancorsini*[5], *Francesca Mancuso*[1‡] *and Giovanni Luca*[1,2,6‡]

[1] Department of Medicine and Surgery, University of Perugia, Perugia, Italy, [2] Department of Medicine and Medical Specialties, Division of Medical Andrology and Endocrinology of Reproduction, University of Terni, Terni, Italy, [3] Division of Anatomic Pathology and Histology, Department of Experimental Medicine, University of Perugia, Perugia, Italy, [4] Unit of Andrology and Reproductive Medicine, Department of Medicine, School of Medicine and Surgery, University of Padua, Padua, Italy, [5] Section of Pathology (Terni), Department of Medicine and Surgery, University of Perugia, Perugia, Italy, [6] International Biotechnological Center for Endocrine, Metabolic and Embryo-Reproductive Translational Research (CIRTEMER), Department of Medicine and Surgery, University of Perugia, Perugia, Italy

OPEN ACCESS

Edited by:
Antonino Belfiore, University of Catania, Italy

Reviewed by:
Giuseppe Grande, Catholic University of the Sacred Heart, Rome, Italy
Robin Mark Hobbs, Monash University, Australia

***Correspondence:**
Elena Eugeni
eugeni.elena@gmail.com

[†]*These authors have contributed equally to this work and share first authorship*

[‡]*These authors have contributed equally to this work and share last authorship*

Specialty section:
This article was submitted to Cancer Endocrinology, a section of the journal Frontiers in Endocrinology

Received: *16 February 2022*
Accepted: *25 April 2022*
Published: *16 June 2022*

Citation:
Eugeni E, Arato I, Del Sordo R, Sidoni A, Garolla A, Ferlin A, Calafiore R, Brancorsini S, Mancuso F and Luca G (2022) Fertility Preservation and Restoration Options for Pre-Pubertal Male Cancer Patients: Current Approaches. Front. Endocrinol. 13:877537. doi: 10.3389/fendo.2022.877537

Fertility preservation for prepubertal male patients undergoing gonadotoxic therapies, potentially depleting spermatogonial cells, is an expanding necessity, yet most of the feasible options are still in the experimental phase. We present our experience and a summary of current and novel possibilities regarding the different strategies to protect or restore fertility in young male patients, before proceeding with chemotherapy or radiotherapy for malignances or other diseases. Adult oncological patients should always be counselled to cryopreserve the semen before starting treatment, however this approach is not suitable for prepubertal boys, who aren't capable to produce sperm yet. Fortunately, since the survival rate of pediatric cancer patients has skyrocketed in the last decade and it's over 84%, safeguarding their future fertility is becoming a major concern for reproductive medicine. Surgical and medical approaches to personalize treatment or protect the gonads could be a valid first step to take. Testicular tissue autologous grafting or xenografting, and spermatogonial stem cells (SSCs) transplantation, are the main experimental options available, but spermatogenesis *in vitro* is becoming an intriguing alternative. All of these methods feature both strong and weak prospects. There is also relevant controversy regarding the type of testicular material to preserve and the cryopreservation methods. Since transplanted cells are bound to survive based on SSCs number, many ways to enrich their population in cultures have been proposed, as well as different sites of injection inside the testis. Testicular tissue graft has been experimented on mice, rabbits, rhesus macaques and porcine, allowing the birth of live offspring after performing intracytoplasmic sperm injection (ICSI), however it has never been performed on human males yet. *In vitro* spermatogenesis remains a mirage, although many steps in the right direction have been performed. The manufacturing of 3D scaffolds and artificial spermatogenetic niche, providing support to stem cells in cultures, seems like the best way to further advance in this field.

Keywords: fertility, spermatogonial cell, gonadotoxic cancer treatment, cryopreservation, testicular tissue transplantation, SSCs transplantation, *de novo* morphogenesis, *In vitro* spermatogenesis

INTRODUCTION

The increasing incidence of cancer during childhood and the rising survival rate, currently estimated around 84% after 5 years from diagnosis (1), is leaving behind a large population of young male patients whose fertility is at stake (2, 3). The most common cancers in children are leukemias, lymphomas, tumors involving the brain or CNS, bone or soft tissue sarcomas, germ cell tumors, and embryonal tumors (4)

In adult patients, cryopreservation of seminal fluid is a safe and proven approach to preserve fertility prior to initiating gonadotropic treatments and should be routinely proposed by the caregiver in consultation with a reproductive medicine specialist (5, 6). Pre-pubertal patients are not capable yet of producing spermatozoa; therefore, this approach is not sustainable in their course of treatment (7, 8).

Although several valid studies have been published in recent years regarding methods to protect or restore fertility in children, and some practices are now likely to be ready for clinical use, these options still remain exclusive to the experimental field.

It is estimated that about half of adult patients with an history of pediatric malignancy will have difficulty conceiving children, with a major impact on their quality of life (9–11).

A variety of oncological treatments could threaten testicular function (12–16), such as surgery, chemotherapy, radiotherapy, or combination therapy, with potential synergistic effects in causing gonadal toxicity. In the pre-pubescent male patient, the seminiferous tubules are populated by Spermatogonial Stem Cells (SSCs) which, being actively proliferating, are particularly sensitive to damage by chemotherapy or radiotherapy (17, 18). A fraction of SSCs is not rapidly proliferating and constitutes a reserve of stem cells. Such cells, referred as A dark spermatogonia or State 0 SSCs, have been widely investigated over the years and are expressed in higher percentage in the testis of humans and non-human primates than in rodents (22% vs 0.3%). These SSCs are less chemosensitive, but their damage might lead to a condition of irreversible infertility, as the pool of SSCs is no longer able to proliferate and subsequently differentiate (19, 20).

Several chemotherapeutic agents have been associated with risk of testicular toxicity, mainly alkylating agents (19–21), platinum agents (22, 23) or cytarabine (21). Therapy with cyclophosphamide or the combination of chlormethine and procarbazine may cause alterations in spermatogenesis, and this risk increases as the dose increases (21). Other chemotherapies that may be implicated in spermatogenesis damage include ifosfamide, busulfan/cyclophosphamide or fludarabine/melphalan, used in some protocols for Hematopoietic stem-cell transplantation (HSCT) conditioning, although studies that evaluate the specific adverse effects for some of them are lacking and their toxicity is only deemed as probable (21). Risk assessment of the impact of chemotherapy on spermatogenesis is not straightforward, as many protocols involve the administration of several drugs together or in combination with radiotherapy, and the patient's age and follow-up time are also relevant, given the potential recovery of spermatogenetic capacity after a period of time. Even taking all these elements into account, individual patient variability and genetic predisposition may play a major role in the gonadotoxic effect of therapy (21).

Leydig cells are more resistant to the toxic action of chemotherapeutic agents and their function is generally preserved (24). Combined treatments with alkylating agents and pelvic radiotherapy, however, may impair their function, bringing to a clinical condition characterized by increased LH and decreased Testosterone (25). Pre- hematopoietic cell transplantation conditioning protocols and treatments including chemotherapy and irradiation are generally capable of damaging both germ cells and Leydig cells (26, 27).

Given their known toxicity, alkylating agents are used with caution in pediatric oncology protocols, either by attempting to reduce the cumulative dose or by choosing drugs with a more favorable harmful profile (28), but this is often not feasible in cancer in advanced stages. The risk of testicular toxicity increases when multiple alkylating agents are used together, when treatments are prolonged, or when the patient is young (28).

Several scores such as alkylating agent dose (AAD) (29) or cyclophosphamide equivalent dose (CED) (30) are available to quantify exposure to alkylating agents and assess the risk of potential adverse events, but they do not account for all drugs currently in use. The recovery of spermatogenesis after therapy depends on the ability of quiescent SCCs to survive and resume differentiation, so the duration of azoospermia increases progressively depending on the extent of damage and the scarcity of the residual stem cell population (31).

Radiation therapy is also capable of damaging the delicate SCCs, as the germinal epithelium is very sensitive to radiation. Cranial radiotherapy could also damage the hypothalamic-pituitary region and cause a form of central hypogonadism, triggered by impaired stimulation of the testis by the lack of LH and FSH. Even doses of 0.1 Gy can temporarily alter spermatogenesis (32, 33), while doses greater than 6 Gy permanently damage the subject's spermatogenetic capacity causing irreversible azoospermia (34). Gonadotoxic protocols include abdomen, pelvis, and total body irradiation, total node irradiation, and cranial radiotherapy, which can cause alterations in the pituitary- testicle axis, leading to hypogonadotropic hypogonadism if administered at doses above 35-40 Gy (21). Leydig cells are more resistant to these effects, but even fractional doses of testicular irradiation of 12 Gy can increase LH values in pre-pubertal patients, thus suggesting a toxic effect (35). Doses greater than 20 Gy generally require hormone replacement therapy to achieve normal pubertal development. In the adult male, however, the irreversibly toxic dose is greater than 30 Gy (36).

The overall gonadotoxic effect of radiation therapy is related to total dose, irradiated volume, fractionated dose, and patient age (37).

Green et al. (38) demonstrated that patients exposed at pre-pubescent age to testicular radiotherapy at cumulative doses > 7.5 Gy, an AAD > 2, or treatment with procarbazine or high dose of cyclophosphamide showed reduction in their ability to

procreate. Specifically, patients included in the study who survived childhood cancers were half as likely to produce offspring as their siblings (Hazard Ratio of pregnancy of 0.56 versus 0.91). Treatment doses and patterns are relevant to this risk, as is age at the diagnosis.

Unilateral orchiectomy for the treatment of testicular tumors can reduce the number of germ cells available, but it is not generally associated with azoospermia. An observational study showed that 85% of patients who underwent unilateral orchiectomy were able to procreate during the subsequent 11-year follow-up (13). The combination of surgical treatment, chemotherapy and radiation therapy increases the risk of long-term gonadotoxicity in the child.

Preserving and protecting the fertility of young cancer patients is now a shared goal within their treatment plan, but nevertheless many doubts still remain about which strategies should be proposed to the patient and family, as many approaches are still considered in the experimental and research phase.

Current guidelines (5, 6) recommend informing the patient and family about the potential infertility risk of planned therapies and referring them to a reproductive medicine specialist at the earliest possible opportunity, to help them to evaluate the available options for preserving future fertility (**Figure 1**).

PHARMACOLOGICAL APPROACHES TO PRESERVE TESTICULAR FUNCTION

One of the hypothesized gonadoprotective strategies is the use of molecules capable of inhibiting the pituitary secretion of LH and FSH, the hormones that stimulate the testis to produce testosterone and spermatozoa. Agonists or antagonists of the pituitary receptor of GnRH are able to block this hormonal production, generating a state of hypogonadotropic hypogonadism that could be exploited to protect the gonads. However, the use of GnRH agonist or antagonist for gonado-protective purposes during or before treatment for neoplasms does not appear to be useful in humans, and it is not recommended in ASCO guidelines. Such a strategy had appeared promising following some studies in rats (39–41) in which administration of GnRH before, during, or after therapy with alkylating agents or radiotherapy resulted in a marked increase in proliferating germ cells and a resumption of spermatogenic capacity. A similar effect has not been demonstrated in humans in several studies in which GnRH antagonist was associated with Testosterone (42–45). A single study (46) in which only Testosterone was administered showed positive results, although under conditions, as in the treatment of nephrotic syndrome and during therapy with cyclophosphamide alone (46). Several studies in nonhuman primates have confirmed this disappointing fact (47). However, GnRH agonist treatment seems to have a positive effect on the success of SCC transplantation, as proven in rats (48, 49). Testosterone suppression induced by such treatment, however, may induce an increased immune response (50), and this may justify the conflicting data obtained in the same pre-transplant treatment in nonhuman primates (47).

Some *in vivo* and *in vitro* studies in animal models have tested the protective effect of anti-apoptotic substances, such as sphingosine-1-phosphate (51) or immunomodulatory substances such as AS101 (52). In mice, these compounds offer some testicular protection against radiation or cyclophosphamide damage, but no relevant effect has been demonstrated in humans so far. Similar approaches have been used to test the protective effect of L- Carnitine (53), and several antioxidant substances, including curcumine nanocrystals (54), Moringa oleifera (55), alpha-tocopherol-succinate (56) and ascorbic acid

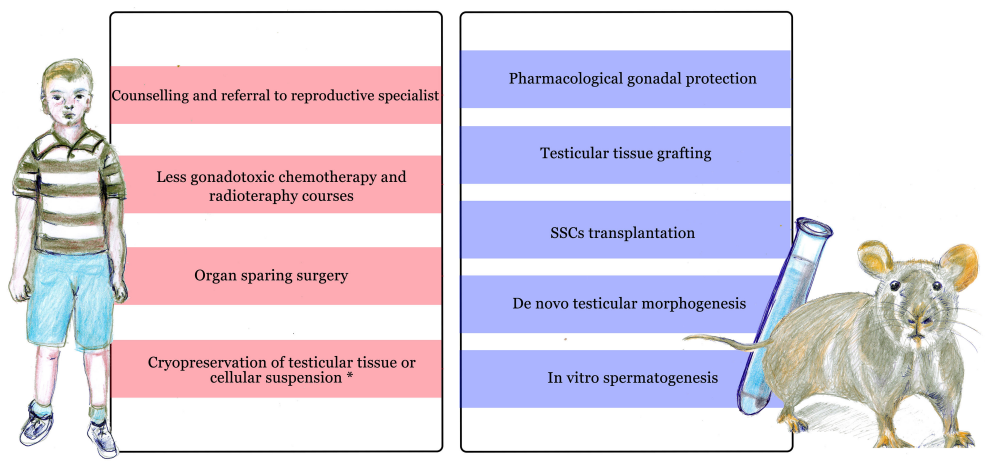

FIGURE 1 | Current approaches to preserve and restore fertility in prepubertal males undergoing cancer treatment. On the left side: current clinical approaches available before and during treatment. On the right side: experimental methods, mainly tested on animal models (including rodents, non human primates and others) or *in vitro*. *Cryopreservation of testicular material is only available in selected centers during experimental protocols.

(57), all tested on the gonads of cyclophosphamide-exposed rodents, with encouraging results but yet to be proven in humans.

The rationale behind the use of these substances is that some chemotherapy drugs, such as cyclophosphamide, are capable of generating radical oxygen species (ROS) and causing cellular apoptosis or altering DNA synthesis (51–56). Oxidative stress can activate enzymes such as sphingomyelinases, which can release ceramide from cell membranes and trigger cell apoptosis, and substances such as S1P might inhibit this specific process (51). A different detrimental effect of some chemotherapy drugs is the fragmentation of cellular DNA, resulting in an abnormal chromatin structure, a condition that reduces seminal quality and is known to decrease fertility (52). Immunomodulatory substances capable of limiting this alteration would be very useful for their gonadoprotective action. On the other hand, the administration of substances with antioxidant power may be able to reduce the oxidative stress produced by chemotherapic agents such as cyclophosphamide, which also seems to be able to damage the structure of the blood-testis barrier, altering the expression of Occludin proteins, produced by Sertoli cells (53).

To understand how to pharmacologically protect the testis in pre-pubertal children, it is thus essential to study the mechanisms involved in cytotoxic damage and survival of the SSCs population, as well as understanding the functioning of the complex spermatogenetic niche (**Figure 2**). The ability of germinal spermatogonial cells to ensure a continuous population of cells that can differentiate is essential for spermatogenic capacity (58). Several studies have investigated the recovery capabilities of spermatogonial stem cells after chemotherapeutic damage (59, 60). Many papers published by Parker et al. (61, 62) have focused on the effect of glial cell line-derived neurotrophic factor (GDNF) produced by Sertoli cells and essential for the survival of SSCs. GDNF is a member of the TGF-β superfamily, and by binding to its receptor and RET/GFRA1 on SCCs it regulates their survival and differentiation (63, 64).

Evidence in mice suggest that GDNF expression levels decrease with ageing, while it might increase with stem cell depletion (65). After a treatment with low dose busulfan, GDNF expression was found to be increased and that might be necessary to restore the pool of SSCs and their subsequent proliferation (65).

However, when this factor is lacking, the germline population gradually declines, reducing its replication and increasing downstream differentiation, down to a condition where the tubules are populated solely by Sertoli cells (SCO) (61). Providing GDNF stimulation again may allow for a new expansion of the cell pool (62).

One of the potential ways in which chemotherapeutic agents might reduce GDNF expression is through DNA methylation, the main epigenetic mechanism capable of affecting male fertility. Several agents, including cisplatin (66) and doxurubicin (67) have been proven to induce important epigenetic modifications to cellular DNA. Methylation of some sequences called CpG islands, rich in dinucleotides composed of Cytosine and Guanine, is able to block access to transcription factors and reduce the expression of some genes (68, 69). This would make the employ of some demethylating agents promising, such as eicosapentaenoic acid (EPA) which is able to activate several enzymes that can counteract cytosine methylation, promoting the re-expression of silenced genes (69).

Our group has studied the effect of cisplatin, doxurubicin, and 4-Hydroperoxycyclophosphamide, chemotherapeutics known to be gonadotoxic, *in vitro* on pre-pubescent porcine Sertoli cells (70), a model known to be adequate for toxicity study (71). Drug exposure resulted in reduced expression of the GDNF gene and protein, as well as reduced expression of AMH and Inhibin B,

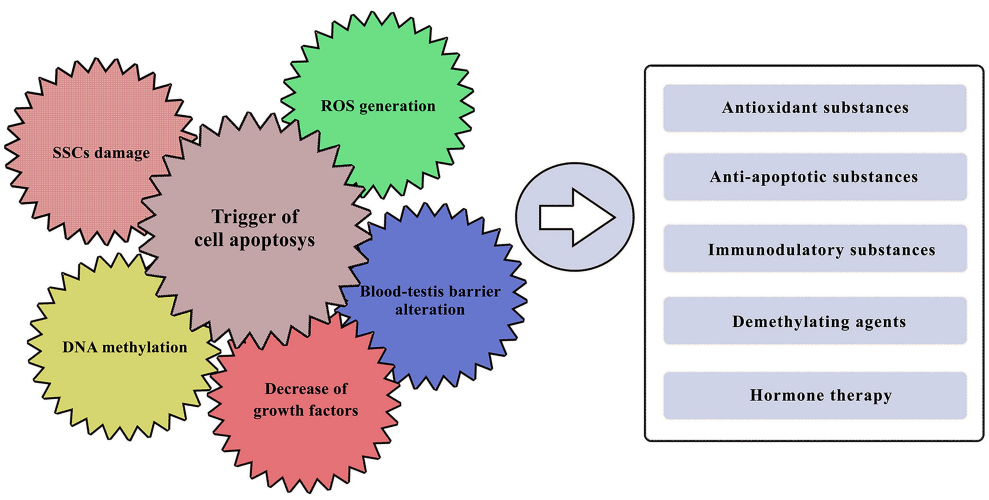

FIGURE 2 | Known gonadotoxic damage of cancer treatments and potential pharmacological approaches. On the left side: the major effects with which various chemotherapeutic agents could impair testicular function. On the right side: potential pharmacological approaches that have been tested so far, with more or less promising results in protecting the male gonad.

which are markers of function in pre-pubertal Sertoli cells. In cultures treated with high dose of cisplatin and EPA, there was a recovery of GDNF, AMH and Inhibin B expression, showing a protective effect on the male gonad. Treatment with cisplatin and d 5-aza-2'-deoxy- cytidine, a known demethylating agent used in several chemotherapy protocols, allowed to obtain similar results, supporting the hypothesis of the ability of EPA to protect against epigenetic alterations of DNA and opening the future to further studies to evaluate the effect of this substance on the human pre-pubescent testis.

Despite promising evidence in animal models, guidelines do not currently include the use of protective substances during cancer therapy in children (5, 6).

SURGICAL APPROACHES TO PRESERVE TESTICULAR FUNCTION

Pediatric testicular tumors are rare nosological entities, the most common being germ cell tumors, but they can occur bilaterally and synchronous or metachronous in up to 5% of cases (72). In such cases, a treatment with enucleation of the neoplasm (73, 74) instead of a total bilateral orchidectomy can be considered, if the tumor is of a small size and it is confined to the testis. Careful follow-up is necessary, as there is a risk of recurrence after enucleation of about 5%. The same approach is possible with Leydig cell tumors, in which the risk of recurrence after conservative treatment appears low (75).

There are several clinical cases reported in the literature, the first dating back to more than 30 years (76), in which a testicular transposition was performed to protect the residual gonad from adjuvant radiotherapy treatment. The healthy testis was transposed at the inguinal (77), abdominal (78) or leg region (79) and then repositioned in the scrotum at the end of therapy. It is interesting to note that in one clinical case report (80), the testis was able to resume spermatogenesis during the following months after post-traumatic repositioning in a subcutaneous pocket at tight level.

In cases of scrotal neoplasia in which extensive excision of skin and muscle layers is necessary, displacement of the testis in the contralateral hemiscrotum has been attempted to preserve its function (81). However, such approaches should be considered experimental and are not currently recommended in guidelines until further investigation (5, 6).

CRYOPRESERVATION: TESTICULAR TISSUE OR CELL SUSPENSION

Young peripubertal patients might be able to produce spermatozoa and a semen sample can be obtained as early as 12 years old (82). Once spermatogenesis is initiated, seminal parameters are comparable to those of adult patients (83, 84). In younger patients, in whom the sperm production has not started yet or who for whatever reason are unable to produce seminal fluid, only experimental approaches are available, such as preservation of testicular tissue obtained by biopsy or orchiectomy, when required for the treatment course of the clinical condition.

The experience of several centers both in Europe (85) and in the USA (86) is remarkable with respect to the possibility of cryopreserving pre-pubescent testicular tissue for use in approaches aimed at restoring fertility in the future. Proposed freezing protocols are numerous (86–92), including fast or slow freezing and the use of various cryoprotectants. Most centers employ slow freezing combined with the use of Dimethylsulfoxide (DMSO) to protect cells from damage (88, 93) while other facilities use DMSO and sucrose, DMSO and human serum albumin or DMSO & ethylene glycol (93). Some studies have alternatively tested vitrification, a protocol of ultrarapid freezing associated with different concentrations of cryo-protective substances, with the aim of preventing the formation of ice crystals (94).

This approach appears promising, but further studies are needed to verify its actual superiority. It is also possible to choose to freeze a testicular cell suspension, which would reduce some complications due to the freezing of a macroscopic tissue sample, such as creating an uneven cellular cooling rate. This procedure would not allow to preserve the spermatogenetic niche in its entirety (95, 96) and has also been studied in humans less intensively (97). Freezing cells rather than tissue fragments will make it impossible to employ some techniques, such as testicular graft transplantation or tissue culture, whereas a cryopreserved tissue fragment could undergo further enzymatic digestion to obtain SSCs and other testicular cells (98). It is essential to improve the freezing protocol, trying to reduce the generation of alterations in thawed sperm quality (99).

A questionnaire proposed to 24 facilities by the European Society for Human Reproduction and Embryology (ESHRE) in 2012 reported that several centers in Europe offered this possibility and have already involved 260 young patients (85). A subsequent survey in 2019 (86) brought the number of patients involved up to 1033, more than a 4-fold increase. Numerous hospital facilities in the US (86) are currently able to cryopreserve testicular tissue, and the current goal is to create networks with a well-defined common protocol to offer this possibility to as many patients as possible. It is also important to note that approximately one third of the patients enrolled had already started cycles of gonadotoxic chemotherapy, which can potentially compromise the quality of the preserved tissue.

Current guidelines (5, 6) recommend that cryopreservation of testicular tissue be performed only during approved clinical trials or experimental protocols.

FERTILITY RESTORATION EMPLOYING TESTICULAR TISSUE

Testicular Tissue Transplantation

One of the potential options to restore fertility in a patient undergoing gonadotoxic therapies is the transplantation of

previously frozen testicular tissue. This option has been under investigation for several years and numerous studies have been published on animals, the majority of which have tested testicular tissue xenograft into adult immunodeficient nude mice. Xenotransplantation of pre-pubescent human testicular tissue into laboratory animals is not a technique that is expected to be employed to restore fertility in patients undergoing gonadotoxic therapies, due to the high risk of zoonosis transmission (100), nevertheless it is useful to study the mechanisms of transplantation and the survival of spermatogonial cells after it has been performed. Moreover, this technique could be in the future exploited to exclude the presence of neoplastic cells contamination in the testicular tissue, in preparation for a future autograft in the patient (101)

Data is available regarding xenotransplantation of tissue obtained from goats, pigs, mice (102), horses (103), cats (104), cattle (105), rhesus monkeys (106), dogs (107), hamsters (108), and rabbits (109). In all these species, once the transplanted tissue was recovered from mice and analyzed, complete donor spermatogenesis was demonstrated, and in some of these experiments (109–113) live and healthy progeny has been obtained.

Despite the undoubtedly promising results, several questions remain to be clarified. Studies that have performed xenografts of pre-pubertal human testicular tissue (92, 100, 114) have not shown appearance of complete spermatogenesis yet. There could be several obstacles, including placement of the transplant in an ectopic or orthotopic location. Early attempts at xenotransplantation, both from human and animal donors, were almost all placed in the ectopic site, but transplantation placed in the testicular site has been shown to have a higher probability of survival and maturation, probably on account of the different local temperature (114, 115). In contrast, whether the tissue is fresh or thawed from previous cryopreservation does not seem to make a difference (116, 117).

Xenograft experiments from pre-pubescent human donors have, however, demonstrated prolonged (up to 9 months) survival of SSCs and Sertoli cells, and obtained secondary spermatocytes (114) or spermatid- like cells (92).

Nevertheless, the survival of spermatogonial cells in transplants is not high (117) and it seems to be closely related to the future of tissue vascularization, which must proceed with capillary formation that is supplied by host vessels (118), since the graft is transplanted without any vascular anastomoses. To improve tissue survival, several approaches with pro-angiogenic,anti-apoptotic and anti-oxidant molecules have been attempted. The use of recombinant FSH (119) and Testosterone (120) has not shown encouraging results on testicular graft survival.

Bovine testicular tissue treated with vascular endothelial growth factor (VEGF) at the time of implantation in mice (121) was heavier at recovery than the untreated control and showed a higher percentage of seminiferous tubules containing differentiated cells. Since the early approaches, numerous experiments have begun to treat the tissue with VEGF, whether in the context of autografts in mice (122), bovine tissue xenografts (123), and even pre-pubescent human testis xenografts (124).

On the pre-pubescent human testis, *in vitro* pretreatment with VEGF appears to increase vascularization and survival of SSCs and seminiferous tubule integrity (124). Subsequent experiments (122) on autograft in mice tested the combined effect of VEGF and platelet-derived growth (PDGF) nanoparticles, showing that the combination of the two factors appears to further improve vascularization. The use of necrosis inhibitor substances also seems promising (125).

Autotransplantation, the method more desirably applicable to pre-pubertal patients undergoing gonadotropic therapies, has been tested on nonhuman primates (111, 126, 127). These studies demonstrated on marmosets (126) better survival of transplants at the orthopedic site, which achieved complete spermatogenesis, probably because of reduced scrotal temperature compared with other body regions, and better results of tissues taken from pre-pubertal animals compared with adults, perhaps because of greater resistance to hypoxia. A study in rhesus monkeys (127) showed the achievement of complete spermatogenesis after orthotopic autotransplantation of testicular tissue, subjected to cryopreservation for a period longer than two years. A subsequent study in rhesus monkeys (111) showed complete spermatogenesis obtained from autologous transplants of testicular tissue placed subcutaneously either in the scrotum or behind the back, cryopreserved or fresh. Spermatozoa were also shown to fertilize oocytes, and *via* ICSI viable and healthy offspring were generated.

In a study of autotransplantation of testicular tissue in mice (128), alginate-encapsulated tissue with or without the addition of VEGF nanoparticles also appeared to improve spermatogonial recovery post-transplantation.

It should be emphasized that testicular tissue transplantation is not able to restore fertility in the recipient in the absence of medically assisted procreation, since it has not been proven that the graft is able to create anastomoses with the seminal tract, thus leading to ejaculation of spermatozoa with seminal fluid and fertilization during natural sexual intercourse. As today, these methods appear to be entirely experimental and have not yet been tested on human patients, either pre-pubescent or adult.

Spermatogenesis *In Vitro* From Testicular Tissue

Achieving spermatogenesis *in vitro* from testicular tissue would allow to avoid the risks related to other methods, in particular the transmission of zoonosis *via* xenografts (100) and the possible neoplastic contamination of tissues obtained from cancer patients (101, 129–132). This approach has been studied for many years (133, 134), but it is still experimental, and the current goal is to optimize culture systems in order to further progress in this direction (135).

In mouse, *in vitro* spermatogenesis has been obtained from testicular tissue cultures (135–137) and these spermatozoa were found to be able of fertilizing embryos and producing healthy offspring. Sato et al's (137) experiments developed a culture system called "*in vitro* transplantation" (IVT), in which SSCs from one donor are injected into the empty seminiferous tubules of another animal, and the result is incubated in a culture system.

In other studies (138) the air- liquid interphase method has been used, obtaining competent spermatozoa capable of generating healthy and fertile offspring, even exploiting previously cryopreserved tissue. The quality of spermatozoa obtained with such cultures has been evaluated (139), showing that the majority of them are characterized by normal haplody, non-fragmented DNA and condensed chromatin.

Full *in vitro* spermatogenesis was reached even in bovine (140) and rat (141) testicular tissue culture

Obtaining human spermatozoa *in vitro* has proven more challenging. Numerous attempts have been made to understand the best culture conditions of testicular fragments (142), investigating proper temperature, serum, and wheter gonadotropin stimulation is necessary.

So far, postmeiotic haploid cells have been obtained from pre-pubescent human testicular tissue fragments, both in organotypic culture (143) and exploiting a 3D culture system (144). One study (145) obtained haploid spermatids from SSCs obtained from testes of cryptorchid patients cultured in 2D systems enriched with arachidonic acid and stem cell factor (SCF). Such spermatids were able to fertilize murine oocytes by Microinjection of round spermatids (ROSI).

Recreating the complex microenvironment of the spermatogenic niche seems to be essential to achieve progress (135, 146) so there has been a clear shift towards 3D culture systems over the old 2D systems. Also, the potential of the culture to generate an intact and functioning blood-testicular barrier (147) seems to be relevant, as occurs *in vivo* during puberty.

FERTILITY RESTORATION EMPLOYING CELL SUSPENSION

SSCS Transplantation

Different approaches exploiting testicular cell suspension are under study. A promising one is SSCs autotransplantation. This mechanism has been described since 1994 in mice (148) and over the years has been the subject of numerous studies on different experimental animals, also it appears to be the only one potentially able to restore fertility without the need to employ medically assisted procreation. The ability to colonize seminiferous tubules, as well as the possibility to initiate spermatogenesis, is related to the amount of SSCs transplanted (149). Furthermore, it has been estimated that only 10% of transplanted spermatogonial stem cells are able to form colonies (149). Such cells are rare, representing approximately 1 in 3500 cells in the adult mouse testis (150), and the amount of testicular tissue that can be harvested in the pre-pubescent would not be sufficient to provide an adequate number of cells.

For this reason, several methods have been developed to generate efficient culture systems of SSCs, amplifying their number *in vitro* before transplantation, and this approach has been initially studied in mice (151). The collected testicular tissue undergoes enzymatic digestion in several steps according to well-defined protocols (152, 153) and great attention has been paid to find a method that allows to efficiently isolate SCCs as soon as this stage (154).

A further complication is the difficulty in identifying SSCs, based on the markers they express and the proteins they produce (155, 156) since a large proportion of them are also expressed by testicular somatic cells and differentiating them appears complex (157). The ability to characterize these cells, purify and amplify them is essential for successful colonization of the seminiferous tubules in the recipient. Stage- specific embryonic antigen-4 (SSEA-4) (158) is one of the many promising markers of this cell population. However, in recent studies, this marker has shown reduced expression in quiescent State 0 cells, making SSEA-4 less suitable for the isolation of SSCs. The search for the most appropriate marker remains ongoing (159).

Many potential growth factors to achieve adequate proliferation of these cells have been extensively evaluated (160–163), including proposed leukemia inhibitory factor (LIF), epidermal growth factor (EGF), basic fibroblast growth factor (bFGF), Insulin like grow factor 1 (IGF-1), Colony stimulating factor 1 (CSF-1) and the importance of GDNF, and the possible addition of its soluble receptor alpha-1 in culture has been demonstrated (160). The required growth factors appear to be identical in rats and mice (164) and therefore some kind of conservation between species has been hypothesized.

In vitro proliferation of SSCs obtained from different animals, including mice and rats (151, 164, 165) porcine (166), cattle (167) and tree shrew (168), has been achieved. The same approach has allowed *in vitro* proliferation of human SSCs, taken from testicular tissue obtained from pre-pubertal patients during orchidopexy (169), for cryopreservation in cancer patients (170) or from adult patients undergoing orchiectomy (171), from patients with obstructive or non-obstructive azoospermia (172) or from deceased organ donors (158).

Using subcultures, human adult SSCs were cultured and propagated up to 28 weeks and their numbers increased more than 18,000-fold (171). The proliferation capacity of SSCs from pre-pubertal patients seems to be even higher (169). Nevertheless, the long-term fate of SSCs cultures seems unclear. Several promising studies have been carried out to elucidate the best culture conditions, but many of them have not characterized SSCs with suitable surface markers, nor defined the ideal conditions for promoting the development of cells at different stages of maturation. More recent work has been able to identify the full gene expression of SSCs and to assess the molecular pathways activated in their proliferation. This approach appears useful for better understanding their development and improve our culture system (173).

Cancer patients, especially those with hematological diseases, may harbor neoplastic infiltrates in the testicle, as shown in pre-treatment biopsies of children with Acute Lymphocytic Leukemia (174). Such neoplastic cells if transplanted can give

rise to new neoplasms (101, 129–132) so it is essential to ensure purification of the SSCs sample. It has been proven that in rats it is enough to transplant in the testis only 20 leukemic cells, mixed with germ cells, to initiate a relapse of the disease (175).

The most studied mechanics so far are culture systems (176), Fluorescence-activated cell sorting (FACS) (129, 130, 132), and Magnetic-activated cell sorting (MACS) (131, 177) but their evaluation has shown conflicting and sometimes not sufficient results to ensure the safety of the method, making further studies necessary.

The first approach for SSCs transplantation was characterized by multiple microinjections into the seminiferous tubules of the recipient mouse (148), a procedure that required open surgery with exteriorization of the testis and reflection of the vaginal tunica. Afterwards, different approaches were tried on dissected mouse, bovine, monkey and human testes (178), attempting injection of SSCs into the efferent duct or into rete testis network under ultrasound guidance, the latter method being the most promising. Some studies on human testis obtained from cadavers have tested injections of contrast agent (179) or murine SSCs (180, 181) to study the best possible operating conditions, showing that a single injection into rete testis network seems to be effective (179) and that it is necessary to find the right filling pressure, perhaps using an infusion pump, to adequately fill the tubules and reduce fluid leaking into the testicular interstitium (180, 181).

Allografting of SSCs has been tested in sheep (182), goats (183), and nonhuman primates (47, 184), generating healthy live offspring. Only one human clinical trial is reported (185), in which some adult patients who had cryopreserved SSCs prior to chemo-radiotherapy treatment underwent transplantation of such cells with intra-testicular injections. Unfortunately, there are no reports on subsequent follow-up and their seminal parameters (186).

The main doubts to be dispelled, concern the safety of these protocols and the absence of major alterations in the progeny. In mouse SSCs allografts, first and second-generation offspring appear to develop with comparable weight and height to controls and do not appear to show differences in methylation patterns of maternal, paternal, or non-imprinted genes (187). However, seminal parameters after transplantation were worse than controls, with reduced sperm concentration and motility (188). A subsequent study on a similar murine allograft showed no notable genetic alterations in either spermatozoa or progeny (189), such as chromosome number alterations, deletions, or amplifications.

in vitro Spermatogenesis From SSCS and From *De Novo* Testicular Morphogenesis

Cryopreserved or fresh SSCs suspension could also be used to try to achieve *in vitro*-spermatogenesis, in specific culture systems. A type of approach is developing culture systems in which injecting SSCs, exploiting different types of matrixes, such as soft agar or methylcellulose (190) or microfuidic system (191) that allowed to obtain functioning spermatozoa in some studies.

The construction of testicular organoids (192) seems promising to create the right supportive environment for the development of SSCs. A wide variety of proposals is available, including models relying on extracellular matrix (ECM) (193) or ECM- free (194), the use of microwells (195) or 3D printing with particular bio-inks (196). A scaffold-based and scaffold-free approach has also been applied to generate human testis organoids (197) and this strategy opens the way to new future prospectives.

A different method that has been studied, is performing, under the back skin of immunodeficient mice, a graft of testicular cell suspension containing other cells besides SSCs, including Sertoli cells, Leydig cells and peritubular myoid cells, in a definite proportion (198). Such a cell mix seems to be able to organize into a testis-like structure, *via* a complex process that has been named *de novo* testicular morphogenesis, generating a spermatogenic niche and recovering steroidogenic capacity, up to complete spermatogenesis (198). This approach has been studied utilizing cells obtained from rodents (199, 200) zebrafish (201), sheep (202) and cattle (203), as well as from pigs (198, 204). Some of these studies have included the cell suspension in matrices as scaffolds to support their growth (205, 206). Seminiferous tubule formation has also been noted after cell suspension grafting inside the testis of rhesus monkeys (207) with resumption of donor spermatogenesis.

This possibility seems to be very interesting to study the interactions between different testicular cell types and to better understand the mechanisms of gonadal development (203, 205).

CONCLUSION: FUTURE CHALLENGES AND PROMISING METHODS

During the last years we have witnessed a swift progress in studies regarding potential approaches to preserve and restore male fertility, but few of these methods are currently clinically applicable in the prepubertal oncological patient. Current clinical guidelines and approaches involve prompt counseling with a reproductive medicine specialist, reduction of gonadotoxicity of the chosen therapy when possible, and potential participation in experimental protocols where offered.

Cryopreservation of testicular tissue or cell suspension is offered in the context of experimental protocols in several centers around the world, which have developed shared methods and a considerable experience on this field, however there is still no certainty about which are the best methods and the potential damage to sperm quality. Cryopreserved testicular material, either tissue fragment or cell suspension, has shown in several experimental animals the ability to re-initiate spermatogenesis and even to generate healthy living offspring, but there is not yet sufficient evidence in humans. Out-of-body approaches, such as *in vitro* spermatogenesis, are promising but early in their development. We believe that there is a need to pursue these approaches, while continuing to evaluate the potential efficacy of numerous chemicals and pharmacological substances that could help to protect the delicate prepubescent testis from the insult of oncological therapies.

AUTHOR CONTRIBUTIONS

All authors listed have made a substantial, direct, and intellectual contribution to the work and approved it for publication.

FUNDING

This research was founded by Fondazione CARIT Cassa di Risparmio di Terni, code or Project FCTR21UNIPG. EE is a recipient of an University of Perugia PhD research grant

REFERENCES

1. American Cancer Society. *Cancer Facts & Figures 2021*. Atlanta, Ga: American Cancer Society (2021).
2. Howell SJ, Shalet SM. Testicular Function Following Chemotherapy. *Hum Reprod Update* (2001) 7:363–9. doi: 10.1093/humupd/7.4.363
3. Byrne J, Mulvihill JJ, Myers MH, Connelly RR, Naughton MD, Krauss MR, et al. Effects of Treatment on Fertility in Long-Term Survivors of Childhood or Adolescent Cancer. *N Engl J Med* (1987) 317:1315–21. doi: 10.1056/NEJM198711193172104
4. Siegel RL, Miller KD, Jemal A. Cancer Statistics, 2016. *CA Cancer J Clin* (2016) 66:7–30. doi: 10.3322/caac.21332
5. Oktay K, Harvey BE, Loren AW. Fertility Preservation in Patients With Cancer: Asco Clinical Practice Guideline Update Summary. *J Oncol Pract* (2018) 14:381–5. doi: 10.1200/JOP.18.00160
6. Tozawa A, Kimura F, Takai Y, Nakajima T, Ushijima K, Kobayashi H, et al. Japan Society of Clinical Oncology Clinical Practice Guidelines 2017 for Fertility Preservation in Childhood, Adolescent, and Young Adult Cancer Patients: Part 2. *Int J Clin Oncol* (2022) 27:281–300. doi: 10.1007/s10147-021-02076-7
7. Wallace WHB. Oncofertility and Preservation of Reproductive Capacity in Children and Young Adults. *Cancer* (2011) 117:2301–10. doi: 10.1002/cncr.2604521
8. Mitchell RT, Nahata L, Quinn GP. Fertility Preservation: Don't Forget the Boys. *BMJ* (2017) 356:j495. doi: 10.1136/bmj.j495
9. Green D, Galvin H, Horne B. The Psycho-Social Impact of Infertility on Young Male Cancer Survivors: A Qualitative Investigation. *Psychooncology* (2003) 12:141–52. doi: 10.1002/pon.622
10. Wasilewski-Masker K, Seidel KD, Leisenring W, Mertens AC, Shnorhavorian M, Ritenour CW, et al. Male Infertility in Long-Term Survivors of Pediatric Cancer: A Report From the Childhood Cancer Survivor Study. *J Cancer Surviv* (2014) 8:437–47. doi: 10.1007/s11764-014-0354-6
11. Kaatsch P. Epidemiology of Childhood Cancer. *Cancer Treat Rev* (2010) 36:277–85. doi: 10.1016/j.ctrv.2010.02.003
12. Hensle TW, Burbige KA, Shepard BR, Marboe CC, Blanc WA, Wigger JH. Chemotherapy and its Effect on Testicular Morphology in Children. *J Urol* (1984) 131:1142–4. doi: 10.1016/s0022-5347(17)50847-2
13. Huddart RA, Norman A, Moynihan C, Horwich A, Parker C, Nicholls E, et al. Fertility, Gonadal and Sexual Function in Survivors of Testicular Cancer. *Br J Cancer* (2005) 93:200–7. doi: 10.1038/sj.bjc.6602677
14. Ash P. The Influence of Radiation on Fertility in Man. *Br J Radiol* (1980) 53:271–8. doi: 10.1259/0007-1285-53-628-271
15. Shalet SM. Effect of Irradiation Treatment on Gonadal Function in Men Treated for Germ Cell Cancer. *Eur Urol* (1993) 23:148–51. doi: 10.1159/000474584
16. Kinsella TJ, Trivette G, Rowland J, Sorace R, Miller R, Fraass B, et al. Long-Term Follow-Up of Testicular Function Following Radiation Therapy for Early-Stage Hodgkin's Disease. *J Clin Oncol* (1989) 7:718–24. doi: 10.1200/JCO.1989.7.6.718
17. De Rooij DG, Creemers LB, den Ouden K, Izadyar F. Spermatogonial Stem Cell Development. In: FFG Rommerts and KJ Teerds, editors. *Testicular Tangrams, 1st*, vol. 15 . Berlin/Heidelberg, Germany: Springer Press (2002). p. 121–38.
18. Jahnukainen K, Ehmcke J, Hou M, Schlatt S. Testicular Function and Fertility Preservation in Male Cancer Patients. *Best Pract Res Clin Endocrinol Metab* (2011) 25:287–302. doi: 10.1016/j.beem.2010.09.007
19. Delessard M, Saulnier J, Rives A, Dumont L, Rondanino C, Rives N. Exposure to Chemotherapy During Childhood or Adulthood and Consequences on Spermatogenesis Ad Male Fertility. *Int J Mol Sci* (2020) 21:1454. doi: 10.3390/ijms21041454
20. Fayomi AP, Orwig KE. Spermatogonial Stem Cells and Spermatogenesis in Mice, Monkeys and Men. *Stem Cell Res* (2018) 29:207–14. doi: 10.1016/j.scr.2018.04.009
21. Skinner R, Mulder RL, Kremer LC, Hudson MM, Constine LS, Bardi E, et al. Recommendations for Gonadotoxicity Surveillance in Male Childhood, Adolescent, and Young Adult Cancer Survivors: A Report From the International Late Effects of Childhood Cancer Guideline Harmonization Group in Collaboration With the PanCareSurFup Consortium. *Lancet Oncol* (2017) 18:e75–90. doi: 10.1016/S1470-2045(17)30026-8
22. Tian En L, Brougham MFH, Wallace WHB, Mitchell RT. Impacts of Platinum-Based Chemotherapy on Subsequent Testicular Function and Fertility in Boys With Cancer. *Hum Reprod Update* (2020) 26:874–85. doi: 10.1093/humupd/dmaa04
23. Favareto APA, Fernandez CDB, Fossato da Silva DA, Anselmo-Franci JA, De Grava Kempinas W. Persistent Impairment of Testicular Histology and Sperm Motility in Adult Rats Treated With Cisplatin at Peri-Puberty. *Basic Clin Pharmacol Toxicol* (2011) 109:85–96. doi: 10.1111/j.1742-7843.2011.00688.x
24. Shalet SM, Tsatsoulis A, Whitehead E, Read G. Vulnerability of the Human Leydig Cell to Radiation Damage is Dependent Upon Age. *J Endocrinol* (1989) 120:161–5. doi: 10.1677/joe.0.1200161
25. Ridola V, Fawaz O, Aubier F, Bergeron C, de Vathaire F, Pichon F, et al. Testicular Function of Survivors of Childhood Cancer: A Comparative Study Between Ifosfamide- and Cyclophosphamide-Based Regimens. *Eur J Cancer* (2009) 45:814–8. doi: 10.1016/j.ejca.2009.01.002
26. Stukenborg JB, Jahnukainen K, Hutka M, Mitchell RT. Cancer Treatment in Childhood and Testicular Function: The Importance of the Somatic Environment. *Endocr Connect* (2018) 7:R69–87. doi: 10.1530/EC-17-0382
27. Müller J. Impact of Cancer Therapy on the Reproductive Axis. *Horm Res* (2003) 59 Suppl 1:12–20. doi: 10.1159/000067835
28. Hudson MM. Reproductive Outcomes for Survivors of Childhood Cancer. *Obstet Gynecol* (2010) 116:1171–83. doi: 10.1097/AOG.0b013e3181f87c4b
29. Green DM, Liu W, Kutteh WH, Ke RW, Shelton KC, Sklar CA, et al. Cumulative Alkylating Agent Exposure and Semen Parameters in Adult Survivors of Childhood Cancer: A Report From the St Jude Lifetime Cohort Study. *Lancet Oncol* (2014) 15:1215–23. doi: 10.1016/S1470-2045(14)70408-5
30. Green DM, Nolan VG, Goodman PJ, Whitton JA, Srivastava D, Leisenring WM, et al. The Cyclophosphamide Equivalent Dose as an Approach for Quantifying Alkylating Agent Exposure: A Report From the Childhood Cancer Survivor Study. *Pediatr Blood Cancer* (2014) 61:53–67. doi: 10.1002/pbc.24679
31. Meistrich ML, Wilson G, Brown BW, da Cunha MF, Lipshultz LI. Impact of Cyclophosphamide on Long-Term Reduction in Sperm Count in Men Treated With Combination Chemotherapy for Ewing and Soft Tissue Sarcomas. *Cancer* (1992) 70:2703–12. doi: 10.1002/10970142(19921201)70:11<2703::aid-cncr2820701123>3.0.co;2-x
32. Hahn EW, Feingold SM, Simpson L, Batata M. Recovery From Aspermia Induced by Low-Dose Radiation in Seminoma Patients. *Cancer* (1982) 50:337–40. doi: 10.1002/1097-0142(19820715)50:2<337::aid-cncr2820500229>3.0.co;2-6
33. Rowley MJ, Leach DR, Warner GA, Heller CG. Effect of Graded Doses of Ionizing Radiation on the Human Testis. *Radiat Res* (1974) 59:665–78. doi: 10.2307/3574084
34. Centola GM, Keller JW, Henzler M, Rubin P. Effect of Low-Dose Testicular Irradiation on Sperm Count and Fertility in Patients With Testicular Seminoma. *J Androl* (1994) 15:608–13. doi: 10.1002/j.1939-4640.1994.tb00507.x

35. Sklar C. Reproductive Physiology and Treatment-Related Loss of Sex Hormone Production. *Med Pediatr Oncol* (1999) 33:2–8. doi: 10.1002/(sici)1096-911x(199907)33:1<2::aid-mpo2>3.0.co;2-7
36. Izard MA. Leydig Cell Function and Radiation: A Review of the Literature. *Radiother Oncol* (1995) 34:1–8. doi: 10.1016/0167-8140(94)01501-s
37. Gleeson HK, Shalet SM. The Impact of Cancer Therapy on the Endocrine System in Survivors of Childhood Brain Tumours. *Endocr Relat Cancer* (2004) 11:589–602. doi: 10.1677/erc.1.00779
38. Green DM, Kawashima T, Stovall M, Leisenring W, Sklar CA, Mertens AC, et al. Fertility of Male Survivors of Childhood Cancer: A Report From the Childhood Cancer Survivor Study. *J Clin Oncol* (2010) 28:332–9. doi: 10.1200/JCO.2009.24.9037
39. Shetty G, Meistrich ML. Hormonal Approaches to Preservation and Restoration of Male Fertility After Cancer Treatment. *J Natl Cancer Inst Monogr* (2005) 34:36–9. doi: 10.1093/jncimonographs/lgi002
40. Meistrich ML, Kangasniemi M. Hormone Treatment After Irradiation Stimulates Recovery of Rat Spermatogenesis From Surviving Spermatogonia. *J Androl* (1997) 18:80–7. doi: 10.1002/j.1939-4640.1997.tb01879.x
41. Kurdoglu B, Wilson G, Parchuri N, Ye W-S, Meistrich ML. Protection From Radiation-Induced Damage to Spermatogenesis by Hormone Treatment. *Radiat Res* (1994) 139:97 – 102. doi: 10.2307/3578738
42. Waxman JH, Ahmed R, Smith D, Wrigley PF, Gregory W, Shalet S, et al. Failure to Preserve Fertility in Patients With Hodgkin's Disease. *Cancer Chemother Pharmacol* (1987) 19:159–62. doi: 10.1007/BF00254570
43. Redman JR, Bajorunas DR. Suppression of Germ Cell Proliferation to Prevent Gonadal Toxicity Associated With Cancer Treatment. In: *Workshop on Psychosexual and Reproductive Issues Affecting Patients With Cancer*. New York: American Cancer Society (1987). p. 90 – 94.
44. Fosså SD, Klepp O, Norman N. Lack of Gonadal Protection by Medroxyprogesterone Acetate-Induced Transient Medical Castration During Chemotherapy for Testicular Cancer. *Br J Urol* (1988) 62:449–53. doi: 10.1111/j.1464-410x.1988.tb04395.x
45. Kreuser ED, Hetzel WD, Hautmann R, Pfeiffer EF. Reproductive Toxicity With and Without LHRHA Administration During Adjuvant Chemotherapy in Patients With Germ Cell Tumors. *Horm Metab Res* (1990) 22:494–8. doi: 10.1055/s-2007-1004954
46. Masala A, Faedda R, Alagna S, Satta A, Chiarelli G, Rovasio PP, et al. Use of Testosterone to Prevent Cyclophosphamide-Induced Azoospermia. *Ann Intern Med* (1997) 126:292–5. doi: 10.7326/0003-4819-126-4-199702150-00005
47. Shetty G, Mitchell JM, Lam TNA, Phan TT, Zhang J, Tailor RC, et al. Postpubertal Spermatogonial Stem Cell Transplantation Restores Functional Sperm Production in Rhesus Monkeys Irradiated Before and After Puberty. *Andrology* (2021) 9:1603–16. doi: 10.1111/andr.13033
48. Ogawa T, Dobrinski I, Avarbock MR, Brinster RL. Leuprolide, a Gonadotropin-Releasing Hormone Agonist, Enhances Colonization After Spermatogonial Transplantation Into Mouse Testes. *Tissue Cell* (1998) 30:583–8. doi: 10.1016/s0040-8166(98)80039-6
49. Dobrinski I, Ogawa T, Avarbock MR, Brinster RL. Effect of the GnRH-agonist Leuprolide on Colonization of Recipient Testes by Donor Spermatogonial Stem Cells After Transplantation in Mice. *Tissue Cell* (2001) 33:200–7. doi: 10.1054/tice.2001.0177
50. Gubbels Bupp MR, Jorgensen TN. Androgen-Induced Immunosuppression. *Front Immunol* (2018) 9:794. doi: 10.3389/fimmu.2018.00794
51. Suomalainen L, Pentikäinen V, Dunkel L. Sphingosine-1-phosphate Inhibits Nuclear Factor Kappab Activation and Germ Cell Apoptosis in the Human Testis Independently of its Receptors. *Am J Pathol* (2005) 166:773–81. doi: 10.1016/s0002-9440(10)62298-5
52. Carmely A, Meirow D, Peretz A, Albeck M, Bartoov B, Sredni B. Protective Effect of the Immunomodulator AS101 Against Cyclophosphamide-Induced Testicular Damage in Mice. *Hum Reprod* (2009) 24:1322–9. doi: 10.1093/humrep/den481
53. Cao Y, Wang X, Li S, Wang H, Yu L, Wang P. The Effects of L-Carnitine Against Cyclophosphamide-Induced Injuries in Mouse Testis. *Basic Clin Pharmacol Toxicol* (2017) 120:152–8. doi: 10.1111/bcpt.12679
54. Poojary KK, Nayak G, Vasani A, Kumari S, Dcunha R, Kunhiraman JP, et al. Curcumin Nanocrystals Attenuate Cyclophosphamide-Induced Testicular Toxicity in Mice. *Toxicol Appl Pharmacol* (2021) 433:115772. doi: 10.1016/j.taap.2021.115772
55. Nayak G, Rao A, Mullick P, Mutalik S, Kalthur SG, Adiga SK, et al. Ethanolic Extract of Moringa Oleifera Leaves Alleviate Cyclophosphamide-Induced Testicular Toxicity by Improving Endocrine Function and Modulating Cell Specific Gene Expression in Mouse Testis. *J Ethnopharmacol* (2020) 259:112922. doi: 10.1016/j.jep.2020.112922
56. Ghosh D, Das UB, Misro M. Protective Role of Alpha-Tocopherol-Succinate (provitamin-E) in Cyclophosphamide Induced Testicular Gametogenic and Steroidogenic Disorders: A Correlative Approach to Oxidative Stress. *Free Radic Res* (2002) 36:1209–18. doi: 10.1080/1071576021000016472
57. Das UB, Mallick M, Debnath JM, Ghosh D. Protective Effect of Ascorbic Acid on Cyclophosphamide- Induced Testicular Gametogenic and Androgenic Disorders in Male Rats. *Asian J Androl* (2002) 4(3):201–7.
58. Caires K, Broady J, McLean D. Maintaining the Male Germline: Regulation of Spermatogonial Stem Cells. *J Endocrinol* (2010) 205:133–45. doi: 10.1677/JOE-09-0275
59. La HM, Mäkelä JA, Chan AL, Rossello FJ, Nefzger CM, Legrand JMD, et al. Identification of Dynamic Undifferentiated Cell States Within the Male Germline. *Nat Commun* (2018) 9:2819. doi: 10.1038/s41467-018-04827-z
60. Carrieri C, Comazzetto S, Grover A, Morgan M, Buness A, Nerlov C, et al. A Transit-Amplifying Population Underpins the Efficient Regenerative Capacity of the Testis. *J Exp Med* (2017) 214:1631–41. doi: 10.1084/jem.20161371
61. Parker N, Falk H, Singh D, Fidaleo A, Smith B, Lopez MS, et al. Responses to Glial Cell Line-Derived Neurotrophic Factor Change in Mice as Spermatogonial Stem Cells Form Progenitor Spermatogonia Which Replicate and Give Rise to More Differentiated Progeny. *Biol Reprod* (2014) 91:92. doi: 10.1095/biolreprod.114.119099
62. Parker N, Laychur A, Sukwani M, Orwig KE, Oatley JM, Zhang C, et al. Spermatogonial Stem Cell Numbers are Reduced by Transient Inhibition of GDNF Signaling But Restored by Self-Renewing Replication When Signaling Resumes. *Stem Cell Rep* (2021) 16:597–609. doi: 10.1016/j.stemcr.2021.01.015
63. Naughton CK, Jain S, Strickland AM, Gupta A, Milbrandt J. Glial Cell-Line Derived Neurotrophic Factor-Mediated RET Signaling Regulates Spermatogonial Stem Cell Fate. *Biol Reprod* (2006) 74:314–21. doi: 10.1095/biolreprod.105.04736530
64. Jing S, Wen D, Yu Y, Holst PL, Luo Y, Fang M, et al. Gdnf-Induced Activation of the Ret Protein Tyrosine Kinase is Mediated by GDNFR-alpha, a Novel Receptor for GDNF. *Cell* (1996) 85:1113–24. doi: 10.1016/s0092-8674(00)81311-2
65. Sakai M, Masaki K, Aiba S, Tone M, Takashima S. Expression Dynamics of Self-Renewal Factors for Spermatogonial Stem Cells in the Mouse Testis. *J Reprod Dev* (2018) 64:267–75. doi: 10.1262/jrd.2018-015
66. Quintanilha JCF, Saavedra KF, Visacri MB, Moriel P, Salazar LA. Role of Epigenetic Mechanisms in Cisplatin-Induced Toxicity. *Crit Rev Oncol Hematol* (2019) 137:131–42. doi: 10.1016/j.critrevonc.2019.03.00436
67. Hanf A, Oelze M, Manea A, Li H, Münzel T, Daiber A. The Anti-Cancer Drug Doxorubicin Induces Substantial Epigenetic Changes in Cultured Cardiomyocytes. *Chem Biol Interact* (2019) 313:108834. doi: 10.1016/j.cbi.2019.108834
68. Davis CD, Uthus EO. Dna Methylation, Cancer Susceptibility, and Nutrient Interactions. *Exp Biol Med* (2004) 229:988–95. doi: 10.1177/153537020422901002
69. Kläver R, Tüttelmann F, Bleiziffer A, Haaf T, Kliesch S, Gromoll J. Dna Methylation in Spermatozoa a as a Prospective Marker in Andrology. *Andrology* (2013) 1:731–40. doi: 10.1111/j.2047-2927.2013.00118.x
70. Arato I, Ceccarelli V, Mancuso F, Bellucci C, Lilli C, Ferolla P, et al. Effect of EPA on Neonatal Pig Sertoli Cells "*In Vitro*": A Possible Treatment to Help Maintain Fertility in Pre-Pubertal Boys Undergoing Treatment With Gonado-Toxic Therapies. *Front Endocrinol (Lausanne)* (2021) 12:694796. doi: 10.3389/fendo.2021.694796
71. Luca G, Mancuso F, Calvitti M, Arato I, Falabella G, Bufalari A, et al. Long-Term Stability, Functional Competence, and Safety of Microencapsulated Specific Pathogen-Free Neonatal Porcine Sertoli Cells: A Potential Product for Cell Transplant Therapy. *Xenotransplantation* (2015) 22(4):273–83. doi: 10.1111/xen.12175

72. Zequi Sde C, da Costa WH, Santana TB, Favaretto RL, Sacomani CA, Guimaraes GC. Bilateral Testicular Germ Cell Tumours: A Systematic Review. *BJU Int* (2012) 110:1102–9. doi: 10.1111/j.1464-410X.2012.11056.x
73. Zhu L, Chen G, Shen Y, Wang X, Gao L, Zhao Y, et al. Infantile Synchronous Primary Bilateral Testicular Germ Cell Tumor: A Case Report and Review of the Literature. *Transl Androl Urol* (2019) 8:540–7. doi: 10.21037/tau.2019.09.21
74. Heidenreich A, Weissbach L, Höltl W, Albers P, Kliesch S, Köhrmann KU, et al. Organ Sparing Surgery for Malignant Germ Cell Tumor of the Testis. *J Urol* (2001) 166:2161–5. doi: 10.1016/s0022-5347(05)65526-7
75. Suardi N, Strada E, Colombo R, Freschi M, Salonia A, Lania C, et al. Leydig Cell Tumour of the Testis: Presentation, Therapy, Long-Term Follow-Up and the Role of Organ-Sparing Surgery in a Single-Institution Experience. *BJU Int* (2009) 103:197–200. doi: 10.1111/j.1464-410X.2008.08016.x
76. Cheng BS, King LR, Kinney TR. Testicle Transposition in Children Who Undergo Low-Pelvic or Scrotal Irradiation. *Urology* (1987) 1987:39–41.
77. Hussein AA, Tran ND, Smith JF. Fertility Preservation for Boys and Adolescents Facing Sterilizing Medical Therapy. *Transl Androl Urol* (2014) 3:382–90. doi: 10.3978/j.issn.2223-4683.2014.11.06
78. Acosta JM, Tiao G, Stein JE, Mahour GH. Temporary Relocation of Testes to the Anterior Abdominal Wall Before Radiation Therapy of the Pelvis or Perineum. *J Pediatr Surg* (2002) 37:1232–3. doi: 10.1053/jpsu.2002.34488
79. Grüschow K, Kyank U, Stuhldreier G, Fietkau R. Surgical Repositioning of the Contralateral Testicle Before Irradiation of a Paratesticular Rhabdomyosarcoma for Preservation of Hormone Production. *Pediatr Hematol Oncol* (2007) 24:371–7. doi: 10.1080/08880010701394998
80. Allegretti E, Luca G, Arato I, Falabella G, Garolla A, Maffia R, et al. Full Restoration of Spermatogenesis and Male Fertility After Post-Traumatic Ectopic Testis Implant. *Ann Ital Chir* (2014) 85:S2239253X14021860.
81. Arango O, Bielsa O, Lorente JA, De Leon E, Mas AG. Hemiscrotectomy With Contralateral Testicular Transposition for Scrotal Cancer. *J Urol* (2002) 168:1406–7. doi: 10.1097/01.ju.0000026387.51062.26
82. Bahadur G, Spoudeas H, Davies MC, Ralph D. Factors Affecting Sperm Banking for Adolescent Cancer Patients. *Arch Dis Child* (2006) 91:715– 716.
83. Ried HL, Zietz H, Jaffe N. Cryopreservation of Semen From Adolescent Patients With Malignancies. *Med Pediatr Oncol* (1997) 28:322–3. doi: 10.1002/(sici)1096-911x(199704)28:4<322::aid-mpo16>3.0.co;2-e
84. Kamischke A, Jürgens H, Hertle L, Berdel WE, Nieschlag E. Cryopreservation of Sperm From Adolescents and Adults With Malignancies. *J Androl* (2004) 25:586–92. doi: 10.1002/j.1939-4640.2004.tb02829.x
85. Picton HM, Wyns C, Anderson RA, Goossens E, Jahnukainen K, Kliesch S, et al. A European Perspective on Testicular Tissue Cryopreservation for Fertility Preservation in Prepubertal and Adolescent Boys. *Hum Reprod* (2015) 30:2463–75. doi: 10.1093/humrep/dev190
86. Valli-Pulaski H, Peters KA, Gassei K, Steimer SR, Sukhwani M, Hermann BP, et al. Testicular Tissue Cryopreservation: 8 Years of Experience From a Coordinated Network of Academic Centers. *Hum Reprod* (2019) 34:966–77. doi: 10.1093/humrep/dez043
87. Keros V, Hultenby K, Borgström B, Fridström M, Jahnukainen K, Hovatta O. Methods of Cryopreservation of Testicular Tissue With Viable Spermatogonia in Pre-Pubertal Boys Undergoing Gonadotoxic Cancer Treatment. *Hum Reprod* (2007) 22:1384–95. doi: 10.1093/humrep/del508
88. Keros V, Rosenlund B, Hultenby K, Aghajanova L, Levkov L, Hovatta O. Optimizing Cryopreservation of Human Testicular Tissue: Comparison of Protocols With Glycerol, Propanediol and Dimethylsulphoxide as Cryoprotectants. *Hum Reprod* (2005) 20:1676–87. doi: 10.1093/humrep/deh797
89. Curaba M, Poels J, van Langendonckt A, Donnez J, Wyns C. Can Prepubertal Human Testicular Tissue be Cryopreserved by Vitrification. *Fertil Steril* (2011) 95:2123.e9–12. doi: 10.1016/j.fertnstert.2011.01.014
90. Poels J, Van Langendonckt A, Many MC, Wese FX, Wyns C. Vitrification Preserves Proliferation Capacity in Human Spermatogonia. *Hum Reprod* (2013) 28:578–89. doi: 10.1093/humrep/des455
91. Kvist K, Thorup J, Byskov AG, Høyer PE, Møllgård K, Yding Andersen C. Cryopreservation of Intact Testicular Tissue From Boys With Cryptorchidism. *Hum Reprod* (2006) 21:484–91. doi: 10.1093/humrep/dei331
92. Wyns C, Van Langendonckt A, Wese FX, Donnez J, Curaba M. Long-Term Spermatogonial Survival in Cryopreserved and Xenografted Immature Human Testicular Tissue. *Hum Reprod* (2008) 23:2402–14. doi: 10.1093/humrep/den272
93. Goossens E, Jahnukainen K, Mitchell RT, van Pelt A, Pennings G, Rives N, et al. Fertility Preservation in Boys: Recent Developments and New Insights. *Hum Reprod Open* (2020) 2020(3):hoaa016. doi: 10.1093/hropen/hoaa016
94. Li YX, Zhou L, Lv MQ, Ge P, Liu YC, Zhou DX. Vitrification and Conventional Freezing Methods in Sperm Cryopreservation: A Systematic Review and Meta-Analysis. *Eur J Obstet Gynecol Reprod Biol* (2019) 233:84–92. doi: 10.1016/j.ejogrb.2018.11.028
95. Zarandi NP, Galdon G, Kogan S, Atala A, Sadri-Ardekani H. Cryostorage of Immature and Mature Human Testis Tissue to Preserve Spermatogonial Stem Cells (Sscs): A Systematic Review of Current Experiences Toward Clinical Applications. *Stem Cells Cloning* (2018) 11:23–38. doi: 10.2147/SCCAA.S137873
96. Pelzman DL, Orwig KE, Hwang K. Progress in Translational Reproductive Science: Testicular Tissue Transplantation and *In Vitro* Spermatogenesis. *Fertil Steril* (2020) 113:500–9. doi: 10.1016/j.fertnstert.2020.01.038
97. Yango P, Altman E, Smith JF, Klatsky PC, Tran ND. Optimizing Cryopreservation of Human Spermatogonial Stem Cells: Comparing the Effectiveness of Testicular Tissue and Single Cell Suspension Cryopreservation. *Fertil Steril* (2014) 102:1491–1498.e1. doi: 10.1016/j.fertnstert.2014.07.1250
98. Kanbar M, de Michele F, Wyns C. Cryostorage of Testicular Tissue and Retransplantation of Spermatogonial Stem Cells in the Infertile Male. *Best Pract Res Clin Endocrinol Metab* (2019) 33:103–15. doi: 10.1016/j.beem.2018.10.003
99. MacKenna A, Crosby J, Huidobro C, Correa E, Duque G. Semen Quality Before Cryopreservation and After Thawing in 543 Patients With Testicular Cancer. *JBRA Assist Reprod* (2017) 21:31–4. doi: 10.5935/1518-0557.20170009
100. Goossens E, Geens M, De Block G, Tournaye H. Spermatogonial Survival in Long-Term Human Prepubertal Xenografts. *Fertil Steril* (2008) 90:2019–22. doi: 10.1016/j.fertnstert.2007.09.044
101. Hou M, Andersson M, Eksborg S, Söder O, Jahnukainen K. Xenotransplantation of Testicular Tissue Into Nude Mice can be Used for Detecting Leukemic Cell Contamination. *Hum Reprod* (2007) 22:1899–906. doi: 10.1093/humrep/dem085
102. Honaramooz A, Snedaker A, Boiani M, Schöler H, Dobrinski I, Schlatt S. Sperm From Neonatal Mammalian Testes Grafted in Mice. *Nature* (2002) 418:778–81. doi: 10.1038/nature00918
103. Rathi R, Honaramooz A, Zeng W, Turner R, Dobrinski I. Germ Cell Development in Equine Testis Tissue Xenografted Into Mice. *Reproduction* (2006) 131:1091–8. doi: 10.1530/rep.1.01101
104. Snedaker AK, Honaramooz A, Dobrinski I. A Game of Cat and Mouse: Xenografting of Testis Tissue From Domestic Kittens Results in Complete Cat Spermatogenesis in a Mouse Host. *J Androl* (2004) 25:926–30. doi: 10.1002/j.1939-4640.2004.tb03163.x
105. Oatley JM, de Avila DM, Reeves JJ, McLean DJ. Spermatogenesis and Germ Cell Transgene Expression in Xenografted Bovine Testicular Tissue. *Biol Reprod* (2004) 71:494–501. doi: 10.1095/biolreprod.104.027953
106. Honaramooz A, Li MW, Penedo MC, Meyers S, Dobrinski I. Accelerated Maturation of Primate Testis by Xenografting Into Mice. *Biol Reprod* (2004) 70:1500–3. doi: 10.1095/biolreprod.103.025536
107. Abrishami M, Abbasi S, Honaramooz A. The Effect of Donor Age on Progression of Spermatogenesis in Canine Testicular Tissue After Xenografting Into Immunodeficient Mice. *Theriogenology* (2010) 73:512–22. doi: 10.1016/j.theriogenology.2009.09.035
108. Schlatt S, Kim SS, Gosden R. Spermatogenesis and Steroidogenesis in Mouse, Hamster and Monkey Testicular Tissue After Cryopreservation and Heterotopic Grafting to Castrated Hosts. *Reproduction* (2002) 124:339–46. doi: 10.1530/rep.0.1240339
109. Shinohara T, Inoue K, Ogonuki N, Kanatsu-Shinohara M, Miki H, Nakata K, et al. Birth of Offspring Following Transplantation of Cryopreserved Immature Testicular Pieces and *in-Vitro* Microinsemination. *Hum Reprod* (2002) 17:3039–45. doi: 10.1093/humrep/17.12.3039

110. Liu Z, Nie YH, Zhang CC, Cai YJ, Wang Y, Lu HP, et al. Generation of Macaques With Sperm Derived From Juvenile Monkey Testicular Xenografts. *Cell Res* (2016) 26:139–42. doi: 10.1038/cr.2015.112
111. Fayomi AP, Peters K, Sukhwani M, Valli-Pulaski H, Shetty G, Meistrich ML, et al. Autologous Grafting of Cryopreserved Prepubertal Rhesus Testis Produces Sperm and Offspring. *Science* (2019) 363:1314–9. doi: 10.1126/science.aav2914
112. Schlatt S, Honaramooz A, Boiani M, Schöler HR, Dobrinski I. Progeny From Sperm Obtained After Ectopic Grafting of Neonatal Mouse Testes. *Biol Reprod* (2003) 68:2331–5. doi: 10.1095/biolreprod.102.014894
113. Nakai M, Kaneko H, Somfai T, Maedomari N, Ozawa M, Noguchi J, et al. Production of Viable Piglets for the First Time Using Sperm Derived From Ectopic Testicular Xenografts. *Reproduction* (2010) 139:331–5. doi: 10.1530/REP-09-0509
114. Van Saen D, Goossens E, Bourgain C, Ferster A, Tournaye H. Meiotic Activity in Orthotopic Xenografts Derived From Human Postpubertal Testicular Tissue. *Hum Reprod* (2011) 26:282–93. doi: 10.1093/humrep/deq321
115. Ntemou E, Kadam P, Van Saen D, Wistuba J, Mitchell RT, Schlatt S, et al. Complete Spermatogenesis in Intratesticular Testis Tissue Xenotransplants From Immature non-Human Primate. *Hum Reprod* (2019) 34:403–13. doi: 10.1093/humrep/dey373
116. Van Saen D, Goossens E, De Block G, Tournaye H. Regeneration of Spermatogenesis by Grafting Testicular Tissue or Injecting Testicular Cells Into the Testes of Sterile Mice: A Comparative Study. *Fertil Steril* (2009) 91:2264–72. doi: 10.1016/j.fertnstert.2008.02.100
117. Wyns C, Curaba M, Martinez-Madrid B, Van Langendonckt A, François-Xavier W, Donnez J. Spermatogonial Survival After Cryopreservation and Short-Term Orthotopic Immature Human Cryptorchid Testicular Tissue Grafting to Immunodeficient Mice. *Hum Reprod* (2007) 22:1603–11. doi: 10.1093/humrep/dem062
118. Schlatt S, Westernströer B, Gassei K, Ehmcke J. Donor-Host Involvement in Immature Rat Testis Xenografting Into Nude Mouse Hosts. *Biol Reprod* (2010) 82:888–95. doi: 10.1095/biolreprod.109.082073
119. Van Saen D, Goossens E, Haentjens P, Baert Y, Tournaye H. Exogenous Administration of Recombinant Human FSH Does Not Improve Germ Cell Survival in Human Prepubertal Xenografts. *Reprod BioMed Online* (2013) 26:286–98. doi: 10.1016/j.rbmo.2012.11.013
120. Poels J, Abou-Ghannam G, Herman S, Van Langendonckt A, Wese FX, Wyns C. In Search of Better Spermatogonial Preservation by Supplementation of Cryopreserved Human Immature Testicular Tissue Xenografts With N-acetylcysteine and Testosterone. *Front Surg* (2014) 1:47. doi: 10.3389/fsurg.2014.00047
121. Schmidt JA, de Avila JM, McLean DJ. Effect of Vascular Endothelial Growth Factor and Testis Tissue Culture on Spermatogenesis in Bovine Ectopic Testis Tissue Xenografts. *Biol Reprod* (2006) 75:167–75. doi: 10.1095/biolreprod.105.049817
122. Del Vento F, Poels J, Vermeulen M, Ucakar B, Giudice MG, Kanbar M, et al. Accelerated and Improved Vascular Maturity After Transplantation of Testicular Tissue in Hydrogels Supplemented With VEGF- and PDGF-Loaded Nanoparticles. *Int J Mol Sci* (2021) 22:5779. doi: 10.3390/ijms22115779
123. Caires KC, de Avila J, McLean DJ. Vascular Endothelial Growth Factor Regulates Germ Cell Survival During Establishment of Spermatogenesis in the Bovine Testis. *Reproduction* (2009) 138:667–77. doi: 10.1530/REP-09-0020
124. Ntemou E, Kadam P, Van Laere S, Van Saen D, Vicini E, Goossens E. Effect of Recombinant Human Vascular Endothelial Growth Factor on Testis Tissue Xenotransplants From Prepubertal Boys: A Three-Case Study. *Reprod BioMed Online* (2019) 39:119–33. doi: 10.1016/j.rbmo.2019.02.012
125. Del Vento F, Vermeulen M, Ucakar B, Poels J, des Rieux A, Wyns C. Significant Benefits of Nanoparticles Containing a Necrosis Inhibitor on Mice Testicular Tissue Autografts Outcomes. *Int J Mol Sci* (2019) 20:E5833. doi: 10.3390/ijms20235833
126. Luetjens CM, Stukenborg JB, Nieschlag E, Simoni M, Wistuba J. Complete Spermatogenesis in Orthotopic But Not in Ectopic Transplants of Autologously Grafted Marmoset Testicular Tissue. *Endocrinology* (2008) 149:1736–47. doi: 10.1210/en.2007-1325
127. Jahnukainen K, Ehmcke J, Nurmio M, Schlatt S. Autologous Ectopic Grafting of Cryopreserved Testicular Tissue Preserves the Fertility of Prepubescent Monkeys That Receive Sterilizing Cytotoxic Therapy. *Cancer Res* (2012) 72:5174–8. doi: 10.1158/0008-5472.CAN-12-1317
128. Poels J, Abou-Ghannam G, Decamps A, Leyman M, Ad R, Wyns C. Transplantation of Testicular Tissue in Alginate Hydrogel Loaded With VEGF Nanoparticles Improves Spermatogonial Recovery. *J Control Release* (2016) 234:79–89. doi: 10.1016/j.jconrel.2016.05.037
129. Dovey SL, Valli H, Hermann BP, Sukhwani M, Donohue J, Castro CA, et al. Eliminating Malignant Contamination From Therapeutic Human Spermatogonial Stem Cells. *J Clin Invest* (2013) 123:1833–43. doi: 10.1172/JCI65822
130. Fujita K, Ohta H, Tsujimura A, Takao T, Miyagawa Y, Takada S, et al. Transplantation of Spermatogonial Stem Cells Isolated From Leukemic Mice Restores Fertility Without Inducing Leukemia. *J Clin Invest* (2005) 115:1855–61. doi: 10.1172/JCI24189
131. Geens M, Van de Velde H, De Block G, Goossens E, Van Steirteghem A, Tournaye H. The Efficiency of Magnetic-Activated Cell Sorting and Fluorescence-Activated Cell Sorting in the Decontamination of Testicular Cell Suspensions in Cancer Patients. *Hum Reprod* (2007) 22:733–42. doi: 10.1093/humrep/del418
132. Hermann BP, Sukhwani M, Salati J, Sheng Y, Chu T, Orwig KE. Separating Spermatogonia From Cancer Cells in Contaminated Prepubertal Primate Testis Cell Suspensions. *Hum Reprod* (2011) 26:3222–31. doi: 10.1093/humrep/der343
133. Steinberger A, Steinberger E. Perloff Wh. Mammalian Testes in Organ Culture. *Exp Cell Res* (1964) 36:19–27. doi: 10.1016/0014-4827(64)90156-9
134. Tesarik J, Bahceci M, Ozcan C, Greco E, Mendoza C. Restoration of Fertility by *in-Vitro* Spermatogenesis. *Lancet* (1999) 353:555–6. doi: 10.1016/S0140-6736(98)04784-9
135. Oliver E, Stukenborg JB. Rebuilding the Human Testis *In Vitro*. *Andrology* (2020) 8:825–34. doi: 10.1111/andr.12710
136. Sato T, Katagiri K, Yokonishi T, Kubota Y, Inoue K, Ogonuki N, et al. *In Vitro* Production of Fertile Sperm From Murine Spermatogonial Stem Cell Lines. *Nat Commun* (2011) 2:472. doi: 10.1038/ncomms1478
137. Sato T, Katagiri K, Kubota Y, Ogawa T. *In Vitro* Sperm Production From Mouse Spermatogonial Stem Cell Lines Using an Organ Culture Method. *Nat Protoc* (2013) 8:2098–104. doi: 10.1038/nprot.2013.138
138. Yokonishi T, Sato T, Komeya M, Katagiri K, Kubota Y, Nakabayashi K, et al. Offspring Production With Sperm Grown *In Vitro* From Cryopreserved Testis Tissues. *Nat Commun* (2014) 5:4320. doi: 10.1038/ncomms5320
139. Oblette A, Rives N, Dumont L, Rives A, Verhaeghe F, Jumeau F, et al. Assessment of Sperm Nuclear Quality After *In Vitro* Maturation of Fresh or Frozen/Thawed Mouse Pre-Pubertal Testes. *Mol Hum Reprod* (2017) 23:674–84. doi: 10.1093/molehr/gax048
140. Kim KJ, Kim BG, Kim YH. *Et al. In Vitro* Spermatogenesis Using Bovine Testis Tissue Culture Techniques. *Tissue Eng Regener Med* (2015) 12:314–23. doi: 10.1007/s13770-015-0045-z
141. Liu F, Cai C, Wu X, Cheng Y, Lin T, Wei G, et al. Effect of KnockOut Serum Replacement on Germ Cell Development of Immature Testis Tissue Culture. *Theriogenology* (2016) 85:193–9. doi: 10.1016/j.theriogenology.2015.09.012
142. Medrano JV, Vilanova-Pérez T, Fornés-Ferrer V, Navarro-Gomezlechon A, Martínez-Triguero ML, García S, et al. Influence of Temperature, Serum, and Gonadotropin Supplementation in Short- and Long-Term Organotypic Culture of Human Immature Testicular Tissue. *Fertil Steril* (2018) 110:1045–1057.e3. doi: 10.1016/j.fertnstert.2018.07.018
143. de Michele F, Poels J, Vermeulen M, Ambroise J, Gruson D, Guiot Y, et al. Haploid Germ Cells Generated in Organotypic Culture of Testicular Tissue From Prepubertal Boys. *Front Physiol* (2018) 9:1413. doi: 10.3389/fphys.2018.01413
144. Abofoul-Azab M, AbuMadighem A, Lunenfeld E, Kapelushnik J, Shi Q, Pinkas H, et al. Development of Postmeiotic Cells *In Vitro* From Spermatogonial Cells of Prepubertal Cancer Patients. *Stem Cells Dev* (2018) 27:1007–20. doi: 10.1089/scd.2017.0301
145. Yang S, Ping P, Ma M, Li P, Tian R, Yang H, et al. Generation of Haploid Spermatids With Fertilization and Development Capacity From Human Spermatogonial Stem Cells of Cryptorchid Patients. *Stem Cell Rep* (2014) 3:663–75. doi: 10.1016/j.stemcr.2014.08.004

146. Stukenborg JB, Wistuba J, Luetjens CM, Elhija MA, Huleihel M, Lunenfeld E, et al. Coculture of Spermatogonia With Somatic Cells in a Novel Three-Dimensional Soft-Agar-Culture-System. *J Androl* (2008) 29:312–29. doi: 10.2164/jandrol.107.002857
147. de Michele F, Poels J, Giudice MG, De Smedt F, Ambroise J, Vermeulen M, et al. *In Vitro* Formation of the Blood-Testis Barrier During Long-Term Organotypic Culture of Human Prepubertal Tissue: Comparison With a Large Cohort of Pre/Peripubertal Boys. *Mol Hum Reprod* (2018) 24:271–82. doi: 10.1093/molehr/gay012
148. Brinster RL, Zimmermann JW. Spermatogenesis Following Male Germ-Cell Transplantation. *Proc Natl Acad Sci USA* (1994) 91:11298–302. doi: 10.1073/pnas.91.24.11298
149. Dobrinski I, Ogawa T, Avarbock MR, Brinster RL. Computer Assisted Image Analysis to Assess Colonization of Recipient Seminiferous Tubules by Spermatogonial Stem Cells From Transgenic Donor Mice. *Mol Reprod Dev* (1999) 53:142–8. doi: 10.1002/(SICI)1098-2795(199906)53:2<142::AID-MRD3>3.0.CO;2-O
150. Kerr CL, Shamblott MJ, Gearhart JD. Pluripotent Stem Cells From Germ Cells. *Methods Enzymol* (2006) 419:400–26. doi: 10.1016/S0076-6879(06)19016-3
151. Kanatsu-Shinohara M, Ogonuki N, Inoue K, Miki H, Ogura A, Toyokuni S, et al. Long-Term Proliferation in Culture and Germline Transmission of Mouse Male Germline Stem Cells. *Biol Reprod* (2003) 69:612–6. doi: 10.1095/biolreprod.103.017012
152. Maki CB, Pacchiarotti J, Ramos T, Pascual M, Pham J, Kinjo J, et al. Phenotypic and Molecular Characterization of Spermatogonial Stem Cells in Adult Primate Testes. *Hum Reprod* (2009) 24:1480–91. doi: 10.1093/humrep/dep033
153. Kossack N, Meneses J, Shefi S, Nguyen HN, Chavez S, Nicholas C, et al. Isolation and Characterization of Pluripotent Human Spermatogonial Stem Cell-Derived Cells. *Stem Cells* (2009) 27:138–49. doi: 10.1634/stemcells.2008-0439
154. Yang Y, Yarahmadi M, Honaramooz A. Development of Novel Strategies for the Isolation of Piglet Testis Cells With a High Proportion of Gonocytes. *Reprod Fertil Dev* (2010) 22:1057–65. doi: 10.1071/RD09316
155. He Z, Kokkinaki M, Jiang J, Dobrinski I, Dym M. Isolation, Characterization, and Culture of Human Spermatogonia. *Biol Reprod* (2010) 82:363–72. doi: 10.1095/biolreprod.109.078550
156. Zheng Y, Thomas A, Schmidt CM, Dann CT. Quantitative Detection of Human Spermatogonia for Optimization of Spermatogonial Stem Cell Culture. *Hum Reprod* (2014) 29:2497–511. doi: 10.1093/humrep/deu232
157. Guo J, Grow EJ, Mlcochova H, Maher GJ, Lindskog C, Nie X, et al. The Adult Human Testis Transcriptional Cell Atlas. *Cell Res* (2018) 28:1141–57. doi: 10.1038/s41422-018-0099-2
158. Kokkinaki M, Djourabtchi A, Golestaneh N. Long-Term Culture of Human Ssea-4 Positive Spermatogonial Stem Cells (Sscs). *J Stem Cell Res Ther* (2011) 2:2488. doi: 10.4172/2157-7633.S2-003
159. Shami AN, Zheng X, Munyoki SK, Ma Q, Manske GL, Green CD, et al. Single-Cell RNA Sequencing of Human, Macaque, and Mouse Testes Uncovers Conserved and Divergent Features of Mammalian Spermatogenesis. *Dev Cell* (2020) 54:529–547.e12. doi: 10.1016/j.devcel.2020.05.010
160. Kubota H, Avarbock MR, Brinster RL. Growth Factors Essential for Self-Renewal and Expansion of Mouse Spermatogonial Stem Cells. *Proc Natl Acad Sci USA* (2004) 101:16489–94. doi: 10.1073/pnas.0407063101
161. Meng X, Lindahl M, Hyvönen ME, Parvinen M, de Rooij DG, Hess MW, et al. Regulation of Cell Fate Decision of Undifferentiated Spermatogonia by GDNF. *Science* (2000) 287:1489–93. doi: 10.1126/science.287.5457.1489
162. Huang YH, Chin CC, Ho HN, Chou CK, Shen CN, Kuo HC, et al. Pluripotency of Mouse Spermatogonial Stem Cells Maintained by IGF-1-Dependent Pathway. *FASEB J* (2009) 23:2076–87. doi: 10.1096/fj.08-121939
163. Oatley JM, Oatley MJ, Avarbock MR, Tobias JW, Brinster RL. Colony Stimulating Factor 1 is an Extrinsic Stimulator of Mouse Spermatogonial Stem Cell Self-Renewal. *Development* (2009) 136:1191–9. doi: 10.1242/dev.032243
164. Ryu BY, Kubota H, Avarbock MR, Brinster RL. Conservation of Spermatogonial Stem Cell Self-Renewal Signaling Between Mouse and Rat. *Proc Natl Acad Sci USA* (2005) 102:14302–7. doi: 10.1073/pnas.0506970102
165. Hamra FK, Chapman KM, Nguyen DM, Williams-Stephens AA, Hammer RE, Garbers DL. Self Renewal, Expansion, and Transfection of Rat Spermatogonial Stem Cells in Culture. *Proc Natl Acad Sci USA* (2005) 102:17430–5. doi: 10.1073/pnas.0508780102
166. Zhang P, Chen X, Zheng Y, Zhu J, Qin Y, Lv Y, et al. Long-Term Propagation of Porcine Undifferentiated Spermatogonia. *Stem Cells Dev* (2017) 26:1121–31. doi: 10.1089/scd.2017.0018
167. Aponte PM, Soda T, Teerds KJ, Mizrak SC, van de Kant HJ, de Rooij DG. Propagation of Bovine Spermatogonial Stem Cells *In Vitro*. *Reproduction* (2008) 136:543–57. doi: 10.1530/REP-07-0419
168. Li CH, Yan LZ, Ban WZ, Tu Q, Wu Y, Wang L, et al. Long-Term Propagation of Tree Shrew Spermatogonial Stem Cells in Culture and Successful Generation of Transgenic Offspring. *Cell Res* (2017) 27:241–52. doi: 10.1038/cr.2016.156
169. Dong L, Kristensen SG, Hildorf S, Gul M, Clasen-Linde E, Fedder J, et al. Propagation of Spermatogonial Stem Cell-Like Cells From Infant Boys. *Front Physiol* (2019) 10:1155. doi: 10.3389/fphys.2019.01155
170. Sadri-Ardekani H, Akhondi MA, van der Veen F, Repping S, van Pelt AM. *In Vitro* Propagation of Human Prepubertal Spermatogonial Stem Cells. *JAMA* (2011) 305:2416–8. doi: 10.1001/jama.2011.791
171. Sadri-Ardekani H, Mizrak SC, van Daalen SK, Korver CM, Roepers-Gajadien HL, Koruji M, et al. Propagation of Human Spermatogonial Stem Cells *In Vitro*. *JAMA* (2009) 302:2127–34. doi: 10.1001/jama.2009.1689
172. Lim JJ, Sung SY, Kim HJ, Song SH, Hong JY, Yoon TK, et al. Long-Term Proliferation and Characterization of Human Spermatogonial Stem Cells Obtained From Obstructive and non-Obstructive Azoospermia Under Exogenous Feeder-Free Culture Conditions. *Cell Prolif* (2010) 43:405–17. doi: 10.1111/j.1365-2184.2010.00691.x
173. Tan K, Song HW, Thompson M, Munyoki S, Sukhwani M, Hsieh TC, et al. Transcriptome Profiling Reveals Signaling Conditions Dictating Human Spermatogonia Fate *In Vitro*. *Proc Natl Acad Sci USA* (2020) 117:17832–41. doi: 10.1073/pnas.2000362117
174. Kim TH, Hargreaves HK, Brynes RK, Hawkins HK, Lui VK, Woodard J, et al. Pretreatment Testicular Biopsy in Childhood Acute Lymphocytic Leukaemia. *Lancet* (1981) 2:657–8. doi: 10.1016/s0140-6736(81)90996-x
175. Jahnukainen K, Hou M, Petersen C, Setchell B, Söder O. Intratesticular Transplantation of Testicular Cells From Leukemic Rats Causes Transmission of Leukemia. *Cancer Res* (2001) 61:706–10.
176. Sadri-Ardekani H, Homburg CH, van Capel TM, van den Berg H, van der Veen F, van der Schoot CE, et al. Eliminating Acute Lymphoblastic Leukemia Cells From Human Testicular Cell Cultures: A Pilot Study. *Fertil Steril* (2014) 101:1072–1078.e1. doi: 10.1016/j.fertnstert.2014.01.014
177. Geens M, Goossens E, Tournaye H. Cell Selection by Selective Matrix Adhesion is Not Sufficiently Efficient for Complete Malignant Cell Depletion From Contaminated Human Testicular Cell Suspensions. *Fertil Steril* (2011) 95:787–91. doi: 10.1016/j.fertnstert.2010.09.054
178. Schlatt S, Rosiepen G, Weinbauer GF, Rolf C, Brook PF, Nieschlag E. Germ Cell Transfer Into Rat, Bovine, Monkey and Human Testes. *Hum Reprod* (1999) 14:144–50. doi: 10.1093/humrep/14.1.144
179. Ning L, Meng J, Goossens E, Lahoutte T, Marichal M, Tournaye H. In Search of an Efficient Injection Technique for Future Clinical Application of Into Rhesus Testes: Infusion of Contrast Dyes in Isolated Cadaveric Human Testes. *Fertil Steril* (2012) 98:1443–8.e1. doi: 10.1016/j.fertnstert.2012.08.023
180. Faes K, Lahoutte T, Hoorens A, Tournaye H, Goossens E. In Search of an Improved Injection Technique for the Clinical Application of Spermatogonial Stem Cell Transplantation. *Reprod BioMed Online* (2017) 34:291–7. doi: 10.1016/j.rbmo.2016.12.007
181. Faes K, Tournaye H, Goethals L, Lahoutte T, Hoorens A, Goossens E. Testicular Cell Transplantation Into the Human Testes. *Fertil Steril* (2013) 100:981–8. doi: 10.1016/j.fertnstert.2013.06.016
182. Herrid M, Olejnik J, Jackson M, Suchowerska N, Stockwell S, Davey R, et al. Irradiation Enhances the Efficiency of Testicular Germ Cell Transplantation in Sheep. *Biol Reprod* (2009) 81:898–905. doi: 10.1095/biolreprod.109.078279
183. Honaramooz A, Behboodi E, Megee SO, Overton SA, Galantino-Homer H, Echelard Y, et al. Fertility and Germline Transmission of Donor Haplotype Following Germ Cell Transplantation in Immunocompetent Goats. *Biol Reprod* (2003) 69:1260–4. doi: 10.1095/biolreprod.103.018788

184. Hermann BP, Sukhwani M, Winkler F, Pascarella JN, Peters KA, Sheng Y, et al. Spermatogonial Stem Cell Transplantation Into Rhesus Testes Regenerates Spermatogenesis Producing Functional Sperm. *Cell Stem Cell* (2012) 11:715–26. doi: 10.1016/j.stem.2012.07.017
185. Radford J. Fertility After Treatment for Cancer. *BMJ* (1999) 319:9. doi: 10.1136/bmj.319.7215.935
186. Radford J. Restoration of Fertility After Treatment for Cancer. *Horm Res* (2003) 59 Suppl 1:21–3. doi: 10.1159/000067840
187. Goossens E, De Rycke M, Haentjens P, Tournaye H. DNA Methylation Patterns of Spermatozoa and Two Generations of Offspring Obtained After Murine Spermatogonial Stem Cell Transplantation. *Hum Reprod* (2009) 24:2255–63. doi: 10.1093/humrep/dep213
188. Goossens E, Van Saen D, Tournaye H. Spermatogonial Stem Cell Preservation and Transplantation: From Research to Clinic. *Hum Reprod* (2013) 28:897–907. doi: 10.1093/humrep/det039
189. Goossens E, de Vos P, Tournaye H. Array Comparative Genomic Hybridization Analysis Does Not Show Genetic Alterations in Spermatozoa and Offspring Generated After Spermatogonial Stem Cell Transplantation in the Mouse. *Hum Reprod* (2010) 25:1836–42. doi: 10.1093/humrep/deq108
190. Stukenborg JB, Schlatt S, Simoni M, Yeung CH, Elhija MA, Luetjens CM, et al. New Horizons for *In Vitro* Spermatogenesis? An Update on Novel Three-Dimensional Culture Systems as Tools for Meiotic and Post-Meiotic Differentiation of Testicular Germ Cells. *Mol Hum Reprod* (2009) 15:521–9. doi: 10.1093/molehr/gap052
191. Komeya M, Hayashi K, Nakamura H, Yamanaka H, Sanjo H, Kojima K, et al. Pumpless Microfluidic System Driven by Hydrostatic Pressure Induces and Maintains Mouse Spermatogenesis In Vitro. *Sci Rep* (2017) 7:15459. doi: 10.1038/s41598-017-15799-3
192. Alves-Lopes JP, Stukenborg JB. Testicular Organoids: A New Model to Study the Testicular Microenvironment *In Vitro*. *Hum Reprod Update* (2018) 24:176–91. doi: 10.1093/humupd/dmx036
193. Brown BN, Badylak SF. Extracellular Matrix as an Inductive Scaffold for Functional Tissue Reconstruction. *Transl Res* (2014) 163:268–85. doi: 10.1016/j.trsl.2013.11.003
194. Edmonds ME, Forshee MD, Woodruff TK. Extra Cellular Matrix-Based and Extra Cellular Matrix-Free Generation of Murine Testicular Organoids. *J Vis Exp* (2020) (164):e61403. doi: 10.3791/61403
195. Sakib S, Yu Y, Voigt A, Ungrin M, Dobrinski I. Generation of Porcine Testicular Organoids With Testis Specific Architecture Using Microwell Culture. *J Vis Exp* (2019) (152):e60387. doi: 10.3791/60387
196. Bashiri Z, Amiri I, Gholipourmalekabadi M, Falak R, Asgari H, Maki CB, et al. Artificial Testis: A Testicular Tissue Extracellular Matrix as a Potential Bio-Ink for 3D Printing. *Biomater Sci* (2021) 9:3465–84. doi: 10.1039/d0bm02209h
197. Baert Y, Rombaut C, Goossens E. Scaffold-Based and Scaffold-Free Testicular Organoids From Primary Human Testicular Cells. *Methods Mol Biol* (2019) 1576:283–90. doi: 10.1007/7651_2017_48
198. Dobrinski I. *De Novo* Morphogenesis of Functional Testis Tissue After Ectopic Transplantation of Isolated Cells. *Organogenesis* (2007) 3:79–82. doi: 10.4161/org.3.2.4944
199. Gassei K, Schlatt S, Ehmcke J. *De Novo* Morphogenesis of Seminiferous Tubules From Dissociated Immature Rat Testicular Cells in Xenografts. *J Androl* (2006) 27:611–8. doi: 10.2164/jandrol.05207
200. Kita K, Watanabe T, Ohsaka K, Hayashi H, Kubota Y, Nagashima Y, et al. Production of Functional Spermatids From Mouse Germline Stem Cells in Ectopically Reconstituted Seminiferous Tubules. *Biol Reprod* (2007) 76:211–7. doi: 10.1095/biolreprod.106.056895
201. Kawasaki T, Saito K, Shinya M, Olsen LC, Sakai N. Regeneration of Spermatogenesis and Production of Functional Sperm by Grafting of Testicular Cell Aggregates in Zebrafish (Danio Rerio). *Biol Reprod* (2010) 83:533–9. doi: 10.1095/biolreprod.110.085159
202. Arregui L, Rathi R, Megee SO, Honaramooz A, Gomendio M, Roldan ER, et al. Xenografting of Sheep Testis Tissue and Isolated Cells as a Model for Preservation of Genetic Material From Endangered Ungulates. *Reproduction* (2008) 136:85–93. doi: 10.1530/REP-07-0433
203. Zhang Z, Hill J, Holland M, Kurihara Y, Loveland KL. Bovine Sertoli Cells Colonize and Form Tubules in Murine Hosts Following Transplantation and Grafting Procedures. *J Androl* (2008) 29:418–30. doi: 10.2164/jandrol.107.004465
204. Honaramooz A, Megee SO, Rathi R, Dobrinski I. Building a Testis: Formation of Functional Testis Tissue After Transplantation of Isolated Porcine (Sus Scrofa) Testis Cells. *Biol Reprod* (2007) 76:43–7. doi: 10.1095/biolreprod.106.054999
205. Dores C, Dobrinski I. *De Novo* Morphogenesis of Testis Tissue: An Improved Bioassay to Investigate the Role of VEGF165 During Testis Formation. *Reproduction* (2014) 148:109–17. doi: 10.1530/REP-13-0303
206. Gassei K, Orwig KE. Experimental Methods to Preserve Male Fertility and Treat Male Factor Infertility. *Fertil Steril* (2016) 105:256–66. doi: 10.1016/j.fertnstert.2015.12.020
207. Shetty G, Mitchell JM, Lam TNA, Wu Z, Zhang J, Hill L, et al. Donor Spermatogenesis in *De Novo* Formed Seminiferous Tubules From Transplanted Testicular Cells in Rhesus Monkey Testis. *Hum Reprod* (2018) 33:2249–55. doi: 10.1093/humrep/dey316

Conflict of Interest: The authors declare that the research was conducted in the absence of any commercial or financial relationships that could be construed as a potential conflict of interest.

Publisher's Note: All claims expressed in this article are solely those of the authors and do not necessarily represent those of their affiliated organizations, or those of the publisher, the editors and the reviewers. Any product that may be evaluated in this article, or claim that may be made by its manufacturer, is not guaranteed or endorsed by the publisher.

frontiers | Frontiers in Endocrinology

MINI REVIEW
published: 17 June 2022
doi: 10.3389/fendo.2022.911079

Activation *Versus* Inhibition of IGF1R: A Dual Role in Breast Tumorigenesis

Joseph J. Bulatowicz and Teresa L. Wood *

Department of Pharmacology, Physiology, & Neuroscience, Center for Cell Signaling and Cancer Institute of New Jersey, Rutgers Biomedical and Health Sciences, Newark, NJ, United States

Historically, the body of literature surrounding the insulin-like growth factor type 1 receptor (IGF1R) has described a largely pro-tumorigenic role in breast cancer cells and in several transgenic or xenograft mouse models of breast cancer. Interestingly, however, more recent evidence has emerged that suggests an additional, previously undescribed, tumor and metastasis suppressive function for IGF1R in both human breast tumors and mammary oncogenesis in mice. These seemingly conflicting reports can be reconciled when considering what is currently known about IGF1R function in the context of tissue development and cancer as it relates to cellular growth, proliferation, and differentiation. In this mini review, we will summarize the currently existing data with a particular focus on mouse models that have been developed to study IGF1R function in mammary development, tumorigenesis, and metastasis *in vivo* and propose hypotheses for how both the tumor-promoting and tumor-suppressing schools of thought regarding IGF1R in these histological contexts are compatible.

Keywords: IGF1R, breast cancer, mammary gland, development, metastasis, differentiation

OPEN ACCESS

Edited by:
Claire Perks,
University of Bristol, United Kingdom

Reviewed by:
Fumihiko Hakuno,
The University of Tokyo, Japan
Briony Forbes,
Flinders University, Australia

***Correspondence:**
Teresa L. Wood
terri.wood@rutgers.edu

Specialty section:
This article was submitted to Cancer Endocrinology, a section of the journal Frontiers in Endocrinology

Received: *01 April 2022*
Accepted: *11 May 2022*
Published: *17 June 2022*

Citation:
Bulatowicz JJ and Wood TL (2022) Activation Versus Inhibition of IGF1R: A Dual Role in Breast Tumorigenesis. Front. Endocrinol. 13:911079. doi: 10.3389/fendo.2022.911079

INTRODUCTION

The critical functions of the insulin-like growth factor (IGF)/IGF type 1 receptor (IGF1R) signaling axis in normal biological development (both systemic and tissue specific) have been extensively studied in several genetically altered mouse models. *In vivo* systemic deletion of IGF ligands or their receptors has resulted in related, but distinct, phenotypes exhibiting varying degrees of developmental impairment and/or lethality (1, 2). Perinatal lethality following systemic deletion of *Igf1r* necessitated the need for subsequent transplantation assays in order to define the role of the receptor in the mammary gland (3). Work performed with these models laid the foundation for the field's current understanding of the importance of IGF1R function during embryogenesis and development of the mammary gland during puberty.

In addition to earlier studies focused on IGF1R developmental functions, more recent mouse models have been developed to investigate the receptor's role in primary tumorigenesis. Consistent with the status of IGF1R as a receptor tyrosine kinase and its vigorously established function in promoting cell proliferation and survival, it was identified as a promising target for therapeutic intervention in human cancer patients. This led to the initiation of a number of clinical trials to disrupt IGF1R function in human tumors utilizing monoclonal antibody or small-molecule tyrosine kinase inhibitor-based therapies. Unfortunately, while early results were promising, the eventual

conclusion from these trials was less than encouraging and, in some instances, led to worse outcomes denoted by systemic toxicity or worse patient prognosis [for reviews, see (4–7)].

In this mini review, we summarize the phenotypes of existing mouse models of modified IGF1R expression in mammary tissue (**Table 1**) and discuss observations made using human breast cancer data. We then attempt to reconcile these observations in order to shed light on the seemingly contradictory roles for IGF1R in breast cancer with a focus on mammary gland biology and tumorigenesis.

IGF1R IN MOUSE MAMMARY GLAND DEVELOPMENT

A number of techniques and mouse models (**Table 1**) have been developed to study the role of IGF1R in mammary gland development. Due to the immediate postnatal lethal phenotype exhibited by *Igf1r*$^{-/-}$ animals, alternative approaches were necessitated to study how loss of *Igf1r* influences mammary gland development (1). To bypass this technical limitation, pioneering experiments by Bonnette and Hadsell utilized tissue transplantation of mammary buds from *Igf1r*$^{-/-}$ embryos into host mice with mammary fat pads cleared of endogenous epithelium to examine epithelial growth during both puberty and pregnancy (3). Eight weeks post-transplantation, the *Igf1r*$^{-/-}$ transplanted animals had a significant decrease in the number of developed glands, as well as macroscopic abnormalities in ductal branching and terminal end bud (TEB) growth. Despite normal cellular organization of the ducts and TEBs in these animals, BrdU and TUNEL staining of 4-week post-transplantation mammary outgrowths revealed a significant decrease in proliferation and no evidence of cell death in TEB cells, specifically in the cap cell layer, which is responsible for most ductal outgrowth during puberty and harbors stem/progenitor populations necessary for formation of the ductal tree. This phenotype is strikingly similar to the developmental phenotype in the *Igf1* knockout mouse, where the number of TEBs and ductal expansion through the mammary fat pad was dramatically reduced, independently validating these observations (14). In contrast, mice with a heterozygous knockout of *Igf* had defects in alveogenesis during pregnancy, however, the lumens of preexisting alveoli were occluded with clusters of hyperproliferative epithelial cells (15). The phenotype observed in the *Igf1r*$^{-/-}$ transplantation model was partially rescued during pregnancy, where the pregnant *Igf1r*$^{-/-}$ transplanted animals exhibited a larger, hormone-induced fat pad outgrowth than wildtype transplanted mice relative to their virgin counterparts (3). This finding may be a result of a hypothetical decrease in dependence on IGF signaling and an increase in progesterone and prolactin signaling that takes place during the early stages of pregnancy and drives cellular proliferation and differentiation to fill the fat pad in preparation for lactogenesis (16, 17). Another potential explanation could be compensatory insulin receptor (INSR) signaling in the absence of *Igf1r* expression, supported by the observations that INSR substrates 1 and 2 undergo significant hormone-mediated changes during pregnancy (18).

To further define how IGF1R signaling influences mammary gland development during pregnancy, Sun *et al.* developed a model denoted as WAP-*dnIGF1R* (8). In this mouse model, the whey acid protein (WAP) promoter controls expression of a dominant-negative human IGF1R that is activated during mid-pregnancy at the onset of lactogenesis. These mice exhibited decreased alveolar outgrowth accompanied by a decrease in proliferation and no change in apoptosis (similar to the *Igf1r*$^{-/-}$ transplantation studies) suggesting the absence of required growth signals, i.e. IGF1 and IGF2 acting through the IGF1R. Additionally, these glands had alveolar differentiation as well as myoepithelial defects including a less elongated cellular morphology and a decrease in myoepithelial cell number as determined by reduced keratin (*Krt)14* expression (8). Consistent with these *in vivo* observations indicating that IGF1/

TABLE 1 | Summary of the mouse models used to study the function of IGF1R in development and tumorigenesis.

Models of IGF1R Function in the Mammary Gland					
Genotype	**Biological Context**	**IGF1R Status**	**Phenotype**	**Effect on Tumor Phenotype**	**Reference**
Igf1r$^{-/-}$ systemic KO	Development	Deleted	Embryonic lethal, 45% normal birthweight, delayed bone/skin development	N/A	(1)
Igf1r$^{+/+}$, *Igf1r*$^{+/-}$, *Igf1r*$^{-/-}$ transplantation	Development	Deleted	Limited branch outgrowth and TEB formation during puberty	N/A	(3)
WAP-*dnIGF1R*	Pregnancy	Inhibited; mutated receptor	Decreased branching outgrowth, delayed alveolar density/ differentiation during pregnancy	N/A	(8)
MMTV-*dnIGF1R*	Development	Inhibited; mutated receptor	Decreased post-pubertal branching, increased luminal progenitor and basal populations	N/A	(9)
MMTV-*CD8α-IGF1R*	Tumorigenesis	Constitutively activated	Induced tumorigenesis, increased luminal progenitor population	Promoting	(10)
MTB-*IGF1R*	Tumorigenesis	Overexpressed	Induced tumorigenesis	Promoting	(11)
Eef1a1-*Kras**/WAP-*Cre*/ *Igf1r*$^{fl/fl}$	Tumorigenesis	Deleted	Increased tumor latency	Promoting	(12)
MMTV-*Wnt1*/*dnIGF1R*	Tumorigenesis	Inhibited; mutated receptor	Increased luminal progenitor and basal populations, decreased latency, increased metastasis	Suppressing	(9)
MMTV-*Wnt1*/K8-*CreER*^{T}/ *Igf1r*$^{fl/fl}$	Tumorigenesis	Deleted	Increased luminal progenitor and basal populations, decreased latency, increased metastasis	Suppressing	(13)

N/A, Not Applicable.

IGF1R signaling functions in mammary epithelial cell differentiation, Merlo et al. showed that HC11 cells, an immortalized and undifferentiated mouse mammary epithelial cell line, can be induced to differentiate and activate milk protein gene casein (*Csn)2* expression *in vitro* using media containing prolactin, dexamethasone, and IGF1 (19, 20). These studies solidified the importance of IGF1R in normal mammary gland differentiation in addition to TEB cap cell proliferation during puberty.

Much of the subsequent studies and models developed to expand on the role of IGF1R in mammary gland biology were performed in the context of mammary carcinogenesis and, consequently, will be introduced and discussed partly in this section on IGF1R in mammary gland development and elaborated on in the next section. The first such model in order of publication was the MMTV-*CD8α-IGF1R* mouse (10). This line utilizes the mouse mammary tumor virus (MMTV) promoter that is highly active in mammary epithelial cells to express a constitutively active CD8α-IGF1R chimeric protein. The biochemical nature of the CD8α extracellular domain results in homodimerization after expression due to its affinity to form intramolecular disulfide linkages (10, 21). Homodimerization of the chimeric protein induces transphosphorylation and constitutive activation of the intracellular IGF1Rβ subunits. Whole mount staining of these glands during pubertal growth demonstrated an obvious phenotype of reduced TEB and fat pad outgrowth, defective ductal branching, and hyperproliferation of epithelial cells within the lumen of the ducts. As a result, the glands were morphologically dense and hyperplastic, resulting in tumorigenesis at about 8 weeks of age (10).

The MMTV-*CD8α-IGF1R* model addresses the role of constitutively active IGF1R in mammary gland development but may not recapitulate overexpression of IGF1R that would rely on endogenously expressed ligand activation. The MTB-*IGF1R* mouse is a mammary epithelium specific doxycycline-inducible IGF1R overexpression model that was created to investigate this gap in knowledge (11). Interestingly, this group found a similar developmental phenotype to the CD8α-IGF1R mice where ductal outgrowth was ablated and the tissue was densely clustered, hyperplastic, and hyperproliferative. This increase in proliferation was subsequently shown to be controlled by expression of cyclin D1 (22). As with the CD8α-IGF1R model, the hyperplasia eventually developed into palpable mammary tumors with an average latency of 71-78 days (11).

We also generated additional mouse lines to explore IGF1R function in both mammary gland development and tumorigenesis. The results of these studies yielded the MMTV-*dnIGF1R* line that expresses the same kinase-dead IGF1R mutant as the WAP animals referenced above (9). As with the gain of function models, this line with reduced IGF1R signaling makes use of the MMTV promoter that is activated in all mammary epithelial cells early in development. Post-pubertal glands expressing the *dnIGF1R* lacked extensive tertiary ductal alveolar budding at late pubertal stages after multiple estrous cycles, consistent with the *Igf1r*$^{-/-}$ transplantation studies showing reduced alveolar differentiation during pregnancy. Flow cytometry analyses of the MMTV-*dnIGF1R* post-pubertal glands revealed enriched luminal ($Lin^-CD24^+CD29^{low}$) and luminal progenitor ($Lin^-CD24^+CD29^{low}CD61^+$) and decreased myoepithelial ($Lin^-CD24^+CD29^{high}$) cell populations (9).

IGF1R IN MOUSE MAMMARY TUMORIGENESIS

Tumor Promoting Functions

A common conclusion of numerous published reports investigating IGF/IGF1R function in mammary tumorigenesis *in vivo* is that dysregulation of this pathway is sufficient to either induce tumorigenesis or to modulate the primary tumor phenotype (for summary, see **Table 1**). In the CD8α-IGF1R model, the authors described the primary tumors as highly proliferative and histologically homogeneous with areas of apparent necrosis (10). The high proliferation phenotype allowed the authors to culture primary cells and create xenograft models to determine the efficacy of IGF1R inhibitors on tumor cell growth. In this case, inhibition of IGF1R was sufficient to decrease proliferation, suggesting IGF1R as a potential target for chemotherapeutics (10). Farabaugh and colleagues continued to characterize this model and performed flow cytometry to investigate potential changes in epithelial lineages (23). Their findings revealed an increase in the basal population ($Lin^-CD24^+CD29^{high}CD61^+$) in the preneoplastic glands; however, this population was absent in CD8α-IGF1R tumors where, instead, the luminal progenitor population ($Lin^-CD24^+CD29^{low}CD61^+$) was increased (23). Furthermore, when these tumors were dissociated and subjected to *in vitro* differentiation assays, the resulting tumorspheres more closely resembled myoepithelial-like colonies, distinguished from their luminal counterparts by morphological analysis. This is consistent with the observations that luminal progenitors retain the capacity to differentiate into basal cells and further suggests an influence of IGF1R activation on mammary epithelial cell differentiation (24).

Perhaps not surprisingly, the MTB-*IGF1R* overexpression model showed a similar histological tumor phenotype to the CD8α-IGF1R model. Two tumor pathologies were described where smaller tumors histologically presented as solid sheets of cells with sparse extracellular space, similar to CD8α-IGF1R tumors, and larger tumors were more vacuous and likened to the phenotype of Wnt-driven mammary tumors (11). More recently, work in the MTB-*IGF1R* model revealed that expression of the microRNA cluster miR-200b/200a/429 suppresses tumor initiation driven by IGF1R overexpression although the intricacies of the mechanism remain unclear (25). Another, previously unmentioned, mouse mammary tumor model is the Eef1a1-*Kras**/WAP-*Cre*/*Igf1r*$^{fl/fl}$ mouse line. This mouse line contains a mutated *Kras* gene including a premature stop codon, flanked by loxP sites for Cre recombinase recognition, under the control of a translational elongation factor promoter, Eef1a1, that is ubiquitously expressed in all cell types. Constitutive activation of Kras is controlled through tissue specific expression of Cre recombinase in order to remove the premature stop codon, resulting in constitutive Kras activation in a tissue of

interest and subsequent tumor formation. Utilizing the WAP-*Cre* allowed the authors to study tumorigenesis specifically in pregnant mice. Tumors arising in these animals exhibit a basal-like gene expression signature in addition to upregulation of *Igf1r* expression, determined by microarray analysis, which led the authors to identify IGF1R as a viable therapeutic target. This model was developed as a proof-of-concept with the goal of inhibiting tumorigenesis in Eef1a1-*Kras**/WAP-*Cre* animals. Conditional deletion of *Igf1r* significantly increased tumor latency in pregnant mice, reaffirming the status of IGF1R as an oncogene (12). These models provided strong *in vivo* evidence to support the conclusions that IGF1R is indeed pro-tumorigenic and has a particular role in promoting tumor cell proliferation.

Tumor Suppressing Functions

In contrast to the above studies, other transgenic mouse lines exist that provide evidence supporting tumor and metastasis suppressive functions for the IGF1R (**Table 1**). We have generated novel transgenic mouse lines that alter either IGF1R function or expression in the context of Wnt1-driven tumorigenesis. Previously, we crossed the aforementioned MMTV-*dnIGF1R* line with the widely studied MMTV-*Wnt1* mammary tumor model, to generate a double transgenic animal, MMTV-*Wnt1*/*dnIGF1R*, to investigate the role of IGF1R signaling in a basal-like mouse model of breast carcinogenesis. Attenuating IGF1R signaling in this model resulted in a dramatic phenotype characterized by decreased tumor latency, increased tumor multiplicity, and a significant increase in lung metastasis in an otherwise low (<15%) metastatic tumor model, an observation that is unreported in the IGF1R overexpression models. These tumors have enhanced basal cell ($Lin^-CD24^+CD29^{high}$) and luminal progenitor ($Lin^-CD24^+CD29^{low}CD61^+$) populations, suggesting inhibition of IGF1R interferes with differentiation or maintenance of a differentiated state (9). In addition to changes in cell population heterogeneity, these tumors have increased matrix metalloproteinase-secreting monocyte infiltration, collagen staining, as well as decreased epithelial adhesion originating from changes in cadherin expression (13, 26). Working with the MMTV-*Wnt1*/*dnIGF1R* animal model led to the question of cell lineage contribution to tumor initiation and metastasis. This resulted in the development of a novel system with a lineage-specific deletion of *Igf1r* in the context of Wnt-driven mammary gland tumorigenesis. The MMTV-*Wnt1*/K8-$CreER^T$/$Igf1r^{fl/fl}$ line allows for investigation into the role of IGF1R specifically in the luminal lineage and to determine its effect on tumor phenotype. Similar to the dnIGF1R expressing Wnt tumors, luminal specific deletion of IGF1R resulted in lower tumor latency and increased metastasis compared to control animals (13). Work to fully characterize this model is still ongoing.

IGF1R IN HUMAN BREAST CANCER

Early studies investigating IGF1R expression in human breast cancer patients produced conflicting reports as to the prognostic value of IGF1R expression in patient samples (27–29). This was likely due to the varied methodologies employed in each study to determine expression, which was usually limited to immunohistochemical analysis of a small, finite number of relevant markers. In addition, the studies had relatively small sample sizes and lacked other relevant information, such as tumor molecular subtype. Microarray technology to evaluate gene expression in human breast cancer samples allowed researchers to identify gene expression profiles that characterized several genetically distinct tumor subtypes denoted as normal-like, luminal-A, luminal-B, $HER2^+$, and triple-negative/basal-like (30, 31). In one of the earliest and largest (n = 2871) reports applying these criteria in conjunction with IGF1R expression data from human breast cancer patients, Yerushalmi *et al.* found a significant positive correlation between high IGF1R expression (IHC Allred score ≥ 7) and breast-cancer-specific survival (BCSS) in patients with luminal-B tumors. Conversely, high IGF1R expression was elsewhere associated with worse BCSS in patients with HER2/ERBB2-enriched tumors (32). Around the same time, other groups reported a strong positive correlation between IGF1R expression and patients harboring luminal type tumors and with BCSS (33–36). Additionally, a subsequent meta-analysis including data from these publications amongst others (10 studies, 5,406 patients) reiterated the findings that IGF1R expression levels positively correlated with overall survival and BCSS in hormone receptor positive tumors, but negatively correlated with survival in triple negative tumors (37). Taken together, these observations support the hypothesis that the role of IGF1R in the primary tumor phenotype is highly context dependent.

The relatively recent development of free, internet-based genomics tools to help facilitate advancement in cancer research has been become an invaluable resource. One such tool is the cBioPortal which functions to consolidate the ever-increasing number of publicly available human cancer datasets into one, easily searchable, user-friendly application (38, 39). To date, one such analysis through cBioPortal has been published employing The Cancer Genome Atlas (TCGA) RNA-sequencing breast cancer subset to further delineate correlations between IGF and insulin signaling molecule expression and PAM50 tumor molecular subtype (40–42). The major finding of this analysis, that included a number of molecules involved in these pathways was that IGF-related molecules are enriched on the transcriptional level in normal-like, luminal-A, and luminal-B tumors, and decreased in $HER2^+$ and basal-like tumors, consistent with previous reports. Interestingly, INSR signaling has frequently been discussed as a possible compensatory mechanism for tumor cells when IGF1R is inhibited; however, these data suggest a positive correlation between IGF1R expression and INSR expression in human tumors. We performed a similar analysis for IGF1R expression using a different human breast cancer dataset, the Molecular Taxonomy of Breast Cancer International Consortium (METABRIC) database, with a focus on correlations between IGF1R expression and PAM50 subtype, as well as probability of survival (43, 44). This analysis further confirmed a positive association with IGF1R expression and hormone receptor positive tumors and a negative correlation with triple-negative

tumors. Importantly, high IGF1R expression was associated with a better probability of survival, regardless of hormone receptor status (26).

Here, we extend these analyses by using cBioPortal to further explore the human data in both TCGA (TCGA Firehose Legacy) and METABRIC databases. Narrowing the available patient set to only include tumors which express higher than average IGF1R (z-score > 1) and lower than average IGF1R (z-score < -1), we see a shift in the PAM50 subtypes where IGF1R^{high} tumors are more commonly luminal-A and luminal-B and IGF1R^{low} tumors are classified more commonly as basal, ERBB2^{+}/HER2^{+}, or claudin-low (**Figure 1A**). Additionally, in both the METABRIC and TCGA subsets, there are lower levels of hormone receptor expression in the IGF1R^{low} cohort compared to IGF1R^{high} as

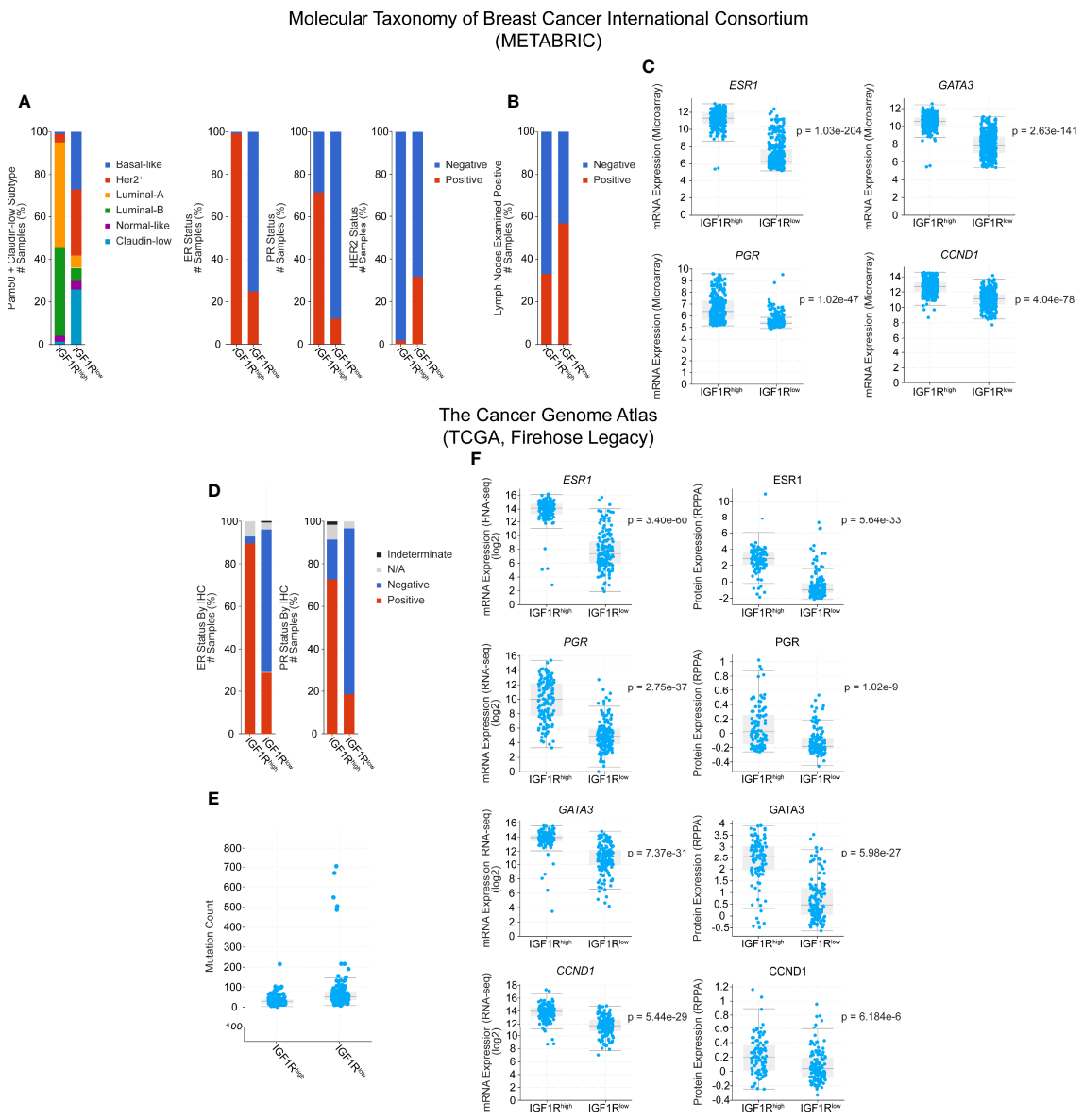

FIGURE 1 | Clinical characteristic and gene expression analysis of IGF1R^{high} and IGF1R^{low} human breast tumors from the Molecular Taxonomy of Breast Cancer International Consortium (METABRIC) and The Cancer Genome Atlas (TCGA) databases. Cohorts were generated by classifying patients by either high (z-score > 1, METABRIC n = 300, TCGA n = 128) or low (z-score < -1, METABRIC n = 415, TCGA n = 153) expression of IGF1R, while average patients (-1 < z-score < 1) were excluded. **(A)** PAM50 classification of patient tumors and hormone receptor expression status. **(B)** Lymph node positivity. **(C)** Gene expression microarray data for *ESR1*, *PGR*, *GATA3*, and *CCND1*. **(D)** Hormone receptor status in the TCGA cohorts. **(E)** Mutation count. **(F)** Gene (left) and protein (right) expression data for *ESR1*, *PGR*, *GATA3*, and *CCND1*. Statistical analyses were generated by cBioPortal and are student t-tests, where significance was defined as $p < 0.05$. N/A, Not Available.

well as a correlation with $HER2^+$ tumor classification (**Figures 1A, C, D, F**), similar to the findings of Farabaugh et al. (41). Interestingly, lymph node positivity, a readout of early-stage metastasis, is ~20% higher in the METABRIC $IGF1R^{low}$ group, providing a human correlation between low IGF1R levels and metastasis, consistent with our previous observations in the MMTV-*Wnt1/dnIGF1R* model [**Figure 1B** (9)]. In the TCGA dataset, these observations are consistent and extend beyond the level of transcription with the protein expression data that is also available for each tumor sample (**Figure 1F**, right). Mutational load was another clinical characteristic that was altered between the groups with $IGF1R^{low}$ patients having a higher mutational burden (**Figure 1E**). Expression of CCND1 in both datasets is increased in the $IGF1R^{high}$ groups and recapitulates the findings from the MTB-*IGF1R* model that tumorigenesis resulting from IGF1R overexpression is cyclin D1-driven [**Figures 1C, F** (22)]. Furthermore, expression of IGF1R is also positively correlated with GATA3, a well characterized promoter of luminal lineage differentiation and whose loss of expression is associated with enrichment of the luminal progenitor population [**Figures 1C, F** (45, 46)].

DISCUSSION

The field's understanding of the role of IGF1R in breast cancer has continued to evolve over decades of study. Early work summarized above convincingly justified the classification of IGF1R as an oncogene with potent value as a therapeutic target in human patients. More recently, though, following the failure of the many clinical trials initiated with the goal of inhibiting IGF1R in human patients, and recent data illustrating the effect of inhibiting IGF1R on enhancement of metastasis, it has become clear that the receptor's role in tumorigenesis is more nuanced and complicated than previously thought. This is also reflected in the literature by a number of studies that attempt to identify different mechanisms of compensation induced by IGF1R inhibition and the efficacy of a dual inhibitory approach with drugs such as cisplatin, trastuzumab, and others (47–51). Conversely, in some contexts, it may be beneficial to subsequently target the IGF pathway in situations where upregulation or activation is observed secondary to administration of therapy (52). Importantly, however, the mechanistic questions still remain as to how both driving and blocking IGF signaling *via* IGF1R result in a tumor promoting phenotype.

Constitutive activation or overexpression of IGF1R is sufficient to induce tumorigenesis characterized by tumors with an increased luminal progenitor population (11, 23). Previous work from our lab utilizing the MMTV-*Wnt1/dnIGF1R* mouse tumor model also observed a similar increase in the tumor luminal progenitor population (9). This seemingly contradictory observation could potentially be explained when considering the different biological processes in which IGF1R plays a role, context (or cell type/stage) specificity, and the unlikely compatibility of data from many of the models outlined above. In the case of the MMTV-*CD8α-IGF1R* model, it is feasible to hypothesize that constitutive activation of IGF1R is driving proliferation of the luminal progenitors at the adolescent stage prior to the onset of puberty, since this is the developmental stage during which the MMTV-LTR activates (53). This is further supported by the data demonstrating that these mice have stunted ductal outgrowth accompanied by hyperproliferation of epithelial cells within the lumens of the rudimentary ductal tree, as well as similar developmental defects also observed in the MTB-*IGF1R* overexpression model. This suggests that the cell-of-origin for the CD8-IGF1R tumors is possibly a luminal progenitor cell whose proliferation may be driven early in development through IGF1R signaling.

On the other hand, the shift seen in the luminal progenitor population of the MMTV-*Wnt1/dnIGF1R* model could be attributed to both the fact that the tumors are formed as a result of *Wnt1* overexpression [which could potentially drive progenitor cell expansion (54)] and the strongly supported role of IGF1R in luminal lineage differentiation. Early work in the MMTV-*Wnt1* model has shown that these tumors express both *Krt6* and *Sca1*, markers for mammary progenitor cells that are not expressed in tumors arising from MMTV-*Neu* or MMTV-*PyMT* animal, suggesting a role of progenitors in initiation of Wnt-driven tumors (54). Tumors resulting from the MMTV-*Wnt1* mouse tumor model are phenotypically basal-like, and historically, basal-like tumors were hypothesized to originate from a transformed myoepithelial progenitor cell (55). However, Molyneux *et al.* demonstrated that basal-like tumors resulting from BRCA1 mutations are derived from luminal progenitors, and not myoepithelial cells (24, 56). Similar to the MMTV-*Wnt1* mouse, tumors containing BRCA1 mutations have a significant population of luminal progenitors. Additionally, BRCA1 plays a role in the DNA damage response, a process that IGF1R has also been shown to positively regulate, suggesting inhibition of BRCA1 could potentially result in a similar phenotype as inhibition of IGF1R [**Figure 1E** (47, 57, 58)]. This mechanism could hypothetically be influenced by a decrease in IGF1R signaling resulting in a block of luminal lineage differentiation while concomitantly hampering the DNA damage response, driving accumulation of luminal progenitors, and increasing the statistical odds of tumor initiation in this population as a result of an increase in mutational burden, especially in the context of Wnt1-driven proliferation.

Another important piece of data unique to the MMTV-*Wnt1/dnIGF1R* model was an observed shift in insulin receptor isoform expression. The gene expression ratio of INSR-A to INSR-B is significantly higher in these tumors and is of importance due to the high affinity of IGF2 for INSR-A, identifying one potential mechanism of resistance to IGF1R inhibition (9). Critically, a similar correlation was seen in human participants of at least one unsuccessful IGF1R-targeting clinical trial where patients, regardless of treatment group, with higher expression levels of INSR-A or INSR-B had significantly shorter progression-free survival (59). These observations serve to further support the translational relevance of the MMTV-*Wnt1/dnIGF1R* model to human disease.

An important distinction between the overexpression/constitutive activation and inhibition models is the fact that tumors arising from inhibition of IGF1R are metastatic, while the existence of metastases in the former has not been reported (9). This is particularly of interest considering metastasis is the overwhelming cause of death in cancer patients (60). A recent study of breast cancer patients published in 2017 revealed a correlation between metastasis and low levels of IGF1R in isolated circulating tumor cells, further supporting the metastatic phenotype seen in our model and the human METABRIC data [**Figure 1B** (61)]. In conclusion, the studies summarized in this mini review highlight the clinical relevance of contextual IGF1R expression during breast cancer tumorigenesis and emphasize the need for further research in order to more thoroughly define the mechanisms distinguishing $IGF1R^{high}$ and $IGF1R^{low}$ tumors with the ultimate goal being more targeted and effective therapeutic strategies for patients.

AUTHOR CONTRIBUTIONS

JB wrote the manuscript, performed the database analyses, and generated the figure and table. JB and TW contributed to the manuscript revision, read, and approved the submitted version.

FUNDING

This work was supported by Public Health Service National Institutes of Health grants NCI R01CA204312 (TW).

ACKNOWLEDGMENTS

This work was conceived, in part, through many constructive discussions with AEO, KRM, and CAG.

REFERENCES

1. Liu JP, Baker J, Perkins AS, Robertson EJ, Efstratiadis A. Mice Carrying Null Mutations of the Genes Encoding Insulin-Like Growth Factor I (Igf-1) and Type 1 IGF Receptor (Igf1r). *Cell* (1993) 75(1):59–72. doi: 10.1016/S0092-8674(05)80084-4
2. Baker J, Liu JP, Robertson EJ, Efstratiadis A. Role of Insulin-Like Growth Factors in Embryonic and Postnatal Growth. *Cell* (1993) 75(1):73–82. doi: 10.1016/S0092-8674(05)80085-6
3. Bonnette SG, Hadsell DL. Targeted Disruption of the IGF-I Receptor Gene Decreases Cellular Proliferation in Mammary Terminal End Buds. *Endocrinology* (2001) 142(11):4937–45. doi: 10.1210/endo.142.11.8500
4. Yang Y, Yee D. Targeting Insulin and Insulin-Like Growth Factor Signaling in Breast Cancer. *J Mammary Gland Biol Neoplasia* (2012) 17(3-4):251–61. doi: 10.1007/s10911-012-9268-y
5. Boone DN, Lee AV. Targeting the Insulin-Like Growth Factor Receptor: Developing Biomarkers From Gene Expression Profiling. *Crit Rev Oncog* (2012) 17(2):161–73. doi: 10.1615/CritRevOncog.v17.i2.30
6. Yee D. Anti-Insulin-Like Growth Factor Therapy in Breast Cancer. *J Mol Endocrinol* (2018) 61(1):T61–T8. doi: 10.1530/JME-17-0261
7. Lero MW, Shaw LM. Diversity of Insulin and IGF Signaling in Breast Cancer: Implications for Therapy. *Mol Cell Endocrinol* (2021) 527:111213. doi: 10.1016/j.mce.2021.111213
8. Sun Z, Shushanov S, LeRoith D, Wood TL. Decreased IGF Type 1 Receptor Signaling in Mammary Epithelium During Pregnancy Leads to Reduced Proliferation, Alveolar Differentiation, and Expression of Insulin Receptor Substrate (IRS)-1 and IRS-2. *Endocrinology* (2011) 152(8):3233–45. doi: 10.1210/en.2010-1296
9. Rota LM, Albanito L, Shin ME, Goyeneche CL, Shushanov S, Gallagher EJ, et al. IGF1R Inhibition in Mammary Epithelia Promotes Canonical Wnt Signaling and Wnt1-Driven Tumors. *Cancer Res* (2014) 74(19):5668–79. doi: 10.1158/0008-5472.CAN-14-0970
10. Carboni JM, Lee AV, Hadsell DL, Rowley BR, Lee FY, Bol DK, et al. Tumor Development by Transgenic Expression of a Constitutively Active Insulin-Like Growth Factor I Receptor. *Cancer Res* (2005) 65(9):3781–7. doi: 10.1158/0008-5472.CAN-04-4602
11. Jones RA, Campbell CI, Gunther EJ, Chodosh LA, Petrik JJ, Khokha R, et al. Transgenic Overexpression of IGF-IR Disrupts Mammary Ductal Morphogenesis and Induces Tumor Formation. *Oncogene* (2007) 26 (11):1636–44. doi: 10.1038/sj.onc.1209955
12. Klinakis A, Szabolcs M, Chen G, Xuan S, Hibshoosh H, Efstratiadis A. Igf1r as a Therapeutic Target in a Mouse Model of Basal-Like Breast Cancer. *Proc Natl Acad Sci USA* (2009) 106(7):2359–64. doi: 10.1073/pnas.0810221106
13. Obr AE, Chang Y-J, Ciliento V, Lemenze A, Maingrette K, Bulatowicz JJ, et al. Breast Tumor Insulin-Like Growth Factor Receptor Regulates Cell Adhesion and Metastasis: Alignment of Mouse Single Cell and Human Breast Cancer Transcriptomics. *bioRxiv* (2021) 2021.08.31.458283. doi: 10.1101/2021.08.31.458283
14. Ruan W, Kleinberg DL. Insulin-Like Growth Factor I Is Essential for Terminal End Bud Formation and Ductal Morphogenesis During Mammary Development. *Endocrinology* (1999) 140(11):5075–81. doi: 10.1210/endo.140.11.7095
15. Loladze AV, Stull MA, Rowzee AM, Demarco J, Lantry JH3rd, Rosen CJ, et al. Epithelial-Specific and Stage-Specific Functions of Insulin-Like Growth Factor-I During Postnatal Mammary Development. *Endocrinology* (2006) 147(11):5412–23. doi: 10.1210/en.2006-0427
16. Lydon JP, DeMayo FJ, Funk CR, Mani SK, Hughes AR, Montgomery CA Jr, et al. Mice Lacking Progesterone Receptor Exhibit Pleiotropic Reproductive Abnormalities. *Genes Dev* (1995) 9(18):2266–78. doi: 10.1101/gad.9.18.2266
17. Ormandy CJ, Camus A, Barra J, Damotte D, Lucas B, Buteau H, et al. Null Mutation of the Prolactin Receptor Gene Produces Multiple Reproductive Defects in the Mouse. *Genes Dev* (1997) 11(2):167–78. doi: 10.1101/gad.11.2.167
18. Lee AV, Zhang P, Ivanova M, Bonnette S, Oesterreich S, Rosen JM, et al. Developmental and Hormonal Signals Dramatically Alter the Localization and Abundance of Insulin Receptor Substrate Proteins in the Mammary Gland. *Endocrinology* (2003) 144(6):2683–94. doi: 10.1210/en.2002-221103
19. Ball RK, Friis RR, Schoenenberger CA, Doppler W, Groner B. Prolactin Regulation of Beta-Casein Gene Expression and of a Cytosolic 120-Kd Protein in a Cloned Mouse Mammary Epithelial Cell Line. *EMBO J* (1988) 7(7):2089–95. doi: 10.1002/j.1460-2075.1988.tb03048.x
20. Merlo GR, Graus-Porta D, Cella N, Marte BM, Taverna D, Hynes NE. Growth, Differentiation and Survival of HC11 Mammary Epithelial Cells: Diverse Effects of Receptor Tyrosine Kinase-Activating Peptide Growth Factors. *Eur J Cell Biol* (1996) 70(2):97–105.
21. Zong C, Yan R, August A, Darnell JEJr., Hanafusa H. Unique Signal Transduction of Eyk: Constitutive Stimulation of the JAK-STAT Pathway by an Oncogenic Receptor-Type Tyrosine Kinase. *EMBO J* (1996) 15 (17):4515–25. doi: 10.1002/j.1460-2075.1996.tb00829.x
22. Jones RA, Campbell CI, Petrik JJ, Moorehead RA. Characterization of a Novel Primary Mammary Tumor Cell Line Reveals That Cyclin D1 Is Regulated by the Type I Insulin-Like Growth Factor Receptor. *Mol Cancer Res* (2008) 6 (5):819–28. doi: 10.1158/1541-7786.MCR-07-2157
23. Farabaugh SM, Litzenburger BC, Elangovan A, Pecar G, Walheim L, Atkinson JM, et al. IGF1R Constitutive Activation Expands Luminal Progenitors and Influences Lineage Differentiation During Breast Tumorigenesis. *Dev Biol* (2020) 463(1):77–87. doi: 10.1016/j.ydbio.2020.04.007
24. Molyneux G, Geyer FC, Magnay FA, McCarthy A, Kendrick H, Natrajan R, et al. BRCA1 Basal-Like Breast Cancers Originate From Luminal Epithelial Progenitors and Not From Basal Stem Cells. *Cell Stem Cell* (2010) 7(3):403–17. doi: 10.1016/j.stem.2010.07.010
25. Watson KL, Yi R, Moorehead RA. Transgenic Overexpression of the miR-200b/200a/429 Cluster Inhibits Mammary Tumor Initiation. *Transl Oncol* (2021) 14(12):101228. doi: 10.1016/j.tranon.2021.101228

26. Obr AE, Kumar S, Chang YJ, Bulatowicz JJ, Barnes BJ, Birge RB, et al. Insulin-Like Growth Factor Receptor Signaling in Breast Tumor Epithelium Protects Cells From Endoplasmic Reticulum Stress and Regulates the Tumor Microenvironment. *Breast Cancer Res* (2018) 20(1):138. doi: 10.1186/s13058-018-1063-2
27. Law JH, Habibi G, Hu K, Masoudi H, Wang MY, Stratford AL, et al. Phosphorylated Insulin-Like Growth Factor-I/Insulin Receptor is Present in All Breast Cancer Subtypes and Is Related to Poor Survival. *Cancer Res* (2008) 68(24):10238–46. doi: 10.1158/0008-5472.CAN-08-2755
28. Shimizu C, Hasegawa T, Tani Y, Takahashi F, Takeuchi M, Watanabe T, et al. Expression of Insulin-Like Growth Factor 1 Receptor in Primary Breast Cancer: Immunohistochemical Analysis. *Hum Pathol* (2004) 35(12):1537–42. doi: 10.1016/j.humpath.2004.09.005
29. Papa V, Gliozzo B, Clark GM, McGuire WL, Moore D, Fujita-Yamaguchi Y, et al. Insulin-Like Growth Factor-I Receptors Are Overexpressed and Predict a Low Risk in Human Breast Cancer. *Cancer Res* (1993) 53(16):3736–40.
30. Sorlie T, Perou CM, Tibshirani R, Aas T, Geisler S, Johnsen H, et al. Gene Expression Patterns of Breast Carcinomas Distinguish Tumor Subclasses With Clinical Implications. *Proc Natl Acad Sci USA* (2001) 98(19):10869–74. doi: 10.1073/pnas.191367098
31. Prat A, Parker JS, Karginova O, Fan C, Livasy C, Herschkowitz JI, et al. Phenotypic and Molecular Characterization of the Claudin-Low Intrinsic Subtype of Breast Cancer. *Breast Cancer Res* (2010) 12(5):R68. doi: 10.1186/bcr2635
32. Yerushalmi R, Gelmon KA, Leung S, Gao D, Cheang M, Pollak M, et al. Insulin-Like Growth Factor Receptor (IGF-1R) in Breast Cancer Subtypes. *Breast Cancer Res Treat* (2012) 132(1):131–42. doi: 10.1007/s10549-011-1529-8
33. Fu P, Ibusuki M, Yamamoto Y, Hayashi M, Murakami K, Zheng S, et al. Insulin-Like Growth Factor-1 Receptor Gene Expression Is Associated With Survival in Breast Cancer: A Comprehensive Analysis of Gene Copy Number, mRNA and Protein Expression. *Breast Cancer Res Treat* (2011) 130(1):307–17. doi: 10.1007/s10549-011-1605-0
34. Hartog H, Horlings HM, van der Vegt B, Kreike B, Ajouaou A, van de Vijver MJ, et al. Divergent Effects of Insulin-Like Growth Factor-1 Receptor Expression on Prognosis of Estrogen Receptor Positive *Versus* Triple Negative Invasive Ductal Breast Carcinoma. *Breast Cancer Res Treat* (2011) 129(3):725–36. doi: 10.1007/s10549-010-1256-6
35. Mountzios G, Aivazi D, Kostopoulos I, Kourea HP, Kouvatseas G, Timotheadou E, et al. Differential Expression of the Insulin-Like Growth Factor Receptor Among Early Breast Cancer Subtypes. *PloS One* (2014) 9(3):e91407. doi: 10.1371/journal.pone.0091407
36. Shin SJ, Gong G, Lee HJ, Kang J, Bae YK, Lee A, et al. Positive Expression of Insulin-Like Growth Factor-1 Receptor Is Associated With a Positive Hormone Receptor Status and a Favorable Prognosis in Breast Cancer. *J Breast Cancer* (2014) 17(2):113–20. doi: 10.4048/jbc.2014.17.2.113
37. Yan S, Jiao X, Li K, Li W, Zou H. The Impact of IGF-1R Expression on the Outcomes of Patients With Breast Cancer: A Meta-Analysis. *Onco Targets Ther* (2015) 8:279–87. doi: 10.2147/OTT.S74774
38. Cerami E, Gao J, Dogrusoz U, Gross BE, Sumer SO, Aksoy BA, et al. The Cbio Cancer Genomics Portal: An Open Platform for Exploring Multidimensional Cancer Genomics Data. *Cancer Discovery* (2012) 2(5):401–4. doi: 10.1158/2159-8290.CD-12-0095
39. Gao J, Aksoy BA, Dogrusoz U, Dresdner G, Gross B, Sumer SO, et al. Integrative Analysis of Complex Cancer Genomics and Clinical Profiles Using the Cbioportal. *Sci Signal* (2013) 6(269):pl1. doi: 10.1126/scisignal.2004088
40. Cancer Genome Atlas N. Comprehensive Molecular Portraits of Human Breast Tumours. *Nature* (2012) 490(7418):61–70. doi: 10.1038/nature11412
41. Farabaugh SM, Boone DN, Lee AV. Role of IGF1R in Breast Cancer Subtypes, Stemness, and Lineage Differentiation. *Front Endocrinol (Lausanne)* (2015) 6:59. doi: 10.3389/fendo.2015.00059
42. Parker JS, Mullins M, Cheang MC, Leung S, Voduc D, Vickery T, et al. Supervised Risk Predictor of Breast Cancer Based on Intrinsic Subtypes. *J Clin Oncol* (2009) 27(8):1160–7. doi: 10.1200/JCO.2008.18.1370
43. Curtis C, Shah SP, Chin SF, Turashvili G, Rueda OM, Dunning MJ, et al. The Genomic and Transcriptomic Architecture of 2,000 Breast Tumours Reveals Novel Subgroups. *Nature* (2012) 486(7403):346–52. doi: 10.1038/nature10983
44. Pereira B, Chin SF, Rueda OM, Vollan HK, Provenzano E, Bardwell HA, et al. The Somatic Mutation Profiles of 2,433 Breast Cancers Refines Their Genomic and Transcriptomic Landscapes. *Nat Commun* (2016) 7:11479. doi: 10.1038/ncomms11479
45. Kouros-Mehr H, Slorach EM, Sternlicht MD, Werb Z. GATA-3 Maintains the Differentiation of the Luminal Cell Fate in the Mammary Gland. *Cell* (2006) 127(5):1041–55. doi: 10.1016/j.cell.2006.09.048
46. Asselin-Labat ML, Sutherland KD, Barker H, Thomas R, Shackleton M, Forrest NC, et al. Gata-3 Is an Essential Regulator of Mammary-Gland Morphogenesis and Luminal-Cell Differentiation. *Nat Cell Biol* (2007) 9(2):201–9. doi: 10.1038/ncb1530
47. O'Flanagan CH, O'Shea S, Lyons A, Fogarty FM, McCabe N, Kennedy RD, et al. IGF-1R Inhibition Sensitizes Breast Cancer Cells to ATM-Related Kinase (ATR) Inhibitor and Cisplatin. *Oncotarget* (2016) 7(35):56826–41. doi: 10.18632/oncotarget.10862
48. Browne BC, Crown J, Venkatesan N, Duffy MJ, Clynes M, Slamon D, et al. Inhibition of IGF1R Activity Enhances Response to Trastuzumab in HER-2-Positive Breast Cancer Cells. *Ann Oncol* (2011) 22(1):68–73. doi: 10.1093/annonc/mdq349
49. Chakraborty A, Hatzis C, DiGiovanna MP. Co-Targeting the HER and IGF/insulin Receptor Axis in Breast Cancer, With Triple Targeting With Endocrine Therapy for Hormone-Sensitive Disease. *Breast Cancer Res Treat* (2017) 163(1):37–50. doi: 10.1007/s10549-017-4169-9
50. Hou X, Huang F, Macedo LF, Harrington SC, Reeves KA, Greer A, et al. Dual IGF-1r/InsR Inhibitor BMS-754807 Synergizes With Hormonal Agents in Treatment of Estrogen-Dependent Breast Cancer. *Cancer Res* (2011) 71(24):7597–607. doi: 10.1158/0008-5472.CAN-11-1080
51. Kurio N, Shimo T, Fukazawa T, Takaoka M, Okui T, Hassan NM, et al. Anti-Tumor Effect in Human Breast Cancer by TAE226, a Dual Inhibitor for FAK and IGF-IR *In Vitro* and *In Vivo*. *Exp Cell Res* (2011) 317(8):1134–46. doi: 10.1016/j.yexcr.2011.02.008
52. Leroy C, Ramos P, Cornille K, Bonenfant D, Fritsch C, Voshol H, et al. Activation of IGF1R/p110beta/AKT/mTOR Confers Resistance to Alpha-Specific PI3K Inhibition. *Breast Cancer Res* (2016) 18(1):41. doi: 10.1186/s13058-016-0697-1
53. Wagner KU, McAllister K, Ward T, Davis B, Wiseman R, Hennighausen L. Spatial and Temporal Expression of the Cre Gene Under the Control of the MMTV-LTR in Different Lines of Transgenic Mice. *Transgenic Res* (2001) 10(6):545–53. doi: 10.1023/A:1013063514007
54. Li Y, Welm B, Podsypanina K, Huang S, Chamorro M, Zhang X, et al. Evidence That Transgenes Encoding Components of the Wnt Signaling Pathway Preferentially Induce Mammary Cancers From Progenitor Cells. *Proc Natl Acad Sci USA* (2003) 100(26):15853–8. doi: 10.1073/pnas.2136825100
55. Melchor L, Benitez J. An Integrative Hypothesis About the Origin and Development of Sporadic and Familial Breast Cancer Subtypes. *Carcinogenesis* (2008) 29(8):1475–82. doi: 10.1093/carcin/bgn157
56. Lim E, Vaillant F, Wu D, Forrest NC, Pal B, Hart AH, et al. Aberrant Luminal Progenitors as the Candidate Target Population for Basal Tumor Development in BRCA1 Mutation Carriers. *Nat Med* (2009) 15(8):907–13. doi: 10.1038/nm.2000
57. Heron-Milhavet L, Karas M, Goldsmith CM, Baum BJ, LeRoith D. Insulin-Like Growth Factor-I (IGF-I) Receptor Activation Rescues UV-Damaged Cells Through a P38 Signaling Pathway. Potential Role of the IGF-I Receptor in DNA Repair. J. *Biol Chem* (2001) 276(21):18185–92. doi: 10.1074/jbc.M011490200
58. Creighton CJ, Casa A, Lazard Z, Huang S, Tsimelzon A, Hilsenbeck SG, et al. Insulin-Like Growth Factor-I Activates Gene Transcription Programs Strongly Associated With Poor Breast Cancer Prognosis. *J Clin Oncol* (2008) 26(25):4078–85. doi: 10.1200/JCO.2007.13.4429
59. Gradishar WJ, Yardley DA, Layman R, Sparano JA, Chuang E, Northfelt DW, et al. Clinical and Translational Results of a Phase II, Randomized Trial of an Anti-IGF-1r (Cixutumumab) in Women With Breast Cancer That Progressed on Endocrine Therapy. *Clin Cancer Res* (2016) 22(2):301–9. doi: 10.1158/1078-0432.CCR-15-0588
60. Chaffer CL, Weinberg RA. A Perspective on Cancer Cell Metastasis. *Science* (2011) 331(6024):1559–64. doi: 10.1126/science.1203543
61. Spiliotaki M, Mavroudis D, Kokotsaki M, Vetsika EK, Stoupis I, Matikas A, et al. Expression of Insulin-Like Growth Factor-1 Receptor in

Circulating Tumor Cells of Patients With Breast Cancer Is Associated With Patient Outcomes. *Mol Oncol* (2018) 12(1):21–32. doi: 10.1002/1878-0261.12114

Conflict of Interest: The authors declare that the research was conducted in the absence of any commercial or financial relationships that could be construed as a potential conflict of interest.

Publisher's Note: All claims expressed in this article are solely those of the authors and do not necessarily represent those of their affiliated organizations, or those of the publisher, the editors and the reviewers. Any product that may be evaluated in this article, or claim that may be made by its manufacturer, is not guaranteed or endorsed by the publisher.

Advantages of publishing in Frontiers

OPEN ACCESS
Articles are free to read for greatest visibility and readership

FAST PUBLICATION
Around 90 days from submission to decision

HIGH QUALITY PEER-REVIEW
Rigorous, collaborative, and constructive peer-review

TRANSPARENT PEER-REVIEW
Editors and reviewers acknowledged by name on published articles

Frontiers
Avenue du Tribunal-Fédéral 34
1005 Lausanne | Switzerland

Visit us: www.frontiersin.org
Contact us: frontiersin.org/about/contact

REPRODUCIBILITY OF RESEARCH
Support open data and methods to enhance research reproducibility

DIGITAL PUBLISHING
Articles designed for optimal readership across devices

FOLLOW US
@frontiersin

IMPACT METRICS
Advanced article metrics track visibility across digital media

EXTENSIVE PROMOTION
Marketing and promotion of impactful research

LOOP RESEARCH NETWORK
Our network increases your article's readership